Chondrogenic differentiation of human amniotic fluid-derived stem cells cultured in alginate and agarose models with CNP and TGFβ

Submitted in partial fulfilment of the requirements of the

Degree of Doctor of Philosophy

(Queen Mary University of London)

Presented by

JAMES ROBERT MILES TAYLOR

2019

Statement of originality

I, James Robert Miles Taylor, confirm that the research included within this thesis is my own work or that where it has been carried out in collaboration with, or supported by others, that this is duly acknowledged below, and my contribution indicated. Previously published material is also acknowledged below.

I attest that I have exercised reasonable care to ensure that the work is original and does not to the best of my knowledge break any UK law, infringe any third party's copyright or other Intellectual Property Right, or contain any confidential material.

I accept that the College has the right to use plagiarism detection software to check the electronic version of the thesis.

I confirm that this thesis has not been previously submitted for the award of a degree by this or any other university.

Date: 16 December 2019

Abstract

The use of stem cells for cartilage repair and treatment of osteoarthritis has been a subject of much debate. To date, there is no consensus on the appropriate cell source that has chondrogenic potential for cartilage repair. The present study examined whether differentiation of stem cells derived from human amniotic fluid (AFSCs) are proliferative and increase gene expression and protein production of extracellular matrix (ECM) components in agarose culture after treatment with growth factors (TGFβ_1 and TGFβ_3) and/or agents which promote natriuretic peptide signalling (CNP, Dex). Following short (up to 7 days) and long-term culture (28 days) of AFSC/agarose constructs, markers for ECM synthesis (GAG, collagen, DNA) were quantified by biochemical assay. Proteoglycan and collagen distribution profiles of AFSC/agarose constructs were examined with Alcian blue staining of histological specimens and by second harmonic generation (SHG) confocal imaging. The gene expression of SOX-9, aggrecan and Type II collagen was examined by RT-qPCR.

In addition, the development of sophisticated scaffold materials which release biologically active agents to incorporated cells is an increasing area of scientific research for tissue engineering applications. In separate experiments, I investigated whether the application of CNP containing microcapsules to bovine chondrocyte/agarose constructs over a 48-hour time period constituted any effect to the GAG synthesis of encapsulated cells compared to exogenous application of CNP. CNP microcapsule structures were characterised via SEM and confocal microscopy and markers for ECM synthesis (GAG, DNA) were quantified by biochemical assay.

GAG synthesis was not stimulated in TGFβ treated AFSCs embedded within alginate bead structures. Alginate beads also suffered from significant structural weakness after prolonged culture periods suggesting they were unsuitable for the chondrogenic differentiation of AFSCs. Co-treatment of AFSC/agarose constructs with either CNP + TGFβ_1, CNP + TGFβ_3 or Dex + TGFβ_1 enhanced GAG synthesis ($p<0.01$) but not collagen synthesis compared to growth factor only conditions after 28 days ($p>0.05$). Weak positive homogenous histological staining was detected in co-treated samples at both core and edge sections of constructs while SHG imaging confirmed some collagen deposition in co-treated samples at the core of constructs investigated. SOX-9, aggrecan and type II collagen gene expression were unaffected by all treatments investigated after 28 days relative to day 0 (all $p>0.05$). Treatment of bovine chondrocyte/agarose

constructs with CNP microcapsules enhanced GAG synthesis relative to exogenous application after 48 hours ($p<0.01$).

In summary, I demonstrate significant upregulation of GAG synthesis but not collagen in AFSC/agarose constructs stimulated with TGF$\beta_{1/3}$ and Dex or CNP for 28 days but not 7 days. In addition, I also show that localised release of CNP is conducive to enhanced GAG synthesis in bovine chondrocyte/agarose constructs after 48 hours relative to exogenous application. The lack of a substantial increases in GAG synthesis upon chondrogenic growth factor treatment in conjunction with CNP or dexamethasone suggest that AFSCs may not be suitable for a cartilage tissue engineering in comparison to other stem cells types. This would therefore have an obvious impact on the use of AFSCs for cartilage engineering field but may have ramifications for their use in other tissue engineering fields. Future investigations should focus build upon the investigations carried out here with a focus on the effect of CNP on hypertrophic/osteogenic gene expression in AFSCs and the effect of CNP microcapsules on the process of AFSC chondrogenic differentiation.

Acknowledgements

I would first like to acknowledge the assistance of my supervisors; Dr Tina Chowdhury, Professor Adrian Hobbs, Professor Anna David and Professor Paolo de Coppi for selecting me for this position and reviewing this thesis to make it the best it can be. To my funders, the Rosetrees Trust medical research charity and the Institute of Bioengineering, I am grateful for your financial support that has made this research possible. I thank the technical staff especially Mr Shafir Iqbal, Dr Dong Sheng Wu, Dr Russell Bailey and Mr Chris Mole for being essential port of calls when asking for training and safety advice. I would like to also thank Dr Stephen Thorpe, Dr Claire Thompson, Dr Hannah Heywood, Professor Gleb Sukhorukov, Dr David Gould, Dr Jordan Read, Dr Eleni Antoniadou and Dr Sindhu Subramaniam for their general help in the lab and advice.

I would like to thank my peers at QMUL; Dr Dinara Ikramova, Dr David Barrett, Dr Stephen Agha, Dr Yamin Abdouni, Dr Salman Hassan Ibne Shams, Dr Gannian Zhang, Dr Feng Yang and Dr Samantha Atienza Gabriel: who have helped make this PhD process survivable and provided many fun nights out away from the lab to stop us all going crazy.

I would like to specially thank Miss Nicola Culshaw, who inspired my scientific curiosity and set me on this long path a long time ago. I will always be immensely thankful for your teaching and sparking my passion for science and teaching. I'm grateful I managed to use the words 'ion' and 'iron' in this thesis which will always make me think of you.

Above all else I would like to acknowledge the love and support of my family (Mum, Dad, Hayley, Lilly, Emily, Charlie and Aunt Linda) who have inspired me to keep going when things were not going so well and reminding me that the work I do is exciting and unique.

Finally, to my love Seora Kim who has continuously supported me in all manner of ways too long to write here and without whom I doubt I'd be in the position I am now to submit this document. Thank you for giving me the motivation to see this through to the end and I look forward to spending the rest of my life with you.

Thank you all from the bottom of my heart.

Table of Contents

List of Figures

List of Tables

Abbreviations

ADAMTS – **A** **D**istintegrin **A**nd **M**etalloproteinase with **T**hrombo**s**pondin motifs

AFSC – **A**mniotic **F**luid **S**tem **C**ell

AGC1 – **A**spartate **G**lutamate **T**ransporter 1

ALP – **Al**kaline **P**hosphatase

ANOVA – **An**alysis **o**f **Va**riance

AP-2 – Activating enhancer-binding **p**rotein 2-epsilon

APC - Allo**p**hyco**c**yanine

ASC – Amniotic stem cell

ATP – Adenosine **T**ri**p**hosphate

BM-MNC – **B**one **M**arrow **M**ono**n**uclear **C**ell

BM-MSC – **B**one **M**arrow derived **M**esenchymal **S**tem **C**ell

ANP – **A**-type **N**atriuretic **P**eptide

bAC – **B**ovine **A**rticular **C**hondrocyte

BMI – **B**ody **M**ass **I**ndex

BMP – **B**one **M**orphogenetic **P**rotein

BNP – **B**-type **N**atriuretic **P**eptide

BSA – **B**ovine **S**erum **A**lbumin

CANTOS – **C**anakinumab **An**ti Inflammatory **T**hrombosis **O**utcomes **S**tudy

CBP/p300 – **C**REB-**b**inding **p**rotein/E1A binding protein **p300**

CD – **C**luster of **D**ifferentiation

cDNA – **C**omplementary **D**eoxyribo**n**ucleic **a**cid

cGMP – **c**yclic **G**uanosine **M**ono**p**hosphate

CNP – **C**-type **N**atriuretic **P**eptide

COL1a1 – **Col**lagen Type **1** **a**lpha **1** chain

COL2a1 – **Col**lagen Type **2** **a**lpha **1** chain

COL2b1 – **Col**lagen Type **2** **b**eta **1** chain

COL10a1 – **Col**lagen Type **10** **a**lpha **1** chain

COMP – **C**artilage **o**ligomeric **m**atrix **p**rotein

CPD – **C**ritical **P**oint **D**rying

DAMPs – **D**amage **A**ssociated **M**olecular **P**atterns

DAPI – 4'6-**d**i**a**midino-2-**p**heny**l**indole

DDR – **D**iscoidin **D**omain **R**eceptor

Dex – **Dex**amethasone

DMBA – **Di**m**e**thylamino-**b**enz**a**ldehyde

DMEM – **D**ulbecco's **M**odified **E**agle's **M**edium

DMMB – 1,9-**dim**ethyl**m**ethlyene **b**lue

DNA – **D**eoxy**r**ibo**n**ucle**i**c **a**cid

dNTP – **D**eoxy**n**ucleotide **t**ri**p**hosphate

D-PBS – **D**ulbecco's **P**hosphate **B**uffered **S**aline

DPX – **D**istyrene **p**lasticiser and **x**ylene

DS – **D**extran **S**ulfate

EB – **E**mbryoid **B**ody

EBSS – **E**arl's **B**alanced **S**alt **S**olution

ECM – **E**xtra**c**ellular **M**atrix

EDTA – **E**thylene**d**iamine**t**etra**a**cetic acid

ERK1/2 – **E**xtracellular signal **r**egulated **k**inase **1/2**

ESC – **E**mbryonic **S**tem **C**ell

FACS – **F**luorescent **A**ctivated **C**ell **S**orting

FBS – **F**oetal **B**ovine **S**erum

FCS – **F**oetal **C**alf **S**erum

FDA – **F**ood and **D**rug **A**dministration

FGFR – **F**ibroblast **G**rowth **F**actor **R**eceptor

FITC – **F**luorescein **i**so**t**hio**c**yanate

GO – **G**raphene **O**xide

GPI - **G**lycosyl**p**hosphatidyl**i**nisotol

GTP – **G**uanosine **T**ri**p**hosphate

HA – **H**yaluronan

H&E – **H**aematoxylin and **E**osin

HCl – **H**ydro**c**hloric **a**cid

HEPES – 4-(2-**h**ydroxy**e**thyl)-1-**p**iperazine**e**thane**s**ulfonic acid

HIF – **H**ypoxia **I**nducible **F**actor

HSP47 – **H**eat **S**hock **P**rotein 47

HUCPVCs – **H**uman **U**mbilical **C**ord **P**eri**v**ascular **c**ells

ICRS – **I**nternational **C**artilage **R**epair **S**ociety

Ihh – **I**ndian **H**edge**h**og

IKDC – **I**nternational **K**nee **D**ocumentation **C**ommittee

IL-1β – **I**nter**l**eukin **1** **β**

IL-1Ra – **I**nter**l**eukin **1** **r**eceptor **a**ntagonist

IMS – **I**ndustrial **M**ethylated **S**pirits

iNOS – inducible **n**itric **o**xide **s**ynthase

iPSC – **I**nduced **P**luripotent **S**tem **C**ell

ITS – **I**nsulin **T**ransferrin **S**elenium

JSN – **J**oint **S**pace **N**arrowing

KOOS – **K**nee injury and **O**steoarthritis **O**utcome **S**core

kV – **K**ilo**v**olt

LbL – **L**ayer **b**y **L**ayer

LED – **L**ight **E**mitting **D**iode

MACS – **M**agnetic **A**ctivated **C**ell **S**orting

MAPK – **M**itogen **A**ctivated **P**rotein **K**inases

MC – **M**icro**c**apsules

MEK1/2 – **M**APK/**E**RK **K**inase

MEM – **M**inimal Essential **M**edium

MHC – **M**ajor **H**istocompatibility **C**omplex

MIA/CD-RAP – **M**elanoma **I**nhibitory **A**ctivity/**C**artilage-**d**erived **R**etinoic **A**cid-sensitive **p**rotein

MMP – **M**atrix **M**etallo**p**roteinase

MOCART – **M**agnetic Resonance **O**bservation of **Ca**rtilage **R**epair **T**issue

mOsm – **M**ili**osm**olar

MRI – **M**agnetic **R**esonance **I**maging

mRNA – **m**essenger **R**ibo**n**ucleic **A**cid

MSC – **M**esenchymal **S**tem **C**ell

N-cad – **N-cad**herin

N-cam – **N**eural **c**ell **a**dhesion **m**olecule

NGF – **N**erve **G**rowth **F**actor

NPPC – **N**atriuretic **P**eptide **P**recursor **C**

NPR – **N**atriuretic **P**eptide **R**eceptor

OA – **O**steo**a**rthritis

OCT – **O**ptimal **C**utting **T**emperature

Osx – **Os**teri**x**

PCM – **P**eri**c**ellular **M**atrix

PDE – **P**hospho**di**e**s**terases

PDI – **P**rotein **D**isulphide **I**somerase

PE – **P**hyco**e**rythrin

PGE_2 – Prosta**g**landi**n** **E_2**

PI3K/Akt – **P**hospho**i**nositide **3**-**k**inase/Protein kinase B

PKGII – **P**rotein **K**inase **G** II

PLA – **P**oly-**l**-**a**rginine hydrochloride

Pth1r – **P**ara**t**hyroid **h**ormone **r**elated peptide 1

PTHrPR – **P**ara**t**hyroid **H**ormone **r**elated **P**eptide **R**eceptor

RA – **R**heumatoid **A**rthritis

RANK – **R**eceptor **a**ctivator of **n**uclear factor **κ** B

RER – **R**ough **E**ndoplasmic **R**eticulum

RGD – Arginyl-glycyl-aspartic acid

ROS – **R**eactive **O**xygen **S**pecies

RPM – **R**evolutions **P**er **M**inute

RT-qPCR – **R**everse **T**ranscription **q**uantitative **P**olymerase **C**hain **R**eaction

Runx2 – **Run**t related transcription factor **2**

SCID – **S**evere **C**ombined **I**mmuno**d**eficient mice

SEM – **S**canning **E**lectron **M**icroscopy **/ S**tandard **E**rror of the **M**ean

siRNA – **S**mall **i**nterfering **R**ibo**n**ucleic **a**cid

SLRPs – **S**mall **L**eucine **R**ich **P**roteoglycans

SOX9 – **S**ex determining region Y-b**ox9**

SPSS – **S**tatistical **P**ackage for **S**ocial **S**ciences

SSC – **S**aline **S**odium **C**itrate

SSEA4 – **S**tage-**s**pecific-**e**mbryonic **a**ntigen 4

TAK1 – **T**ransforming Growth Factor beta **A**ctivated **K**inase **1**

TCF – **T**-**c**ell **f**actor

TGFβ – **T**ransforming **G**rowth **F**actor β

TIMP3 – **TI**MP **M**etallo**p**roteinase Inhibitor **3**

TIMPS – **T**issue **I**nhibitor of **M**etallo**p**roteinase**s**

TNFα – **T**umour **N**ecrosis **F**actor α

TRITC – **T**etramethyl**r**hodamine **I**so**t**hio**c**yanate

TSC22 – **T**GFβ **S**timulated **C**lone **22**

TUNEL – **T**erminal deoxynucleotidyl transferase d**U**TP **n**ick **e**nd **l**abelling

UK – **U**nited **K**ingdom

VAS – **V**isual **A**nalogue **S**cale

VEGFA – **V**ascular **E**ndothelial **G**rowth **F**actor **A**

WNT – **W**ingless I**nt**egrated

WOMAC – **W**estern **O**ntario and **Mc**Master Universities Osteoarthritis Index

Chemicals

Ca – Calcium

$CaCl_2$ – Calcium Chloride

$CaCO_3$ – Calcium Carbonate

CO_2 – Carbon Dioxide

NaCl – Sodium Chloride

Na_2CO_3 – Sodium Carbonate

NaOH – Sodium Hydroxide

O_2 – Oxygen

Facilities

ICH – **I**nstitute of **C**hild **H**ealth

IOB – **I**nstitute **o**f **B**ioengineering

UCL – **U**niversity **C**ollege **L**ondon

UCLH – **U**niversity **C**ollege **L**ondon **H**ospital

Table of reagents

Product name	Company	Product code
1-Propanol	Sigma Aldrich/Merck	402893
αMEM	ThermoFisher Scientific	12561-056
Acetic acid (glacial)	Sigma Aldrich/Merck	537020
Agarase from *Pseudomonas atlantica*	Sigma Aldrich/Merck	A6306
Agarose, low gelling temperature (Type VII-A)	Sigma Aldrich/Merck	A0701
Alcian blue 8GX	Sigma Aldrich/Merck	A3157
Aluminium sulfate hydrate	Sigma Aldrich/Merck	368458
Black assay plate 96 well	4titude	4ti-0263/IND
Bovine Serum Albumin	Sigma Aldrich/Merck	A9418
Buffer QG	Qiagen	19063
Calcium Chloride	Sigma Aldrich/Merck	C1016
Calf thymus DNA	Sigma Aldrich/Merck	D1501
C-chip disposable haemocytometer	NanoEnTek/Labtech	DHC-N01
CD73 antibody	Miltenyi biotec	130-085-183
CD90 antibody	Miltenyi biotec	130-099-208
CD105 antibody	Miltenyi biotec	130-099-888
CD117 antibody	Miltenyi biotec	130-091-734
CD117 microbeads	Miltenyi Biotec	130-091-332
Cell strainer (40 μm)	Corning	352340
Chang B + C	FUJIFILM Irvine Scientific	T101-019
Chloramine T reagent	Sigma Aldrich/Merck	857319
Chondroitin-4-sulphate	Sigma Aldrich/Merck	C4384
Citric acid monohydrate	Sigma Aldrich/Merck	C1909
C-type natriuretic peptide (CNP)	Genscript	RP11110
Collagenase from *Clostridium histolyticum*	Sigma Aldrich/Merck	C9407
Cysteine Hydrochloride	Sigma Aldrich/Merck	C7477
DAPI	Sigma Aldrich/Merck	D9542
Dexamethasone	Sigma Aldrich/Merck	D2915
Dextran sulfate	Sigma Aldrich/Merck	D6924
Dimethylmethylene blue (DMMB)	Sigma Aldrich/Merck	341088

Disposable microtome blade	CellPath	POR010993
4-dimethylamino-benzaldehyde	Sigma Aldrich/Merck	39070
DMEM	Sigma Aldrich/Merck	D5030
Dimethyl sulfoxide (DMSO)	Sigma Aldrich/Merck	D2650
DNA-*free*™ DNA removal kit (recombinant DNase I, 10x DNase I buffer, DNase inactivation reagent, nuclease free water)	Ambion™/ ThermoFisher Scientific	AM1906
DPX	Sigma Aldrich/Merck	44581
Earl's Balance Salt Solution (EBSS)	Sigma Aldrich/Merck	E3024
EDTA	Sigma Aldrich/Merck	E6758
Enhanced Avian Synthesis Kit	Sigma Aldrich/Merck	STR1
Eosin Y	Sigma Aldrich/Merck	E-4382
Ethanol	Sigma Aldrich/Merck	51976
Foetal Bovine Serum	ThermoFisher Scientific	10500064
FcR blocking reagent	Miltenyi Biotec	130-059-901
GlutaMAX	Gibco	35050061
Haematoxylin solution according to Mayer	Sigma Aldrich/Merck	51275
High Glucose-Dulbecco's Modified Eagle Medium (HG-DMEM)	Sigma Aldrich/Merck	D1145
Hydrochloric acid	Sigma Aldrich/Merck	H1758
Isopropanol (Molecular Biology grade)	Sigma Aldrich/Merck	I9516
ITS + 1 Liquid media supplement	Sigma Aldrich/Merck	I2521
Kapa SYBR green I fluorescent dye (2x)	Kappa	KK4601
Kimwipes	Sigma Aldrich/Merck	Z188956
L-Ascorbic acid	Sigma Aldrich/Merck	A4403
L-glutamine	Sigma Aldrich/Merck	G7513
Live/Dead Viability/Cytotoxicity kit, for mammalian cells	ThermoFisher Scientific /Invitrogen	L3224
L-proline	Sigma Aldrich/Merck	P5607
Magnetic bead columns	Miltenyi Biotec	130-042-201
Microtest plate 96 wells - clear	Sarstedt	82.1582.001
Nuclear fast red	VWR	342094W
OCT compound	ThermoFisher Scientific	LAMB-OCT
OCTOMACS separator	Miltenyi Biotec	130-042-109
Papain from *papaya latex*	Sigma Aldrich/Merck	P3125
Paraformaldehyde	Sigma Aldrich/Merck	158127

Phosphate buffered saline (PBS)	Sigma Aldrich/Merck	D8537
PCR tubes (20μl)	BioRad	TFI0201
Penicillin / streptomycin (100x)	Sigma Aldrich/Merck	P4333
Perchloric acid	Sigma Aldrich/Merck	244252
Picric acid	Sigma Aldrich/Merck	197378
Pierce FITC Antibody Labelling Kit	ThermoFisher Scientific	53027
Poly-l-arginine	Sigma Aldrich/Merck	P7762
Polysine slides	ThermoFisher Scientific	J2800AMNT
Pronase from *Streptomyces griseus*	Sigma Aldrich/Merck	10165921001
Recombinant TGFβ_1	R&D Biosystems	240-B-002
Recombinant TGFβ_3	R&D Biosystems	243-B-002
RNase AWAY	ThermoFisher Scientific	10328011
RNeasy minikit (containing RW1, RPE, RLT and Rnase free water)	Qiagen	74104
Round bottom polypropylene tubes	Corning	352058
Sodium acetate trihydrate	Sigma Aldrich/Merck	S7670
Sodium acetate anhydrous	Sigma Aldrich/Merck	S2889
Sodium alginate keltone LV	ISP	1134001
Sodium Carbonate	Sigma Aldrich/Merck	S7795
Sodium Chloride	Sigma Aldrich/Merck	S7653
Sodium Citrate	Sigma Aldrich/Merck	C7254
Sodium Hydroxide	Sigma Aldrich/Merck	655104
Sodium Pyruvate	Sigma Aldrich/Merck	S8636
Sterile non-tissue culture treated bacteriological petri dishes	ThermoFisher Scientific /Corning	351029
Sucrose	Sigma Aldrich/Merck	S0389
Thymol	Alfa Aesar	A14563
Toluidine blue	Sigma Aldrich/Merck	T-0394
Tetramethylrhodamine isothiocyanate mixed isomers (TRITC)	Sigma Aldrich/Merck	87918
Trans-4-hydroxy-L-proline	Sigma Aldrich/Merck	56250
TrypLE	ThermoFisher Scientific	12563-029
Whatman paper	ThermoFisher Scientific	WHA10347509

Chapter 1: Cartilage structure, pathology and tissue repair

1.1 Anatomical features and functions of healthy articular cartilage

Hyaline articular cartilage is a specialised connective tissue that covers the opposing osseous ends of bones in the synovial joint (Fox et al., 2009, Mow et al., 1992). The main functions of cartilage are to distribute loads, minimise the peak stresses in the subchondral bone, and provide a load-bearing surface with minimal friction and wear (Guilak, 2005, Mow et al., 1992, Mow and Guo, 2002). Cartilage is not innervated and is avascular which, combined with a low chondrocyte cell density, explains why the tissue exhibits limited repair capacity when damaged after injury or affected by inflammatory disease (Hunter, 1743). The location of articular cartilage in the synovial joint is illustrated in **Figure 1.1**.

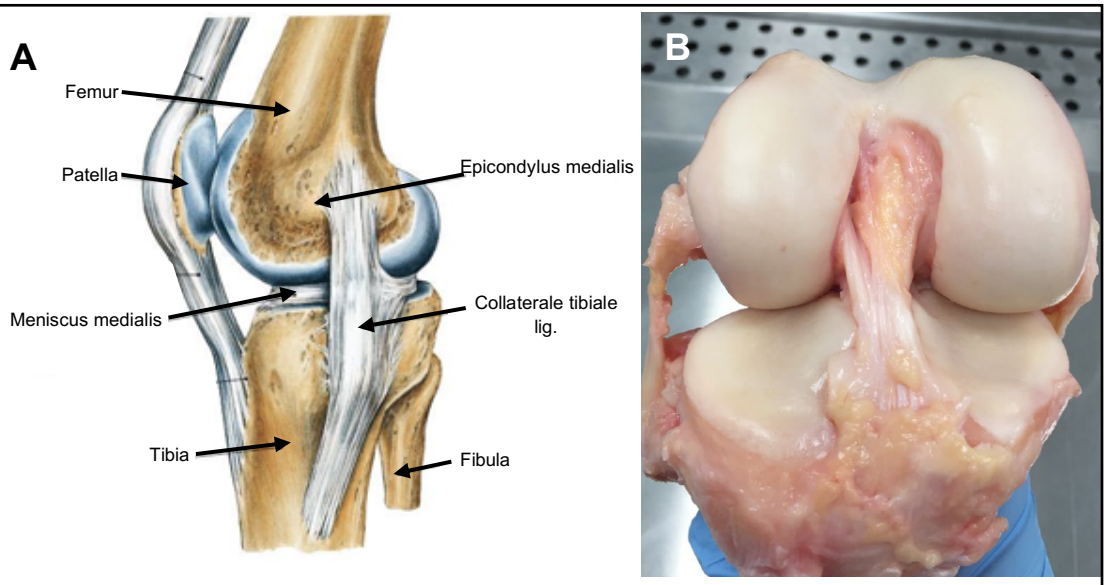

Figure 1.1: Healthy articular cartilage allows smooth articulation. *Anatomical schematic of knee articular joint as a side view of the femoral condyle (**A**) and a frontal view of a healthy human joint (**B**). Figure adapted from (Tillmann, 2005, Peters et al., 2018).*

The most distinguishing features of healthy cartilage are that the tissue appears to be relatively smooth and thin, between 2.2 to 2.5 mm thick, and is primarily white turning marginally yellow with age (Frisbie et al., 2006). Cartilage has unique viscoelastic and compressive properties provided by the extracellular matrix (ECM) and complex interplay of chondrocytes. The presence of nutrients in the synovial fluid and biological factors are transferred to the cells by diffusion from the synovial fluid.

1.2 Structure and composition of articular cartilage

The extracellular matrix has a unique constitution dictated by environmental conditions, cellular components and genetic disposition. The ECM is mainly composed of water (60 - 80%), type II collagen (10 - 20%), proteoglycans (4 - 7%) and glycoproteins (< 5%) (Fox et al., 2009, Ratcliffe and Mow, 1996, Mow et al., 1992). In contrast, chondrocytes contribute to only 1 - 10% of the total tissue volume and are responsible for the synthesis and maintenance of the matrix components (Kim et al., 2008, Muir, 1995, Ratcliffe and Mow, 1996). The composition of the ECM and its complex interactions with chondrocytes give the tissue its load-bearing capacity and in the presence of the synovial fluid, its lubrication and frictionless properties (Mov, Ratcliffe, Poole, 1992). Chondrocytes exist in a unique physiological and mechanical environment in the ECM and exhibit different sizes, shapes, and metabolic activity in the various zones of cartilage. In fact the surrounding ECM limits the number of possible cell-to-cell contacts and also means the cells rely on diffusion from the synovial space for their nutritional supply (Cavanaugh, 2007). The cell/ECM network is therefore able to help regulate important biological processes such as cell proliferation, metabolism, mechanotransduction, ECM synthesis and tissue remodelling mechanisms in an effort to maintain tissue homeostasis (Loeser, 2014, Gelse, 2003).

1.2.1 Collagens

Collagens are a family of extracellular structural proteins with at least 26 genetically distinct chains and are the most abundant fibrous protein within the ECM, accounting for up to two thirds of articular cartilage dry mass (Frantz et al., 2010, Luo et al., 2017, Eyre, 2004). Type II collagen represents 80 - 95% of collagen subtypes with the remaining subtypes identified as I, V, VI, IX, XI. Type II collagen consists of three identical α1 (II) polypeptide chains wound together into a left handed helical pattern and then further wound around each other into right handed helices to produce chains of approximately 300 nm length, 1.5 nm diameter and 1000 amino acids (**Figure 1.2**) (Gelse, 2003, Wu et al., 1987). The collagen network contributes to the tensile strength and torsional stability of the ECM but also help to regulate cell adhesion and support tissue development. This is achieved by interaction between collagens and specific receptors such as glycoprotein VI and integrins.

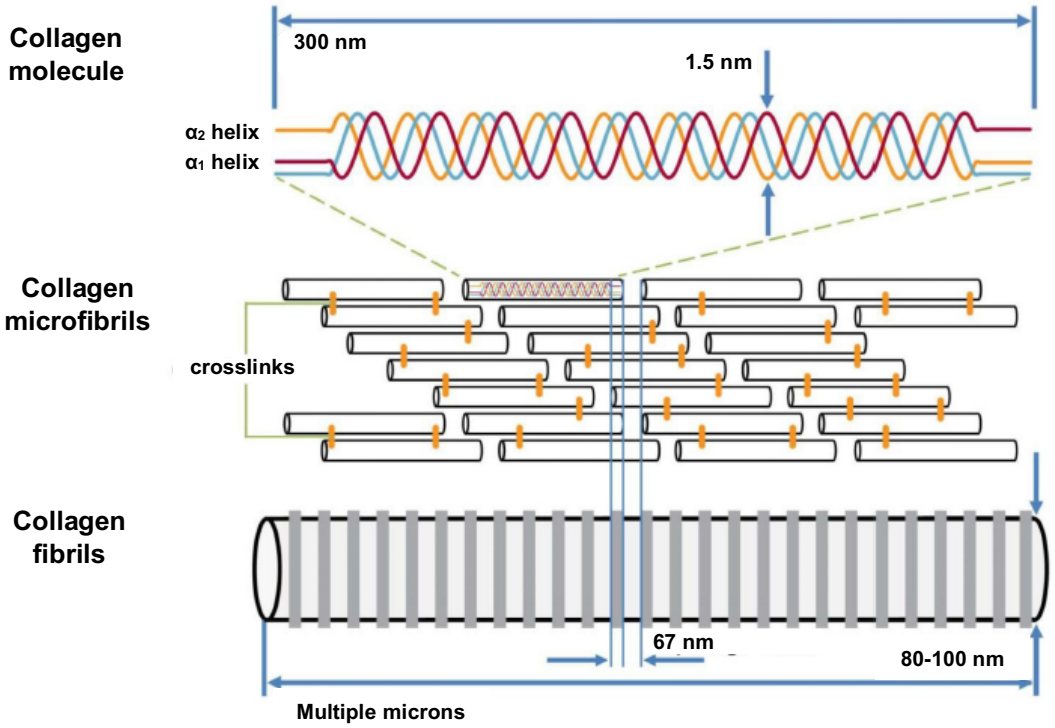

Figure 1.2: Collagen fibril construction. *Each individual collagen helix is arranged in a staggered array with 40 nm gaps between N and C termini of other linear helices to form collagen fibrils. Adapted from (Schwarcz et al., 2017).*

In the initial stages of collagen synthesis, since most genes that encode collagen follow a complex exon-intron pattern, several messenger ribonucleic acid (mRNA) species can be identified, transcribed at different initiation sites and alternatively spliced; a feature first described in type II collagen (Ryan MC, 1990). The events of collagen synthesis within the cell are summarised in **Figure 1.3**. Firstly, the pre-mRNA is capped at its 5' end with polyadenylation occurring at the 3' end whereby it is termed 'mature mRNA'. This mature mRNA is then delivered to the cytoplasm by ribosome binding for translation within the rough endoplasmic reticulum (RER). Once the signal peptide is removed from the N terminus via single peptidase, the procollagen molecules are modified post translationally; for example hydroxyprolation of lysine and proline residues. This post translation modification is essential for the collagen fibrils ability to form stable intramolecular hydrogen bonds which can help crosslinking of other collagen molecules and the attachment of carbohydrate chains. C-propeptide allows the assembly of the 3 α chains together, allowing the C terminals of the chains to align and initiate the triple helix formation up to the N terminus. Heat hock proteins such as HSP47 are essential to ensure correct folding of the procollagen chains (Clarke et al., 1991) whilst inter/intra disulphide bonds between the molecules are regulated by protein disulphide isomerase (Lang et al., 1987). Once the

procollagen structure has been assembled, the structure is transferred to the Golgi apparatus where it can be transported to the extracellular space via secretory vesicles (**Figure 1.3**). Here, C and N terminal propeptides are cleaved via N proteinase and C proteinase. Once complete, the collagen fibrils then self-assemble based on hydrophobic and electrostatic interactions of the collagen monomers which are stabilised by further covalent crosslinks.

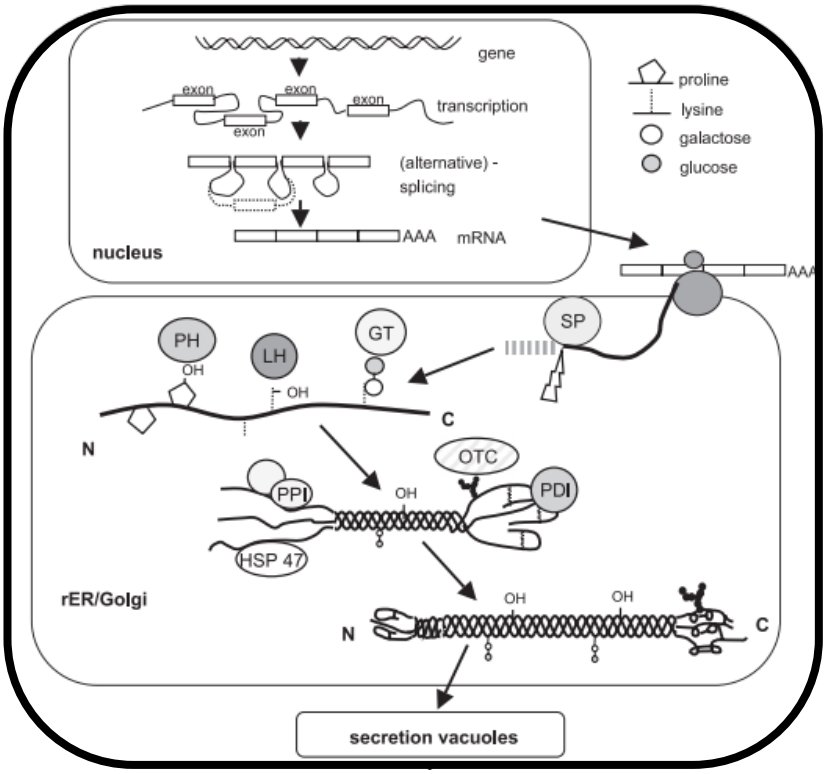

Figure 1.3: Collagen synthesis inside the cell. *Collagen gene expression triggers the transcription of messenger RNA and release from the nucleus. Subsequently, it is modified within the rough endoplasmic reticulum (RER) before packaging within the Golgi apparatus into secretion vacuoles which are released into the pericellular matrix where they can be further modified and reside or diffuse to other regions of the tissue. Figure from (Gelse, 2003).*

1.2.2 Proteoglycans

Proteoglycans consist of glycosaminoglycan (GAG) side chains covalently bound around a protein core. In cartilage, proteoglycans can be broadly divided into three families based on their core proteins, composition and localisation. These families are:

- Small leucine rich proteoglycans (SLRPs) such as decorin + biglycan (class 1), lumican + fibromodulin (class 2) and epiphycan (class 3).
- Lecticans such as aggrecan, versican and perlecan.
- Cell surface proteins such as betaglycan, glypican and syndecan 4.

Importantly, proteoglycans possess covalently attached highly anionic GAG (Yanagishita M., 1993). The sulfate and carboxyl groups on the GAG chains can become ionised due to the distance between the charged groups; approximately 1 - 1.5 nm. A strong opposite charge repulsion is produced which attracts water molecules into the tissue and causes the cartilage tissue to swell. This effect contributes to the compressive stiffness of cartilage up to as much as 50%.

Aggrecan is the predominant proteoglycan found within hyaline cartilage consisting of covalently attached chondroitin sulfate and keratin sulfate surrounding a core protein structure in a bottle brush configuration (**Figure 1.4**). However, they do not exist on their own but rather form aggregates based around a central filament of hyaluronan (HA) via non-covalent attachments stabilised by link protein. HA is synthesised within the cytosol of the cell aided by hyaluronan synthase at the plasma membrane where it is released from the cell directly to the pericellular environment of the chondrocyte (Hubbard et al., 2012, Knudson et al., 2000, Knudson and Knudson, 2001). Once bound by link protein, this unique connection between aggrecan and hyaluronan is non-dissociating and non-displaceable under physiological conditions and as a result represents the principal load bearing proteoglycan of cartilage (Wight et al., 2010). The aggrecan gene is made up of 19 exons, with different exons encoding different regions of the aggrecan structure (G1: exons 3 - 6, G2: 8 - 10 and G3: 13 - 19) (Roughley and Mort, 2014). The core protein of aggrecan is made up of 3 globular regions that are responsible for different interactions. The G1 region is responsible for the interaction between HA and link protein whilst the G3 region plays more of a trafficking function. Between the G2 and G3 domains, glycosaminoglycans are able to bind depending on the domains exposed (Zheng et al., 1998). For example, immediately after the G2 domain is a proline-serine sequence which can attach O-linked oligosaccharides such as those of the linkage region on the GAG keratin sulfate. Following this region is the chondroitin sulfate domain where up to 100 chondroitin sulfate chains can bind. Importantly for cartilage disease, aggrecan possesses domains that are sensitive to protease cleavage (between G1 and G2). Once cleaved, these fragments contain neo-epitopes such as a distinegrin and metalloproteinase with thrombospondin motifs-1 (ADAMTS-1), matrix metalloproteinase-8 (MMP-8) and ADAMTS-4 which have been implicated in osteoarthritis (OA) pathogenesis (Knudson and Knudson, 2001).

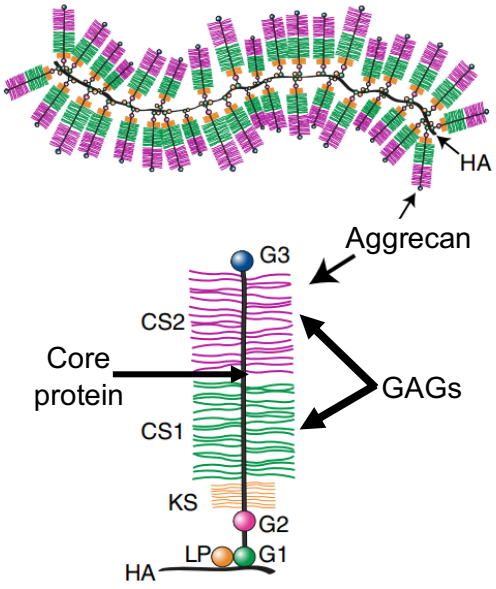

Figure 1.4: Aggrecan monomer structure aids the formation of large aggregates. *Aggrecan globular regions (G1, G2 and G3) are bound around a core protein. Link protein (LP) binds the G1 domain to hyaluronan (HA) and stabilises the structure. Different glycosaminoglycans can bind between G2 and G3 domains creating an overall mass of 1 - 4 x 10^6 Da. Adapted from (Roughley and Mort, 2014).*

1.3 Zonal arrangement of cartilage

The composition of cartilage varies with depth and can be categorised into four zones called the superficial, transitional, deep and calcified layer (**Figure 1.5**) (Hardin et al., 2015, Fox et al., 2009, Mow et al., 1992). The superficial zone has an outer layer called the *lamina splendens* and consists of densely packed collagen fibres within a gel like ECM with fibres orientated parallel to the articulating surface (Rexwinkle et al., 2017). The superficial zone protects the tissue from shear stress, aided by type II and type IX collagen that align parallel to the articular surface in a tangential network arrangement. The chondrocytes within this layer have an ellipsoidal morphology with low proteoglycan levels (Wong et al., 1996).

In the middle layer or transitional zone, the collagen fibrils are thicker and the water content within the layer is lower when compared to the superficial layer. The chondrocytes have a rounded morphology with low cell density and a high proteoglycan content. The collagen fibres are aligned obliquely to the surface in an intersecting transitional network which contributes to the resistance to compressive and shear forces. Below the transitional layer lies the deep zone which gives the tissue its greatest resistance to compressive force primarily due to the perpendicular alignment of collagen fibres and columnar orientation of the chondrocytes to the articular surface. Here the collagen fibres have the largest diameter with an average of 108 nm compared to 55.8 nm and 87.5 nm in the superficial and transitional zones respectively, the greatest level of proteoglycan components and the lowest volume of water (Changoor et al., 2011, Schenk et al., 1986). Beneath this layer is what is known as the deep calcified zone which represents a transition

between the deformable cartilage and the hard bone below, represented by an undulating tidemark (Mow et al., 1999, Pearle et al., 2005). The calcified zone offers a much denser mineralised region than that of the subchondral bone beneath it in order to uniquely transfer and distribute the mechanical forces experienced during physiological loading which is attenuated by the overlying cartilage (Goldring and Goldring, 2016).

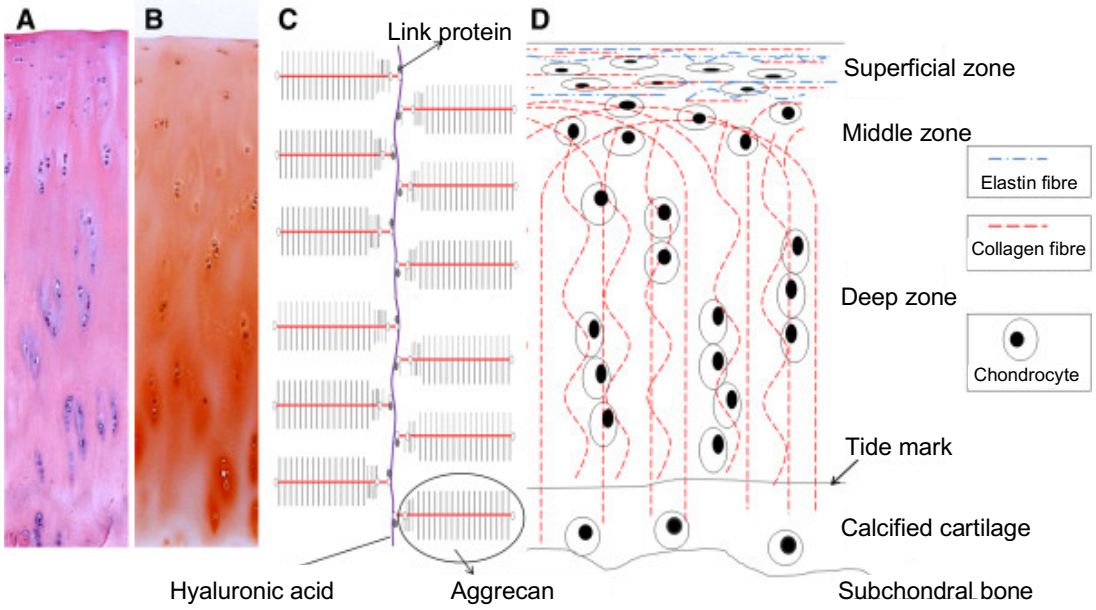

Figure 1.5: Zonal and regional constitution of articular cartilage. *H&E (**A**) and Safranin O (**B**) staining demonstrate how proteoglycan content and cell distribution change with cartilage depth. **D**) Collagen and elastin fibre arrangement change with tissue depth (dashed lines). Figure from (Bo et al., 2014).*

There are also regional divisions based on the proximity to the chondrocyte that are responsible for signal transduction in the pericellular matrix and mechanical stress protection in the territorial matrix and the inter-territorial zone (**Figure 1.6**). The pericellular matrix consists of type VI collagen and high concentrations of proteoglycans which are tightly woven around the chondrocyte to form the basic metabolic unit of hyaline cartilage; the chondron (Poole, 1997, Wang et al., 2008). The territorial matrix consists of thicker collagen fibres in an effort to protect the cells from loading whilst the inter-territorial zone contains the thickest collagen fibres responsible for the visual differences observed between collagen fibre alignments when looking at histological sections. Chondron shape, size and orientation are dependent on the zone where they are observed with chondrons located within the superficial layers taking on a much more discoidal shape compared to those within the deep zone where they are perpendicular to the articular surface and much more rounded (Thompson, 2013). The chondrocyte is able to interact with the pericellular matrix via cell surface integrins (Poole, 1997). However, the pericellular matrix

itself is important to prevent resting chondrocytes from interacting abnormally with components present in the inter-territorial and territorial zones. In doing so, the cells are maintained in their differentiated, low turnover state vital for cartilage homeostasis.

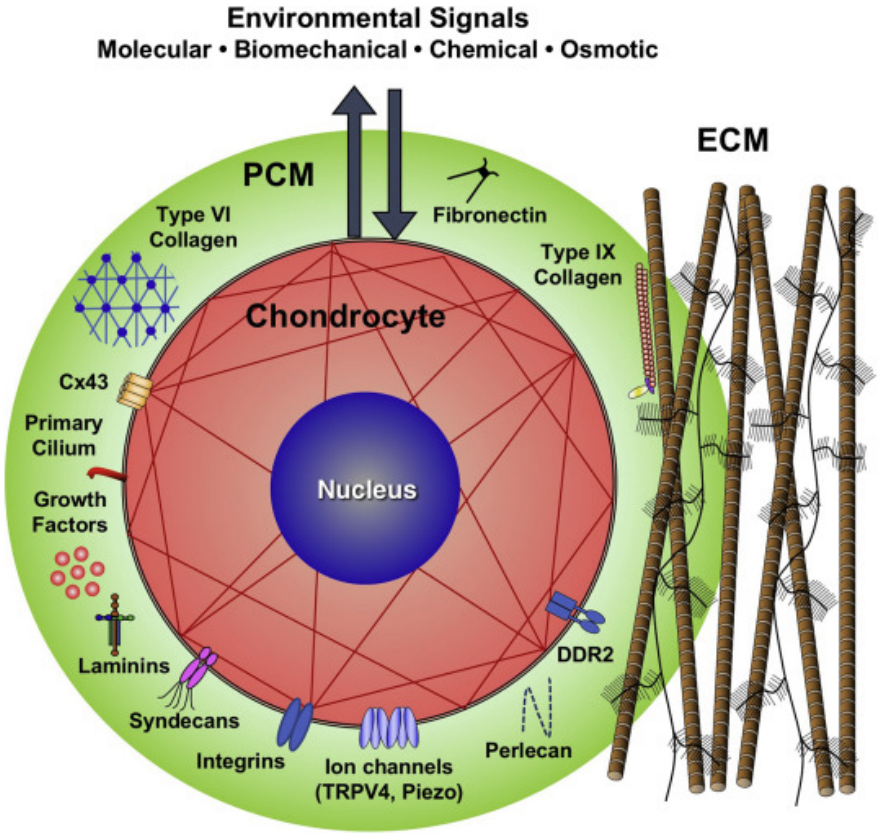

Figure 1.6: Schematic showing the interactions of the pericellular matrix with ECM proteins and chondrocytes. *Pericellular matrix shields the chondrocyte from overstimulation in response to growth factor stimulation, integrin stimulation and ionic channels. In this way, the pericellular matrix is integral for maintaining cartilage homeostasis and ECM tissue remodelling. Figure from (Guilak et al., 2018).*

1.4 Chondrogenic differentiation in development

The process of chondrogenesis is a multistep complex pathway with the molecular events largely contradictory and unclear. Mouse embryonic stem cells are commonly used to study the differentiation processes because the *in vitro* differentiation process closely recapitulates what occurs during early human embryonic development. In broad strokes, lateral plate mesoderm segments into structures called somites whereby the mesenchymal stem cells (MSCs) commit to the chondrogenic lineage within the vertebral skeleton in a process referred to as endochondral bone formation (**Figure 1.7**). During this phase, the mesenchymal condensates formed from MSC aggregation begin to express a range of ECM and cell adhesion molecules including collagen type IIa, N-cadherin, N-cam, tenascin C and most importantly the transcription factor known as SOX-9. This gives rise to what is known as the *cartilage primordia,* with the cells taking on a round phenotype; indicative of immature chondrocytes.

Within the central region of the *cartilage primordia* the cells undergo further maturation and withdraw from the cell cycle becoming enlarged and begin to mineralise; indicating a hypertrophic post mitotic progression. On either side to this area, chondrocytes start to proliferate in a unidirectional manner along the longitudinal axis of the long bone. As the cartilage grows longitudinally, hypertrophic chondrocytes are gradually deposited. These hypertrophic chondrocytes then differentiate further to contribute to the primary ossification centre whereby vascular invasion can occur and bone eventually forms. Mature chondrocytes are then restricted to the bone surface (epiphysis) to become what is known as the growth plate. At puberty, an increase in the number of apoptotic events within the growth plate gradually causes lengthening of the long bone to decrease as the growth plate is slowly replaced with bone until only a surface layer of cartilage lining the bone is left.

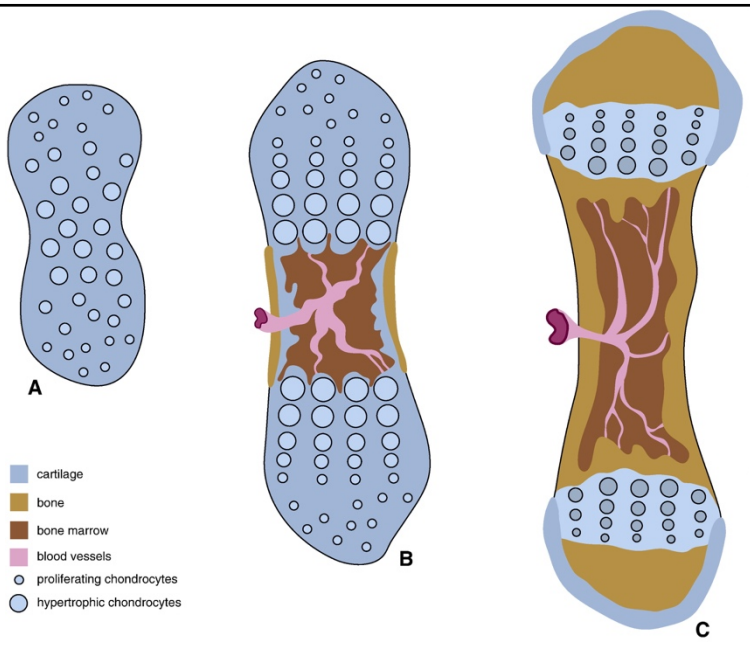

Figure 1.7: Endochondral bone formation. A: *Mesenchymal stem cells proliferate and form condensates which differentiate into chondrocytes and an early analgen to the eventual bone structure.* ***B****: Within the centre of the structure some chondrocytes undergo further maturation which sees an increased proliferation occur before the cell's withdrawal from the cell cycle, indicating hypertrophy. Vascular invasion forms a marrow cavity. Cartilage resorbtion and osteoid deposition begins.* ***C****: Columns of chondrocytes in the growth plate begin to proliferate outwards, become hypertrophic and eventually mineralise their ECM which gradually extends the bone structure. The mineralised ECM is then replaced with new bone over time until the growth plate fuses. Figure from (Teixeira et al., 2008).*

It is in these different regions of the developing bone where the distinct differences in chondrocyte maturation become evident as a result of complex interactions between hormones, growth factors and other signals. This is most notably seen in regard to the changes in gene expression that occur (**Figure 1.8**). Immature chondrocytes express key transcription factors SOX-5, SOX-6, SOX-9, COL2a1 and aggrecan. Mature chondrocytes then begin to also express an alternate splice form of type 2 collagen known as COL2b1 as well as fibroblast growth factor receptor 3 (FGFR3) at low levels. Pre-hypertrophic chondrocytes begin to express markers and peptides such as parathyroid hormone related peptide 1 (Pth1r), alkaline phosphatase (ALP), Indian hedgehog (Ihh), Runx2 and Osterix further aiding differentiation and future mineralisation which controls bone growth (Hegert et al., 2002). Early hypertrophic chondrocytes express COL10a1 with a loss of the transcription factors associated with immature chondrocytes. Late stage hypertrophic chondrocytes then lose expression of COL10a1 and begin to express vascular endothelial growth factor-A (VEGF-A) and matrix metalloproteinase 13 (MMP-13) which indicate

their transference into an osteoblast precursor which work together with osteoclasts to help remodel bone and enhance vascularisation. Terminally differentiated hypertrophic chondrocytes also express MMP-13 to control degradation of the cartilage matrix required for creation of the bone marrow space. Despite the broad knowledge already achieved in this area, the control mechanisms which govern these gene expression changes are still not completely understood. Investigations into events where this process goes wrong enable us to further understand and decipher the complex events that are occurring. One important factor which has gained considerable attention regarding its role as an important regulator of endochondral ossification and abnormal development is C-natriuretic peptide (CNP). The significance of CNP in endochondral bone formation and in cartilage tissue homeostasis is described in further detail in **Chapter 1.9**.

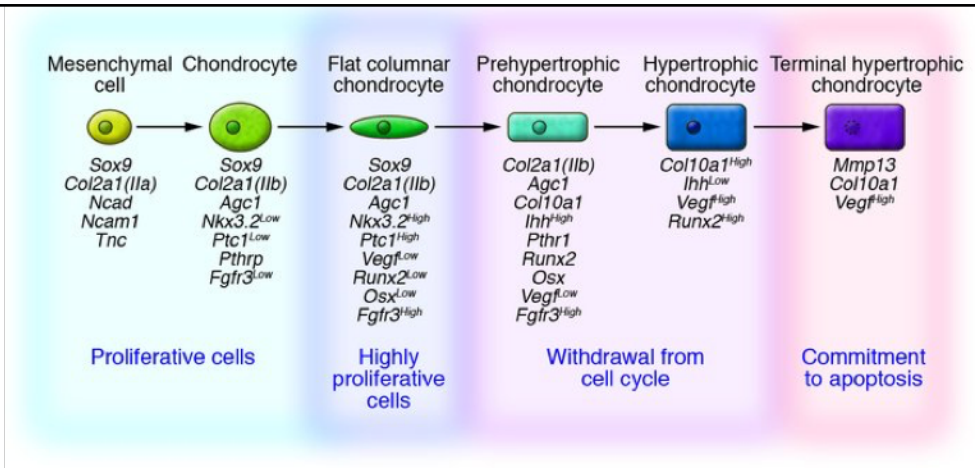

Figure 1.8: Changes in gene expression with chondrocyte maturation. *Chondrocytes undergo extensive genetic changes as they develop to fulfil specific roles within the developing bone. Chondrocytes maintain SOX-9 gene expression for ECM production. However, SOX-9 expression is lost by hypertrophic chondrocytes and osteogenic cells. Figure from (Zuscik et al., 2008).*

1.5 Osteoarthritis

Osteoarthritis is a progressive degenerative joint disease characterised by the breakdown of articular cartilage. This is a different disease to that of rheumatoid arthritis (RA) which is defined as an autoimmune condition characterised by chronic inflammation of multiple synovial joints. The risk of developing OA increases with age with over half of people over the age of 75 seeking treatment for OA in the UK (Arthritis Research UK, 2013). Geriatric individuals or those who live sedentary lifestyles due to obesity, joint abnormalities, occupation or disability are primarily affected by this disease. Overweight (with an average BMI of 28.8) and obese (with an average BMI of 31.0) people are 2.5 and 4.6 times more likely respectively to develop OA relative to those of a normal body weight (Huaqing and Changhong, 2015, Kearns et al., 2014, National Joint Registry, 2017). 4.11 million (18.2%) adults who are aged over 45 in England have OA affecting the knee, with an estimated 8.75 million (33% of the UK population) seeking treatment for OA (Arthritis Research UK, 2018). Treating the most common forms of OA along with rheumatoid arthritis (RA) costs the UK's national health service £10.2 billion in direct costs (healthcare prescriptions and home care), whilst over the next decade the total cost of healthcare for this disease is estimated to reach £118.6 billion (York Health Economics, 2017). In terms of the UK economy, the cost attributed to the number of working days lost to OA is estimated at £2.58 billion in 2017, with that number increasing to £3.43 billion by 2030 (York Health Economics, 2017). A sex difference is also present (**Figure 1.9**), with women accounting for 60% of knee replacements in the UK, of which 90% were due to OA (National Joint Registry, 2017).

Figure 1.9: Effect of age on osteoarthritis incidence in the UK. *Each figure represents 1 million people with orange indicating OA sufferers. Figure from (Arthritis Research UK, 2013).*

1.5.1 Mechanisms/pathophysiology

Joint tissue integrity can be affected either through an acute injury or progressively over time via cell/matrix derived factors that result in an alteration of composition, structure and material properties of the tissue. Whilst individual issues can be selectively affected, due to the intimate functional association between tissues within the articular joint, OA is commonly accepted as a disease that affects all joint structures (Loeser et al., 2012). As no single cause of the disease has been identified to date, studies in animals and analysis of specimens from patients suffering from OA have enabled scientists to establish a general sequence of pathological progression (**Figure 1.10 and 1.11**).

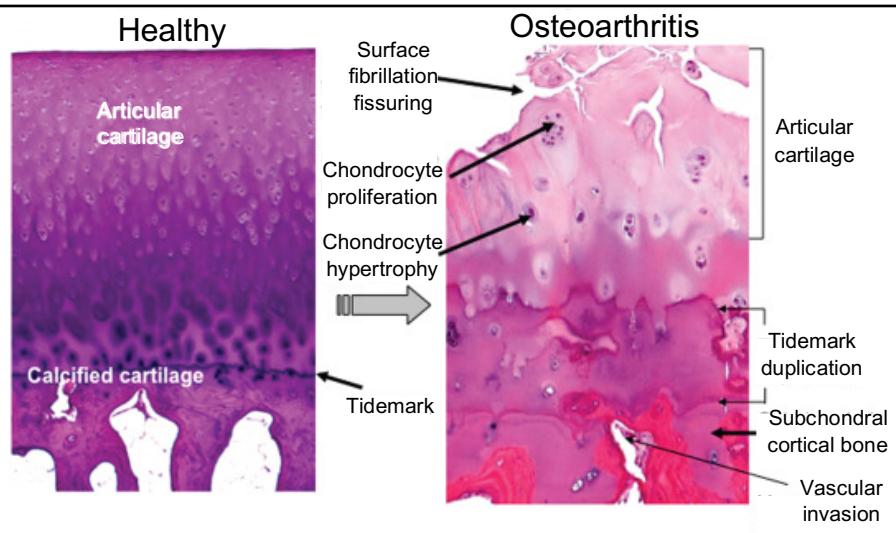

Figure 1.10: Characteristics of damage to cartilage during osteoarthritis. *Osteoarthritic cartilage contains lesional areas in which the tissue has been degraded. The tissue is also much more yellow in appearance than younger cartilage although this is commonly observed as cartilage increases with age. The loss of cartilage in load bearing areas of the tissue causes significant discomfort for the patient when performing basic movements. Figure from (Goldring et al., 2016).*

Initially, changes to the water content of articular cartilage are observed due to a loss of proteoglycans within the tissue resulting in a swelling of the ECM (**Figure 1.11**). This loss of proteoglycans is mediated by aggrecanses of the ADAMTS family which are responsible for the cleavage of the aggrecan core protein. This results in a disruption of interactions between aggrecan and surrounding collagen networks making them more susceptible to degradation by MMPs or by physical forces. Fibrillations within the superficial layer start to form which progress to deep fissures as cartilage fragments exfoliate, delaminate and ultimately result in the exposure of the calcified cartilage and subchondral bone layers. Duplication of the tidemark, which separates calcified cartilage from underlying articular chondrocytes, occurs with the zone of

calcified cartilage gradually expanding and replacing the overlying articular cartilage. Microcracks that form at the osteochondral junctional are penetrated by vascular elements, sympathetic and sensory nerves. Bone then forms around these channels resulting in a resurgence of the endochondral ossification process.

Chondrocytes themselves undergo dramatic phenotypic changes throughout the progression of OA attributed to abnormal mechanical loading which both directly damages the cells themselves but also alters chondrocyte function through interaction with their cell surface mechanoreceptors (Goldring and Goldring, 2016). Chondrocytes initially increase their ECM synthesis activity in an attempt to repair the developing damage as shown by an increase in proteoglycan staining around cells during early stage OA (Lorenzo et al., 2004). However, the disruption of the chondrocyte pericellular matrix deregulates chondrocyte function via surface receptors integrins and discoidin domain receptors (DDR2) interaction with surrounding ECM. As the ECM becomes more depleted, chondrocytes appear in clonal clusters suggesting that a shift in the chondrocyte low turnover rate has occurred resulting in proliferation. However, at late stages of OA chondrocyte density decreases, likely a result of apoptotic events indicated by the presence of cell membrane 'ghosts' and fragmented chondrocyte nuclei. Of the chondrocytes that remain, an increased number demonstrate features of a senescent associated secretory phenotype. This is characterised by the production of MMPs, reactive oxygen species (ROS), angiogenic factors and pro-inflammatory cytokines which aid in the endochondral ossification process. To redress this imbalance, an increase in 'tissue inhibitor of MMPs' (TIMPs) is observed but they are insufficient to match the catabolic processes resulting in the typical cracking and fissuring of the cartilage associated with the disease.

The breakdown of the ECM, as a result of the degradative enzyme release from chondrocytes, also results in the production of cartilage matrix breakdown products such as damage associated molecular patterns (DAMPS) and alarmins. These products can directly affect chondrocyte function thorough their surface receptors but are also capable of inducing inflammation within nearby synovial tissue. Synovitis induction results in hyperplasia and perivascular infiltration of T and B lymphocytes which themselves produce pro-inflammatory products (Goldring, 2010, Man and Mologhianu, 2014). The release of such pro-inflammatory products can then feedback to the remaining chondrocytes and enhance their catabolic state; essentially forming a positive feedback loop. In terms of subchondral bone changes, cortical plate

thickness and volume increases are observed whilst subchondral trabecular bone demonstrates marked architectural changes. Bone turnover is directly affected, resulting in changes to the mineralisation of the bone and its ability to deform under load. Osteophyte and bone cyst formation within the tissue eventually leads to flattening and deformation of the subchondral articular contour resulting in bone attrition (**Figure 1.11**). In areas of denuded cartilage, bone marrow lesions are common since the protection offered by the overlying cartilage to distribute mechanical forces is lost leading to excessive loading of the subchondral bone (Madry et al., 2010).

Whilst OA is often regarded as a non-inflammatory disease, there remains a large number of animal and human studies which indicate that treatments targeting pro-inflammatory cytokines and inflammation in joints have positive effects. IL-1β and TNFα are considered the main pro-inflammatory cytokines involved in OA by driving cartilage destruction and inflammatory cascades respectively. Sources for these cytokines are abundant as they are produced by chondrocytes, osteoblasts, synovial tissues and mononuclear cells. Detectable increases in IL-1β and TNFα have been shown in the synovial fluids, subchondral bone and cartilage of human joints (Saha et al., 1999). TNFα also can induce osteoclastic bone resorption *in vitro*, which may be responsible for subchondral bone remodelling (Bertolini et al., 1986)

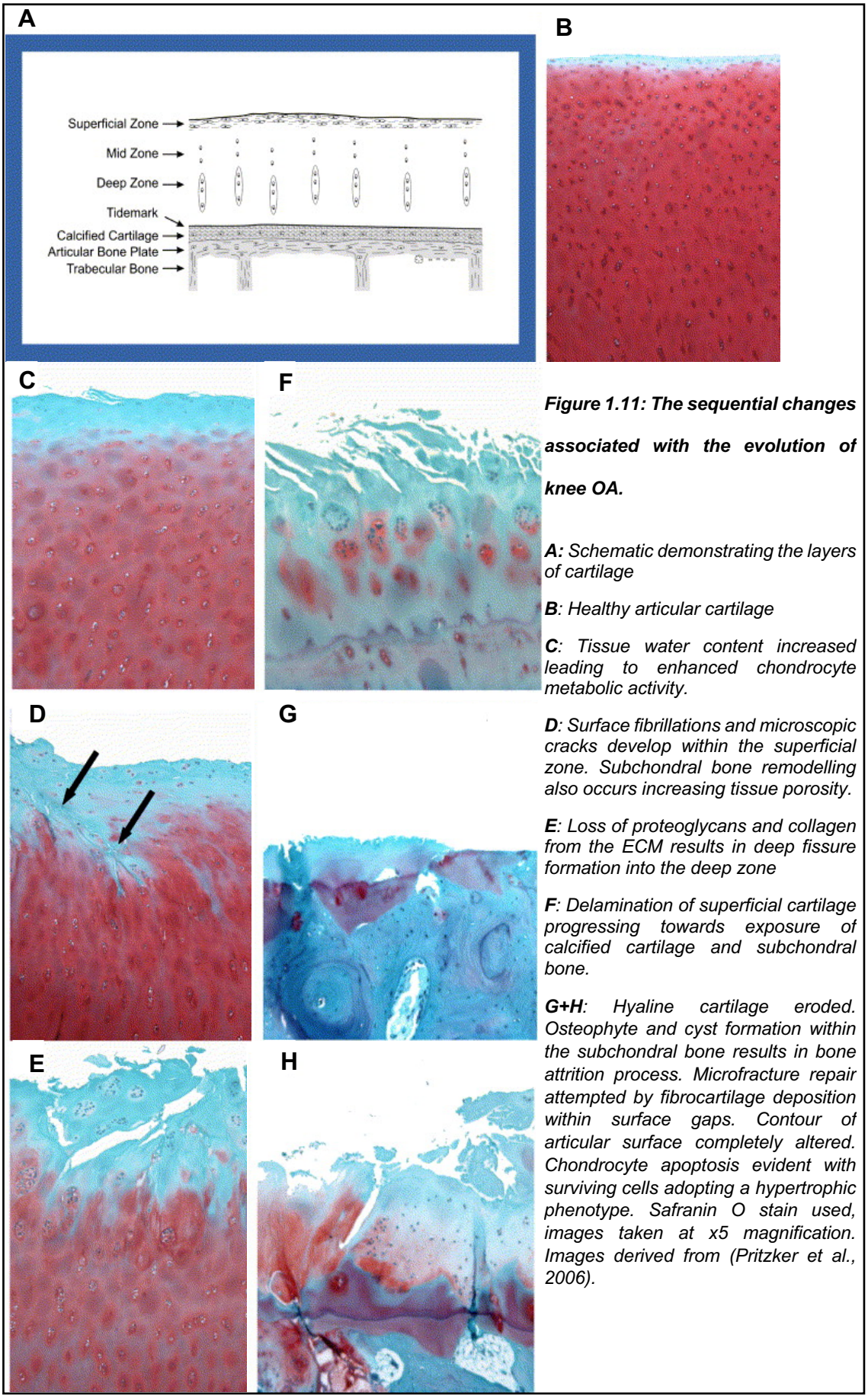

Figure 1.11: The sequential changes associated with the evolution of knee OA.

A: *Schematic demonstrating the layers of cartilage*

B*: Healthy articular cartilage*

C*: Tissue water content increased leading to enhanced chondrocyte metabolic activity.*

D*: Surface fibrillations and microscopic cracks develop within the superficial zone. Subchondral bone remodelling also occurs increasing tissue porosity.*

E*: Loss of proteoglycans and collagen from the ECM results in deep fissure formation into the deep zone*

F*: Delamination of superficial cartilage progressing towards exposure of calcified cartilage and subchondral bone.*

G+H*: Hyaline cartilage eroded. Osteophyte and cyst formation within the subchondral bone results in bone attrition process. Microfracture repair attempted by fibrocartilage deposition within surface gaps. Contour of articular surface completely altered. Chondrocyte apoptosis evident with surviving cells adopting a hypertrophic phenotype. Safranin O stain used, images taken at x5 magnification. Images derived from (Pritzker et al., 2006).*

1.6 Treatment strategies

As diseases of the joints are painful and affect a growing proportion of the population due to increases in life expectancy, interventions for pain relief and disease-modifying therapy for OA are imperative. However, without a clear understanding of how diseases such as OA are caused, attempts to prevent the disease progression are limited. To this end, the majority of current drug treatments are aimed at delivering pharmacological agents to treat pain and maintain function of the joint. Unfortunately, due to the avascular nature and density of the tissue, the delivery of therapeutic agents to provide pain relief or disease treatment are extremely difficult. Also, evaluation of non-surgical interventions often suffer from poor methodology and small sample sizes (Lue et al., 2017). Despite this, there is increasing success in using agents to modify the disease, enhance the native cells resistance to disease progression or the generation of healthy tissue within the laboratory.

1.6.1 Cytokine and receptor antagonists

The presence of TNFα has also been associated with an inhibition of proteoglycan, link protein and type II collagen synthesis (Saklatvala, 1986, Seguin and Bernier, 2003). Indeed, an overproduction of TNFα also results in upregulation of MMP expression (Dayer et al., 1985). TNFα has been utilised successfully as a key target for the treatment of rheumatoid arthritis (RA) due to its high level of expression in RA affected joints (Rau, 2002). Further to this, levels of TNFα have also been shown to be elevated in the synovial fluid and serum of OA affected joints compared to healthy individuals (Hulejova et al., 2007, Smith et al., 1997). However, despite the successful use of anti TNFα therapeutics for RA such as adalimumab, the effect on OA affected joints have provided generally disappointing results. Further to this, the outcomes of the studies have generally focused on pain relief rather than identifying the effect of the drug on disease progression. For example, an open label Phase I/II trial of adalimumab published in 2012 by Maksymowych et al, showed significant improvements in joint pain through Western Ontario and McMaster Universities Osteoarthritis index (WOMAC) assessment, yet assessments such as joint space narrowing (JSN) to determine whether the treatment actually affects disease progression were not performed (Maksymowych et al., 2012). Therefore, further larger studies with JSN incorporated into the study assessments and a homogenous OA patient cohort would be desirable to further investigate the use of adalimumab and other anti TNFα treatments for OA.

Elevated levels of IL-1β are often observed in the synovial fluid of humans and animal models of OA. Since IL-1β stimulates the production of matrix breakdown agents such as MMPs whilst also causing a reduction in proteoglycan synthesis, it is likely that targeting IL-1β production should improve OA symptoms and reduce progression. However, whilst IL-1 receptor antagonists (IL-1Ra) have shown improvements in animal models of OA in terms of cartilage preservation, these effects in humans trials have been difficult to replicate or sustain (Chevalier et al., 2009, Cohen et al., 2011). One of the successful human clinical trials targeting IL-1β was the Canakinumab Anti Inflammatory Thrombosis Outcomes Study (CANTOS) published in 2017. Post hoc analysis of the results from this clinical study showed that incidence rates of total knee replacements, total hip replacements and OA symptoms were reduced upon treatment with different doses of the human antibody canakinumab which targets the IL-1β pathway compared to placebo (Ridker et al., 2017). Further responder analysis of this data is ongoing. One explanation as to why many human trials have difficulty demonstrating an effect of a particular treatment like IL-1β targeting is due to the method of assessing pain in OA patients. Since pain is a subjective method of assessment that differs between individuals, determining whether the effect of a treatment is having a significant effect is extremely difficult and may contribute to the lack of statistical differences observed in many of these studies. Clinical safety of these drugs also needs to be carefully controlled since one fully human monoclonal antibody investigated as an antagonist of IL-1 receptor type I was also associated with a decrease in neutrophil count which could have significant clinical implications for patients if not localised to the articular joint (Hernandez et al., 2015). IL-1 Ra therefore are likely most useful for patients with severe OA, whereby the pain relief and structural benefits offered by the treatments are most desirable.

Nerve growth factor (NGF) is a key player in modulating the expression of pain related substances released peripherally and centrally within the nervous system whilst also sensitising nociceptors adjacent to areas of inflammation (Shang et al., 2017). Inflammatory markers such as IL-1β and mechanical overloading are known to increase the levels of NGF whilst increased levels of NGF are also detected within the synovial fluid of diseased OA joints compared to non-diseased joints. Together this evidence serves to suggest NGF as a potential target for disease treatment (Aloe et al., 1992). Selective antibodies against NGF such as tanezumab have demonstrated significant effects at reducing OA associated knee pain, physical function and stiffness in 450 patient study compared to placebo (Lane et al., 2010). However, it has also been

associated with significant safety issues including osteonecrosis, rapidly progressive and destructive OA and subchondral bone fractures (Food and Administration 2015). The exact cause of these effects is not known currently. However, it has been associated with several different explanations including the pharmacological profile of the drug, unknown effects of inhibiting of the NGF pathway or the fact that the pain relief offered allowed the patients to utilise their joints more intensively than before which results in greater wear and tear of the already damaged cartilage present. Its efficacy and ability to improve pain and function of OA patients means that tanezumab must be studied more intensively.

With the identification of key pathways such as TGF and Wnt/β-catenin signalling pathways in OA, efforts to develop a disease modifying osteoarthritis drug have been approached in earnest. In mouse models, inhibitors of MMP13 and ADAMTS-5 effectively demonstrate a reduction in cartilage destruction progression, ECM production enhancement and a reduction in chondrocyte apoptosis (Wang et al., 2013, Chen et al., 2014). Whilst these findings show extreme promise, the inability to reproduce these effects in humans is troubling. MMP inhibition in particular has been linked with musculoskeletal toxicity in humans, restricting its use for clinical application (Krzeski et al., 2007). Since direct inhibition of these targets might cause unintended events, it might be advantageous to try and target upstream effectors or administer directly into the articular joint. For example, syndecan 4 is a regulator of ADAMTS-5 and therefore has potential to prevent its activation and consequently disease progression.

1.6.2 Surgical interventions

There are significant limitations and prolonged clinical trials required to fully evaluate the efficacy of pharmacological interventions. Because of this, other established methods must be utilised. Autologous cell implantation repairs small articular cartilage defects by using enzymes to isolate chondrocytes from biopsy samples of healthy articular cartilage, expanded and then reinjected under an autologous periosteal flap on the defect (Brittberg et al., 1994, Cancedda et al., 2003). The effectiveness of this treatment is disputed and also dependent on sacrificing normal cartilage tissue for harvest which, by the nature of cartilage, will be slow to heal. This also restricts the application of this technique to small OA lesional repair since larger areas of healthy tissue would need to be harvested for larger defects. Surgical procedures such as bone marrow stimulation technique involve breaking subchondral bone to form microfractures which facilitate stem cell infiltration and cartilage deposition for cartilage repair. Yet these defects are typically

repaired with fibrocartilage (collagen type I) which do not possess the same mechanical properties as type II collagen leading to a focal weakness in the tissue. When mechanical forces are reapplied to the joint, these areas are the first to undergo further degeneration. Mosaicplasty involves the harvesting and implantation of cylindrical 'plugs' of bone and cartilage from donor sites which are less weight bearing. In effect, the hyaline cartilage implanted provides a more durable surface than the fibrocartilage often formed by implanted cells that subsequently differentiate or de-differentiate to a fibrocartilage phenotype. However, complications of excessive postoperative bleeding and thromboembolic developments can occur.

The last resort in terms of surgical options is that of total knee replacement surgery (TKR). Over 700,000 TKR are performed every year in the US (Kurtz et al., 2007). However, even with the best man-made bearing surface such as Teflon, the coefficient of friction is much greater than in the normal articular joints (μ0.04 compared to μ0.01) and does not handle load very well resulting in a low wear product but with higher friction bearings. Over time, the body can react to the foreign materials present in the joint and try to break it down, as seen in circumstances where polyethylene wear and metallic debris accumulation is observed. If the reaction by the body is significant enough, granulomatous tissue masses can form which mimic those of a sarcoma (Mavrogenis et al., 2009). The joint would therefore need replacing and tissue masses removed altogether requiring the patient to undergo another intense significant surgery with the associated months of physiotherapy following.

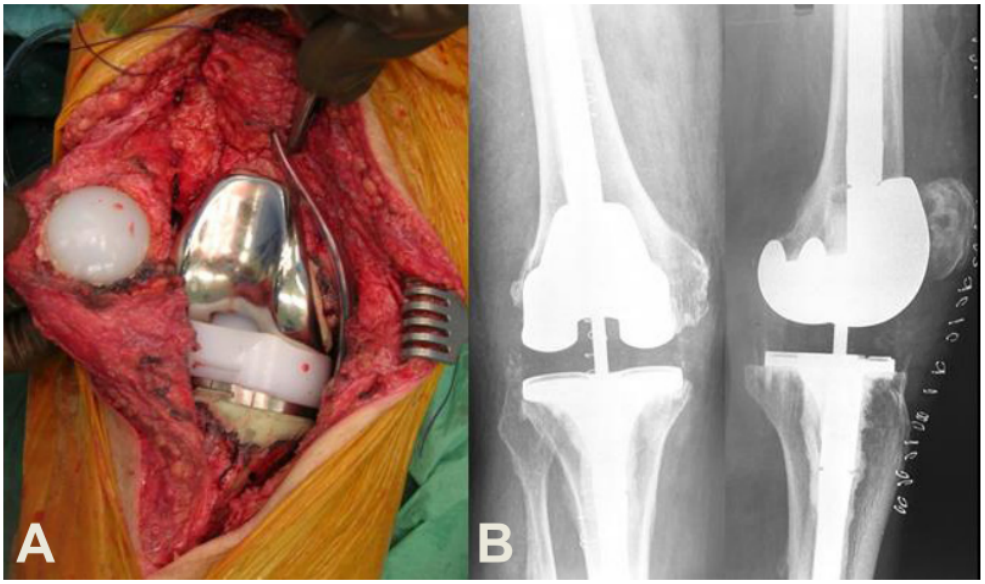

Figure 1.12: **Double tricompartmental knee arthroplasty.** A: The ends of the femur and tibia are removed and replaced with metal components with a plastic spacer between to create a smooth gliding surface. B: Postoperative radiographs of the right knee. Figure from(Mavrogenis et al., 2009).

1.6.3 Cell therapy, gene therapy and tissue engineering technology

In order to work around the pharmacokinetic barriers of drug delivery to the articular joint, the use of gene therapeutics have been investigated and recently approved (Evans et al., 2018). cDNA delivery to cells within the articular joint encode therapeutic products (such as IL-1Ra) which can allow endogenous cells to synthesise therapeutic gene products on a local level. Since turnover of chondrocytes is low, genetic manipulation has the potential to produce long term gene expression compared with those which have a high turnover. One main area of concern regarding gene therapy is possible insertional mutagenesis and tumorigenesis especially in regard to a non-life-threatening disease such as OA. However, recently advances have been made to use allogenic cells that have been irradiated to prevent cell division whilst maintaining growth factor synthesis. The types of viruses used are also a consideration since some viruses are too large to penetrate the ECM *in situ*. However, adeno-associated viruses (AAV) are a popular candidate as they demonstrate low immunogenicity, effectiveness and good safety. However, whilst the advances are promising, there remains a need to monitor and evaluate the results of clinical trials before it can be widely accepted. Only 2 gene therapies have been approved for non-lethal disease treatment in the world as of 2018 (Evans et al., 2018). Genetically engineered chondrocytes transduced to express $TGF\beta_1$ completed phase II trials within the last 3 years whereby the results showed significant improvements to international knee documentation committee score (IKDC), visual analogue scale score (VAS) and pain severity (Cherian et al., 2015). sc-rAAV2.5IL-1Ra is awaiting Phase 1 trial following safety assessment in a mono-iodoacetate-induced OA rat model (Wang et al., 2016). Whilst this technology would be beneficial to those in early stages of cartilage disease whereby lesional areas are small, larger defects or late stage progression OA, it will still require extensive cell culture to provide sufficient cells to implant.

Although surgical interventions such as total knee replacements are commonplace now, the risk of surgical complications cannot be completely eradicated. Cartilage repair using cell-based therapies offers a long-term strategy for the repair and regeneration of cartilage destruction caused by OA, stopping or reversing the progression of the disease as a result. Until now, autologous chondrocyte transplantation is the only approved cellular based therapy that can be used for cartilage restoration (Brittberg et al., 2003, Brittberg et al., 1994). However, the limitations in expanding chondrocytes *ex vivo* and the damage to the donor site required for this technique

limits its utility as a treatment for OA patients. Several seed options are available for use including chondrocytes (Liu et al., 2002), fibroblasts (Zhao et al., 2009), mesenchymal stem cells (MSCs) and induced pluripotent stem cells (iPSCs) (Lietman, 2016). Still, no consensus exists regarding the optimal cell source for orthopaedic tissue engineering application.

Stem cell therapy has become an increasingly popular area of investigation for several reasons. Stem cells are able to differentiate into cartilage tissue, proliferate extensively *in vitro*, require no biopsy of cartilage tissue and demonstrate paracrine release of growth factors and cytokines beneficial to immunoregulation and reduction in inflammatory processes that play an important role in disease progression. Whilst the desired mechanism of action for this treatment is stem cell engraftment into damaged articular cartilage and direct differentiation, the mechanism of action has actually been poorly defined. Despite this, the field is advancing rapidly as several case series and clinically controlled trials have indicated positive result especially in regards to sustained pain relief (Davatchi et al., 2016, Orozco et al., 2013). However, MSC usage specifically has some notable issues. Firstly, the yield of non-committed MSCs from source tissues like bone marrow are quite low. This then requires the significant proliferation and differentiation procedure which is time consuming. MSCs extracted from donor sites can also possess different sub populations. Ultimately MSCs are also capable of differentiating into other lineages in an uncontrolled manner when exposed to inflammatory mediators (Lohan et al., 2014).

An alternative to this is the use of adipose tissue derived MSCs due to their ubiquity and abundance within a mammalian organism. Since these cells can be harvested from the infrapatellar fat pad, they also avoid the implications posed by BM-MSC procurement. One reported example using adipose tissue derived MSCs for OA treatment was performed by Koh et al on a group of 25 patients whereby a significant improvement in WOMAC scores after 2 years when applied with platelet rich plasma was observed (Koh et al., 2013). However, the involvement of the stem cells themselves has been disputed since the group who performed this study also noted that the placebo (in this case platelet rich plasma only) produced the same effect (Koh and Choi, 2012). The main issue currently with assessing cell implantation as a therapy is the small number of case series available. Without larger studies involving prolonged follow up, this technique cannot be effectively applied to more patients than it currently is (Pas et al., 2017). Variation in evidence level of primary studies, inherent bias due to inadequate blinding, high risk

selection bias also does not offer the confidence required to the claims being made by some groups.

Tissue engineering offers an alternative strategy through the seeding of chondrogenic cells within biodegradable scaffolds to produce tissue matching that of native cartilage for defect repair (Langer and Vacanti, 1993). In doing so a tissue engineered product theoretically has the potential to provide consistent clinical results in filling defects and repairing hyaline tissue. In order to be suitable for orthopaedic application, the engineered cartilage must be able to integrate with the healthy cartilage surrounding the defect and the underlying subchondral bone. Mechanical properties that match that of healthy tissue in terms of stable load distribution and mechanotransduction is also an essential requirement to ensure the tissue can survive the biomechanical forces that exists within the joint environment and to avoid strain disparity. Recreation of the complex zonal arrangement of cartilage is also essential to achieve this. Due to these lofty aspirations, no research to date has entirely mimicked these essential properties and structure. In particular, the sheer number of options in terms of cell types, scaffold materials and bioreactor setups has resulted in a lack of consensus regarding the critical components for successful cartilage tissue engineering. This unfortunately has resulted in an inability to move technologies into the clinic, although has not restricted this completely.

Autologous mesenchymal stem cells and chondrocytes to engineer tissues with absorbable biodegradable materials have been described, albeit with varying success (Jungebluth et al., 2012, Behrend et al., 2002). In terms of tissue engineered products, there have been several different materials used and investigated clinically in humans including Biocart™II, Bioseed® C, Cartipatch, MACI, Neocart and NOVOCART. Huang et al. published a comprehensive review of the literature regarding the different materials summarised in **Table 1.1** (Huang et al., 2016). Each scaffold material used is fairly unique, for example a synthetic matrix of polyglactin 910/poly-p-dioxanone fleece is used in the case of Bioseed® C and non-synthetic agarose-alginate hydrogels for Cartipatch. Autologous chondrocytes are used for all of these products, which requires an initial surgery to take place to remove tissue for cell isolation and subsequent *in vitro* expansion before seeding within their respective scaffold materials. Variations in cell density requirements are also observed dependent on the size of the defects they are being used to treat as well as the construct preparation time as seen in the cases of Bioseed® C and

NOVOCART which require only 3 weeks to prepare a construct for implantation whilst Neocart requires 67 days for completion.

Commonalities in surgical procedure are observed as all methods require initial debridement, alteration of the construct material to fit the shape, and attachment in the form of gluing using fibrin gel or suture. Rehabilitation times and methods are also shared, typically beginning with continuous passive motion physiotherapy building up to free walking exercise at the 3-month post op stage. Measurement of clinical benefit outcomes differs between each trial with the different methods of assessment including: WOMAC, International knee documentation committee (IKDC), magnetic resonance observation of cartilage repair tissue (MOCART), knee injury and osteoarthritis outcome score (KOOS), international cartilage repair society (ICRS), IKDC, Lysholm and Noyes, SF36, Tegner, Gillquist, VAS, Cincinnati assessment. Because of this, comparison of the effectiveness of particular products are difficult to make since there is no consensus on the method of assessment. Most importantly these products have primarily been investigated for their use in treating focal defects and osteochondritis dissecans. From these cartilage implant type technologies, there still remains an inability to show significant clinical benefit in comparison to older methodologies such as microfracture and mosaicplasty (**Table 1.1**).

These technologies still cannot treat large defects associated with advanced disease like OA and have limited potential for reconstruction of entire structural units. The complications, safety issues and cost effectiveness of this technology require further development before they can provide distinct clinical gains. More recent research has started looking at the possibility of percutaneous injection. Self-setting cellulose-based hydrogels have previously been investigated in regard to repairing articular cartilage using chondrocytes and MSCs in animal models of OA defects (Vinatier et al., 2009). However, no clinical trials have been performed of this technology at the time of writing.

Table 1.1: Examples of the tissue engineering technologies previously used for clinical OA

Product (patent)	Scaffold	Cell number	Key findings	Reference
Biocart™II (08618258)	Fibrinogen/ HA	500,000/cm^2	Phase I trial (N = 8): For defects up to 8 cm^2 in size with a maximum depth of 5 mm. IKDC score demonstrated improvement at 12-month follow up compared to baseline. Phase I trial (N = 31): For an average defect size of 3.3 cm^2 demonstrated increased IKDC and MOCART scores at 12-month follow up compared to baseline. Phase II: Unavailable currently.	(Nehrer et al., 2008) (Eshed et al., 2012)
Neocart	Type I bovine collagen scaffold	5 - 10 × 10^6 cells/ml	Phase I trial (N = 8): 2 year follow up showed significantly improved pain scores + range of motion compared to baseline. 66% good fill of defects. Phase II (N = 21): 2 year follow up significantly improved KOOS, IKDC, VAS scores compared to microfracture in 9/21 patients. Phase III (N = 245): compared to microfracture ongoing (measurements to be performed KOOS, IKDC and MRI).	(Crawford et al., 2009) (Crawford et al., 2012) (Medicine, 2015c)
Cartipatch	Agarose-alginate hydrogel	10 x 10^7 cells/ml	Phase II trial (N = 17): Multi-center study showed positives results with Cartipatch® treatment. At 2 years follow up, IKDC scores significantly improved compared to baseline. Arthroscope investigation showed normal and nearly normal tissue in 85% of patients but hyaline cartilage detected in only 62% of patients. Phase III (N = 58): Mosaicplasty v Cartipatch showed superior repair quality in mosaicplasty patients at 2 year follow up. Phase III trial comparing Cartipatch to microfracture discontinued.	(Selmi et al., 2008) (Medicine, 2015a) (Medicine, 2015b)
Novocart	Biphasic type I collagen scaffold	1.45 x 10^6 cells/cm^2	Used in over 6000 European patients. Phase I trial (N = 23): 2 year follow up showed NOVOCART increased IKDC, Tegner Noyes and MOCART compared to baseline. Complete or slightly incomplete filling of defect. Phase I trial (N = 41): 6.14 cm^2 average defect size. Coupled with cancellous bone autograft showed improved Lysholm, Cincinnati and MOCART scores at 2 and 5 year follow up but graft hypertrophy evident in 20 - 27% of patients. 3 Phase III trials ongoing.	(Zak et al., 2014) (Niethammer et al., 2014, Pietschmann et al., 2012, Zak et al., 2014)
MACI	Decellularized porcine peritoneal tissue	0.5 - 1 x 10^6 cells/cm^2	Phase III trial (N = 144): for lesions of >3 cm^2. KOOS scores higher in MACI group than microfracture at 2 year follow up with no failures registered in MACI treated group. Phase III trial (N = 60): Lysholm, Tegner and ICRS scores improved compared to microfracture at 2 year follow up. Phase III trial (N = 91): MACI compared to ACI with collagen sponge showed no differences after 1 year but fibrocartilage development in MACI biopsies (36%). Phase III trial (N = 21): 91% of patients had improved clinical scores but 9% failed. 76% possessed normal defect filling.	(Saris et al., 2014); (Basad et al., 2010); (Bartlett et al., 2005); (Ebert et al., 2011).

1.7 Challenges associated with producing tissue engineered cartilage

One of the main issues with any attempt to engineer cartilage is the inability to produce tissue that has exactly the same structural and mechanical properties to that of naturally occurring articular cartilage. Whilst differentiated tissues in the lab are classed as cartilage since they express the essential biomolecules such as collagen type II and proteoglycans, the proportions of these constituents are usually incorrect, with collagen content frequently less than that found in natural cartilage resulting in weak structural tissue (Kafienah et al., 2002, Kafienah et al., 2007, Marijnissen et al., 2002). This has connotations for the loadbearing and tensile abilities of the tissue itself. If implanted within a joint and subjected to physiological forces, these implanted areas become focal points of wear and tear. Similarly, whilst numerous displays of successful chondrogenic differentiation has been demonstrated, a recapitulation of the complex zonal structure of cartilage has been notably absent. From a cellular standpoint, chondrocytes also provide unique challenges in terms of tissue engineering. At maturation, the capacity for chondrocytes to proliferate becomes markedly reduced and whilst chondrocytes explants can be harvested from tissues with relative ease in adults, the number obtained is usually not high enough for the generation of a complete tissue. Chondrocytes are also destined for several fates; progressing from immature cells, mature chondrocytes, hypertrophic cells or trans-differentiation into an osteoblast precursor (**Figure 1.12**). Maintaining the cells at the mature stage in development is therefore an important concern in order to maximise the production of ECM.

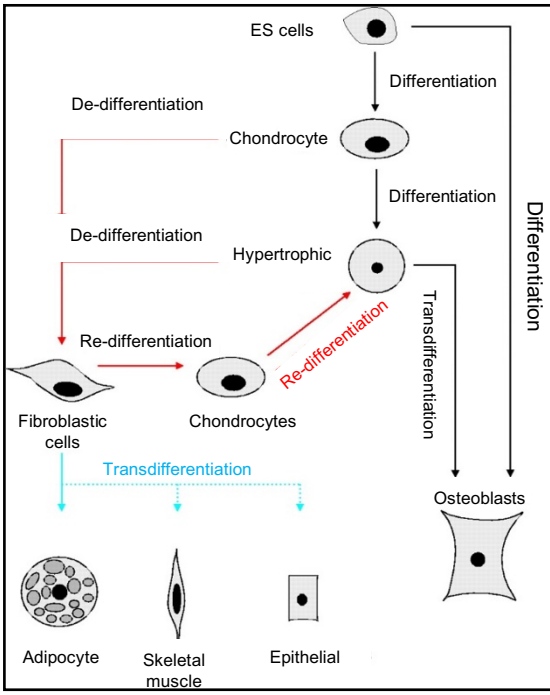

Figure 1.13: The evolution of a chondrocyte from embryonic stem cell. *Monolayer culture of chondrocytes results in the dedifferentiation of chondrocytes into a fibroblastic cell type which produces fibrocartilage rather than the hyaline cartilage required. Re-differentiation of these cells is possible through encapsulation within 3D models but can have a negative impact on ECM synthesis abilities. Mature chondrocytes can also undergo further differentiation further into hypertrophic phenotype which can then transdifferentiate into an osteoblast phenotype. Figure adapted from (Hegert et al., 2002).*

1.8 Chondrogenic differentiation with human multipotent stem cells

Table 1.2 summarises *in vitro* studies investigating chondrogenic differentiation using mesenchymal stem cells (MSCs). MSCs lack both the ethical implications posed by the use of embryonic stem cells (ESCs) and the teratogenic potential of induced pluripotent stem cells (iPSCs). However, in contrast to the pluripotent potential of ESCs, MSCs are only able to differentiate into a select number of cell types. The majority of investigations regarding chondrogenic differentiation of stem cells has involved the use of MSCs. In these experiments, whilst chondrogenic differentiation is detected it is often associated with hypertrophic and osteogenic markers such as alkaline phosphatase (ALP), osteopontin and MMP-13. This of course is a significant observation when considering if the cartilage produced by the cells can be sustained at a functional level (Pelttari et al., 2008, Pelttari et al., 2006). Another consideration for this cell type is the yield of MSCs from tissues. MSC retrieval from tissues within a single donor can be extremely limited, requiring extensive *in vitro* proliferation and a reduction in differentiation potential. In addition, the chondrogenic potential of MSCs was previously shown to be more limited in comparison to iPSCs and ESCs, most likely a consequence of the reduced differentiation potential of these cells in comparison (Ko et al., 2014).

Table 1.2: Human MSC in vitro models for chondrogenic differentiation

Cell type	Model	Time (day)	Agents	Cell density	Key information	Reference
Human MSCs implanted in SCID mice	Pellet	56	Dex (0.1 µM) $TGF\beta_3$ (10 ng/ml)	4-5 x 10^5	Premature onset of COLX and MMP-13 expression in pellets at day 7 before Col2A1 expression. Osteopontin and COL1a1 significantly upregulated at day 14 and continued to day 42. COLX widely distributed in pellets after 14 days via immunostaining. ALP upregulation detected using immunostaining. Not observed in chondrocyte controls. MSC pellets mineralised despite producing aggrecan and type II collagen.	(Pelttari et al., 2006)
Human MSCs and HUCPVCs	Pellet	21	Dex (0.1 µM) $TGF\beta_3$ (10 ng/ml)	2.5 x 10^5	HUCPVCs showed a ↑ proliferative potential, similar levels of proteoglycan staining and more intense collagen staining than MSCs. Statistical differences in GAG content only detected at day 7 ($p<0.05$).	(Baksh et al., 2007)
BM-MSCs	Pellet	21	$TGF\beta_3$ (10 ng/ml) + Dex (100 nM) Selected cases: BMP-2, BMP-4 or BMP-6 (500 ng/ml)	2 × 10^5	All BMPs ↑ chondrogenic differentiation. BMP-2>BMP-4>BMP-6. Chondrogenic genes expressed in response to BMP-2. Heterogeneous differentiation in pellet observed.	(Sekiya et al., 2005)

Amniotic fluid derived stem cells (AFSCs), are a broadly multipotent stem cell type characterised by expression of OCT3/4 (Prusa et al., 2003), stem cell factor (CD117), vimentin, CD90, CD105, SSEA-4 and alkaline phosphatase (Carraro et al., 2008). In particular, OCT3/4 and SSEA-4 are common markers associated with the undifferentiated state of ESCs. Only 1% of the cells found in amniotic fluid derived from amniocentesis samples are referred to as AFSCs. The amniocentesis procedure used to extract the fluid is minimally invasive and ultrasound guided to provide a relatively safe and painless procedure. While AFSCs have no defining unique marker, they are most effectively isolated via immunoselection for the marker CD117 (C-kit). AFSCs have been shown to be capable of differentiating into cells derived from all 3 germ layers, but most importantly have been shown to be capable of differentiating into chondrocytes using several different *in vitro* models (Zuliani et al., 2018, Resca et al., 2015, Kolambkar et al., 2007, Preitschopf et al., 2016). Examples of these studies are included in **Table 1.3**. Again, this successful differentiation is often characterised by the expression of key chondrogenic markers such as COL2a1, SOX-9 and aggrecan as well as proteoglycan production and collagen synthesis in various culture models including monolayer, pellet and hydrogel. However, when directly compared to that of MSCs the robustness of these chondrogenic markers is more limited; potentially indicating a more reduced capacity to differentiate into the chondrogenic lineage (Kolambkar et al., 2007).

Table 1.3: Human AFSC in vitro models for chondrogenic differentiation

Cell type	Model	Time (day)	Agents	Cell density	Key information	Reference
Human AFSCs and MSCs	Pellet and Alginate	21	TGFβ_1 (10 ng/ml) TGFβ_3 (10 ng/ml) BMP-2 (500 ng/ml) IGF-1 (100 ng/ml)	Pellet: 200,000-800,000 Alginate: 2 x 10^7 cells/ml	The growth factors did not affect cell proliferation in pellets but TGFβ_1 supplementation alone increased GAG/DNA synthesis compared to TGFβ_3 alone or TGFβ_3 + BMP-2. Single factor produced greater staining for proteoglycan and type II collagen than combined factor. Increasing pellet cell density ↑ GAG/DNA by 57%. TGFβ increased Type II collagen pericellularly compared to basal control. MSCs produced more robust cartilage compared to AFSCs.	(Kolambkar et al., 2007)
Human AFSCs into AC pellet	Pellet	14	Dex (100 nM) TGFβ_1 (5 ng/ml)	2.5 x 10^5	Quantification of chondrogenic marker expression showed that knockdown of HIF2α reduced SOX-9, aggrecan, and COL2a1 gene expression after day 7 of differentiation and could not be reversed with rapamycin.	(Preitschopf et al., 2016)
Human AFSCs	Monolayer	21	Dex (100 nM) TGFβ_1 (10 ng/ml)	2000 cells/cm^2	Diffuse positive staining for type II collagen detected in ASC (amniotic stem cell) compared to AMC (amniotic mesenchymal cell).	(Resca et al., 2015)

Human AFSCs	Micromass	21	Dex (100 nM) $TGF\beta_3$ (10 ng/ml)	5×10^5	Micromass culture of AFSCs increased SOX-9, aggrecan and COL2 gene expression after $TGF\beta_3$ treatment compared to untreated controls cultured in monolayer for up to 21 days. SOX-9 gene expression was greater than control, but reduced type II collagen and aggrecan expression. Type II collagen detected in culture medium in $TGF\beta_3$ treated micromass samples at 21 days.	(Zuliani et al., 2018)
Human AFSC	Agarose (2%) Starch-polycaprolactone (SPCL) scaffold	21	Dex (1 mM) $TGF\beta_1$ (10 ng/ml)	2×10^6	Early detection of COL2 at 7 days of culture in basal and chondrogenic cultures. COL2 expression is lost at week 2 but reappears at week 3 and increases. Agarose gels demonstrate more consistent expression over time. Aggrecan expression is less than that of collagen II. Encapsulated AFSCs express low aggrecan levels for duration of experiment. Viability unaffected in core and periphery.	(Rodrigues et al., 2012)

However, one of the major problems for the clinical use of MSCs is that they cannot retain their stem cell status for longer than five passages without displaying a reduced differentiation potential, proliferation and expression of specific cell surface markers (Wagner et al., 2008). In contrast, AFSCs have demonstrated the ability to maintain their stemness after 250 population doublings without significant telomere shortening which allows them to be cultured for long periods from one specific donor (De Coppi et al., 2007). The reduced expression of MHC class II or other co stimulatory molecules (CD80, 86) on the surface of AFSCs also indicates that they do not initiate a strong rejection response from the host once implanted (Moorefield et al., 2011). This has positive implications for evaluating AFSC effectiveness within *in vivo* models and clinical application. This is most likely a result of their development stage between that of an embryonic and adult stem cell (Cananzi, 2009). It was also confirmed that AFSCs do not form germ cell line tumours in SCID (severe combined immunodeficient) mice which makes these cells a much more viable choice for clinical application than embryonic and induced pluripotent stem cells (Resca et al., 2015). Whilst ESCs and iPSCs can express chondrogenic markers with less hypertrophic gene expression, AFSCs (at least in the short to medium term) are a much easier cell type to translate to an *in vivo* clinical setting due to ethical and safety reasons.

1.9 Comparison of *in vitro* 3D models for chondrogenic differentiation

Table 1.4 summarises high-density *in vitro* models involving pellet or micromass culture. The principle behind these methods is that by packing the cells together at a high density, there are a greater number of cell to cell contacts and gap junction signalling events which reproduces the embryonic events that occur during limb development and thus aid the progression of cells to the chondrogenic differentiation stage (Augustyniak et al., 2015). Micromass culture differs to pellet culture by the fact that the cells are initially suspended within a small volume of liquid, typically 10 – 20 μl, to induce the pellet formation instead of using centrifugation. From **Table 1.4**, it is clear that the application of high density cultures, often treated with TGFβ, induces chondrogenic gene expression and increased histological staining of either proteoglycans or collagens (Johnstone et al., 1998). Comparison experiments between micromass and pellet cultures have shown that while both methods lead to chondrogenic differentiation of MSCs, micromass cultures demonstrate an enhanced efficiency of MSC chondrogenic differentiation compared to pellet culture in terms of specific earlier gene expression including the upregulation of cartilage specific COL2a1 and aggrecan in addition to downregulation of fibrocartilage markers like COL X and COL 1. Proteoglycan deposition and a reduction in core cell necrosis is also clearly evident (Zhang et al., 2010). However, the upregulation in gene expression is not always observed for all chondrogenic differentiation genes such as SOX-9. The importance of markers such as SOX-9 have been supported in instances whereby decreases in SOX-9 expression resulted in decreased aggrecan and collagen II markers (Ruedel et al., 2013). However, whilst a downregulation of fibrocartilage markers is evident when comparing pellet to micromass models, MSCs used in these models still demonstrate an increased expression of these markers compared to controls (Barry et al., 2001, Sekiya et al., 2002, Pelttari et al., 2008). Supplementation of culture medium with TGFβ and dexamethasone has actually been shown to slow down the hypertrophic progression of MSCs in pellet models and reduce these fibrocartilage markers (Mueller et al., 2010). It is therefore possible that the use of high-density culture method is conducive to hypertrophic differentiation rather than immature/mature chondrocyte differentiation and that the addition of exogenous growth factors is essential to reduce this incidence.

Table 1.4: Examples of high-density culture methods for chondrogenic differentiation using MSCs.

Model	Time (days)	Agents	Cell density	Key information	Reference
Pellet	21	Dex (1 mM) TGFβ$_3$ (10 ng/ml) BMP-6 (500 ng/ml)	200,000	Increased proteoglycan mRNA, type II, IX, X, XI collagen, FGFR-2, PTHrPR, and transcription factors SOX-5, SOX-6, and SOX-9. Increased toluidine blue in line with culture time.	(Sekiya et al., 2002)
Pellet	14 28 42	TGFβ$_1$ (10 ng/ml) TGFβ$_3$ (10 ng/ml)	200,000	No statistical differences in GAG synthesis, DNA content or histological differences between TGFβ isoforms. Type II collagen staining weak at day 14 but positive on day 28 and localised to central area. Type X collagen in periphery at day 28 and 42 in chondrogenic controls compared to hypertrophic treated. TGFβ$_1$ and dex removal required to allow hypertrophic expression of type X collagen and ALP.	(Mueller et al., 2010)
Pellet	21	TGFβ$_3$ (10 ng/ml) Dex (100 nM) BMP-2 (500 ng/ml) FGF-2 (2 ng/ml)	200-2000 x 10^3	Single factors did not induce chondrogenesis. TGFβ$_3$ or dex increased pellet size but no significant accumulation of GAG. BMP-2 + TGFβ$_3$ and dex increased growth of pellet and ECM production. DNA content per pellet ↓ during chondrogenesis. Runx2 expression unchanged with culture period.	(Shirasawa et al., 2006)
Micromass vs pellet	21	TGFβ$_3$ (10 ng/ml) Dex (100 nM)	2 x 10^7 vs 2 x 10^5	Wet weight of micromass tissue larger than pellet. Increased toluidine blue staining in micromass compared to pellet (day 7 - 21). Higher Collagen II in micromass with lower collagen I and X compared to pellet. TUNEL assay showed positive cells in central region of pellet but fewer in micromass. Micromass: significantly higher collagen II and aggrecan ($p<0.01$) but downregulated collagen I and X ($p<0.01$). SOX-9 expression did not change in either culture method, stayed low.	(Zhang et al., 2010)
Micromass vs pellet	33	Dex (1 μM)	50,000 cells/ml vs 2.5 x 10^5	Hanging drop method showed increased collagen type II, SOX-9 and MIA/CD-RAP expression as early as day 2. Not observed in pellet until day 11. Collagen X ad AP-2 expression only weakly induced at day 7. Addition of TGFβ enhances expression of these markers at day 2. siRNA treatment to decrease SOX-9 expression reduced aggrecan, collagen II, MIA/CD-RAP expression also reduced.	(Ruedel et al., 2013)

In general, high density cultures have several advantages compared to other *in vitro* models since they are quick and easy to form and do not require complex enzymatic digestions to remove any surrounding structures like hydrogels. In this way, the chondrogenic potential of cells can be quickly evaluated along with the investigation of different signalling pathways (Pelttari et al., 2008). These models are often used by commercial chondrogenic differentiation kits such as STEMPRO (Thermofisher Scientific, UK). However, the production of dense ECM after long culture periods by the incumbent differentiating cells can be a problem when trying to isolate cells for further investigation, requiring high intensity manual lysis methods which can result in a loss of sample or risk of contamination. Another common problem associated with these methods is the presence of undifferentiated and necrotized cells within the central regions of the

pellet/micromass compared to the differentiated outer layer cells (**Figure 1.13**) (Mueller and Tuan, 2008, Kafienah et al., 2007). This is due to the way in which the model is formed. By packing the cells at a high cell density, a low oxygen tension environment is produced with poor nutrient diffusion. Together these constraints increase cellular stress events and cause cells to die within the central region of the model. Despite successes some of the main drawbacks for micromass culture are the limitations in size, quantity and overall mechanical instability of the constructs once implanted *in vivo* (Tare et al., 2005, Panadero et al., 2016). High density models are therefore limited to more investigative roles instead of practical application.

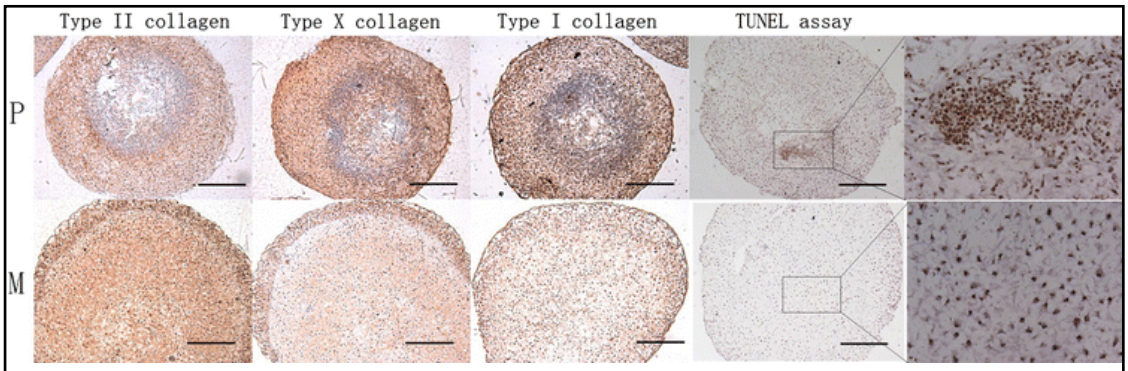

Figure 1.14 Cell necrosis is reduced in micromass compared to pellet culture for chondrogenic differentiation of MSCs. *Core regions of pellets show clear differences in staining for specific cartilage and fibrocartilage markers indicating a lack of homogenous differentiation within the pellet structure. In addition, the results of the terminal deoxynucleotidyl transferase dUTP Nick-End Labelling (TUNEL) assay indicate areas of apoptotic cell death within the central region in contrast to that observed within the micromass model. Scale bar represents 100μm. Figure from (Zhang et al., 2010).*

Alginate is an anionic linear polysaccharide composed of alpha-L-guluronic and 1-4 linked beta-d-mannuronic acid, as detailed in **Figure 1.14** (Hernandez et al., 2010, Guo J, 1989). Due to the inert nature of alginate, interactions between the hydrogel itself and cells encapsulated within it are limited and do not present any toxic products which can affect cell viability allowing it to be used for human trials (Tonnesen and Karlsen, 2002). This biocompatibility can be further enhanced through the attachment of peptide sequences to the alginate chains itself which allows cell integrin interactions e.g. RGD motifs (Shachar et al., 2011). Cells can be distributed homogenously within alginate with little impact on cell viability using chelators such as citrates, phosphates, carbonates and lactates or incubation in solutions with a reduced calcium concentration solutions (Olderoy et al., 2014, Gleghorn et al., 2008). The high permeability enables movement of low molecular weight nutrients, oxygen, metabolites and catabolic products

(Hernandez et al., 2010). However, porosity is dependent on factors such as the ratio of its constituents (guluronic acids to mannuronic acids), temperature, pH and gelation method (Lundberg and Kuchel, 1997).

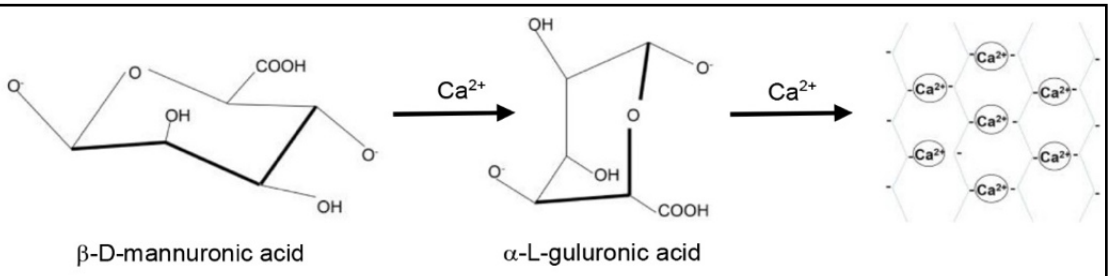

Figure 1.15 Chemical structure of the repeated units of alginate: β-D-mannuronic acid and α-L-guluronic acid. *Divalent cations such as calcium (Ca^{2+}) ions bind to the exposed guluronic acid residues creating a solution-gel transition material. Crosslinks between Ca^{2+} and the guluronic residues forms a stiff egg box structure responsible for the viscoelastic behaviour of the hydrogel (LeRoux et al., 1999).*

Table 1.5 shows examples of MSC chondrogenic differentiation using alginate hydrogels as demonstrated by increased safranin O staining and immunostaining for aggrecan and collagen (Kolambkar et al., 2007, Xu et al., 2008, Herlofsen et al., 2011). GAG accumulation increases were also associated with alginate and fibrin encapsulation compared to monolayer culture. Cell proliferation was also shown to be possible within alginate hydrogels but whilst high viability values are always noted, a reduction in viability has been observed after prolonged periods of culture (Xu et al., 2008). This is a potentially significant issue since chondrogenic differentiation typically takes place over a protracted time period of 3 - 4 weeks. Comparisons of alginate bead models to monolayer and pellet culture showed that alginate encapsulation initially caused an upregulation of hypertrophic markers but after prolonged culture resulted in a significant downregulation compared to these other models (Dashtdar et al., 2016). Subcutaneous implantation of MSC seeded alginate hydrogels was also associated with significant chondrogenic gene expression and histological staining for collagen markers indicating the suitability for alginate hydrogels for *in vivo* application (de Vries-van Melle et al., 2014).

Table 1.5: Examples of alginate hydrogels for chondrogenic differentiation of human MSCs

Model	Time (day)	Agents	Cell density	Key information	Reference
Alginate (2%)	24	TGFβ$_3$ (10 ng/ml)	1 x 10^6	Cell proliferation increased with culture period (76.5%). Cell viability reduced (14 - 18%) at day 24. Increased safranin O staining with culture period in chondrogenic constructs compared to day 0. Aggrecan and collagen immunostaining observed intracellular and pericellularly as early as day 6 in chondrogenic constructs whilst increased Type II collagen II, X, COMP and aggrecan gene expression temporally.	(Xu et al., 2008)
Alginate (1%)	21	Dex (0.1 μM) TGFβ$_1$ (10 ng/ml)	5 x 10^6/ml	High viability throughout alginate culture. COL1 was initially expressed at high levels in monolayer culture and decreased slightly over time. In comparison, COL2, COL10, SOX-5, SOX-6, SOX-9 and aggrecan ↑ at day 7 while COL1 and versican ↓. Collagen and aggrecan showed dispersion through the ECM after 21 days whilst COL10 showed intra/pericellular localisation.	(Herlofsen et al., 2011)
Alginate (1.2%) and/or HA (1%) within an OA defect	28	Dex (100 nM) TGFβ$_1$ (10 ng/ml)	1 x 10^7/ml	Glycosaminoglycan deposition and chondrogenic gene expression (COL2 and aggrecan) significantly ↑ in alginate hydrogels and fibrin hydrogels. Supplementation of HA to alginate did not have an effect. When implanted subcutaneously, alginate hydrogels had significantly ↑ cartilage gene expression after 28 days than fibrin and significantly ↑ safranin O staining after 12 weeks *in vivo*. DNA content ↓ with time in alginate structures. Expression of COL X and ALP ↑ for all materials tested compared to negative control.	(de Vries-van Melle et al., 2014)
Monolayer v Pellet v Alginate (1.2%)	21	Dex (100 nM) TGFβ$_3$ (10 ng/ml)	2.5 x 10^5 per pellet 80,000 per bead	Alginate bead encapsulation and pellet culture significantly ↑ immunohistochemical staining of collagen and aggrecan compared to monolayer. GAG content and expression of aggrecan, SOX-9 and collagen II were significantly higher in alginate bead samples compared to pellet culture samples at all time points tested ($p<0.05$). Hypertrophic markers COLX and Runx2 significantly higher in alginate samples compared to pellet at early point of culture (day 3; $p<0.05$) but were significantly ↓ at later time points (days 12 and 21).	(Dashtdar et al., 2016)

Alternatively, agarose is a polymer that consists of disaccharide units with variable numbers of methoxy groups which stabilise by hydrogen bonding between galactose residue hydroxyl groups and water resulting in pores that can range between 10 - 500 nm in diameter for a 2% w/v gel as detailed in **Figure 1.15**. (Lundberg and Kuchel, 1997).

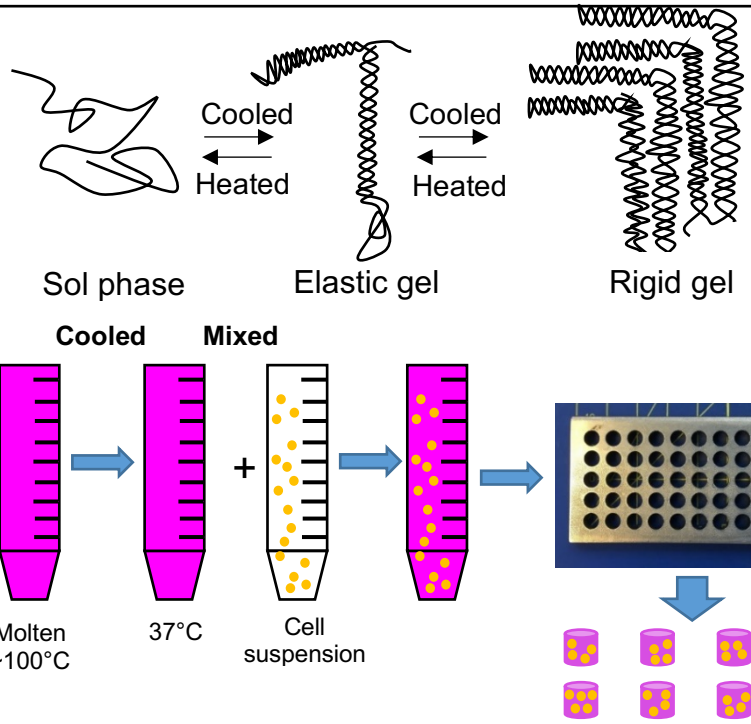

Figure 1.16: Agarose polymer arrangement in different phases. *When heated to high temperature (100°C) agarose polymers exist as individual single chains (sol phase). When cooled these chains start to combine, generally into a helical structure due to low level cross linking (elastic gel phase). When left to cool further these complexes begin to stick together due to the formation of further cross links which makes the gel become much more rigid (rigid gel phase).*

Table 1.6 summarises some examples of agarose models used for chondrogenic differentiation of MSCs. Within these, an increase in type II collagen expression, variable proteoglycan content, increased collagen staining and chondrogenic gene expression have all been noted using agarose hydrogels when treated with dexamethasone and TGFβ (Rodrigues et al., 2012, Tangtrongsup and Kisiday, 2016). However, these increases have also been associated with an enhancement of hypertrophic/osteogenic markers such as type X collagen and ALP (Thorpe et al., 2012). Whilst superior differentiation has been noted in self-assembled polypeptide scaffold materials, agarose encapsulation was also shown to be conducive to chondrogenic differentiation although more so for bovine MSCs than human MSCs (Florine et al., 2013). In contrast, TGFβ$_3$ mediated chondrogenesis within agarose was shown to be superior to fibrin gels

as shown by enhanced staining for type II collagen, whilst fibrin seemed to support greater myogenic differentiation (Thorpe et al., 2012). Markers for hypertrophic chondrocytes were also noted to be higher in agarose constructs compared to fibrin. Testing of chondrogenic differentiated MSCs within agarose constructs also showed significant accumulation of cartilaginous matrix but the mechanical properties were shown to be diminished compared to mature chondrocytes cultured under identical conditions (Mauck et al., 2006). However, it was also suggested that further optimisation of the model through a longer induction period or the application of mechanical loading to differentiated MSCs could potentially overcome these issues and enhance the mechanical properties of the resulting cartilage. In support of this, the effect of mechanical loading on MSC chondrogenic differentiation has been well examined using agarose hydrogels (Mouw et al., 2007, Mauck et al., 2007, Kisiday et al., 2009, Huang et al., 2010).

Table 1.6: Examples of agarose hydrogels used for chondrogenic differentiation

Cell type	Model	Time (day)	Agents	Cell density	Key findings	Reference
Equine MSCs	Agarose (2%)	21	Dex (1 or 100nM) $TGF\beta_1$ (5 ng/ml)	1.2×10^7 per ml	GAG accumulation, toluidine staining, collagen II staining, chondrogenic gene expression and hydroxyproline content showed no significant difference when dex concentration reduced from 100 nM to 1 nM. In dex free, GAG accumulation significantly ↓ compared to dex treated. DNA content unchanged but type I collagen gene expression significantly ↑. Collagen II gene expression ↑ in response to 100 nM dex with 52-fold increase between 3 and 15 days. Collagen I expression showed 2.5-fold increase at day 15. Type X collagen and alkaline phosphatase ↑ in response to 100 nM dex. MMP ↑ in 1 nm dex compared to 100 nM. ADAMTS4 ↓ in response to 100 nM dex. Withdrawal of dex caused ↓ in hydroxyproline but not GAG relative to controls after 6 days.	(Tangtrongsup and Kisiday, 2016)
Human and Bovine BM-MSCs	Agarose (2%) and/or V RADA	21	$TGF\beta_1$ (10 ng/ml) Dex (100 nM)	1×10^7 cells/ml	$TGF\beta_1$ with dex significantly ↑ GAG accumulation compared to $TGF\beta_1$ alone in agarose hydrogels but ↓ in RAD scaffolds. DNA content ↑ in response to dex treatment in agarose constructs. TGFβ and dex showed significant proteoglycan synthesis ↑ compared to TGFβ alone at day 14 and 21. Hydroxyproline content ↑ over time in both scaffolds. In agarose no statistical difference between dex and TGFβ alone at any time point. Immunohistochemistry showed collagen II staining in RADA but not agarose. More collagen type II in TGFβ alone gels compared to dexamethasone and TGFβ. Collagen I staining not evident in agarose or RADA. Apoptosis levels ↑ in agarose gels (20-30%) compared to RADA gels (2%). TGFβ and dex resulted in ↓ apoptosis compared to TGF alone in agarose.	(Florine et al., 2013)

					RU-486 significantly ↓ GAG synthesis levels in TGFβ + dex treated samples in agarose and RADA. Seeding of constructs with human BMSC showed minimal GAG increases in agarose hydrogels and levels 50% of that of bovine cells in RADA.	
Human AFSC	Agarose (2%)	21	Dex (1 mM) $TGF\beta_1$ (10 ng/ml)	2 x 10^6	Early detection of COL2 at 7 days of culture in basal and chondrogenic cultures. COL2 expression is lost at week 2 but reappears at week 3 and increases. Agarose gels demonstrate more consistent expression over time. Aggrecan expression is less than that of collagen II. Encapsulated AFSCs express low aggrecan levels for duration of experiment. Viability unaffected in core and periphery.	(Rodrigues et al., 2012)
Porcine MSCs	Agarose (2%)	22 or 42	$TGF\beta_3$ (1 or 10 ng/ml)	1.5 x 10^7 /ml	Agarose embedded MSCs showed spherical morphology compared to spread morphology in fibrin matrix. Free swelling agarose showed positive chondrogenic staining but also mineral staining indicating a progression towards terminal differentiation. Free swelling fibrin constructs differentiated towards myogenic pathway. Dynamic compression application reduced differentiation short-term but long-term extrinsic loading supported chondrogenic differentiation.	(Thorpe et al., 2012)

Overall, the sheer number of growth factor treatments, *in vitro* models, cell types, scaffold materials, gelation methods and cell densities used to achieve chondrogenic differentiation of stem cells is vast and confusing. Contradictory findings are rife and has led to a lack of consensus in regard to even basic considerations when it comes to approaching the synthesis of a tissue engineered cartilage product. As such, any approaches to investigate stem cell chondrogenic differentiation or the development of new models requires a step wise evaluation.

1.10 Role of C-type natriuretic peptide in bone homeostasis

In addition to the cells and scaffold materials used to engineer specific tissues, the addition of biological agents that can stimulate a desired cellular response is a significant determination to be made. One of the most significant small peptides with growing evidence to support its role in cartilage and bone homeostasis is that of CNP.

1.10.1 CNP expression and signalling

Activation of the *Nppc* gene, chromosomally located at 2q24-qter. synthesises a 126 amino acid long pre-pro form of CNP (**Figure 1.16**). Removal of the N-terminal signal peptide allows the cleavage of pro-CNP, via the endoprotease furin into 2 products; a 50 amino acid long amino terminal pro peptide (NT-proCNP) and a 53 amino acid long active CNP. These products can be excreted from the cell, but ordinarily the 53 amino acid peptide is cleaved again into a mature 22 amino acid long product. CNP-22 is much more potent than the uncleaved 53 amino acid long peptide (Wu et al., 2003) but has a considerably shorter plasma half-life.

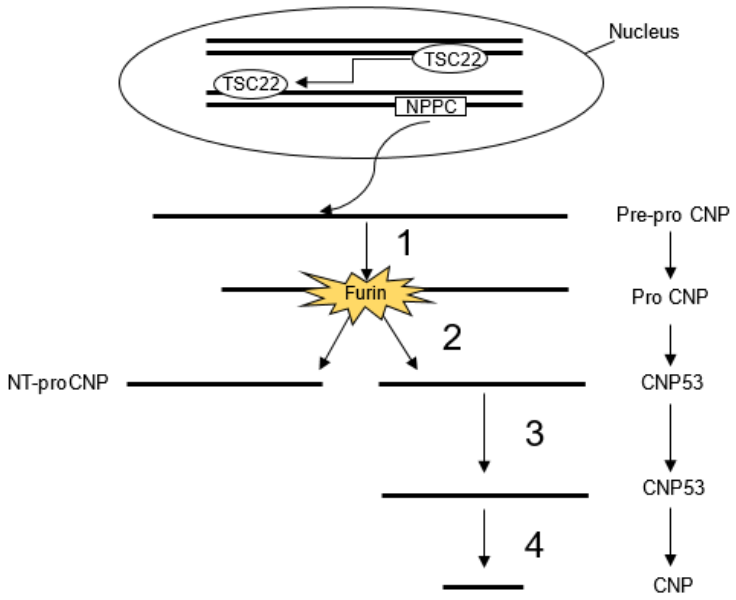

Figure 1.17: CNP synthesis. *The transcription factor TSC22 stimulates the NPPC gene to trigger production of a 126 amino acid pre-pro CNP with a signal peptide attached. Subsequent removal of this signal peptide forms 'Pro-CNP' which then allows cleavage by an endoprotease (furin) into 2 components: an active 53 amino acid CNP along with an amino terminal pro-peptide. Secretion of these out of the cell allows further cleavage of CNP-53 into mature CNP-22.*

Whilst sharing a similar peptide main structure with a 17 amino acid loop structure to its family members, atrial natriuretic peptide (ANP) and brain natriuretic peptide (BNP), the

distribution of CNP within the body is distinct (ANP and BNP are predominantly produced by the heart) localised to the CNS and to a lesser extent within vital organs such as the lung, liver, kidney and most importantly the growth plate of cartilage (Chusho et al., 2001).

CNP acts through a membrane bound guanylyl cyclase receptor; natriuretic peptide receptor (NPR)2 and another receptor that lacks a guanylyl cyclase functionality called NPR-3. These 2 receptors are important for two different reasons. Binding of CNP to the glycosylated NPR-2 homodimer triggers the binding of an ATP molecule which acts to instigate a conformational change within the guanylyl cyclase domains, bringing them together. This movement activates the conversion of GTP to cyclic GMP which can go on to stimulate the activation of a host of downstream targets ranging from cGMP dependent kinases (the main intracellular cGMP target, such as PKGII), cGMP regulated phosphodiesterases and cyclic nucleotide gated ion channels (Pilz and Casteel, 2003). Dephosphorylation of the ATP binding domain causes the conformational change to reverse as ATP is released and the initial CNP ligand is released from the receptor (Potter, 1998). Breakdown of CNP within the extracellular space is performed by matrix membrane metalloendopeptidase, principally neprilysin, resulting in CNP's rapid half-life (Kenny et al., 1993).

1.10.2 Evidence of the role of CNP in bone and cartilage homeostasis

The evidence to support the role of CNP during limb development has been indicated from several *in vivo* knockout studies that either disrupt CNP or one of its cognate receptors such as NPR-2. For example, dwarfism results with severe growth retardation postnatally due to growth reduction in endochondral bones (Chusho et al., 2001, Yasoda et al., 2004). In contrast, overexpression of CNP or deletion of NPR-3, which is thought to be responsible for clearance of natriuretic peptides from the circulation rescues the phenotype of CNP knockout mice (Matsukawa et al., 1999). These effects are not only seen in murine models but also clinically, as is the case for acromesomelic dysplasias type Maroteaux (Bartels et al., 2004, Olney, 2006) which results from *Nppc* or *Npr2* mutations. It has been suggested that CNP plays a direct role in regulating when chondrocytes exit the cell cycle, whereby the proliferative zone of the growth plate is directly affected (Chusho et al., 2001, Yasoda et al., 2004). By removing CNP, the length of time that these cells are able to remain within the synthesis phase (S phase) of the cell cycle is reduced and therefore directly reduces the length of the proliferating zone resulting in growth retardation. More significantly, when CNP is removed a shortening of the hypertrophic zone is

apparent. Treatment of endochondral long bones with CNP increases the size and number of hypertrophic cells without an effect on cell apoptosis (Agoston et al., 2007). In terms of *in vitro* investigations, CNP has been associated with regulating osteoblast activity by increasing osteogenic gene expression markers such as ALP and osteocalcin in osteoblastic MC3T3-E1 cells and osteoblast like cells from foetal rat calvaria (Yeh et al., 2006, Suda et al., 1996). Furthermore, CNP was also previously associated with increasing osteoclast bone resorption activity in osteoclast containing mouse bone marrow cultures (Holliday et al., 1995). These and other investigations suggest that CNP plays an important role in regulating osteoblast activity which directly affects bone formation

Importantly, CNP supplementation has been shown to induce proteoglycan synthesis and reduce enzymes associated with ECM breakdown (Krejci et al., 2005, Woods et al., 2007). In addition to its local effects, CNP has also been associated with controlling the secretion of pituitary growth hormone, known to directly regulate endochondral bone growth (McArdle et al., 1994), as well as chondroprotective effects against inflammatory challenge by inflammatory cytokines such as IL-1β (Peake et al., 2015), an effect further enhanced by the application of mechanical loading (**Table 1.7**). This increase in ECM synthesis caused by CNP application has been attributed to an increase in the activity of the enzymes responsible for chondroitin sulfate synthesis and therefore GAG production (Woods et al., 2007). The principle mechanism that drives this chondroprotective effect in human chondrocytes has been characterised via cGMP production and subsequent activation of PKGII. Therefore, the role of CNP in bone formation and the maintenance of healthy articular cartilage is clearly evident and has subsequently driven research into its potential role in the chondrogenic differentiation process.

Table 1.7: Examples of functional studies looking at the role of CNP in chondrocyte signalling

Species	Model	Agents	Key findings	References
Human	Agarose (3%) / bioreactor	Il-1β 10 (ng/ml) CNP (0.1 – 1000 nM)	CNP reduces IL-1 induced NO + PGE_2 release in dose dependent manner Dynamic compression with CNP reduced iNOS and COX2 expression at 6 hours of culture CNP treated unstrained samples show increases in aggrecan and collagen type 2 expression - concentration dependent effect	(Ramachandran et al., 2011)
Human	Agarose (3%) / bioreactor	CNP (100 nM) IL-1β (10 ng/ml)	Co-treatment of constructs with CNP and IL-1β reduced catabolic effects of IL-1 via reduction in NO. Inhibition of NPR2 prevented this effect Activation of NPR3 reduced NO and PGE_2 release in co-treated constructs CNP presence significantly enhanced GAG synthesis and cGMP levels	(Peake et al., 2013)
Bovine	Pellet	CNP (10 pM – 10 nM)	Low doses of CNP stimulated proliferation but no ECM accumulation High doses of CNP resulted in significant ECM accumulation with no increase in cellularity CNP stimulated cells more rounded morphology than untreated Dose dependent decrease in Collagen X expression when CNP applied	(Waldman et al., 2007)

1.11 Aims & Objectives

This project investigated the chondrogenic potential of human amniotic fluid-derived stem cells in alginate and agarose 3D models upon treatment with different TGFβ isoforms. AFSCs isolated from human amniotic fluid were expanded in conditioned media supplemented with either growth factor TGFβ$_1$, TGFβ$_3$, CNP and/or dexamethasone (Dex). In order to identify which model was optimal for long-term differentiation and production of chondrogenic markers, AFSCs were either encapsulated in alginate beads or seeded into agarose constructs (**Chapters 2 and 3**), and the differential effects of either CNP, growth factors or Dex on protein synthesis (collagen, GAG) and gene expression (aggrecan, type II collagen, SOX-9) were investigated in AFSC/agarose constructs (**Chapter 4**). In a separate study, I explored the potential of CNP containing microcapsules to promote GAG synthesis in chondrocyte/agarose constructs (**Chapter 5**).

AIM 1: Short-term culture effects of AFSCs either encapsulated in alginate beads or seeded into agarose constructs.

OBJECTIVES: I developed a model to expand AFSCs and culture in either alginate beads or agarose constructs for up to 14 days in the presence and absence of either TGFβ$_1$ or TGFβ$_3$. Biochemical assays were used to quantify GAG synthesis and DNA content. Confocal microscopy was used to examine cell viability in the centre and edge of AFSC/agarose constructs. Epifluorescence microscopy was used to examine cell viability in cross sections of AFSC/alginate beads. Fluorescence activated cell sorting (FACS) was also used to examine cell surface markers of AFSCs used in these experiments.

PROJECT OUTCOMES: *AFSC/agarose constructs:* Treatment with either TGFβ$_1$ or TGFβ$_3$ significantly increased DNA content compared to controls whilst maintaining cell viability in core and edge of constructs after culture for up to 14 days. GAG synthesis in AFSC/agarose constructs was elevated in TGFβ treated samples relative to only basal control samples after 14 days of culture. *AFSC/alginate beads:* Treatment with TGFβ demonstrated statistically significant increases in DNA content compared to controls but no statistically significant increases in GAG synthesis were detected. Alginate beads were not stable after short-term treatment with growth factors and the structure appeared to diminish making it a poor model for cell differentiation.

AIM 2: Long-term culture effects of either TGFβ$_1$ or TGFβ$_3$ in AFSC/agarose constructs.

OBJECTIVES: Following cell expansion, AFSCs were cultured in agarose constructs for up to 28 days in the presence and absence of either TGFβ$_1$ or TGFβ$_3$. Confocal microscopy was used to examine cell viability in the centre and edge of the AFSC/agarose constructs. Biochemical assays were used to quantify GAG synthesis, collagen synthesis and DNA levels. The differential effects of the TGFβ isoforms on GAG synthesis and collagen content in AFSC/agarose constructs were investigated up to 28 days of culture.

PROJECT OUTCOMES: Treatment with either TGFβ$_1$ or TGFβ$_3$ in AFSC/agarose constructs significantly increased GAG synthesis, collagen levels, DNA content and maintained homogeneous cell viability after culture for up to 28 days when compared to day = 0.

AIM 3: Long-term culture effects of either CNP, TGFβ$_1$, TGFβ$_3$ or Dex in AFSC/agarose constructs.

OBJECTIVES: Following cell expansion, AFSC/agarose constructs were cultured for up to 28 days in the presence and absence of either CNP, TGFβ$_1$, TGFβ$_3$ and/or Dex. At the end of the experiment, GAG synthesis, collagen levels and DNA levels were quantified by biochemical assay. Histology was used to examine proteoglycan content with alcian blue staining. RT-qPCR was used to examine SOX-9, Type II collagen (COL2a1) and aggrecan gene expression. SHG imaging and confocal microscopy was used to examine collagen fibre organisation in the centre of the AFSC/agarose constructs.

PROJECT OUTCOMES: Co-stimulation with CNP and either TGFβ$_1$ or TGFβ$_3$ significantly increased GAG synthesis and collagen levels in in AFSC/agarose constructs cultured for up to 28 days. I observed greater levels of alcian blue staining and increased SOX-9 gene expression in co-stimulated samples when compared to day = 0. Pericellular deposition of collagen was also detected in co-stimulated samples according to SHG imaging.

AIM 4: Short term culture effects of CNP containing microcapsules in bovine articular chondrocyte/agarose constructs.

OBJECTIVES: CNP microcapsules were made using layer by layer assembly of the alternately charged polyelectrolytes poly-L-arginine and dextran sulfate around a dissolvable calcium carbonate core with CNP incorporated within. Bovine chondrocytes from articular joints of 18 – 24-month old steers were isolated from tissue and cultured in 3% agarose constructs in the presence and absence of CNP microcapsules for up to 48 hours and compared to treatment with exogenous CNP, empty microcapsules and day 0 control. Biochemical assays were used to quantify GAG synthesis and DNA content. Confocal and SEM microscopy were used to characterise and observe microcapsule distribution in the core of agarose constructs.

PROJECT OUTCOMES: Treatment with CNP microcapsules resulted in a statistically significant increase in GAG synthesis compared to day 0 and exogenous CNP application. CNP containing microcapsules were shown to have no morphological differences with empty microcapsules. Cellular and microcapsule distribution were shown to be homogeneously distributed in the centre of the constructs.

Chapter 2: Assessment of alginate and agarose hydrogels for early amniotic fluid derived stem cell differentiation

2.1 Introduction

This chapter investigates the chondrogenic differentiation of AFSCs embedded within alginate beads and agarose constructs using TGFβ$_1$ or TGFβ$_3$. TGFβ$_1$ is typically secreted as a 290 kDa latent complex whereby a latent binding protein is directly linked via a disulphide bridge to the TGFβ$_1$ precursor (latency associated peptide) (Kanzaki et al., 1990). Initial binding of TGFβ to type I (TGFβR1) and type II (TGFβR2) serine/threonine kinase receptors on the surface of the cell triggers downstream phosphorylation of Smad2/3 to form a hetero-oligomeric complex with Smad4 which is then able to migrate into the nucleus and instigate the transcription of target genes such as COL2a1, aggrecan, SOX-9 (**Figure 2.1**). CBP/p300 are then recruited to the transcription factor and further increase SOX-9 transcriptional activity. TGFβ$_1$ can also activate other non-smad signalling pathways such as the MAPK pathway via TGFβ activated kinase (TAK1), ERK1/2 via TIMP-3 and PI3K/Akt–MAPK signalling. These pathways aid in the control of wnt mediated signalling through the intracellular β-catenin TCF pathway which in turn controls N-cadherin expression. N-cadherin upregulation allows the formation of cell adhesion complexes during MSC chondrogenesis (Tuli et al., 2003). ERK1/2 controls the anabolic activity of chondrocytes and cellular growth as well as expression of AGC1, COL2a1 and cartilage link proteins (Vater, 2011).

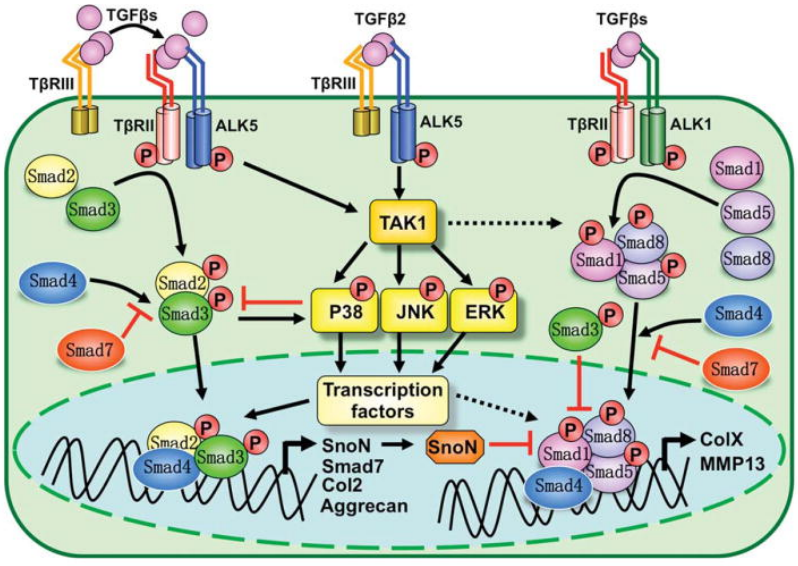

Figure 2.1: TGFβ signalling canonically and non-canonically. *Canonical pathways utilise Smad signalling to instigate changes to chondrogenic gene transcription. Non-canonical pathways have been associated with determining the functional outcome of TGFβ including tissue repair* (Mu et al., 2012, Gilbert et al., 2016, Wang et al., 2014). Figure taken from Mu et al., 2012.

Table 2.1 summarises some *in vitro* examples of the effect of TGFβ on MSC differentiation. Of the 3 prototypic TGFβ isoforms, most investigators utilise either $TGF\beta_1$ (Yoo, 1998, Johnstone et al., 1998, Bock et al., 2018, Zhu et al., 2018, Bertolo et al., 2015) or $TGF\beta_3$ (Sekiya et al., 2002, Bian et al., 2011, Mahboudi et al., 2018). Most studies have supported the use of $TGF\beta_1$ for the differentiation of stem cells to a chondrocyte phenotype (Blunk et al., 2002) and hypertrophy prevention (Mueller and Tuan, 2008).

However, contrasting studies have been published suggesting specific TGFβ isoforms are superior to the others for chondrogenic differentiation of stem cells. For example, Barry et al in 2001 suggested that $TGF\beta_3$ results in a more rapid differentiation of BM-MSCs than other TGFβ isoforms (Barry et al., 2001). Conversely, in 2007 Kolambkar et al suggested the opposite with greater GAG synthesis detected in pellet cultures treated with $TGF\beta_1$ compared to $TGF\beta_3$ (Kolambkar et al., 2007). Finally in 2014, Jakobsen et al suggested that at least on a gene expression level, no difference in the expression of chondrogenic or non-chondrogenic genes was detected when comparing $TGF\beta_1$ and $TGF\beta_3$ treatment (Jakobsen et al., 2014).

Table 2.1 **Examples of TGFβ isoforms for chondrogenic differentiation using BM-MSCs**

Model	Time (day)	Agents	Cell density	Key findings	Reference
Pellet	21	Dex (100 nM) $TGF\beta_3$, $TGF\beta_2$, $TGF\beta_1$ (10 ng/ml)	200,000	No changes in DNA content for all conditions. $TGF\beta_1$ showed less GAG compared to $TGF\beta_2$ and $TGF\beta_3$ at all time points (7, 14, 21 days) due to lower synthesis rate per cell. $TGF\beta_1$ showed lowest chondrogenic differentiation at all time points and largest distinct difference between core and periphery in terms of collagen II staining. Type I collagen gene expression throughout culture for all treatments but type II gradually increased. Type X collagen rapidly upregulated and maintained.	(Barry et al., 2001)
PES scaffold	21	Dex (100 mM) $TGF\beta_3$ (10 ng/ml)	2×10^5	Collagen type II and aggrecan markers positive via immunocytochemistry at day 21, but also detected in controls. Chondrogenic gene expression higher for scaffold treated cells compared to scaffold free, collagen I expression lower in scaffold group at end of culture. Statistically significant gene expression of aggrecan and collagen II at 21 days of culture higher in scaffold compared to scaffold free. No significant difference in SOX-9 expression for either culture.	(Mahboudi et al., 2018)
Alginate disc	21	$TGF\beta_1$, $TGF\beta_2$, $TGF\beta_3$ (10 ng/ml) Dex (100 nM) BMP-2 (500 ng/ml) BMP-4 (500 ng/ml) BMP-6 (500 ng/ml) FGF-2 (10 ng/ml) IGF-1 (100 ng/ml)	1.25×10^6 or 2×10^7/ml	**Wanted genes**: aggrecan, biglycan, collagen XI, COL2a1, COL9a1, COMP, decorin, fibromodulin. **Unwanted genes**: ALP, COLXa1, osteoglycin, Runx2, osteopontin and versican. $TGF\beta_1$, Dex and BMP-2 directly increased wanted markers whilst FGF-2 decreased the wanted markers. Dex was essential for $TGF\beta_1$ induction of wanted markers, $TGF\beta_1$ alone had a much smaller effect. Downregulation of osteocalcin also observed. $TGF\beta_1$ with BMP-2 caused a lower increase in wanted marker expression compared to $TGF\beta_1$ alone. Supplementation with all 3 markers decreased the total effect but still increased wanted marker expression. Dex alone did not have significant effect on markers. $TGF\beta_1$ or BMP-2 caused increases in unwanted marker expression but when used in combination did not further enhance this. In all cases unwanted gene expression was evident despite increases in wanted gene expression. $TGF\beta_2$ and $TGF\beta_3$ can replace $TGF\beta_1$ positive effects of chondrogenic differentiation.	(Jakobsen et al., 2014)

Given the varied and contradictory findings of the effects demonstrated by previous research by other groups, I sought to distinguish if any difference in the effect of TGFβ isoforms on chondrogenic differentiation could be detected. To achieve this, based on the advantages and disadvantages laid out in **Chapter 1**, I utilised 2 basic hydrogel models to investigate their effects; alginate beads and agarose constructs. I also utilised AFSCs as the cell type to undergo chondrogenic differentiation since they have been shown capable of undertaking this process, are relatively easy to procure and have been less readily researched compared to other more commonly used stem cell types. This chapter furthers our understanding of how AFSCs react to growth factor stimulation within 3D hydrogel models at an early stage of a chondrogenic differentiation protocol (up to 14 days) by investigating common biochemical markers which signify ECM synthesis indicative of chondrogenic differentiation. Using this method, I sought to determine whether there were any differences in the effect of $TGF\beta_1$ or $TGF\beta_3$ supplementation on this process.

2.2 Methods

2.2.1 Ethics

Ethical approval was granted by the joint UCL/UCLH Committees on the Ethics of Human Research (REC: 14/LO/0863). Human amniotic fluid (N = 8) was collected with informed consent from women undergoing elective amniocentesis, amniodrainage or laser procedures for foetal karyotyping, polyhydramnios or therapeutic procedures at University College London Hospital NHS Foundation Trust. The outlines of the research and what the samples would be used for were explained before informed consent was provided. The collection procedure for amniocentesis involved ultrasound guided placement of a needle into the amniotic cavity whereby amniotic fluid was extracted using sterile syringes (50 - 2000 ml). Cells with an abnormal karyotype were excluded from the study. Example consent forms are included in the appendix of this thesis. Clinical data was recorded for cells used in all experiments (**Tables 2.2 and 2.3**).

Table 2.2: Clinical data pertaining to cells collected for alginate 7- and 14-day experiments*

Alginate 7- and 14-day experiments				
Code ID	*Gestational age*	*Source*	*Karyotype*	*Maternal Age*
H0303	15 weeks + 5 days	Amniocentesis	Normal	38
H0294	18 weeks + 1 days	Amniocentesis	Normal	33
H0318	14 weeks + 2 days	Amniocentesis	Normal	32
H0272	20 weeks + 6 days	Amniodrainage	Normal	23
H0300	21 weeks + 5 days	Amniocentesis	Normal	28

Table 2.3: Clinical data pertaining to cells collected for agarose experiments*

Agarose 14-day experiments				
Code ID	*Gestational age*	*Source*	*Karyotype*	*Maternal Age*
H0344	29 weeks	Laser	Normal	32
H0298	15 weeks + 1 day	Amniocentesis	Normal	38
H0273	25 weeks + 2 days	Laser	Normal	33
H0315	15 weeks + 3 days	Amniocentesis	Normal	41

**Data retrieved includes the gestational age of the foetus from which the sample was extracted, the procedure undertaken to remove the fluid, the resulting karyotype of the cells extracted from the fluid and the maternal age.*

2.2.2 AFSC isolation and culture

Fluid samples were provided an identification number to protect the patient's identity and for record keeping (for example H0123). To culture and preserve the stemness of the AFSCs, culture medium containing αMEM (Thermofisher Scientific, UK), FBS (Thermofisher Scientific, UK), L-glutamine (Sigma-Aldrich Ltd, UK), penicillin with streptomycin (Sigma-Aldrich Ltd, UK), Chang B and Chang C supplements (FUJIFILM Irvine Scientific, UK) was used. Of the Chang supplements used here, Chang B is a basal medium whilst Chang C is a lyophilised component which contains 6% v/v Newborn calf serum, fibroblast growth factors, insulin and no antibiotics.

This media formulation will hence forth be referred to as Chang medium (**Table 2.4**). Amniotic fluid samples were filtered through a 40 /μm cell strainer into a 50 ml volume Falcon tube to remove debris from the sample. Filtered samples were then centrifuged at 300 x g for 5 minutes and the resulting supernatant removed prior to resuspension in 2 ml of defined Chang medium. 500,000 cells were transferred to each sterile non-tissue culture treated bacteriological petri dishes containing 10 ml of warm Chang medium and incubated at 37°C with 5% CO_2 (HeraCell Incubator, Thermofisher Scientific, UK).

Reagent	Concentration	Source
αMEM	n/a	Sigma
FBS	16%	Sigma
L-glutamine	2 mM	Sigma
Penicillin/Streptomycin	1000 U/μg	Sigma
Chang B	18%	Irvine Scientific
Chang C	2%	Irvine Scientific

Table 2.4: **Chang medium constituents for AFSC culture.**

NB: It was noted that upon transfer of the cells between institutes, the cells would struggle to adhere to the bacteriological plates that are used for AFSC culture at the Institute of Child Health (ICH). As the vials all remained frozen during transit it was thought unlikely to be causing this problem. However, the one area where methods differed in culture was in culture medium filtration. At ICH, a vacuum pump system was used with a Merck-Millipore Stericup set up to filter the solution rapidly within a few seconds. At the Institute of Bioengineering (IOB), without access to a vacuum pump system I used hand-made filters using 0.22 μm filter papers, autoclavable filter

holders and syringes. This process took considerably longer to perform and possibly withheld some growth factors from transferring through. Due to this, culture of the AFSCs was moved back to ICH for all further experiments.

2.2.3 Cell counting - Trypan blue exclusion principle

Cells were diluted 1:1 with 0.4% trypan blue solution (Sigma-Aldrich Ltd, UK). 10 µl of the cell suspension/trypan blue solution was then placed into the 0.1 mm deep chamber of the haemocytometer under the coverslip and visualised using a Leica DM1000 LED microscope at 10x magnification. The presence of Newton's rings was checked to ensure the coverslip was adequately adhered to the haemocytometer by suction. The cells were then counted within the central 5 x 5 grid or 4 x 4 corner grids for high and low cell densities respectively (**Figure 2.2**). Any cells that were blue in colour were counted as dead. Equation A was used to determine cell number in 1 ml for low cell densities and equation B was used to determine cell number in 1 ml for high cell densities:

A $$\text{Number of cells in 1ml} = \frac{\text{Number of cells counted}}{\text{Number of squares counted}} \times 2 \times 10{,}000$$

B $$\text{Number of cells in 1ml} = \frac{\text{Number of cells counted}}{5} \times 2 \times 25 \times 10{,}000$$

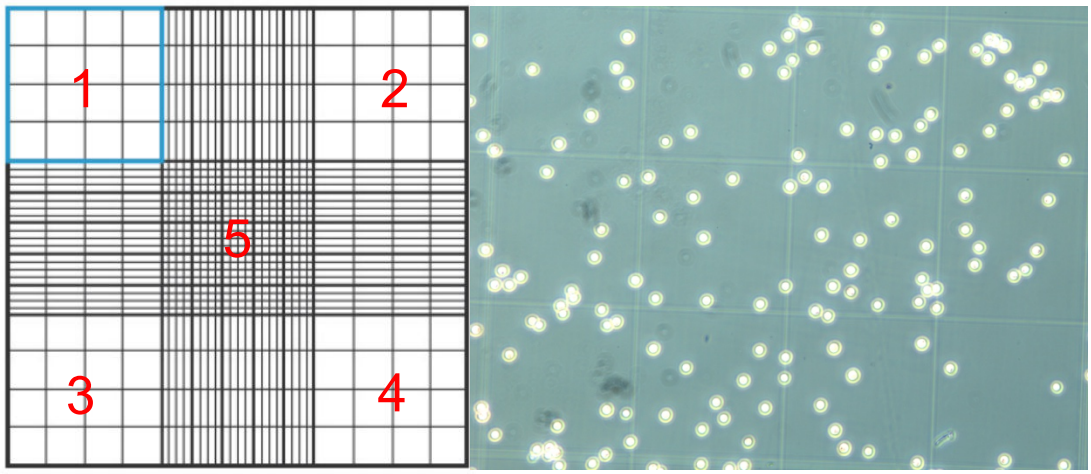

Figure 2.2: Cell counting. *Left: A standard haemocytometer grid. Corners labelled 1, 2, 3 and 4 are used for low densities whilst grid 5 is used for high densities. Right: Displayed is one of the 4 x 4 grids used to count AFSCs on the haemocytometer. AFSCs are in suspension and stained with Trypan blue to help with visualisation and to distinguish dead cells. Image taken at x10 magnification.*

2.2.4 Magnetic activated cell sorting (MACS)

When cell confluency reached 70 - 80%, Chang C culture medium was removed from the petri dish which was then washed using 5 ml PBS (Sigma-Aldrich Ltd, UK) to remove any residual culture medium. 3 ml of TrypLE (Thermofisher Scientific, UK) was applied and the dish placed in an incubator for 5 minutes to detach the cells. This was checked via observation of the cells in a light microscope where the cells should be free floating and have a circular morphology. In circumstances where the detachment was incomplete, a further 2 minutes in the incubator was possible. TrypLE was deactivated via the application of an equal quantity of Chang C culture medium and this mixture was then centrifuged at 300 x g for 5 minutes. While this centrifugation took place, the MACS buffer solution was made (**Table 2.5**).

Table 2.5: MACS buffer solution*

Reagent	Concentration	Company
PBS	1x	Sigma
BSA	5 mg/ml	Sigma
EDTA	2 nm	Sigma

**Mix and filter using a 0.2 µm filter. Store at 2 - 8°C and keep on ice before use.*

Following centrifugation, the supernatant was removed and the cell pellet re-suspended in 300 µl of buffer per 10^8 cells. 100 µl of FcR blocking reagent (Miltenyi Biotec Ltd, UK) and 100 µl of CD117 microbeads (Miltenyi Biotec Ltd, UK) were then added to the sample and incubated on ice for 15 minutes. 1ml of buffer was then used to wash the cells and then centrifuged (300 x g, 10 minutes). The supernatant was removed and 500 µl of buffer was added per 10^8 cells. A magnetic bead column ((Miltenyi Biotec Ltd, UK) was placed within an OCTOMACS separator (Miltenyi Biotec Ltd, UK) attached to a MACS multistand. Round bottom polypropylene tubes were labelled as either waste, CD117 positive and CD117 negative. The tube labelled ‘waste’ was first placed beneath the column which was subsequently washed with 500 µl of buffer into the waste tube (no physical input was applied). Next, the CD117 negative tube was placed beneath the column. The cell suspension was then added and allowed to pass through again with no physical input. 500 µl of buffer was added through the column 3 more times. The column was then removed

from the OCTOMACS and placed over the CD117 positive tube where 1 ml of buffer was added and the syringe applied to the column to forcefully eject the trapped cells into the collecting tube (**Figure 2.3**). The CD117 positive tube was then centrifuged at 300 x g for 5 minutes and resuspended in 1ml of Chang medium where the cells were then placed back into monolayer expansion whilst the negative cells were discarded. Following selection, Chang culture medium was changed every 48 - 72 hours from the day of plating. When the cells reached 70 - 80% confluency the cells were passaged, counted and split into 2 new plates in 10 ml culture medium (500,000 cells per plate).

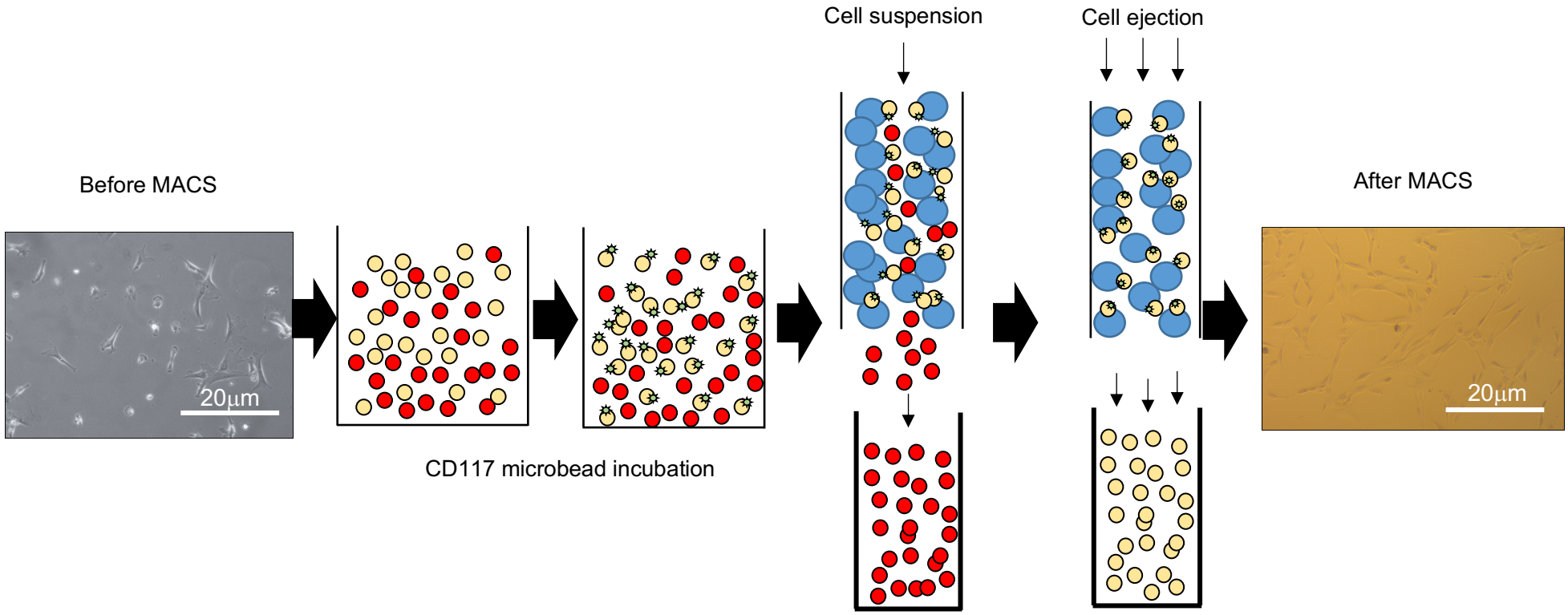

Figure 2.3: Magnetic activated cell sorting (MACS). *AFSCs are sorted for the cell surface marker CD117 from a heterogeneous sample population. Cells are incubated with magnetic microbeads ( ) specific for CD117. Following incubation, the cells were placed into a MACS column and passed through using gravity to remove the negative cells ( ). Finally a plunger was applied to forcefully eject the CD117 positive cells ( ) held within the column. Positive cells are returned to culture while negative cells are either frozen or discarded. Cell culture images taken at x10 magnification.*

2.2.5 FACS

AFSCs were incubated in 300 µl MACS buffer solution (**Table 2.25**). 100 µl of FCR blocking reagent (Miltenyi Biotec Ltd, UK) and 1 µg/ml of different fluorophores were then added to this solution (**Table 2.6**) before being incubated on ice for 15 minutes. 1 ml of buffer was used to wash the cells, centrifuged (300 x g, 10 mins). 4'6-diamidino-2-phenylindole (DAPI) staining was also added to quantify the number of alive cells within the sample. The supernatant was removed, washed in 500 µl of buffer and then transferred to the flow cytometer for analysis. For each test, 1 x 10^5 cells were used in 100 µl of buffer. Cells were analysed using LSRII cytometer with BD FACSDiva Software v.6.1.3. Subsequent analysis was performed using FlowJo10 software (Treestar, USA). All fluorophores listed supplied by BD Biosciences.

Fluorophore	Peak emission/nm	Target	Target function
PE-A	578	CD117	Stem cell marker involved in signalling activation and proliferation
APC-CY7	774	CD34	Transmembrane glycoprotein expressed on hematopoietic stem, endothelial progenitor and foetal stem cells
APC-A	660	CD73	Membrane bound enzyme which hydroylses adenosine monophosphate (AMP) to bioactive adenosine. Expressed on lymphocytes, follicular dendritic cells and marrow stromal cells
Brilliant Violet 421	421	CD90	GPI anchored protein of Ig superfamily. Expressed on neurons, foetal liver cells and hematopoietic stem cells
PE-CY5	667	CD105	Endoglin, receptor for growth factors $TGF\beta_1$ and $TGF\beta_3$
FITC	520	CD45	Leukocyte common antigen. Type 1 transmembrane protein involved in cell growth, mitotic cycle and oncogenic transformation.
DAPI	461	Dead cells	Dye that can stain the nuclei of dead cells; live if used at high enough concentrations

Table 2.6: Fluorophores used for cluster of differentiation detection on AFSCs*

2.2.6 AFSC encapsulation in alginate

The working sodium alginate solution was formed using sodium alginate keltone LV (ISP, Germany). A 6% alginate solution (0.06 g alginate per ml of sterile Earls balanced salt solution (EBSS)) was mixed overnight on rollers at 37°C and sterilised by autoclaving. The 100 mM $CaCl_2$ gelling solution was made by adding 7.35 g $CaCl_2$ (Sigma-Aldrich Ltd, UK) to 500ml of standard chondrocyte growth medium (DMEM + 20% FBS). The solution was then mixed thoroughly and filtered through a 0.2 µm filter. An equal volume of cell suspension was added to the sterile alginate and placed on rollers for 10 minutes to allow adequate mixing. The cell suspension/alginate mixture was then transferred to a new sterile 1 ml syringe with a 21Ga needle attached. The calcium chloride solution was then placed into a 25 ml sterile beaker. The cell alginate mixture was added dropwise to the calcium chloride solution from a fixed height of 10 cm whereby bead structures instantly formed upon impact with the solution. Care was taken to prevent the formation of air bubbles within the solution as this would introduce bubbles into the beads causing immediate rupture. The beads were then incubated in the calcium/DMEM solution for 10 minutes before being washed in EBSS and then added to a 24 well plate and suspended in a minimum volume of 3 ml of chondrogenic differentiation medium. Each bead was calculated to contain 4 x 10^6 cells/ml. Day 0 samples were immediately frozen at -20°C or snap frozen to preserve them as control samples.

2.2.7 AFSC encapsulation in agarose

6% low gelling agarose (Sigma-Aldrich Ltd, UK) solution was made (0.06 g agarose per ml EBSS) and autoclaved for 30 minutes then placed in a 37°C oven to cool down. The cell suspension was then added to the sol agarose suspension in a 1:1 ration and mixed on rollers inside the 37°C oven. After 5 minutes, the agarose/cell mixture was removed from the oven and quickly pipetted into the prepared mould using a Pasteur pipette. Any excess mixture was removed from the overflowing mould and a glass cover was then applied to the top of the mould to secure the constructs inside. The mould was then transferred a large petri dish, sealed and then moved to a 5°C fridge for 5 minutes before returning to the culture hood. A Pasteur pipette was then used to push the constructs out from the mould holes and the constructs immediately placed inside well plates containing the same volume of culture medium used in alginate bead culture. Each construct was calculated to contain 4 x 10^6 cells/ml. Day 0 samples were immediately frozen either at -20°C or snap frozen using liquid nitrogen within a plastic dewar.

2.2.8 Chondrogenic differentiation culture

Chondrogenic differentiation medium consisted of high glucose Dulbecco modified eagle medium (HG-DMEM), insulin, transferrin, selenium (ITS), bovine serum albumin (BSA), GlutaMAX, penicillin streptomycin, L-proline, sodium pyruvate, L-ascorbic acid and linoleic acid sourced from Sigma-Aldrich Ltd, UK (**Table 2.7**). Each construct or bead was supplied with 3 ml of chondrogenic differentiation media and cultured within a 24 well plate. For all differentiation experiments in this chapter, samples were treated either with Chang medium (control), basal chondrogenic medium (control), 10 ng/ml TGFβ_3 (R&D Biosystems, USA) or 10 ng/ml TGFβ_1 (R&D Biosystems, USA). Culture experiments lasted for either 7 or 14 in the case of alginate beads and 14 days for agarose constructs. Day 0 samples were immediately frozen and stored at -20°C for analysis.

Table 2.7: Constituents of basal chondrogenic medium*

Reagent	Concentration	Company
HGDMEM (phenol free)	n/a	Sigma
Penicillin/Streptomycin	1000U/100 μg/ml	Sigma
L-proline	40 mg/ml	Sigma
Sodium pyruvate	100 mM	Sigma
BSA	1 mg/ml	Sigma
GlutaMAX	200 mM	Gibco

Day of use additions:

Reagent	Concentration	Company
ITS+1 liquid media supplement	100x	Sigma
L-ascorbic acid	50 mg/ml	Sigma

**Standard combination of chondrogenic differentiation components can be added at the same time and will last up to 1 month when stored at 4°C.*

2.2.9 Digestion of AFSC seeded alginate beads

Constituents of the alginate digest buffer were added to 480 ml of PBS and adjusted to pH 6.0 using sodium hydroxide (NaOH, Sigma-Aldrich Ltd, UK) before adding up to a final volume of 500 ml (**Table 2.8**). Constructs were then submerged in 1 ml of digest buffer within an O ringed tube then agitated overnight at 60°C. Digested samples were then stored long term at -20°C or assayed immediately.

***Table 2.8*: *Constituents of alginate digest buffer*.**

Reagent	Concentration
Sodium chloride	150 mM
Sodium citrate	55 mM
EDTA	5 mM
Cysteine hydrochloride	5 mM
Papain	0.56 units/ml

2.2.10 Digestion of AFSC seeded agarose constructs

Constituents were added to 480 ml PBS and adjusted to pH 6.0 using NaOH before making up to final volume of 500 ml (**Table 2.9**). Constructs were placed within standard 2 ml Eppendorf tubes and heated to 70°C for 1 hour within a temperature-controlled oven. The samples were then allowed to cool within a 37°C oven before 10 µl of agarose (Sigma-Aldrich Ltd, UK) and 5 µl of papain (Sigma-Aldrich Ltd, UK) was added to each sample. The constructs were then digested overnight at 37°C to allow for agarase digestion. Once complete the samples were returned to the 60°C oven for 1 hour to allow papain digestion of the remaining polymers. Samples were then assayed immediately or stored at -20°C.

Table 2.9: Constituents of agarose digest buffer

Reagent	Concentration
PBS	1x
Cysteine hydrochloride monohydrate	9 µM
EDTA	2.76 µM

2.2.11 Viability profiling using live dead assay

Cell viability within the hydrogel specimen was determined using a two-colour assay to stain and identify viable or non-viable cells within the hydrogel using Calcein-AM (Molecular Probes, UK) and Ethidium homodimer-1 (Calbiochem, UK), respectively. Each hydrogel specimen was bisected using a no. 11 scalpel and immersed in 1 ml of DMEM + 20% FBS containing 5 µm of Calcein-AM and Ethidium homodimer-1 for 30 minutes at 37°C with gentle agitation. Each specimen was then mounted on a glass slide before imaging. Calcein-AM is able to permeate cells and upon contact with intracellular ubiquitous esterases is converted into a highly fluorescent polyanionic calcein which is retained within the live cell. This fluorescence produces an intense uniform green fluorescence emission at ~515 nm when excited at ~495 nm. Ethidium homodimer-1enters non-viable cells where the cell membrane has been perforated and non-covalently binds to the nucleic acids; producing a 40-fold increase in fluorescence. In non-viable cells, Ethidium homodimer-1 will bind DNA and emit a fluorescence at ~635 nm when excited with green light at 495 nm. Viability was determined using a systematic sampling procedure whereby a standard sample area of 0.5 x 0.25 mm under a x20 objective and the sampling area was run from the top of the specimen to the base with the number of live cells (green) and dead cells (red) were counted (**Figure 2.4**). Alginate beads and agarose constructs were visualised using a Zeiss confocal microscope at x 20 objective. Viability was assessed using a systematic sampling procedure for both hydrogels but was localised at edge and core regions of the agarose construct due to its size. The percentage viability was then calculated [(viable cells/total cells) * 100]. The mean percentage viability was calculated from 3 replicate cell counts from different field views and data represented with standard error of the mean.

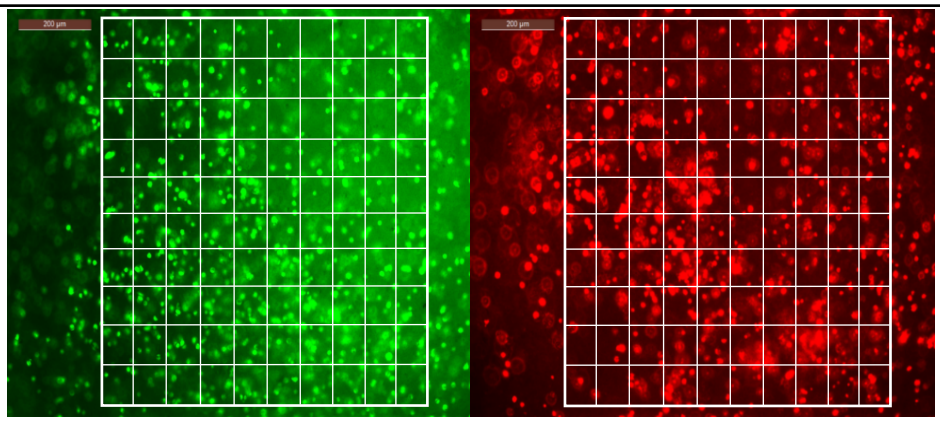

Figure 2.4: Measuring viability using grid system. *Each cell counted within the grid was counted using standard exclusion principles through both green and red wavelength excitations. This was repeated 6 times through each sample before quantification.*

2.2.12 Hoechst assay

The DNA content was measured using the DNA specific fluorometric Hoechst 33258 to generate a standard curve. The binding of Hoechst to adjacent adenine thymine pairs of DNA results in a fluorescence that can be measured taken at 360 nm excitation and 460 nm emission wavelengths. Concentration of DNA was extrapolated from deoxyribonucleic acid sodium salt from calf thymus (Sigma-Aldrich Ltd, UK) to establish a standard curve for DNA content. DNA standard (1 mg/ml) was first diluted to a working concentration (20 μg/ml) was performed using 980 µl 2xSSC/digest buffer (**Table 2.10 and 2.11**) and 20 µl of stock standard. A serial double dilution using 2xSSC/digest buffer as the 0 µg/ml standard was performed producing concentrations of 20, 10, 5, 2.5, 1.25, 0.666 and 0.333 µg/ml of DNA. Subsequently, 100 µl of standard and samples was pipetted into each well of a 96 well plate. Working solution of Hoechst was made using 19.98 ml of SSC/digest buffer and 20 µl of Hoechst stock solution. 100 µl of Hoechst reagent was then added to all wells. The plate was then transferred to a BMG FLUOstar OPTIMA microplate reader to be scanned (FLUOstar, BMG Labtech Ltd, UK). DNA concentration of unknown samples was then calculated from the equation of the linear regression line applied to the standard concentrations (**Figure 2.5**).

Table 2.10: Digest buffer sodium citrate buffer constituents.

Digest buffer	
Reagent	**Weight/g**
Cysteine Hydrochloride	0.788
EDTA	0.403

Digest buffer*: Make up to approximately 480 ml with PBS and adjust to pH 6.0 with NaOH. Make up to 500 ml finally and freeze aliquots at -20°C.*

Table 2.11: Sodium citrate buffer constituents

20x sodium citrate buffer	
Reagent	**Weight/g**
Sodium Chloride	87.65
Trisodium Citrate	44.1

20x SSC stock buffer*: Make up to approximately 480 ml then pH adjusted to 7.0 using 1 M NaOH/1 M HCl. Make up to 500 ml and sterilise by autoclaving. For 2 x working buffer used in the assay, dilute 25 ml of 20 x SSC buffer in 225 ml of* dH_2O.

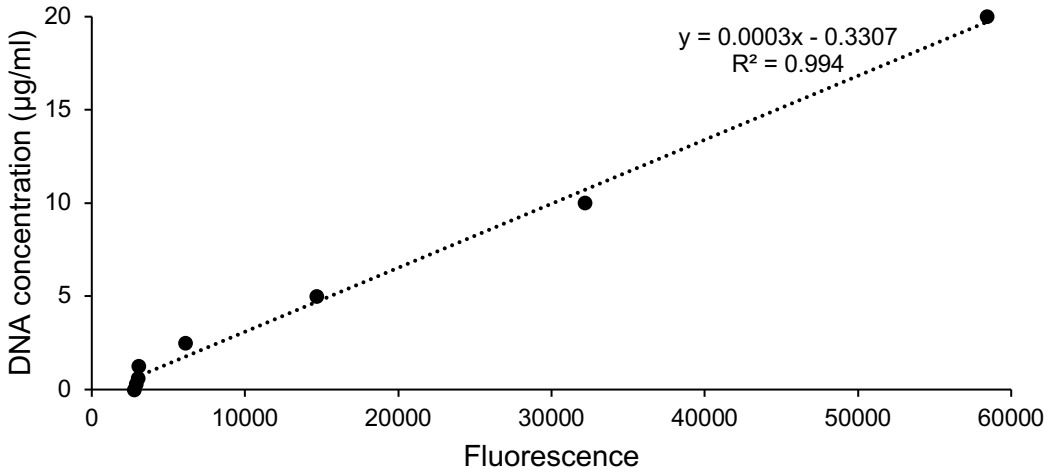

Figure 2.5: Example DNA assay standard curve with linear regression applied. *The curve demonstrates the relationship between the fluorescence intensity and the DNA concentration. Linear regression model applied to the data to allow calculation of DNA content of our unknown samples. Rearrangement for x allows input of the fluorescence values to provide data regarding DNA concentration.*

2.2.13 Optimisation of DMMB assay for sulphated glycosaminoglycans

Principle

1,9-dimethylmethylene blue (DMMB) is a highly metachromatic dye first introduced for the histological detection of glycosaminoglycans (GAGs) by Taylor and Jeffree in 1969, with an analytical method for quantitative determination of GAG content proposed by Farndale in 1982 (Taylor and Jeffree, 1969, Farndale, 1982). In principle, when DMMB forms complexes with negatively charged carboxyl groups and sulphate groups which are present on GAGs, this initiates a metachromatic shift in the absorbance maximum of the dye (600 nm to 525 nm). As such the reduction in absorbance as measured at 595 nm with increasing GAG concentration can be measured and GAG concentration accurately determined. One complication for DMMB assay application for use in alginate embedded cells is that alginate contains carboxyl groups which also bind to the DMMB used in this assay. This can therefore affect the accuracy of the measurement. In 1996, Enobakhare et al. demonstrated that acidification of the DMMB preparation to below pH 2 retains the high affinity binding of the sulphate groups present on sulphated GAG but blocks binding of it to the carboxyl groups present on the alginate polymer (Enobakhare et al., 1996). However, despite following this protocol accurately, it was frequently observed that positive values would be registered in control day 0 samples in which there should have been no GAG present. This observation was present for both alginate and agarose hydrogels. Therefore, I investigated the use of different pH DMMB reagents on day 0 samples for both agarose and alginate samples to assess which pH DMMB would produce the weakest false positive result from day 0 samples.

Optimisation method

Day 0 samples of alginate beads and agarose constructs were stored and digested using the standard enzymatic protocol. Following digestion, samples were stored at -20°C or analysed immediately. DMMB solutions were prepared within a fume hood following standard procedures. Firstly, 0.016 g of DMMB (Sigma-Aldrich Ltd, UK) was added to ethanol (5 ml, Sigma-Aldrich Ltd, UK) and allowed to dissolve into solution. 2 grams of sodium formate (Sigma-Aldrich Ltd, UK) was subsequently added to deionised H_2O (850 ml). The two solutions were then mixed and made up to 1 litre using deionised H_2O. Finally, the pH was adjusted to pH 3.0 or 1.5 using formic acid for the purposes of optimisation. Due to light sensitivity, the solutions were covered in foil and

kept in the dark prior to use. Standard concentrations of chondroitin sulphate (Sigma-Aldrich Ltd, UK) were used to create a standard curve based on the absorbance at 525 nm which could then be used to compare and determine the GAG concentration of the unknown samples, within the range of 0 - 50 µg/ml (**Figure 2.6A**). In brief, 1 mg/ml of standard was diluted 1:10 with digest buffer before preparation of the dilution series. Prior to plating within a clear 96 well plate, all samples and standards were vortexed. Samples and standards were run in triplicate (40 µl/well) before a multichannel pipette was used to add DMMB reagent to the wells (250 µl/well). For detection, a SpectrostarNano system (BMG Labtech Ltd, UK) was used whereby plates were initially shaken at 360 RPM, orbital for 10 seconds prior to measurement at 595 nm. A 95% confidence limit of GAG concentration is maintained due to the minimal deviations for the standard from a linear fit. R^2 values close to 1 were used.

Optimisation results

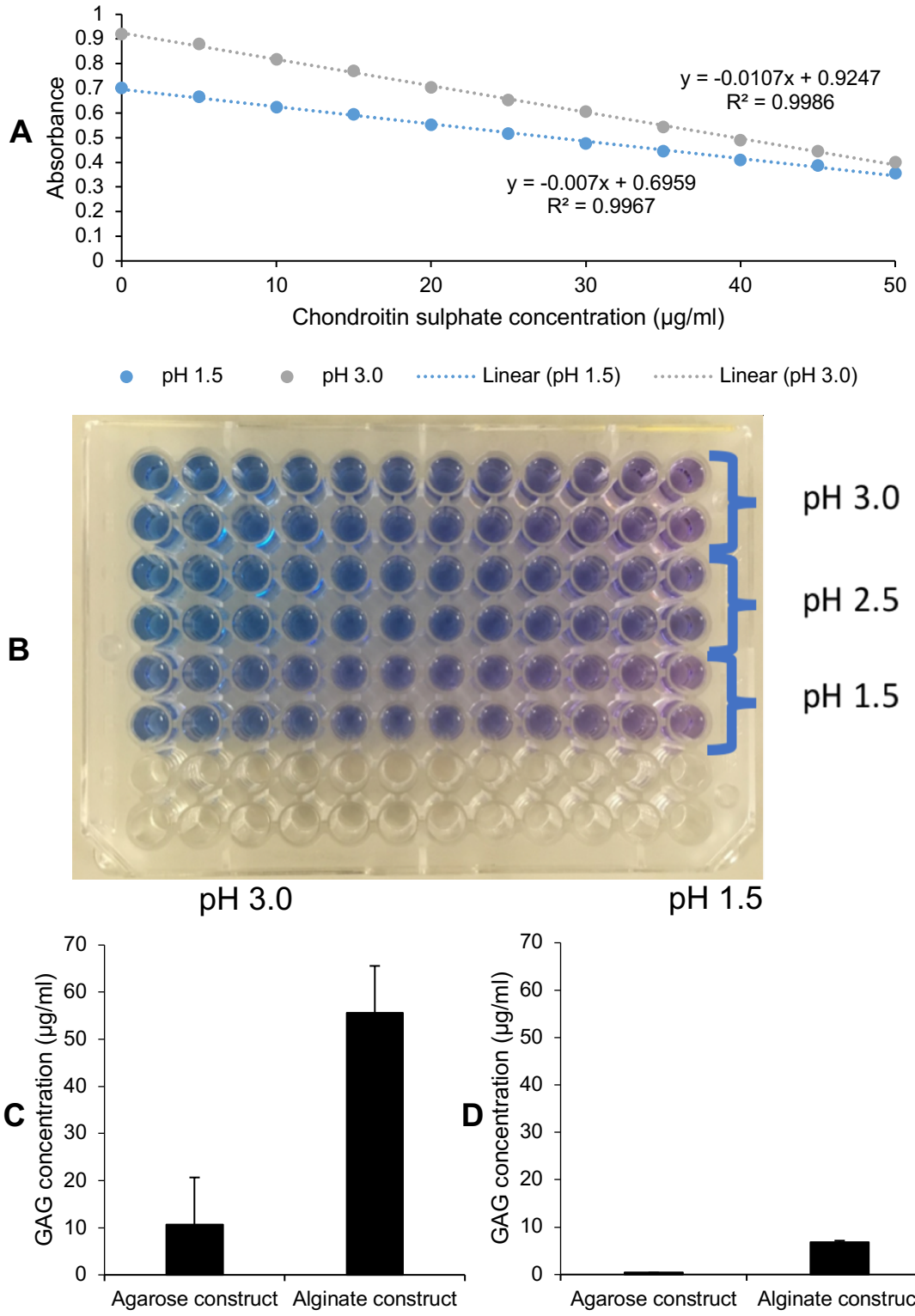

Figure 2.6: Results of DMMB assay optimisation. **A:** Lowering of DMMB pH results in a reduced gradient standard curve but maintains distinction between each standard concentration. **B**: A distinct colour change is associated with increasing concentration of chondroitin sulphate standards typically associated with DMMB assay at both concentrations investigated. **C+D**: Lowering of pH completely removes false positive GAG concentration readings in digested cell free agarose samples but retains positive reading in alginate samples. N = 3. Error bars = ± SEM.

Reduction of DMMB pH from 3.0 to 1.5 resulted in an expected flattening of the standard curve associated with increasing GAG concentration used for the assay (**Figure 2.6A**). This is attributed to a reduction in the metachromatic shift associated with the interaction between DMMB and sulphated GAG (**Figure 2.6B**).The presence of digested alginate exposed to DMMB reagent at pH 3.0 was certainly unsuitable for this assay, in line with previous observations made by Enobakhare et al (**Figure 2.6C**). At the same pH, agarose samples registered smaller amounts of GAG even in blank constructs, but at much lower levels in comparison to the alginate. Reduction of the DMMB pH to 1.5 reduced the DMMB reaction significantly in regard to alginate samples (a 5 - fold decrease in GAG concentration) but still registered a positive GAG value at levels comparable to that of agarose constructs observed at pH 3.0 (**Figure 2.6D**). In regard to agarose, the reduction in pH to 1.5 greatly reduced positive day 0 control readings in the sample, as should be expected from a blank control construct. Therefore, for the biochemical analysis of digested alginate and agarose constructs a reduced pH DMMB of 1.5 was used.

Final DMMB method used for analysis following optimisation

Standard solutions of chondroitin sulphate (Sigma-Aldrich Ltd, UK) were used to create a standard curve based on the absorbance at 525 nm which could then be used to compare and determine the GAG concentration of the unknown samples, within the range of 0 - 20 µg/ml. A SpectrostarNano system (BMG Labtech Ltd, UK) was used for this detection. A 95% confidence limit of GAG concentration was maintained due to the minimal deviations for the standard from a linear fit. R^2 values close to 1 were observed. The concentration of unknown samples was determined by rearranging the equation of the trendline in terms of x. Total GAG synthesis in each digest and its corresponding medium was then calculated and normalised to its DNA concentration to provide GAG synthesis.

2.2.14 Statistics

To determine which statistical test to use, all biochemistry data was checked for normal distribution using a Shapiro-Wilk normality test in SPSS (SPSS version 10, IBM, USA). A QQ plot was included in this analysis (**Figure 2.7**).

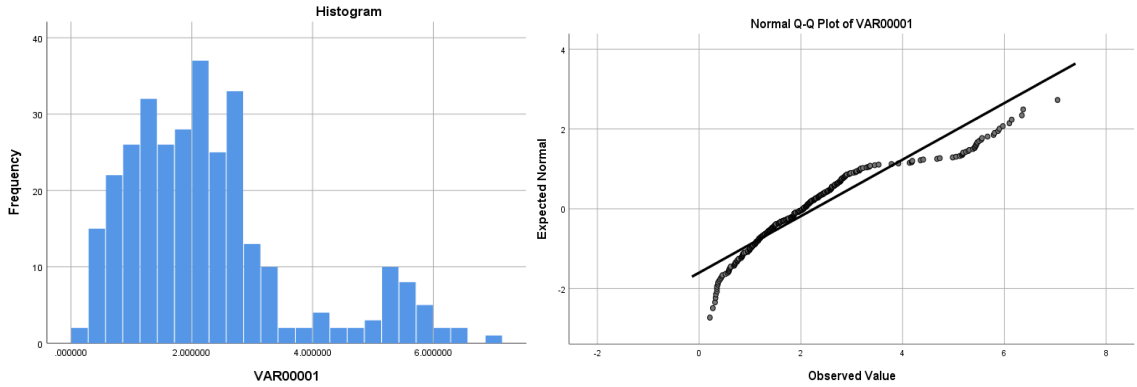

Figure 2.7: Representative histogram and QQ plot of abnormal data. *Clear kurtosis and skewness present within the dataset, therefore the data fails the first assumption required for parametric testing.*

The histogram and QQ plots of the raw GAG synthesis data demonstrated a non-normal distribution with the Shapiro-Wilk test giving a statistically significant value of 0.000095. This reduces the number and strength of statistical tests that can be performed on the data. In order to circumvent this, the raw data was transformed to its natural log and log10. Following the transformation of the data the resulting QQ plot changed significantly from before (**Figure 2.8**):

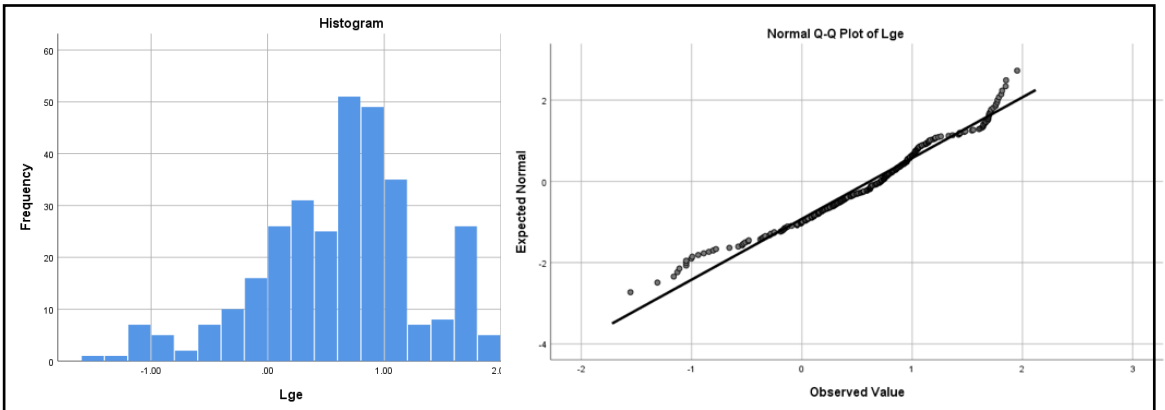

Figure 2.8: Natural log transformation of raw GAG synthesis data. *Despite transformation of the data, there is still an inherent skew that still makes the data follow a non-normal distribution.*

However, despite the log transformations performed, the Shapiro-Wilk test still retained statistically significant results ($p<0.05$) indicating that the data was not normal. Normal distribution assumption is a requirement for standard t tests and ANOVA statistical tests. Because of this, a non-parametric test was used on the raw biochemistry and viability data. The statistical test

selected for analysis was the Mann-Whitney U test. All results in this study were shown as the mean from replicates and individual experiments with error bars representing the standard error of the mean (SEM). The number of patients and replicates are indicated in figure legends. In all comparisons, $p<0.05$ was considered statistically significantly for tests comparing treatment conditions vs controls and inter-treatment comparisons.

2.3 Results

2.3.1 FACS analysis of CD117 selected AFSCs following 3 passages and MACS selection.

A sample of AFSCs (source: H0315) post CD117 MACS selection and prior to culture experiments was investigated to look at the expression of common stem cell surface markers. Analysis of the sample showed a high expression for the markers CD73, CD90, CD117 indicative of common stem cell features (**Figure 2.9**)**.** Further analysis of the cell sample showed positive expression of CD34 and CD105 (88 and 93.8% respectively) but showed negative expression of the non-stem marker CD45 (<3%) (**Figure 2.10**).

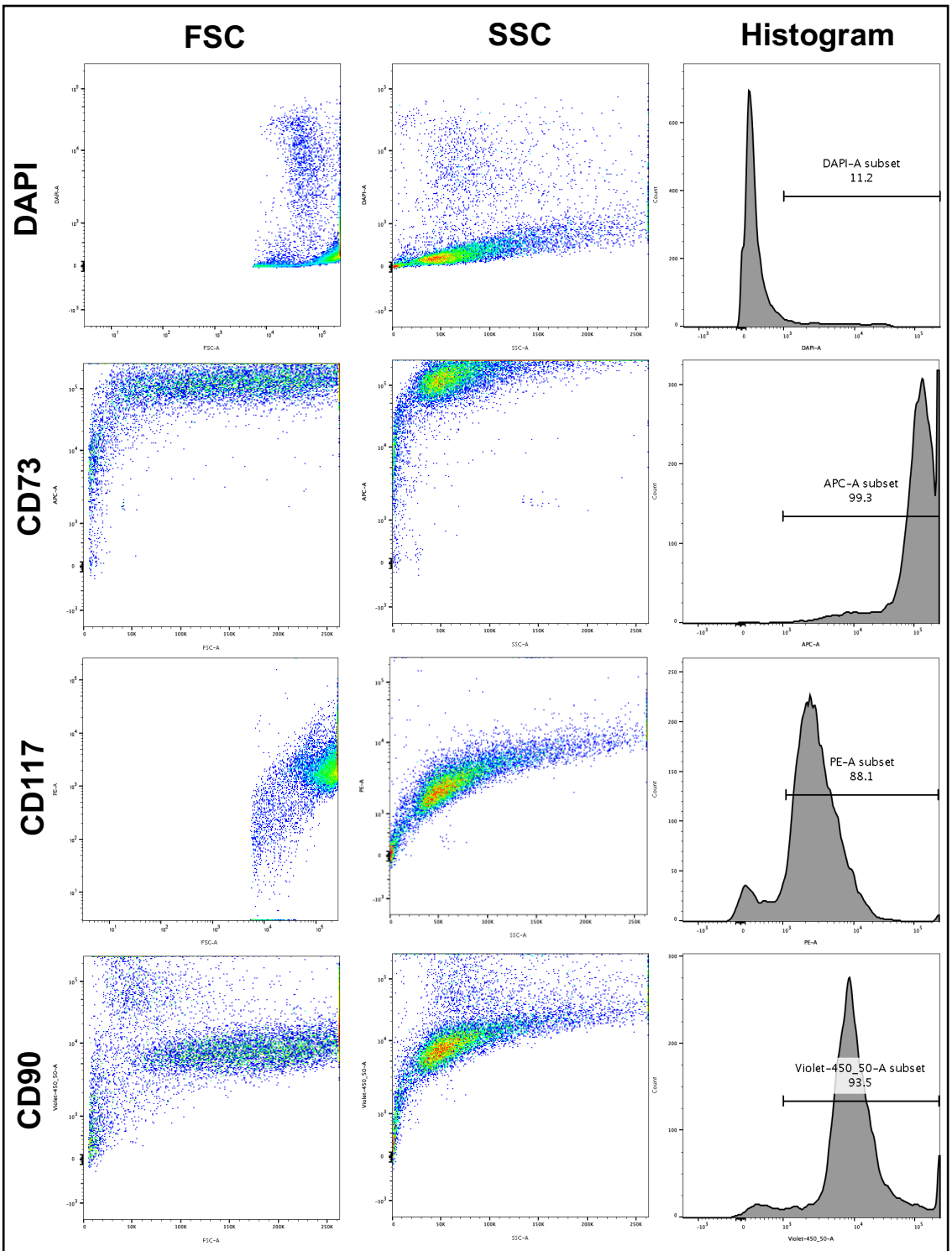

Figure 2.9: Flow cytometry analysis of stem cell marker expression following 3 passages and MACS selection. *Analysis of human AFSCs demonstrated that the cells were strongly positive for the stem cell markers CD73 and CD90 (**Figure 2.9B** and **D**; >90% of population expressed the markers) including the selected marker CD117 (**Figure 2.9C**; 88.1%). DAPI staining indicated that the majority of cells were alive post MACS selection and prior to encapsulation (**Figure 2.9A**; viability of 88.8%). N = 1, independent experiments, representative examples shown in figure). Percentages of positive cells for the specific marker displayed based on histogram plot.*

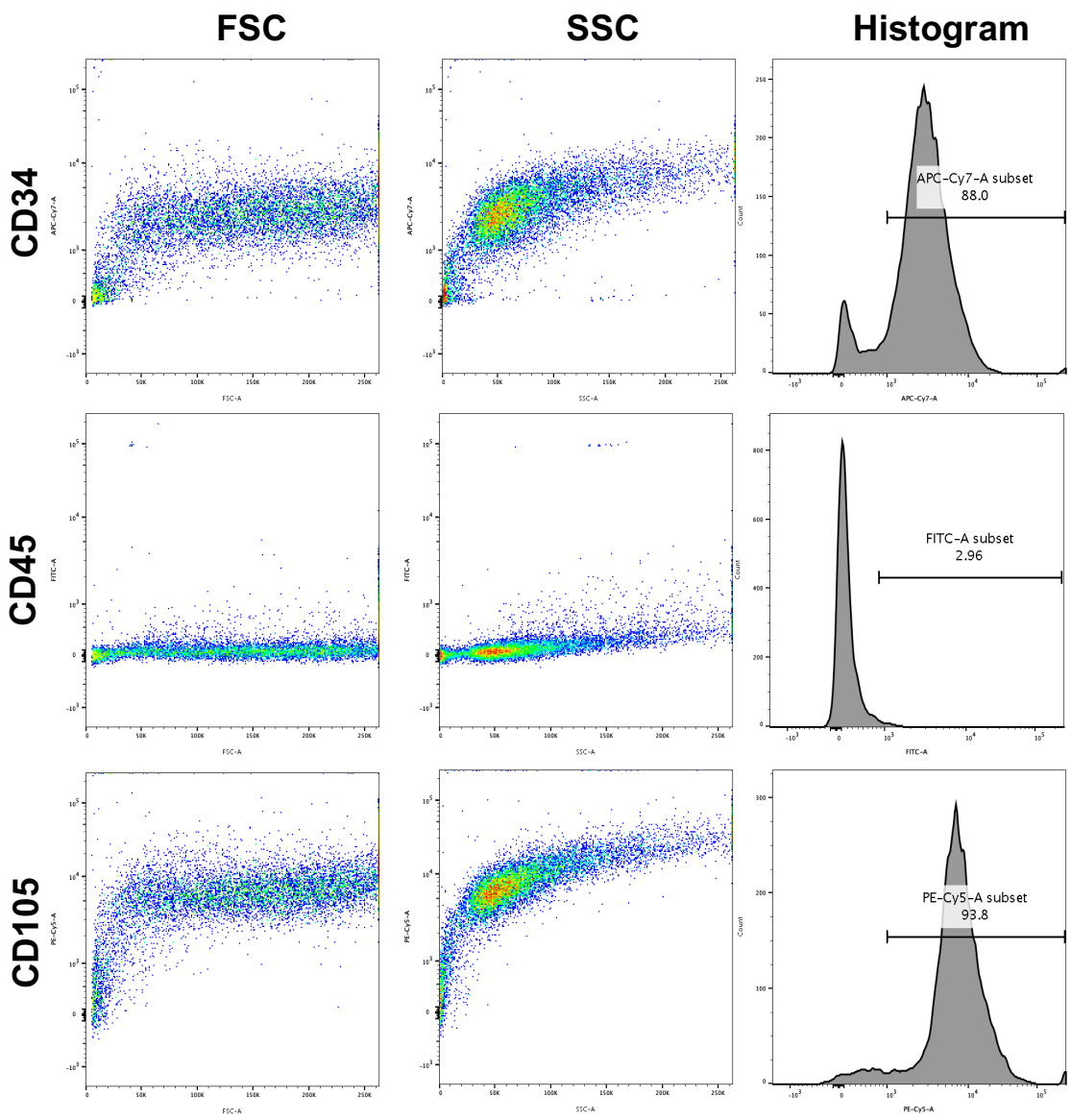

Figure 2.10: Further analysis of stem cell and non-stem cell markers prior to hydrogel encapsulation. *MACS selected AFSCs from the same sample group were negative for the non-stem cell marker CD45 (**Figure 2.10F**; <3% of population) but positive for CD34 and CD105 expression (**Figure 2.10E** and **G**; 88 and 93.8% respectively). N = 1, percentages of positive cells for the specific marker displayed based on histogram plot.*

2.3.2 Temporal effect of hydrogel encapsulation on AFSC viability in alginate and agarose materials.

The viability of AFSCs/alginate beads treated with either TGFβ_1 or TGFβ_3 was performed at 7 and 14 days of culture using a live-dead assay. AFSC/agarose constructs treated with TGFβ_1 or TGFβ_3 were also assessed for viability using this method but only for constructs cultured at 14 days. All samples were compared to Chang, basal chondrogenic medium and day 0 samples.

Viability of AFSC/alginate beads was initially detected at > 90% at day 0 with good distribution of cells within the bead. No statistical differences were detected when comparing day 7 TGFβ treated AFSC/alginate beads with day 0 controls (**Figure 2.11**; $p>0.05$). The same situation was observed when comparing day 14 TGFβ treated AFSC/alginate beads with day 0 controls also (**Figure 2.12**; $p>0.05$). No obvious differences were detected between TGFβ treated samples and Chang/Basal chondrogenic medium controls ($p>0.05$). No clear difference was detected between TGFβ isoform treatments ($p>0.05$).

Viability of cells within the core and edge of AFSC/agarose constructs was initially detected at >80% and 70% respectively at day 0 (**Figure 2.13**). No differences were detected when comparing TGFβ treated samples with day 0 controls ($p>0.05$). Similarly, no obvious differences were detected between all treatment options at 14-days of culture ($p>0.05$). No marked differences were detected between core and edge viability indicating homogenous cell viability throughout the constructs. No statistical differences were also detected between TGFβ isoform treatments ($p>0.05$).

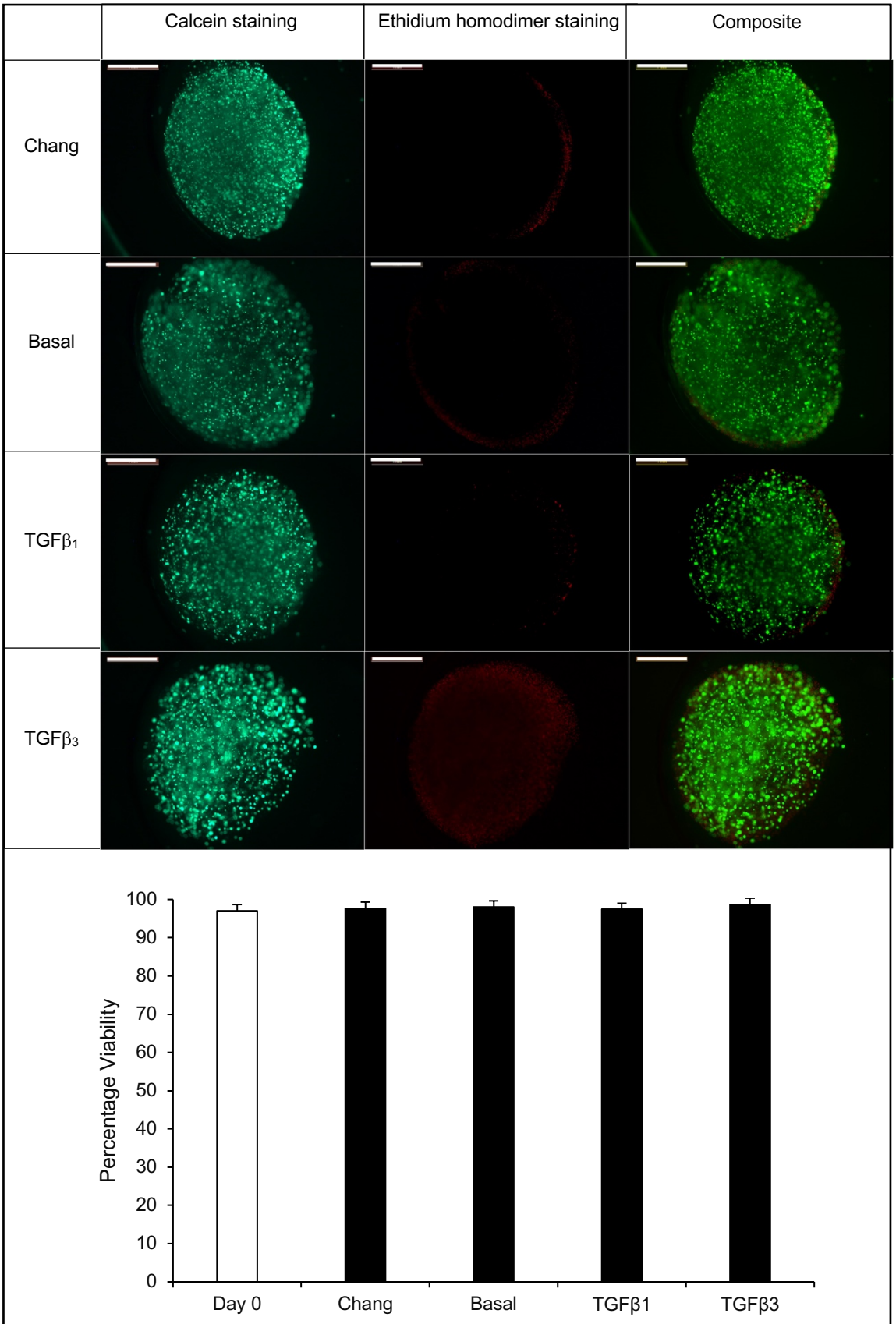

Figure 2.11: Viability of AFSCs within alginate beads is not affected by short term 7-day culture. *No statistical differences detected between different treatment conditions and controls after 7 days in culture. Error bars represent ± SEM. N = 3. White bar in images indicates 1 mm scale bar.*

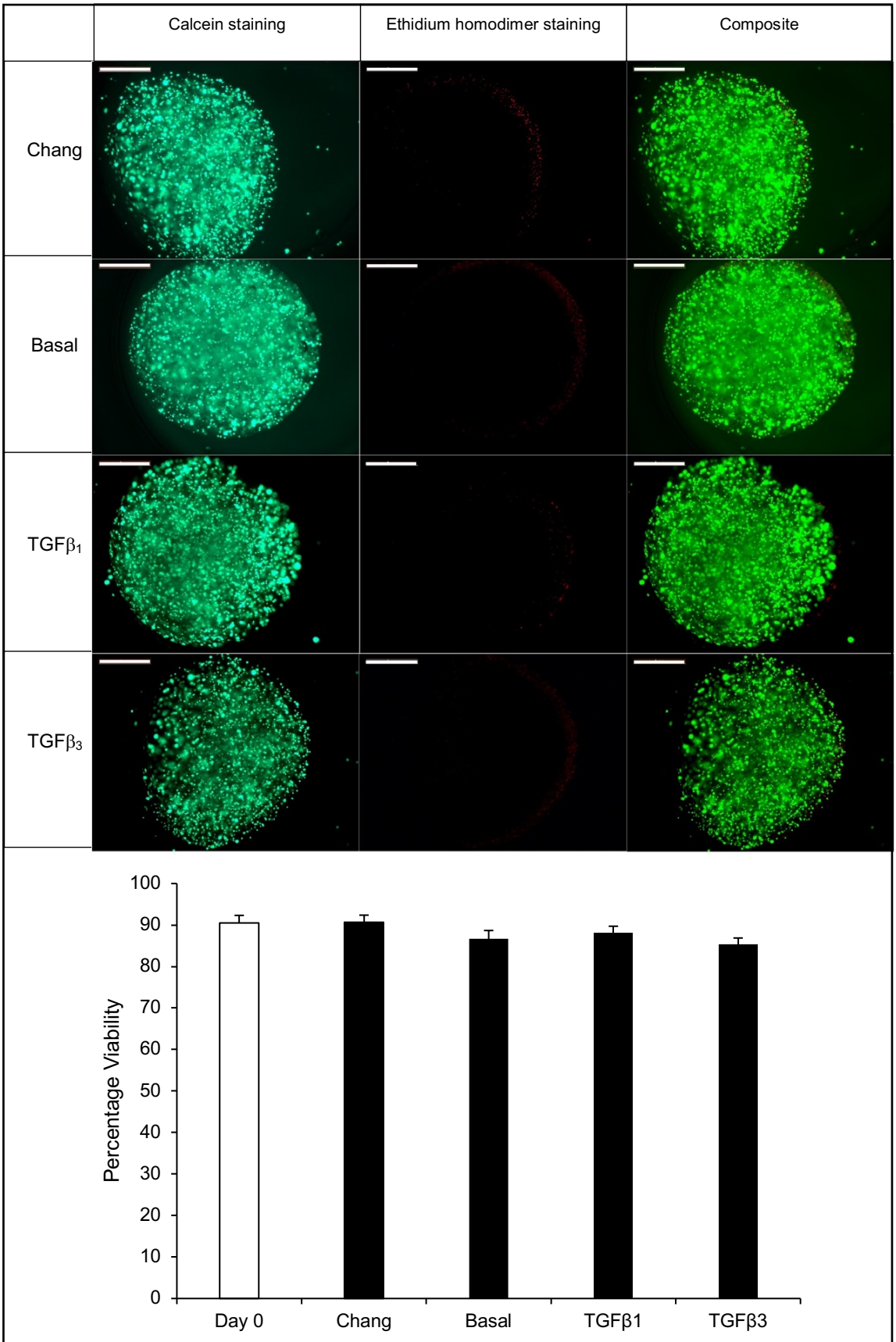

Figure 2.12: Viability of AFSCs within alginate beads is not affected by 14-day culture. *Quantification of viable cells after 14 days of treatment indicated. Error bars represent ± SEM. N = 3. White bar in images indicates 1 mm scale bar.*

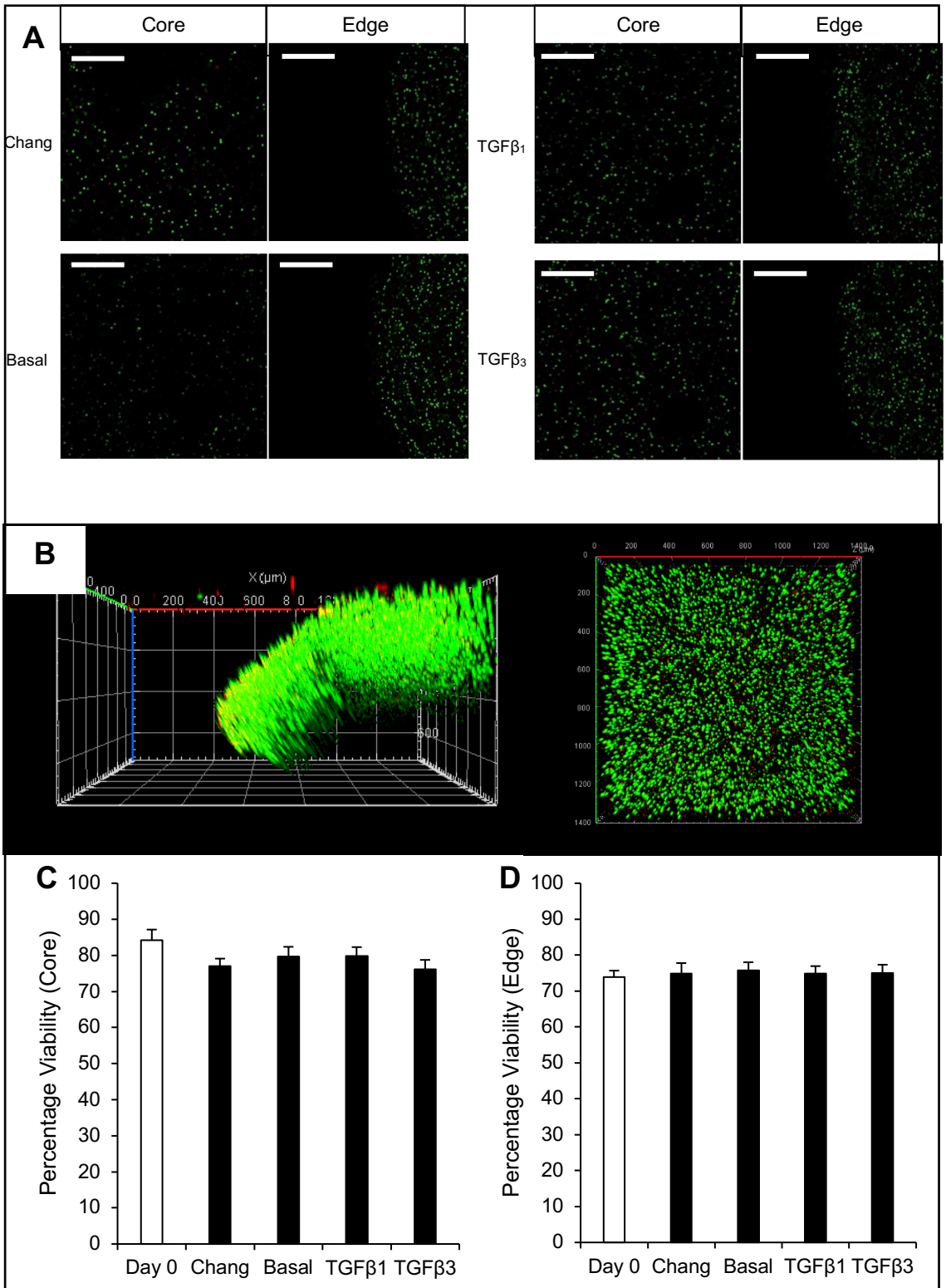

Figure 2.13: Viability of cells is unaffected after 14 days of culture compared to control. A: *Agarose constructs maintained a high level of cellular viability after 14 days of culture in core and edge of the constructs (>80 and >70%).* ***B****: The size of the agarose constructs required the use of a confocal microscope to assess the number of viable cells in core and edge images.* ***C + D****: No statistical differences were observed between treated samples and controls at edge and core ($p>0.05$). No statistical differences were also detected between TGFβ isoform treated samples also at edge and core sections ($p>0.05$). Error bars represent $\pm$ SEM. N = 3. White scale bar represents 1 mm.*

2.3.3 Effect of TGFβ treatment on GAG synthesis and DNA content of AFSC/alginate and AFSC/agarose constructs.

AFSC/alginate beads

AFSC/alginate beads treated with 10 ng/ml of exogenous TGFβ_3, showed no statistically significant increases in GAG synthesis compared to Chang medium, basal chondrogenic medium and day 0 controls ($p>0.05$; **Figure 2.14A**). Samples treated with TGFβ_1 or TGFb3 showed no differences compared to control samples ($p>0.05$). Control samples demonstrated marked decreases in GAG synthesis compared to day 0 samples ($p<0.01$). DNA content significantly increased when comparing samples treated with exogenous TGFβ_1 or TGFβ_3 to all controls at day 7 and at day 14 (**Figure 2.14B**). No obvious differences were detected between TGFβ_1 and TGFβ_3 samples in terms of GAG synthesis or DNA content changes ($p>0.05$).

AFSC/agarose constructs

Treatment of AFSC/agarose constructs with 10 ng/ml of exogenous TGFβ_1 or TGFβ_3, showed a statistically significant increase in GAG synthesis relative to basal control medium treatment but not Chang medium (**Figure 2.15A**). Only exogenous application of TGFβ_1 or TGFβ_3 samples showed an increase in DNA content compared to all control samples (**Figure 2.15B**). No marked differences in DNA content were detected between control samples. Further to this, no statistical differences were detected between TGFβ_1 and TGFβ_3 within AFSC/agarose constructs in terms of GAG synthesis or DNA content changes ($p>0.05$).

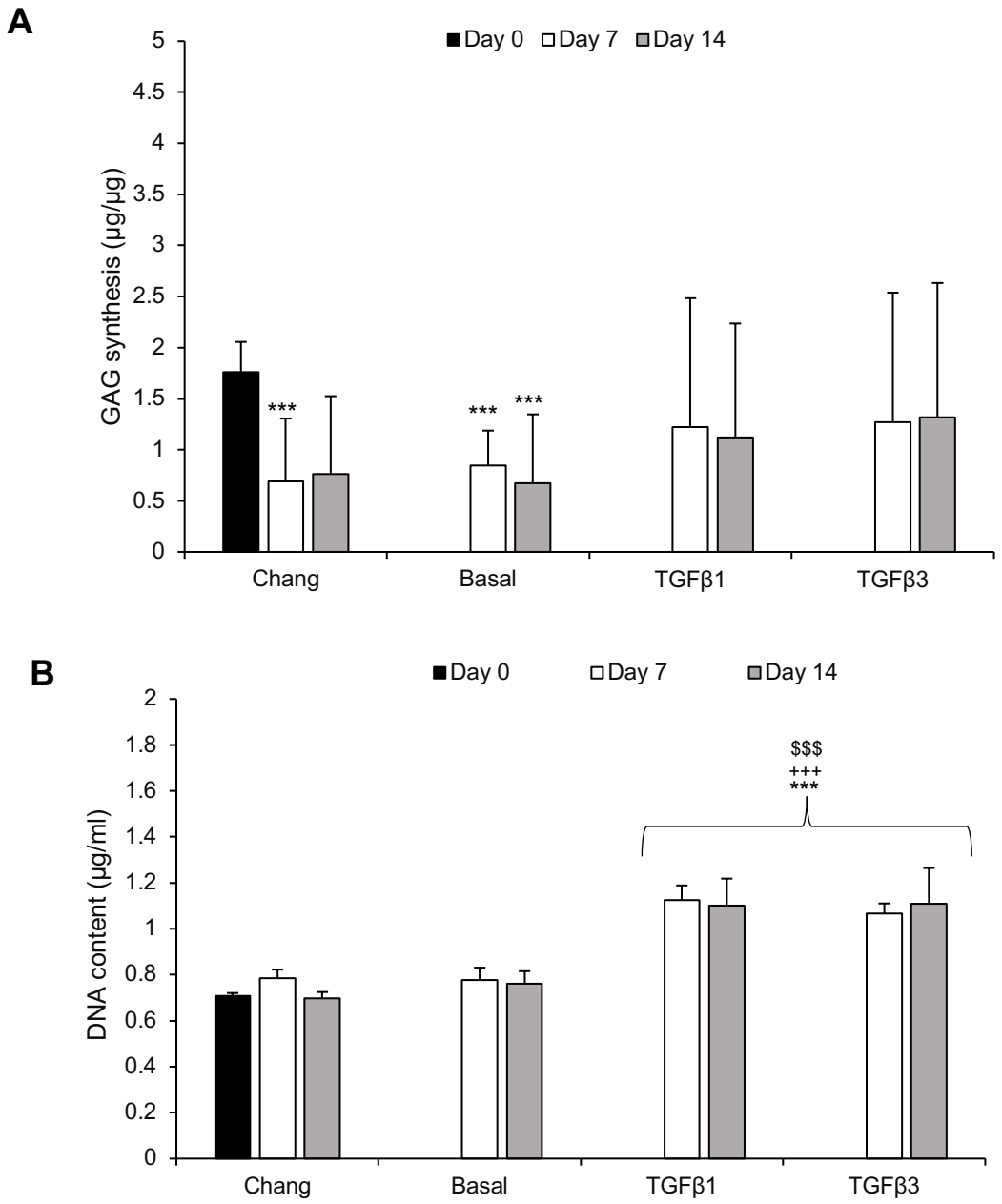

Figure 2.14: Alginate encapsulation of AFSCs and treatment with TGFβ results in significant DNA content increases. *Statistically significant decreases in GAG synthesis were detected between basal, Chang control groups compared to day 0 control with no differences detected with the TGF$\beta_{1/3}$ treated samples (**A**). DNA quantification demonstrated statistically significant differences following TGF$\beta_{1/3}$ treatment after 7 days compared to day 0 controls, basal and Chang treatments (**B**). No statistical differences are detected between treatment of each TGFβ isoform in terms of GAG synthesis and DNA content. * = p<0.05 and *** = p<0.01. Error bars represent $\pm$ half range. N = 8 for each condition. Samples sourced from 2 different patients. *** indicates sample compared to day 0, +++ indicates sample compared with Chang, $$$ indicates sample compared with basal control. Day 0 data included to indicate effect of alginate presence on assay.*

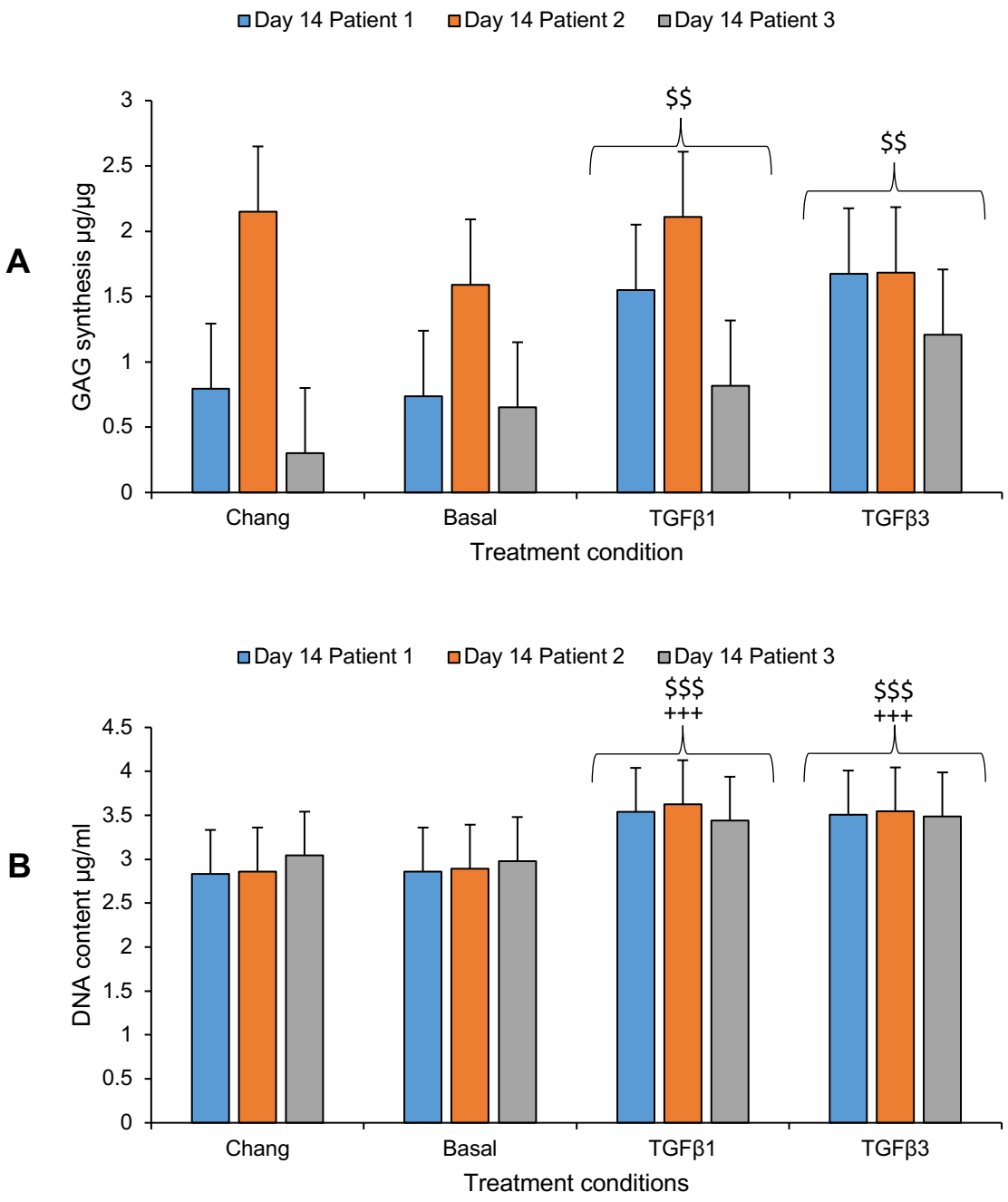

Figure 2.15: AFSCs embedded within agarose constructs initiates GAG synthesis increases in all treatment conditions but cell proliferation only observed in TGFβ treated samples. *For GAG synthesis, statistically significant differences were detected when comparing the average of TGFβ_1 and TGFβ_3 treated samples to the average of basal chondrogenic medium treated samples. Treatment of samples with either TGFβ_1 or TGFβ_3 isoforms resulted in a statistically significant increase in DNA content compared to all control samples. No significant differences were detected between TGFβ isoforms detected in terms of GAG synthesis and DNA content increases. Error bars represent SEM. N = 12 for each condition. Samples sourced from 3 different patients. +++ indicates sample compared with Chang treatment (p<0.01), $$$ indicates sample compared with basal medium treatment (p<0.01). All data normalised to day 0.*

2.3.4 Alginate beads demonstrate fragility and failure after 14 days of culture

AFSC/alginate beads become increasingly fragile as time in culture increases resulting in a splitting of the alginate bead structure after 14 days (**Figure 2.16A**). This phenomenon is also associated with an increase in AFSC/alginate weight over time in culture (**Figure 2.16B**). This observation is independent of the treatment applied to each culture. Agarose constructs did not demonstrate any structural failings at the same culture time points.

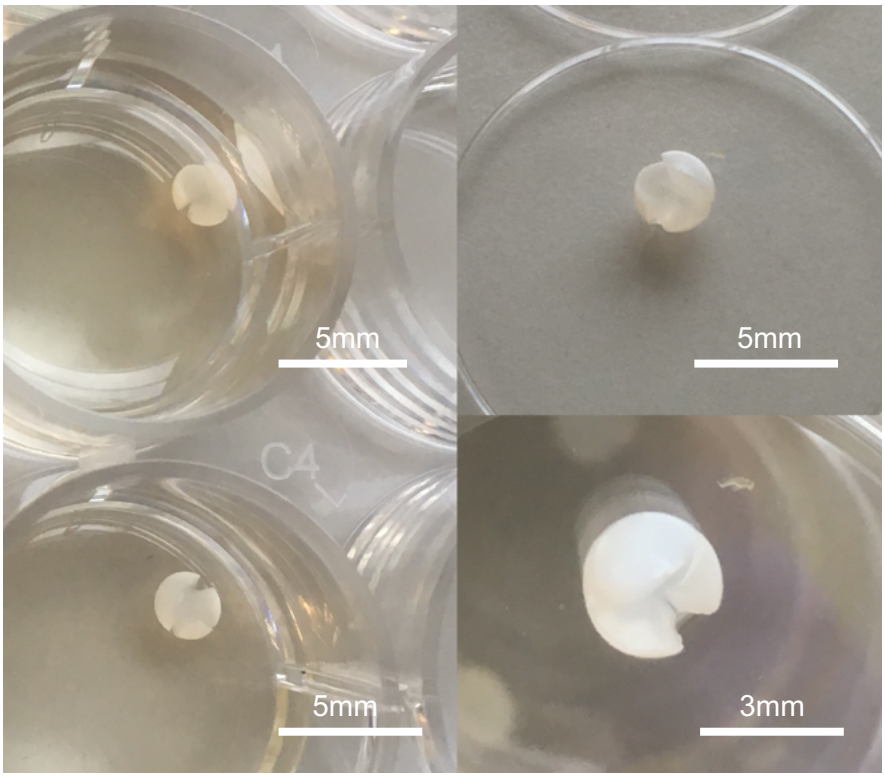

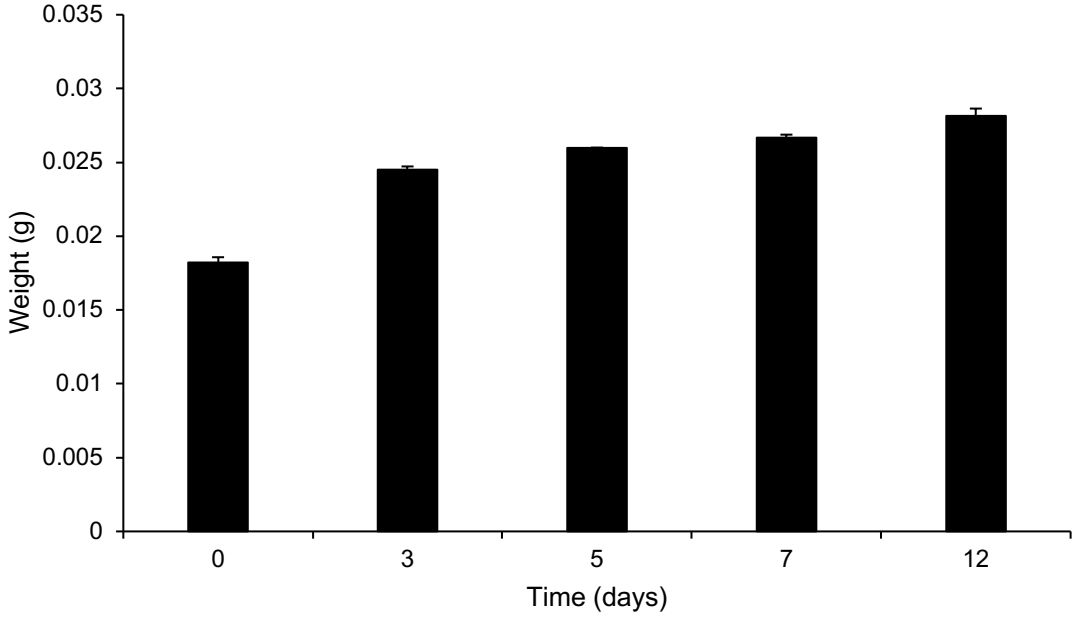

Figure 2.16: AFSC/alginate bead structures begins to rupture or disintegrate after prolonged culture up to 14 days. A*: AFSC/alginate beads after 14 days of culture begin to split demonstrating structural weakness of the structure after prolonged culture.* ***B****: Positive correlation between AFSC/alginate bead weight and time in culture is present, suggesting a swelling of the bead structure. N = 6 per time point. Error bars indicate ± SEM.*

2.4 Summary of results

- AFSCs used for the chondrogenic differentiation experiments within alginate and agarose hydrogels demonstrated high expression of stem cell markers and low expression of non-stem markers.
- AFSCs embedded within alginate hydrogels maintained cellular viability with no statistical differences detected up to 7 days of chondrogenic differentiation culture.
- AFSCs embedded within alginate hydrogels showed statistically significant decreases in viability after 14 days of culture for all treatments and controls compared to day 0 samples but was most significant for TGFβ treated samples.
- AFSC/agarose constructs demonstrated no statistically significant changes in viability after 14 days of culture for all treatments and controls.
- A statistically significant increase in GAG synthesis was detected in $TGF\beta_1$ treated sample after 14 days of culture in AFSC/alginate beads compared to day 0 but not in $TGF\beta_3$ samples.
- DNA content of AFSC/alginate beads statistically increased in $TGF\beta_1$ or $TGF\beta_3$ treated samples compared to all controls at day 7.
- DNA content of AFSC/alginate beads showed only a statistically significant increase when comparing $TGF\beta_3$ treated samples and Chang medium control sample after 14 days.
- GAG synthesis statistically increased in agarose constructs treated with either TGFβ or control medium compared to day 0.
- DNA content statistically increased in only $TGF\beta_1$ or $TGF\beta_3$ treated samples compared to all controls.
- No differences between TGFβ isoforms in terms of GAG synthesis and DNA content increases in AFSC/agarose constructs.
- AFSC/alginate beads rupture following 14 days of culture.

2.5 Discussion

This aspect of my thesis set out to investigate the effect of TGFβ_1 and TGFβ_3 on the chondrogenic differentiation of AFSCs within the first 14 days of culture. GAG synthesis, DNA content and viability were examined and compared to control samples of non-growth factor supplemented medium (basal), stem cell medium (Chang) and day 0 samples. Furthermore, the study used here optimised the methods for examining GAG synthesis in the different hydrogels used which can be applied for further investigations.

2.5.1 AFSCs are heterogeneous cell population with mesenchymal surface markers.

AFSCs are heterogeneous cell population derived from all three germ layers; ectoderm, endoderm and mesoderm. As such the key markers which characterise AFSCs are typically associated with mesenchymal marker expression; CD90, CD105, CD44 etc. In addition, haematopoietic markers such as CD34 and 45 are absent from this population of cells as well as the lack of HLA-DR antigen which contributes to the immunologic properties of the cell type.

FACS analysis AFSCs used in these experiments was performed in order to confirm that after passaging, the cells retained the surface marker profile associated with AFSCs and had not differentiated prior to encapsulation. Expression levels observed from FACS analysis were consistent with the literature for AFSCs with strong mesenchymal marker expression and weak haematopoietic expression. CD117 expression was also confirmed to be high following the MACS selection process.

Since AFSCs are a heterogenous population of cells, this has potential implications for differentiation experiments as cells from different donors or different surface expression markers could have an impact on the level of differentiation into specific lineages. Since the FACS performed here was for informative purposes only, this could have an impact on the cellular responses to the chondrogenic differentiation protocols employed in later chapters of this thesis. In order to circumvent this in the future, it would be beneficial to utilise FACS to sort the cells on their expression profile more selectively, to produce a more homogeneous clonal cellular population and therefore eliminate any variation between cells from different populations. Given the time/cost constraints and labour intensiveness of such a procedure however this was not performed for these experiments. Previous experiments by other groups have indicated that AFSCs from different subpopulations express the same markers as each other but may differ in

terms of the level of expression. This could therefore have an impact of a particular AFSCs ability to differentiate into a specific lineage compared to another. The extent to which this effects chondrogenic differentiation has not previously been investigated but could be a potential area of future work.

2.5.2 TGFβ_1 or TGFβ_3 treatment does not affect GAG synthesis in AFSC/alginate and AFSC/agarose hydrogels at 14 days of culture.

The findings establish that in AFSC/alginate beads supplementation of TGFβ_1 to culture medium results in a statistically significant decrease in GAG synthesis at day 7 of culture when compared to day 0 values, but no other statistically significant observations are made at either time point investigated for both TGFβ_1 and TGFβ_3 treated samples (**Figure 2.14**). Furthermore, this investigation determines that for AFSC/agarose constructs, all treatment conditions investigated increase GAG synthesis relative to day 0 control but only TGFβ_3 treatment presents an increase relative to Chang medium control at day 14 of culture (**Figure 2.15**).

The observation that GAG synthesis values did not statistically differ between TGFβ_1 or TGFβ_3 treated samples is demonstrated in this study. However, the study documents that the application of either TGFβ isoform did constitute an obvious increase in DNA content compared to control samples within both agarose and alginate hydrogels. This suggests that TGFβ plays a role in instigating *in vitro* proliferation in the early stages of the chondrogenic differentiation protocol used here. This observation is consistent with groups such as Awad et al that demonstrated that TGFβ is a potent instigator of cellular proliferation during the early stages of chondrogenic differentiation but an initiator of chondrogenesis *in vitro* at later time points (Kim et al., 2014, Awad et al., 2004). The level of GAG synthesis achieved here is slightly lower than what was reported by Awad et al, although this could simply be due to the increased number of cells used in that study (1×10^7 cells/ml) relative to my study (4×10^6 cells/ml) (Awad et al., 2004). Furthermore, Dexheimer et al previously suggested from their study that proliferation was positively associated with chondrogenesis of MSCs within a pellet culture model (Dexheimer et al., 2012). In contrast, Florine et al. identified no changes to DNA content when culturing bovine BM-MSCs in agarose constructs but did confirm no statistically significant changes in terms of proteoglycan synthesis when culturing BM-MSC/agarose constructs supplemented with TGFβ_1 within the first 14 days (Florine et al., 2013).

This then poses a question of why control conditions of basal chondrogenic medium (HG-DMEM with no growth factors added) and Chang medium (stem cell culture medium) caused an increase in GAG synthesis compared to day 0 in alginate and agarose hydrogels. One explanation for this may be due to the suspension of the cells within a 3D environment. The actin cytoskeleton is an integral part of chondrocyte differentiation, so much so that in dedifferentiated chondrocytes the addition of actin polymerisation inhibitors (such as cytochalasin D) results in a return to rounded morphology and return of chondrogenic gene expression and GAG production (Daniels and Solursh, 1991, Loty et al., 1995). By maintaining the stem cells in a rounded morphology as opposed to the one they maintain when cultured in 2D, the rearrangement of the actin cytoskeleton may instigate different signalling pathways associated with chondrogenesis resulting in the cells trying to generate their own microenvironment to enable cell survival. In doing so, lower levels of GAG synthesis are observed.

An alternative explanation is that the optimisation of the DMMB assay to detect the presence of sulphated GAGs is still not sufficient. The reduced pH used for the DMMB assay makes the binding of DMMB to sulphated GAGs more likely given the higher pKa compared to that of alginate. However, by reducing the pH so significantly it is possible that the reduction in pH reduces the sensitivity of the assay to sulfated GAGs present in the sample. Given the fact that levels of GAG synthesis are very low in the early stages of the chondrogenic differentiation protocol, this could result in the decreases observed in my study.

2.5.3 Viability is not affected in TGFβ_1 or TGFβ_3 treated AFSC/agarose constructs or AFSC/alginate beads after 14 days of culture.

In further *in vitro* studies I determined that the encapsulation of AFSCs within alginate beads resulted in no loss of viability over the first 14 days of culture (**Figures 2.11** and **2.12**). The same observation was made in AFSC/agarose constructs which also maintained a high viability of cells throughout the 14 days of culture with no statistically significant increases or decreases (**Figure 2.13**).

The only major difference between the two hydrogel materials is the initial viability of day 0 samples. In AFSC/alginate bead samples, the initial percentage viability recorded at day 0 was in excess of 90% indicating a minimal loss of cells during the encapsulation process. In contrast, AFSC/agarose constructs showed an initial viability of between 70 – 80%. A possible explanation

for this is the difference in the construction of the hydrogel structures. Since alginate bead construction simply requires addition of cells to a sterile alginate solution and then into a cation gelling solution, the cells are not stressed by the procedure, provided that the temperature of the solutions is maintained at a constant 37°C. In contrast, agarose encapsulation requires the agarose to be in a liquid state which can only be achieved by first melting the agarose at a high temperature. Whilst the solution is allowed to cool before addition to the cells, the only method of temperature evaluation available was through the use of a thermometer. If the solution was allowed to cool down too much, the agarose would set requiring the solution to be heated once again into its sol state. Once the AFSC/agarose solution is added to the mould, it is then transferred to a fridge for 5 minutes in order to speed up the gelling process. The cells are therefore exposed to a variety of temperatures through the construct assembly process which could potentially cause cellular stress and the activation of an apoptotic response in some cells resulting in a reduced initial viability compared to those of alginate beads for example.

However, the maintenance of viability in agarose constructs observed in my experiments is in agreement with that of Rodrigues et al who demonstrated no loss of viability when using AFSCs in agarose hydrogels also (Rodrigues et al., 2012). My findings also indicate no loss of viability when treated with TGFβ isoforms in agarose constructs or alginate beads.

2.5.4 AFSC/alginate bead rupture occurs after 14 days of culture

Despite successful culture of AFSCs within alginate beads up to 14 days, there were significant issues regarding their utility for a long term chondrogenic differentiation model. Between days 12 and 14 of culture, alginate beads began to display increasing fragility culminating in either rupture or eventual disintegration of the beads themselves (**Figure 2.16A**). Measurements of the bead volumes as they were cultured indicated a positive correlation between the time in culture and the volume of the beads with bead volume increasing by more than 35% of their initial volume as early as 3 days of culture (**Figure 2.16B**). Given the amount of GAG synthesis detected by the GAG assays performed (**Figure 2.14),** it was unlikely that these weight changes were due to proteoglycan deposition. This is a finding common to hydrogel cell culture and is sometimes used for specific applications (Ehrenhofer et al., 2018).

In terms of cellular culture, softening of hydrogels following prolonged culture has previously been noted by several groups who demonstrated that the compressive modulus of

alginate hydrogels decreases over time possibly due to the loss of cross linking calcium ions in the case of alginate (LeRoux et al., 1999, Shoichet et al., 1995, Awad et al., 2004). Awad et al noted that the compressive moduli of the hydrogels did decrease over the first 2 weeks of culture but began to increase between 15 and 28 days of culture; an increase associated with greater matrix synthesis. Unfortunately for the alginate beads used in this experiment, further culture was impossible as the constructs themselves were too fragile and began to split upon replacement of the culture medium.

A possible explanation for the changes in bead volume during culture is due to differences in osmolarity between the culture medium supplied and the fluid of the hydrogel; resulting in an influx of fluid into the bead. Using an osmometer, the osmolarity of the alginate used to encapsulate the cells was measured at 234 mOsm whereas the osmolarity of the HG-DMEM used was measured at around 90 mOsm. Whilst this effect may be beneficial for cells within the construct to enable adequate delivery of cellular nutrients vital for cell metabolism, it also puts an increased strain on the delicate alginate structure. As culture medium requires removal and replacement every 48 - 72 hours, this consistent change in osmolarity may cause excessive influx and efflux of fluid from the hydrogel resulting in a weakening of the structure and a loss of calcium ions from the alginate structure. As calcium ions are removed from the structure, the complex egg box arrangement of the alginate polymers become disrupted and begins to dissociate. This may also explain why the agarose constructs did not appear to weaken as much as the alginate structures since agarose constructs utilise thermal crosslinking which is unaffected by the change in medium as long as the temperature is consistent. Since the culture medium was always heated to 37°C, any weakening of the agarose structure was minimised. The size of the structures may also play a role in this difference, since a larger structure will inherently possess more crosslinks between polymers, conferring greater structural strength. Alternatively, the composition of the alginate itself in terms of mannuronic and guluronic acid could also play a role since other alginate structures have been used successfully by other groups. Therefore, further investigation using other alginate sources might be warranted to clarify the suitability of alginate for stem cell differentiation purposes. Ultimately, since alginate beads presented a poor hydrogel for prolonged chondrogenic differentiation culture, agarose was selected for further investigation instead.

2.6 Summary

In conclusion, this chapter reports novel findings which indicate that at the early stages of human AFSC chondrogenic differentiation, limited GAG synthesis but significant differences in cell division were detected upon TGFβ$_1$ or TGFβ$_3$ stimulation relative to controls in AFSC/agarose and AFSC/alginate hydrogels. This investigation also suggests that there are minimal differences between the use of either TGFβ$_1$ or TGFβ$_3$ at such an early stage of the chondrogenic differentiation process in terms of GAG synthesis or DNA content changes. To my knowledge, no direct comparison of TGFβ isoforms has been performed previously in regard to the chondrogenic differentiation of AFSCs within a hydrogel model in the first 14 days of culture. This study therefore provides an optimised method and a basic examination of the initial biochemical and viability events that occur during chondrogenic differentiation of AFSC within alginate and agarose hydrogels over a time course of 14 days. Characterisation of the changes associated with these processes provides an important foundation for the further investigation of AFSC differentiation and TGFβ's effect on this process.

Chapter 3: Assessment of agarose hydrogels for late stage amniotic fluid derived stem cell differentiation

3.1 Introduction

This chapter outlines the investigation of AFSC/agarose hydrogels using TGFβ_1 or TGFβ_3 over a 28-day period to achieve chondrogenic differentiation. The results of this chapter highlight the effectiveness of TGFβ_1 and TGFβ_3 on enhancing the chondrogenic differentiation of AFSCs, the lack of differences between the isoforms on this process and finally the possibility of applying other treatments to this model for further investigation.

3.1.1 Importance of culture duration on chondrogenic differentiation

Since my previous findings outlined in Chapter 2 indicated that there were no statistically significant differences when comparing TGFβ_1-treated sample with TGFβ_3-treated samples after 14 days of culture, I determined that this was likely to be a consequence of the short culture time employed. Whilst groups such as Barry et al have successfully been able to observe differences in TGFβ isoform mediated chondrogenic differentiation as early as 7 days of differentiation, albeit within a pellet culture model, the majority of investigations regarding stem cell chondrogenic differentiation utilise culture durations in excess of 21 - 28 days or even longer (Barry et al., 2001, Mauck et al., 2006). Findings by Awad et al also support this requirement for a prolonged differentiation culture as they demonstrated that after an initial stage of proliferation within the first 14 days of culture, proliferation began to subsequently decrease while collagen and proteoglycan deposition began to increase at later stages of culture when using adipose derived stem cells (Awad et al., 2004). I therefore hypothesised that differences in the chondrogenic differentiation capacity of TGFβ isoforms within our model might be time dependent and would be more evident if the time in culture was extended, allowing cells to move from the proliferation stage of differentiation to ECM synthesis. This would also enable determination of whether the agarose model I investigated would be sufficiently durable enough to remain intact over a prolonged culture time since alginate beads had already demonstrated significant instability after only 14 days of culture resulting in a diminishment of the structural properties of the gel that prevented further culture (**Figure 2.16A**).

3.1.2 Approach

In addition to the optimised DMMB and Hoechst assays used previously, a hydroxyproline assay was necessary to further assess the effect of TGFβ_1 and TGFβ_3 on the chondrogenic differentiation of AFSCs in terms of their ECM synthesis capabilities over 28 days. Furthermore,

I included a brief investigation that utilised SEM characterisation of AFSCs within agarose constructs to provide high resolution imaging at 2 different time points (day 7 and day 28) to identify any morphological changes that might be occurring during the culture process.

3.2 Methods

3.2.1 Chondrogenic differentiation experiment

Chondrogenic differentiation medium was identical to that described in **Chapter 2.2**. Each construct was supplied with an identical volume of differentiation medium and growth factor concentrations as previously stated also. Culture time was altered to an endpoint of 28 days. Culture medium was exchanged every 3 days as previously performed.

3.2.2 Biochemical assays

DMMB and Hoechst assay protocols were identical to that described in **Chapter 2.2**. Each construct was also processed identically to the methods stated previously.

3.2.3 Hydroxyproline Assay

Digested agarose hydrogel samples within microcentrifuge tubes (100 µl) were initially digested in a 1:1 ratio with concentrated HCl (Sigma-Aldrich Ltd, UK), vortexed, centrifuged briefly and then incubated at 110°C for 18 hours within a temperature-controlled heating block. Samples were then cooled down to room temperature, centrifuged at 11.5 x g for 5 minutes and then dried in a heat block within a fume hood for approximately 48 hours at 50°C with the microcentrifuge lids removed. 250 µl of ultra-pure ddH_2O was used to dissolve the sample and vortexed until re-suspended completely then spun briefly. Samples were stored at 4°C until required.

Fresh solutions required prior to assay included the following:

Hydroxyproline stock solution: 1 mg/ml trans-4-hydroxy-L-proline (Sigma-Aldrich Ltd, UK).

Citrate stock buffer: 5.04 g of citric acid monohydrate (Sigma-Aldrich Ltd, UK) was added to 11.98 g of sodium acetate trihydrate (Sigma-Aldrich Ltd, UK), 7.22 g of anhydryous sodium acetate (Sigma-Aldrich Ltd, UK) and 3.4 g sodium hydroxide (Sigma-Aldrich Ltd, UK) and dissolved in 80 ml of ultra-pure H_2O. Following this, 1.26 ml of glacial acetic acid (Sigma-Aldrich Ltd, UK) was added to the solution and pH adjusted to 6.1. The solution was then made up to 100 ml and filtered using Whatman filter paper.

Assay buffer: 1.5 ml of 1-propanol (Sigma-Aldrich Ltd, UK) was added to 1 ml of ultra-pure H_2O and made up to 7.5 ml using citrate stock buffer.

Chloramine T reagent: 141 mg of chloramine T reagent (Sigma-Aldrich Ltd, UK) was added to 0.5ml of ultra-pure H_2O and heated at 60°C for 10 minutes until completely dissolved. 0.5 ml of

1-propanol and 4 ml of assay buffer was then added. The solution was light sensitive so was wrapped in foil prior to use.

DMBA reagent: 4.5 g of 4-dimethylamino-benzaldehyde (DMBA, Sigma-Aldrich Ltd, UK) was dissolved in 6 ml of 1-propanol and 3 ml of 70% perchloric acid (Sigma-Aldrich Ltd, UK). The solution was light sensitive so was wrapped in foil prior to use.

Hydroxyproline standard: 1 mg/ml hydroxyproline standard was diluted 1 in 20 in PBE solution, vortexed.

Using the 50 µg/ml hydroxyproline standard solution, a standard curve was made using the following concentrations: 0, 15, 60, 120, 210 and 300 ng (**Figures 3.1 and 3.2**). 60 µl of samples and standard were added in triplicate to wells of a clear 96 well microtest plate (Sarstedt Ltd, UK). 20 µl of assay buffer (1-propanol, citrate stock buffer) and 40 µl of chloramine T reagent were then added to each well containing standard and samples. Plates were covered in tinfoil and allowed to incubate at room temperature for 20 minutes to allow hydroxyproline oxidation. 80 µl of DMBA reagent (1-propanol, perchloric acid, DMBA) were subsequently added to each well using a multichannel pipette until mixed well and the solution clear. Plates were sealed and incubated at 60°C for 20 minutes then allowed to cool for 25 minutes. The sealplate was removed and plates read using the SpectroNano Star plate reader at 570 nm optical density. Hydroxyproline content of collagen has been determined as 13% therefore hydroxyproline samples were multiplied by 7.69 to provide an estimation of collagen content of each sample (Ignat'eva et al., 2007).

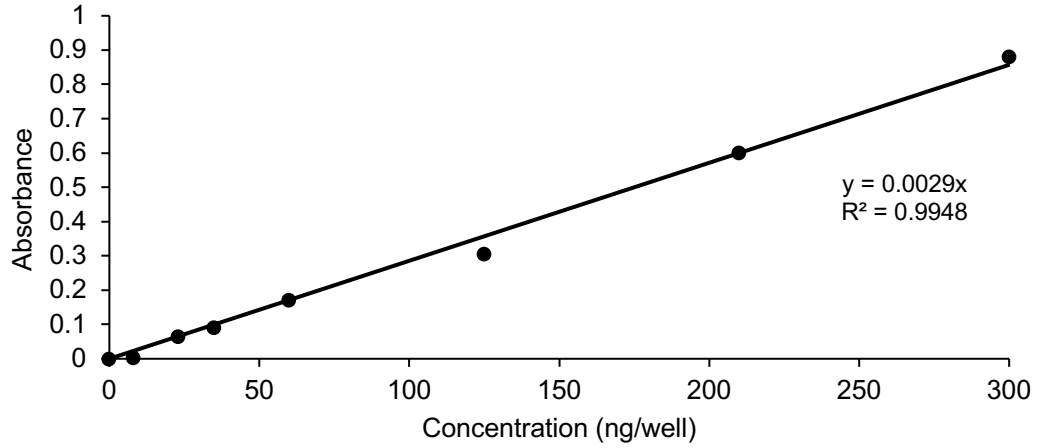

Figure 3.1: **Example hydroxyproline assay curve with linear regression model applied.** *Linear regression provides the equation of the trendline which can then be rearranged to calculate the hydroxyproline content of unknown samples simply by inputting the absorbance values.*

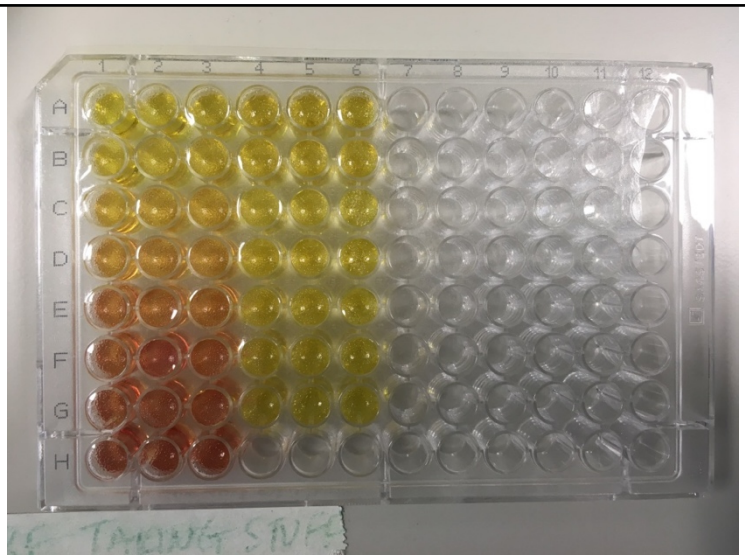

Figure 3.2: Colour change associated with increasing concentration of hydroxyproline content in standards. *Low concentrations of hydroxyproline show no reaction to the DMBA reagent added and maintain a yellow colour. Presence of hydroxyproline initiates a colour change, changing from yellow to dark brown with increasing concentration.*

3.2.4 Optimisation of hydrogel sample preparation for SEM

Principle

For SEM visualisation, the removal of water from the specimen is essential as it can disturb the vacuum used by the microscope to produce detailed images. For some samples simple air drying is suitable to achieve this. Unfortunately for delicate structures such as hydrogels, air drying of specimens can result in severe deformation of the structure leading to its collapse and an inability to visualise cells within the construct. This is primarily due to the effect of surface tension as water moves between its phase boundaries during evaporation. Therefore, the high surface tension of water (72 Nm^{-2} at 20°C) needs to be substituted for a liquid with a much lower surface tension. One typical method of water removal uses a solvent series such as ethanol to replace the majority of water within the sample. However, the surface tension of ethanol is still too high (22 Nm^{-2} at 20°C) and would result in the same effect. Because of this, 2 different methods have been developed in order to remove water without damaging the delicate specimens needed to be imaged; freeze drying and critical point drying (CPD).

CPD works on the principle that when a liquid is contained in a sealed volume it will expand and evaporate at the same time as temperature is increased. As kinetic energy increases, more molecules enter the gaseous phase resulting in a decrease in the density of the liquid and

a simultaneous increase in the density of the gas. When the densities of both phases are equal (the critical point) surface tension effectively becomes zero (Bray, 2000) (**Figure 3.3**). Dehydration of samples containing water using critical point drying is unfeasible as the critical point itself lies at 374°C and 229 atm of pressure which would cause the destruction of the sample (similarly with ethanol; 241°C at 60 atm). Therefore, replacement of the fluid within the construct with one that has a lower surface tension than water and ethanol but at a reasonable critical point is required. In this case, carbon dioxide is used due to its realistic pressure (73 atm), practical temperature (31.1°C) and miscibility with ethyl alcohols. By replacing the water with liquid CO_2, when the temperature is raised above critical temperature the CO_2 changes to vapour form without a change in density thereby avoiding the surface tension affects seen in water dehydration. The gas can then be released slowly, drying the sample without distorting it.

In contrast, freeze drying offers a simpler method of water removal. Freeze drying works by removing specimen water through sublimation. Initially the samples are prepared within loosely capped tubes to allow water vapour to escape, then the samples are frozen to a temperature that results in complete solidification of the contents. Following this the chamber is evacuated in order to reduce the pressure to below the vapour pressure of ice at the temperature of the item. Heat is then applied to provide energy for sublimation of the ice present in the sample (primary drying). The samples are then provided further drying time to allow any adsorbed water to be removed (secondary drying).

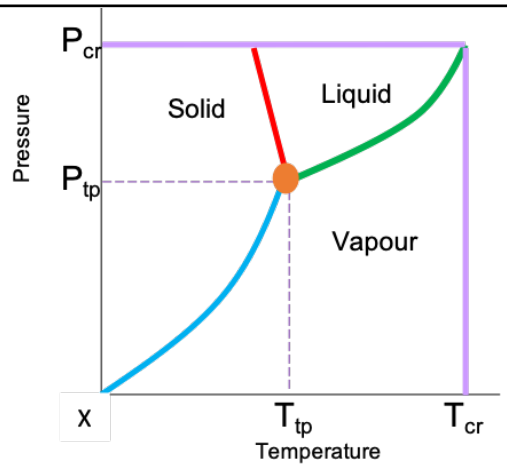

Figure 3.3: The different states of a fluid. *At point X, water exists as a solid. As pressure and temperature increase sublimation begins (blue). Subsequently, the water can either melt (red) or vaporise (green) depending on the pressure and temperature used. Anything below Ptp cannot exist as a liquid. Anything above Pcr and Tcr is known as supercritical. When the triple point is reached (orange) the sample is said to exist in all three states. For freeze drying, the entire process occurs below the triple point, where water moves directly to vapour phases.*

Therefore, to ascertain whether CPD or freeze drying should be used for SEM sample preparation I investigated the use of both methods for AFSC/hydrogel structures.

Optimisation of method

Critical point drying

Fixed bead samples underwent critical point drying following the standard protocol. Briefly, hydrogel samples were fixed in 4% PFA for 1 hour at 4°C. Fixed samples were then dehydrated in an ethanol series for 10 minutes at each concentration (50%, 75%, 96% and 100%) before being placed in the CPD machine (EMS 850, Quorum Technologies, UK). The CO_2 was vented into the machine to cool temperature down to around 5°C (taking care to avoid excessive flow and freezing of the system). Specimens were loaded into the chamber insert and tightened into the machine. The chamber was checked to ensure it was depressurised prior to starting the process. The chamber was then filled by allowing more CO_2 into the system ensuring the meniscus was visible before purging. The heater was applied to increase the temperature up to 35°C (critical point of CO_2) and the pressure was checked to have reached 1250 psi. Following this, the chamber was depressurised slowly (100 psi per minute) then samples removed and stored in a 24 well plate dish sealed with parafilm prior to sputtering.

Freeze drying

Samples were simply inserted into an Eppendorf inside a 50 ml Falcon tube with parafilm wrapped around the exterior of the screw cap, then inserted into the freeze drier overnight at a temperature of -70°C.

Sputter coating

To improve topographical contrast and minimise damage to the specimens, all samples were glued onto standard aluminium stubs using carbon tape and sputter coated (EMITECH Sputter Coater SC7620) with a 5 nm thick layer of gold to allow dissipation of charge.

SEM imaging

Samples were analysed using a 10 - 20 kV electron beam (FEI Inspect F, Oxford Instruments, Netherlands). Voltage was selected at between 10 and 20 kV in order to produce

sufficient resolution whilst providing enough small structural detail. A scalpel was used to cut the constructs in half for an interior look at the specimen.

Optimisation result

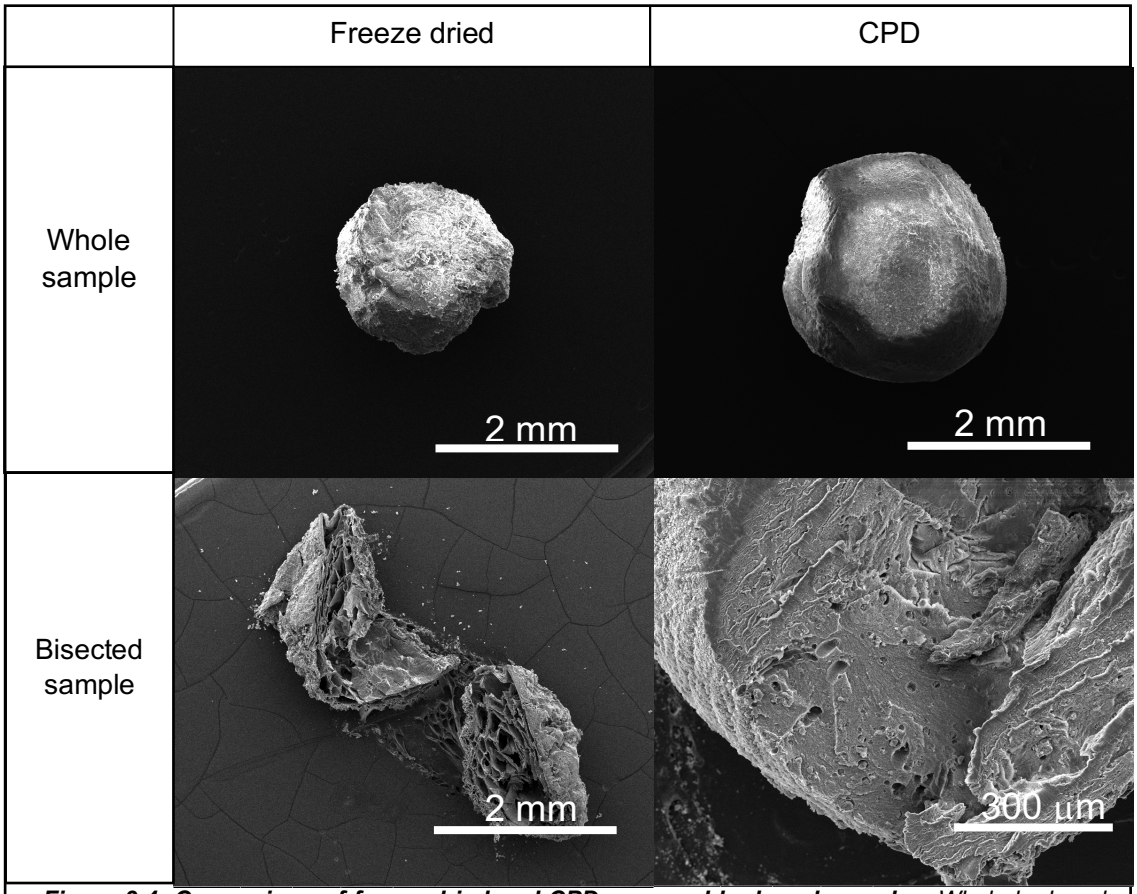

Figure 3.4: Comparison of freeze-dried and CPD prepared hydrogel samples. *Whole hydrogel samples showed small differences between the structures with the freeze-dried sample showing a much rougher surface compared to the CPD prepared sample. Upon bisection, cells could be visualised within the structures but were conspicuously absent from the freeze-dried sample.*

From SEM imaging of the bisected samples it was clear the sample prepared using the freeze-drying method was much weaker structurally compared to the construct prepared using CPD method. This may be due to the preservation of the natural porosity of the structure which become empty when water is removed. Upon bisection using a scalpel, I could not identify any cells within the interior of the constructs. In contrast, CPD offered a more rigid material that upon bisection allowed visualisation of multiple cells embedded within the constructs. However, it is likely that the CPD process altered the structure since there is an evident lack of porosity within the structure in comparison to the freeze-dried sample. To what degree the method affects the cells visualised requires further investigation but for simple visualisation of the cell structures, CPD offered a clear advantage over the freeze-drying.

3.3 Results

3.3.1 TGFβ_1 or TGFβ_3 treatment of AFSC/agarose constructs enhanced GAG and collagen synthesis up to 28 days of culture

The ability of TGFβ_1 or TGFβ_3 to influence GAG synthesis in AFSC/agarose constructs was compared to that of Chang and Basal chondrogenic medium controls over a period of 21 and 28 days. Treatment of constructs with exogenous TGFβ_1 or TGFβ_3 resulted in marked increases in GAG synthesis, DNA content and hydroxyproline synthesis compared to Chang and Basal medium controls after 21 and 28 days of culture (**Figure 3.5A and B, Figure 3.6A and B, Figure 3.7 A and B;** $p<0.01$). Further to this, no statistical differences were detected between TGFβ_1 and TGFβ_3 treated AFSC/agarose constructs in terms of GAG synthesis, DNA content changes and hydroxyproline synthesis (**Figure 3.5A and B, Figure 3.6A and B, Figure 3.7 A and B;** $p>0.05$).

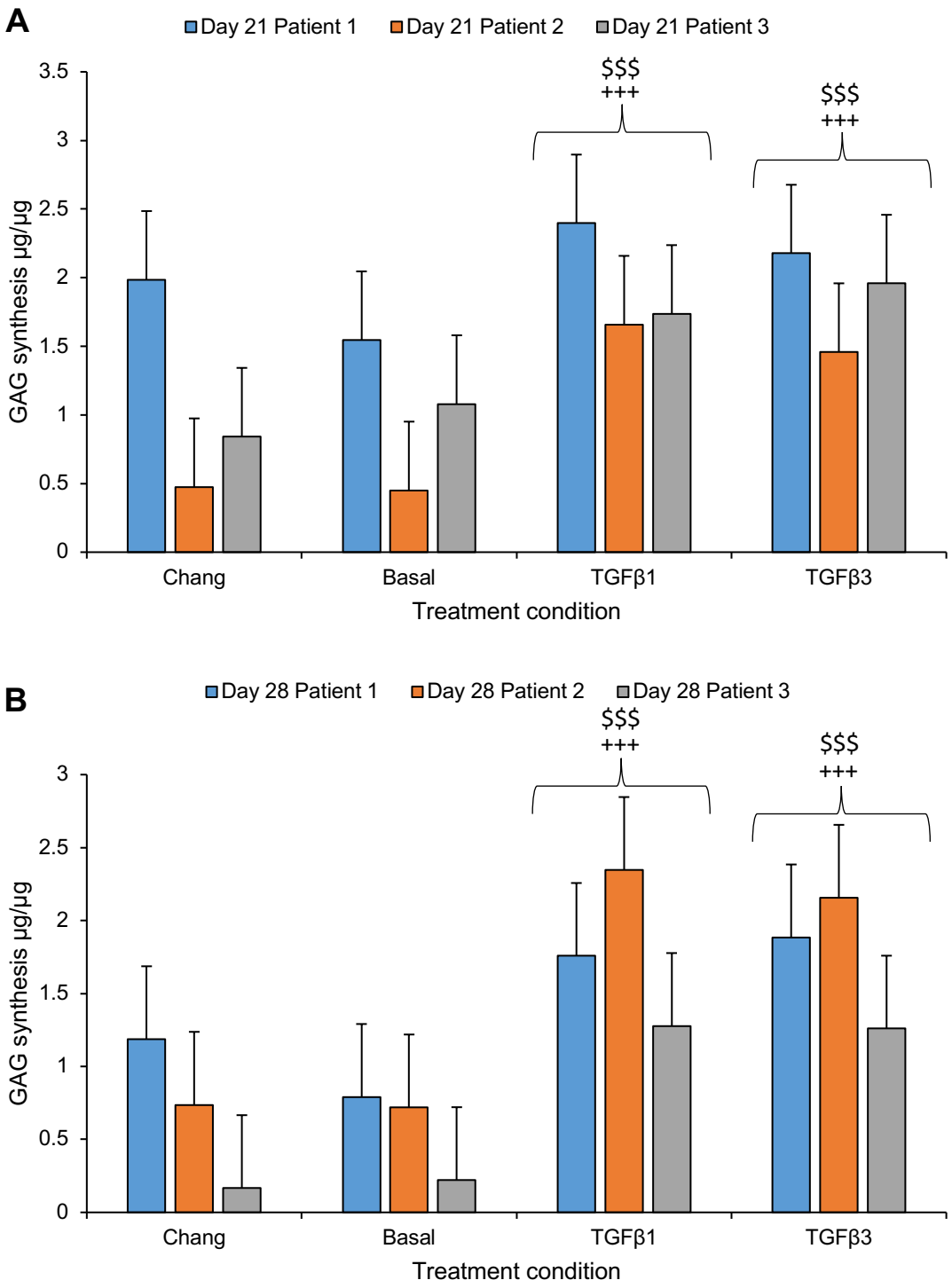

Figure 3.5: Extracellular matrix synthesis is enhanced in response to time in culture and TGFβ_1 or TGFβ_3 supplementation. *Each column indicates a different patient. +++ indicates significant comparison with Chang treatment, $$$ indicates significant comparison with Basal medium +++ = p<0.01, $$$ = p<0.01.*

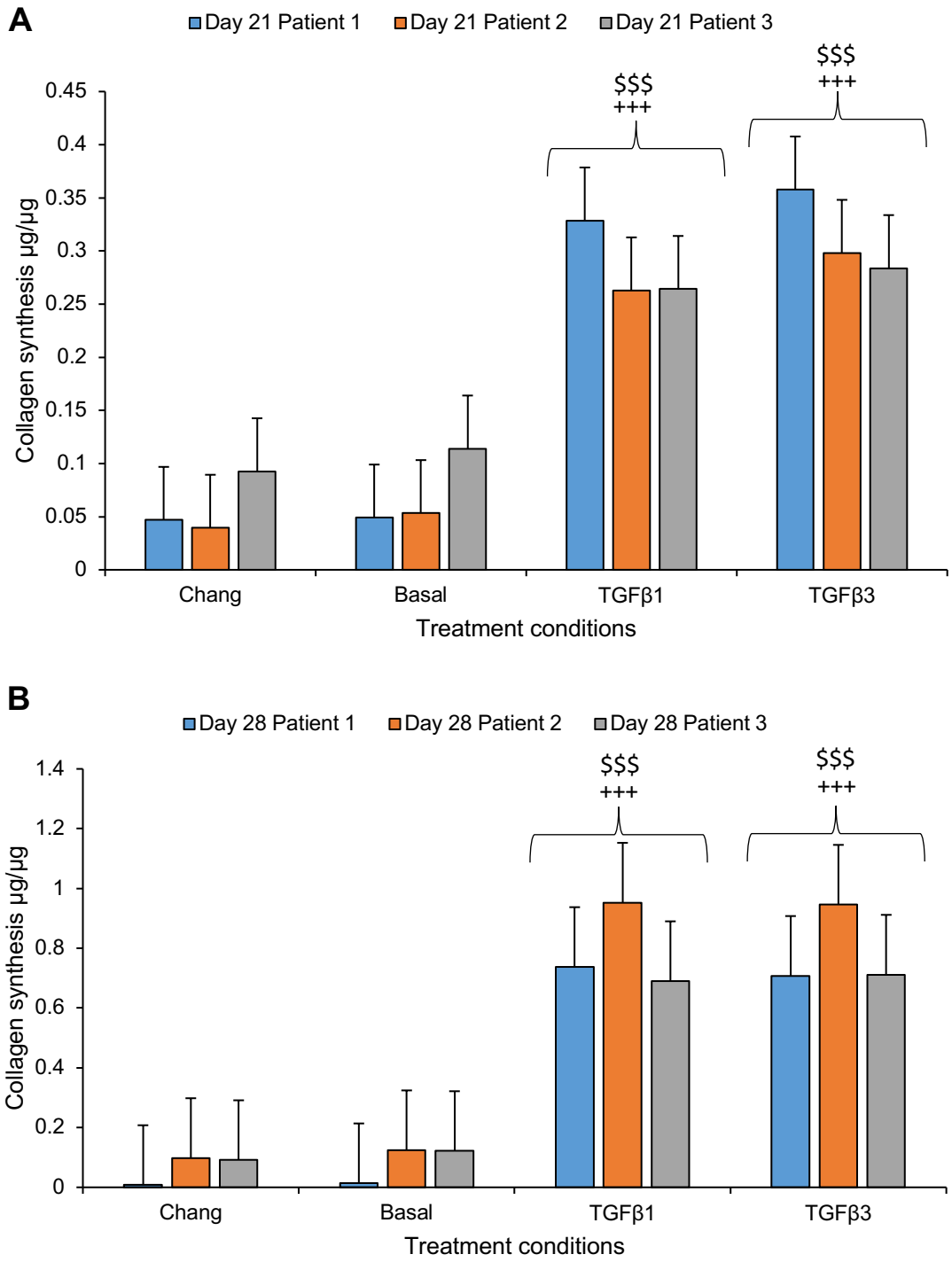

Figure 3.6: Extracellular matrix synthesis is enhanced in response to time in culture and TGFβ_1 or TGFβ_3 supplementation. *+++ indicates significant comparison with Chang treatment $$$ indicates significant comparison with Basal medium treatment. +++ = p<0.01, $$$ = p<0.01.*

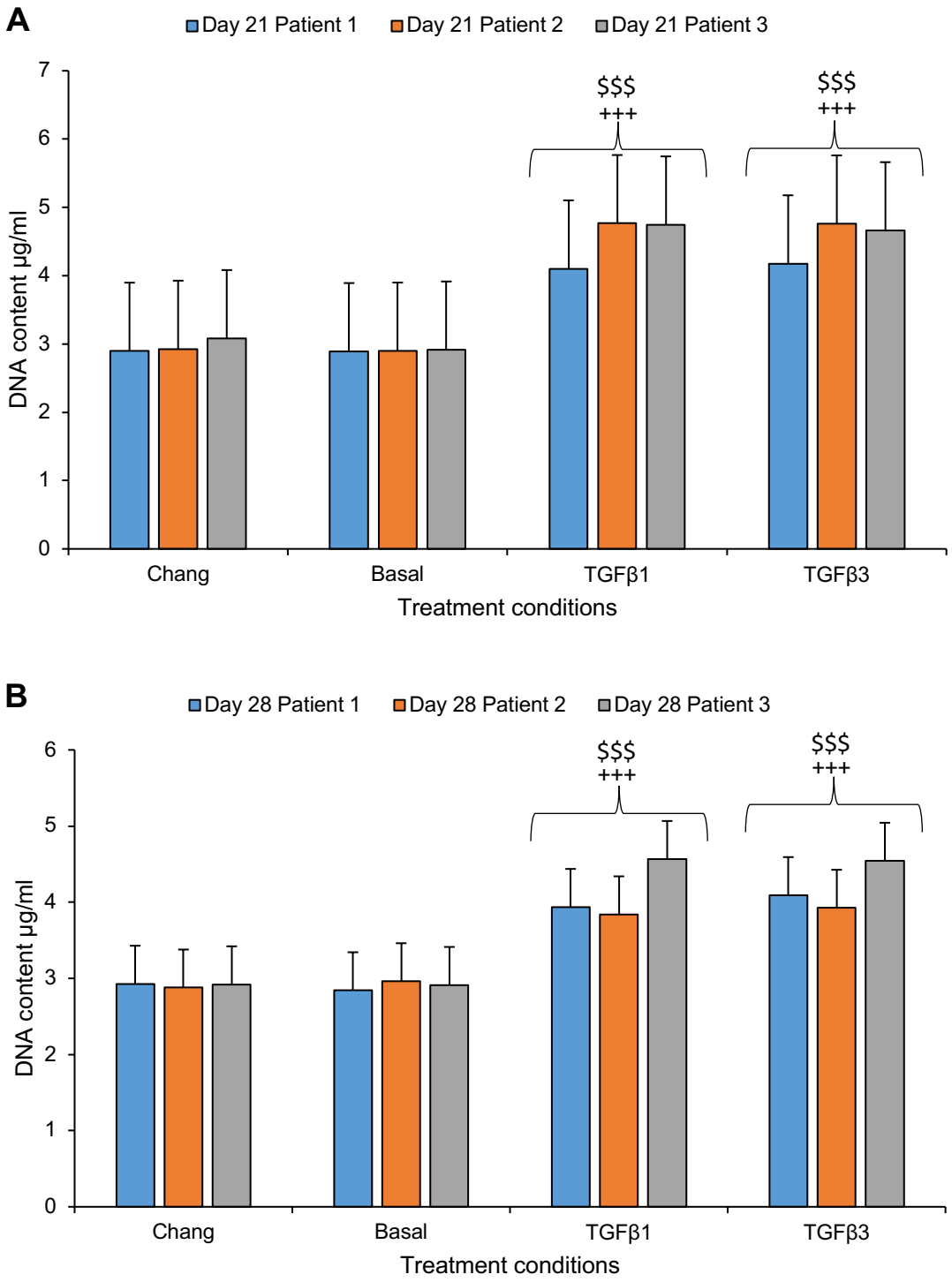

Figure 3.7: Extracellular matrix synthesis is enhanced in response to time in culture and TGFβ_1 or TGFβ_3 supplementation. *+++ indicates significant comparison with Chang treatment, $$$ indicates significant comparison with Basal medium treatment. +++ = p<0.01, $ = p<0.01.*

3.3.2 Scanning electron microscopy imaging of TGFβ_1 treated AFSCs embedded within agarose hydrogels suggests morphological changes over 28 days.

Macroscopic observation of the CPD dehydrated AFSC/agarose sample demonstrated maintenance of the general structure of the construct after the drying and sputtering procedures (**Figure 3.7A**). Indeed, bisection of the construct showed a varied polymer fibre network in some areas of the construct demonstrating some of the porosity of the agarose hydrogel (**Figure 3.7B**). SEM is a poor indicator of cellular distribution considering we can only observe the exposed surface, but it does suggest that some cells are in close proximity to each other within the small section of the gel observed (**Figure 3.7C**). Electron micrographs of the cells at the beginning of encapsulation show the cell surface contains filopodia-like projections (**Figure 3.7E**). Of the cells imaged later on in the differentiation process, these projections are seemingly lost, with a smoother surface evident (**Figure 3.7F**). The size of the cells is maintained throughout culture between 5 - 10 μm.

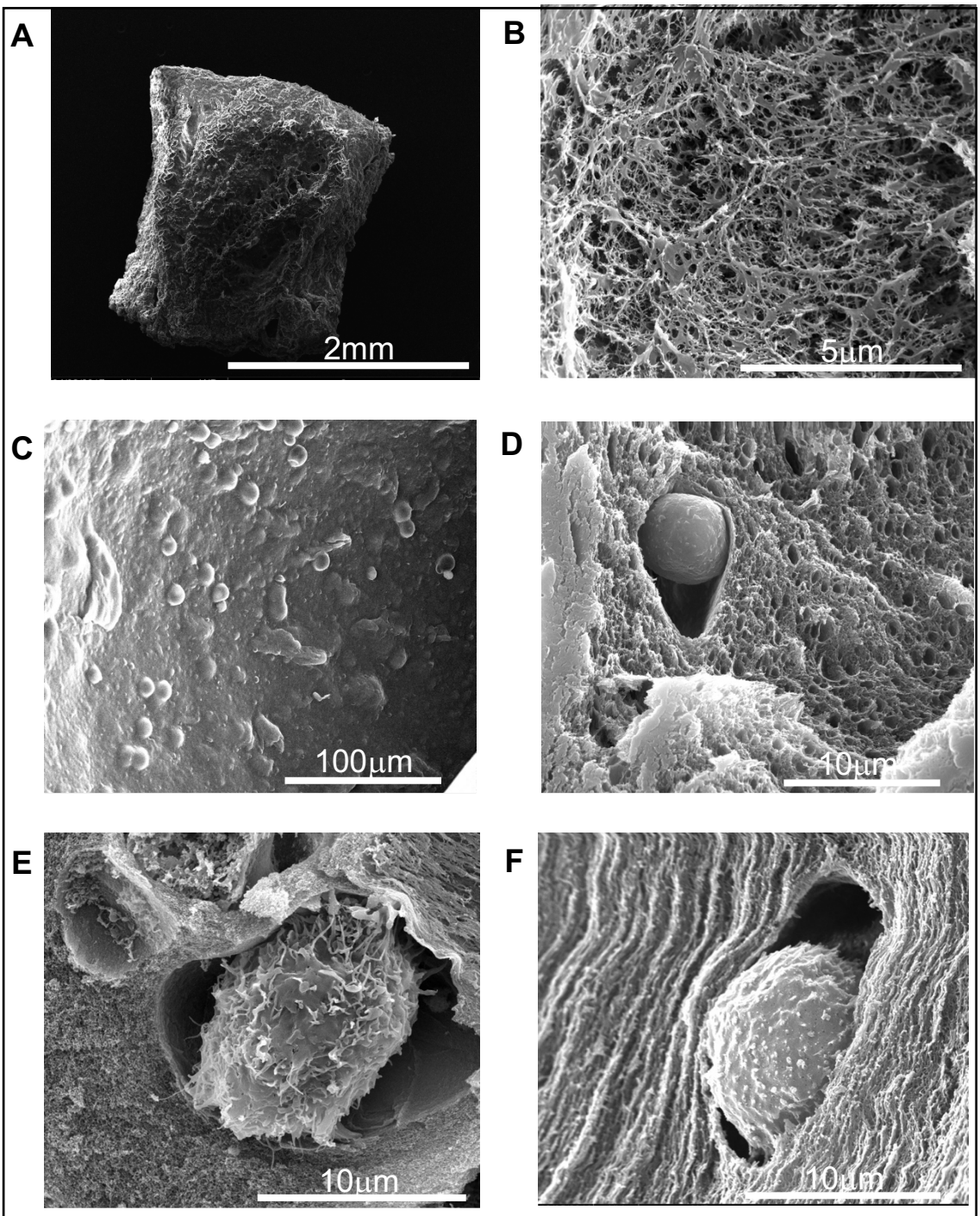

Figure 3.8: Electron micrograph of AFSC/agarose constructs and cells within. *Following CPD processing, the agarose construct remains intact and well preserved (**A**). In some sections, the fibrous polymer nature of the agarose is evident at 26,000 magnification (**B**). Bisection of the construct to look at the cells within is not always successful with overlying gel preventing closer inspection of the AFSCs (**C**), but some AFSCs are exposed and visible within their microenvironment (**D**). Of the exposed cells, AFSCs appear to express finger like projections at day 7 which appear to interact with the environment around them (**E**), whereas in the later stages of culture at 28 days these projections are noticeably absent (**F**). Image A taken at 70x mag., B at 26,000x magnification, C at 914x magnification, D at 9208x magnification, E at 12,000 magnification and F at 23,123 magnification.*

3.4 Summary of results

- GAG synthesis, DNA content and hydroxyproline synthesis of AFSC/agarose constructs statistically increased in all conditions compared to day 0.
- Treatment of AFSC/agarose constructs with TGFβ_1 or TGFβ_3 resulted in statistically significant increases in GAG synthesis, DNA content and hydroxyproline synthesis after 21 and 28 days of culture.
- No differences in GAG synthesis, DNA content and hydroxyproline synthesis were detected when comparing TGFβ_1 treated sample to TGFβ_3.
- Statistically significant increases in hydroxyproline synthesis were detected when comparing day 28 TGFβ_1 or TGFβ_3 treated samples with day 14 TGFβ_1 or TGFβ_3 samples.
- SEM imaging of cells shows rounded morphology and loss of cellular extensions over 28 days of culture compared to day 7.

3.5 Discussion

3.5.1 TGFβ treatment enhances GAG and collagen synthesis in AFSC/agarose constructs up to 28 days.

Following on from my initial 14-day investigation, further culture up to 28 days resulted in a greater deposition of chondrogenic biochemical markers in terms of GAG and hydroxyproline synthesis (**Figure 3.31A and C**). This finding was consistent not only for TGFβ_1 and TGFβ_3 treated samples but also controls when comparing to day 0 values. This was also observed in **Chapter 2** and supports the idea that encapsulation of AFSCs within a 3D environment can contribute to a degree of ECM deposition independent of growth factor stimulation. This observation correlates with recent research carried out by Tuan et al who demonstrated that chondroinductive growth factor independent differentiation of MSCs could be achieved. In that case, graphene oxide was incorporated into a poly-d-l-lactic acid/polyethlyene glycol hydrogel whereby the stiffness of the supportive hydrogel and the graphene oxide (GO) incorporated within it stimulated the production of ECM molecules as well as chondrogenic gene expression (Shen et al., 2018). Even without GO incorporation, which was hypothesised to sequester endogenous growth factors to aid in the chondrogenic differentiation of the cells, hydroxyproline and GAG synthesis was still achieved without growth factor supplementation indicating a level of ECM production similar to that seen in my experiments. However, the application of chondrogenic growth factors still significantly enhances this process. This is shown when TGFβ_1 or TGFβ_3 is applied to the AFSC/agarose constructs whereby a statistically significant increase in GAG synthesis, DNA content and hydroxyproline synthesis is detected compared to Basal and Chang medium controls after 21 and 28 days of culture.

Collagen synthesis was substantially upregulated relative to the effect seen in GAG synthesis when TGFβ is supplemented to the culture medium (**Figure 3.5C).** Increases in collagen synthesis are typically observed during chondrogenic differentiation processes however much more significant increases are usually seen in regard to GAG synthesis also. This potentially could indicate that the AFSCs within my model are not only differentiating to a chondrogenic phenotype but also other lineages. Supplementation of TGFβ has been associated with collagen synthesis increases in cardiac fibroblasts, skeletal muscle fibrosis, tendon fibroblast and even dental pulp cells. Given the broadly multipotent lineages that can derive from AFSCs and the lack

of substantial increases in GAG synthesis there is the potential for the differentiation observed here to be progressing towards a non-chondrogenic phenotype/genotype of either osteogenic, fibroblastic or myogenic. To further investigate this, histological or immuno staining of cells within the hydrogel could be performed to confirm if alternative differentiation is occurring. This could be achieved thorough immunostaining for markers such as α-actin for myogenic lineage detection whilst histological staining using alizarin red could be used to indicate if osteogenesic differentiation is occurring. From a genetic perspective, analysis of markers such as Osx, Alp and Bsp could also be used to determine osteogenic differentiation. If cells could be harvested from within the hydrogel structures, FACS analysis of surface markers such as CD10 and CD92 could also give an indication of osteogenic differentiation. However, the ease with which to extract intact live cells from within agarose hydrogels is challenging requiring optimisation.

In terms of DNA content, the lack of statistically significant increases in the case of TGFβ_3 treated samples from day 21 to day 28, and statistically significant decreases in DNA content following TGFβ_1 treatment within the same time period could indicate the fulfilment of the phenomenon suggested by Awad et al that the cells had essentially switched priorities from cell proliferation to ECM synthesis. This could also indicate that AFSCs require a specific cell density to increase cell to cell contacts. Upon reaching the required cell per volume ratio cells then can withdraw from the proliferative phase of the cell cycle and establish chondrogenic nodule formation. Thus, I may have observed the cells within the model system adjusting to the lack of sufficient cellular contacts by increasing proliferation to meet this requirement. In a way, this could be evidence of the cell attempting to initiate the events of embryonic development whereby mesenchymal stem cell proliferation and condensation to achieve chondrogenic differentiation is seen at early development.

Overall, the basic hydrogel model of AFSCs embedded within agarose constructs shown herein supports a level of ECM deposition. However, when we look at the level of GAG synthesis achieved from these cells is very low. I observed GAG synthesis levels between 2.5 and 3 μg/μg of DNA when treated with either TGFβ_1 or TGFβ_3. In contrast Vinardell et al found GAG synthesis levels of 20 μg/μg DNA after 21 days of culture (Vinardell et al., 2011). Similar comparisons can be made in regard to collagen synthesis, whereby the levels achieved in my investigation were between 0.3 and 0.9 μg/μg DNA after 21 and 28 days of culture. These values are significantly

lower than that shown by Vinardell et al who noted collagen synthesis levels of 20 μg/μg DNA when investigating BM-MSCs in agarose constructs. Whilst the cell density must be taken into consideration (Vinardell et al used 1.5 x 10^7 cells/ml in comparison to 4 x 10^6 cells/ml herein), my data was significantly lower in comparison. This might further indicate the importance of cell seeding density in relation to chondrogenic differentiation of stem cells. Also, while AFSCs are described as having broadly multipotent potential, their chondrogenic differentiation capability has been shown not to be as robust as BM-MSCs (Kolambkar et al., 2007). Therefore, the lack of GAG synthesis in my model could potentially be simply a limitation of the AFSCs ability to differentiate to the chondrogenic lineage.

3.5.2 No differences in GAG and collagen synthesis is detected between TGFβ1 and TGFβ3 treated AFSC/agarose constructs

No biochemical differences in TGFβ1 or TGFβ3 treated AFSC/agarose constructs were detected. Crystallisation studies by Huang et al demonstrate that TGFβ1 or TGFβ3 share considerable homology in terms of structure; they share 71 - 79% identity, similar 3D structures consisting of two cysteine monomers tied by a disulphide bond and similar solution structures. The only way in which they do differ is when placed in solution whereby TGFβ3 favours an open state whilst TGFβ1 favour a closed state. These isoforms are typically indistinguishable in many cell-based reporter gene assays, growth inhibition assays and, importantly, Smad phosphorylation assays. The only major differences are typically seen in chemo-regulated migration assays whereby TGFβ3 is an active promoter of migration whilst TGFβ1 is inactive. TGFβ1 and TGFβ3 also show very similar overall affinities and kinetics with only small differences in dissociation rate from TGFβRI binding by the TGFβ:TGFβ3RII complex. They also share similar association rates but TGFβ3 has a slightly slower dissociation rate indicating a slightly greater affinity. Results by Huang et al indicate that the closed or open state of the particular TGFβ isoform causes the difference in function (albeit in absence of intrinsic dissimilarities) (Huang et al., 2014). Therefore, any differences observed in published chondrogenic differentiation experiments previously may be due to the differences in this dissociation rate, but not directly by the cell signalling pathways activated. In my studies, since TGFβ isoforms were re-supplemented to culture medium after every medium change the likelihood is that this small difference in

dissociation becomes attenuated and could therefore contribute to the lack of a statistical difference observed at all time points investigated.

3.5.3 Morphological changes of AFSCs occur between beginning and end of chondrogenic differentiation protocol

Observation of AFSCs within the agarose construct was important to understand fine detail morphological changes the cells undergo through the chondrogenic differentiation process. The specific cases pictured in **Figure 3.7** show cells imaged within agarose constructs at day 7 and 28. Electron micrographs of the cells at the beginning of the chondrogenic differentiation protocol shows that the cell surface of AFSCs contain filopodia-like projections that are likely the cell's attempt to interact with the surrounding structure or other nearby cells (**Figure 3.7E**). In this way the cells could be exploring their surrounding environment as is often seen in ECM development and migration to identify appropriate adhesion sites. Of the cells imaged later on in the differentiation process, these projections are seemingly lost, with a smoother surface evident (**Figure 3.7F**). Since filopodia are dynamic structures which can rapidly extend and retract this could be a transient observation or an indication that the cell had already suitably altered its surrounding ECM to its requirements. Given the level of GAG and hydroxyproline synthesis detected, it is more likely that this is a transient observation. Further investigation into this phenomenon would be required for a definitive answer.

3.5.4 Implications

Although I have successfully demonstrated that TGFβ supplementation to AFSC/agarose constructs constitutes statistically significant increases in proteoglycan and hydroxyproline synthesis compared to control samples over a period of 28 days, TGFβ treatment alone is rarely used in the majority of chondrogenic differentiation experiments that have been published. Frequently, supplemental factors are utilised to enhance this process with the most common of these being the synthetic glucocorticoid dexamethasone. However, whilst the supplementation of dexamethasone to TGFβ mediated chondrogenic differentiation protocols has been associated with an enhancement of ECM synthesis and chondrogenic gene expression, it is also accompanied with an increase in hypertrophic/osteogenic gene expression and in some cases an inhibitory effect on the chondrogenic differentiation process in some stem cell types. This has resulted in some calls for its omission from this process and investigation into other alternative

agents (Buxton et al., 2011, Shintani and Hunziker, 2011). Since the level of ECM synthesis detected in my preliminary experiments is significantly lower than other established work in this field, I thought it essential to investigate other supplemental factors that could potentially replace or at least recapitulate the effect of dexamethasone in terms of enhancing the chondrogenic differentiation of human AFSCs. Therefore, my next steps in regard to this differentiation model were to characterise the effect of new supplemental factors on TGFβ_1 and TGFβ_3 mediated chondrogenic differentiation of AFSC/agarose constructs. One promising supplemental factor for this purpose is CNP.

3.6 Summary

This chapter reports the biochemical and morphological changes that occur in AFSCs embedded within agarose constructs over a full 28-day culture cycle following an established chondrogenic differentiation protocol. Further to my previous work, no statistically significant differences in the effect each TGFβ isoform had on GAG and hydroxyproline synthesis were detected suggesting a shared mechanism of effect and a transition away from cellular proliferation. These data therefore build upon the work established in **Chapter 2** of this thesis and present a foundational model that can be used for the characterisation of novel treatments for the chondrogenic differentiation of AFSCs over a 28-day period.

Chapter 4: Effect of CNP on amniotic fluid derived stem cell differentiation embedded within agarose constructs

4.1 Introduction

This chapter investigates the effect of the peptide CNP on the chondrogenic differentiation of human AFSCs within agarose constructs over 28 days of culture. To my knowledge, the application of CNP for the chondrogenic differentiation of human AFSCs has not previously been investigated. Biochemical (GAG, DNA, collagen), histological (Alcian blue staining) and gene expression changes to SOX-9, aggrecan and COL2a1 are studied here. By identifying the effect of CNP on this process with human AFSCs, it potentially provides a target for developing future differentiation protocols for cartilage tissue engineering applications.

4.1.1 Effect of CNP on chondrogenic differentiation

While TGFβ is a critical determinant of stem cell differentiation to chondrocyte phenotype/genotype, it has also been associated with upregulating CNP/NPR2 expression in BM-MSCs (Tezcan et al., 2010). **Table 4.1** summarises some of these *in vitro* investigations regarding the effect of CNP on TGFβ-mediated chondrogenic differentiation. Within these examples, alcian blue staining for proteoglycans was shown to be influenced by the presence of CNP during TGFβ mediated chondrogenic differentiation of MSCs. Specifically, CNP supplementation to $TGF\beta_1$ treated MSCs demonstrated a dose dependent increase in alcian blue staining (Tezcan et al., 2010), whilst blocking of CNP and its receptors resulted in a reduction in alcian blue staining (Kocamaz et al., 2012). Moreover, $TGF\beta_1$ supplementation in rat chondrocytes has also been associated with an increase in CNP secretion (Hagiwara et al., 1994). Further links between TGFβ and CNP can be seen when looking at the genetics of CNP production. The gene, *Nppc*, that codes for CNP possesses an enhanced binding site for the TGFβ early response inducible gene TSC22 (Transforming growth factor B stimulated clone-22) within its promoter region, potentially suggesting a close role between TGFβ signalling and CNP synthesis (Kawamata et al., 2004, Ohta et al., 1996, Olney, 2006).

Table 4.1: Examples of CNP involvement in chondrogenic differentiation in pellet models.

Cell type	Time (days)	Agents	Cell density	Key findings	Reference
Chicken BM-MSCs	21	TGFβ_1 (10 ng/ml) CNP (100 nM)	3 x 10^5	TGFβ_1 treatment ↑ CNP-3 mRNA in monolayer culture but ↓ NPR-2 mRNA compared to control. CNP addition ↑ chondrogenesis compared to control ($p<0.01$). Effect removed when antibodies targeting NPR-2 and CNP were used. TGFβ_1 supplementation resulted in spheroid shaped pellets after 21 days which stained positive for Alcian blue. When CNP antibody inhibitors used staining and pellet size ↓. Pellet culture resulted in collagen II mRNA expression but hypertrophic chondrocytes in peripheral regions compared to central regions of pellet. CNP and NPR-2 specific antibodies did not affect collagen II mRNA expression compared to TGFβ_1 treated but alcian blue staining significantly ↓.	(Kocamaz et al., 2012)
Human MSCs	21	Dex (0.1 μM) TGFβ_1 (10 ng/ml) CNP (10^{-6}, 10^{-7} or 10^{-8} M)	3 x 10^5 per pellet	TGFβ_1 induction of chondrogenesis resulted in ↑ of CNP mRNA and NPR-2 precursor at day 4, 10 and 21 compared to control. TGFβ_1 chondrogenic induction with 10^{-7} M CNP significantly ↑ alcian blue uptake in comparison to TGFβ_1 only at day 10 and 21. Similar effects seen with 10^{-8}M CNP with TGFβ_1 compared to TGFβ_1 only but not as strong as 10^{-8} M CNP effect. 10^{-6}M CNP diminished this effect, showing comparable results to TGFβ_1 only. Gene expression analysis of aggrecan, SOX-9 and collagen II did not differ statistically among treatment groups.	(Tezcan et al., 2010)

Phenotype instability is a common problem associated with the differentiation of MSCs to chondrocytes and diseases such as OA. Loss of the chondrocyte phenotype results in cells progressing towards a hypertrophy like phenotype characterised by an abnormal production of matrix proteins and matrix degrading enzymes (Singh et al., 2019). Therefore, maintenance of the chondrocyte phenotype is of utmost importance in order to produce the hyaline cartilage required for tissue engineering endeavours. CNP has been associated as a key regulator of this process for MSC derived chondrocytes, potentially through the downregulation of RANK and Collagen type X expression, in addition to inhibiting calcification formation under an inflammatory environment caused by OA (Shi et al., 2017). In addition, CNP has been shown to downregulate the *Tnfs11* gene which encodes RANKL; a key marker of hypertrophic cartilage. CNP has also been suggested to participate in the Indian hedgehog / parathyroid hormone related protein loop that inhibits pre-hypertrophic chondrocytes from entering the hypertrophic phase (Yamashita et al. 2000, Olney, 2006). Furthermore, while the application of dexamethasone inhibits the longitudinal growth of tibial explants, this effect can be reversed by CNP addition (Ueda, 2016). This potentially signifies a substantial area of improvement over the traditional dexamethasone

mediated method of chondrogenic differentiation which is commonly associated with hypertrophic progression.

So, the question that follows these investigations is how CNP affects this process from a signalling perspective. Overall, the underlying mechanism is thought to be through the modulation of RAF-1 activation (**Figure 4.1**). In brief, activation of NPR-2 through CNP binding to its extracellular domain triggers cGMP generation which can activate a host of different intracellular machinery including phosphodiesterases (PDE), cGMP gated ion channels and cyclic GMP dependent protein kinases I and II (PKGI and PKGII). Activation of PKGII directly activates p38 which can directly interact with RAF-1 resulting in inhibition. Preventing RAF-1 activation directly affects MEK1/2 and ERK1/2 signalling which are known to reduce chondrocyte proliferation, ECM synthesis and differentiation (Krejci et al., 2005). While TGFβ primarily uses its Smad-dependent signalling pathway to trigger cellular response, it also utilises p38 through its non-Smad dependent pathway. Therefore, it can be hypothesised that TGFβ and CNP together can inhibit RAF-1 and thus enhance the chondrogenic differentiation process. However, p38 activation is also noted to be involved in activating MAPK which can directly affect the phosphorylation of the hypertrophic gene Runx2. Therefore, activation of p38 and subsequent inhibition of RAF-1 could also actually be enhancing the expression of hypertrophic genes as well as chondrogenic ones.

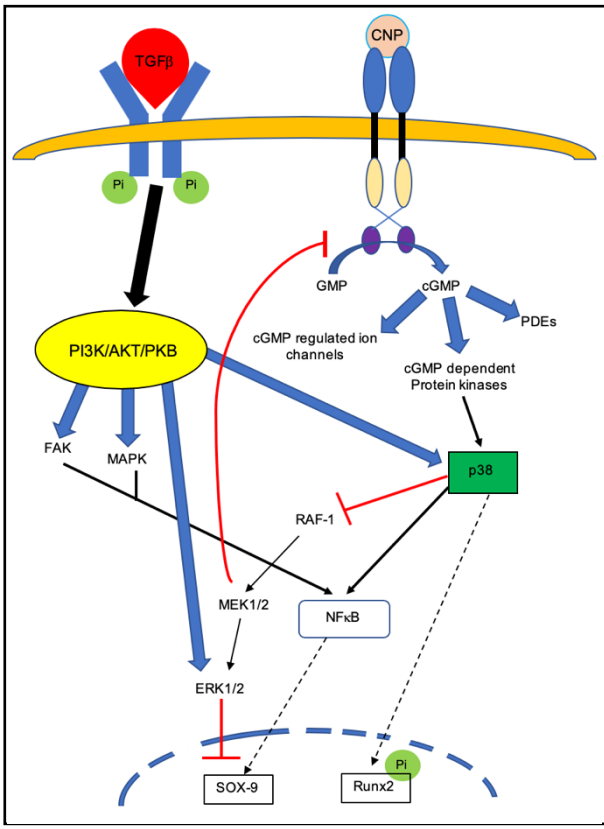

Figure 4.1: Intracellular signalling schematic showing areas of potential crosstalk between TGFβ and CNP signalling pathways. *While TGFβ primarily signals through a Smad dependent pathway, non-canonical signalling also takes place that can affect chondrogenic differentiation. Meanwhile CNP signalling is able to inhibit RAF-1, which directly impacts on MEK and ERK and effectively reduces SOX-9 inhibition.*

In addition to CNP and its close association with TGFβ for chondrogenic differentiation, Agoston et al demonstrated that Dex regulates the expression of CNP and its receptors in chondrocytes (Agoston et al., 2006). Since Dex is consistently used in concert with TGFβ isoforms to achieve chondrogenic differentiation and CNP has been shown to help enhance the effect of TGFβ$_1$ in this process, it stands to reason that CNP could potentially play a role in the chondrogenic differentiation of AFSCs and should therefore be investigated in comparison to Dex + TGFβ$_1$ treatment for this purpose. In addition, no evidence exists to the effect that CNP application without TGFβ has on chondrogenic differentiation of AFSCs. Given the complexity of interaction of these two agents, further work is required to elucidate the nature of this association.

Taken together, I sought to determine the effect of CNP on the chondrogenic differentiation of human AFSCs within agarose constructs over a period of 28 days. Using the established basic agarose model, I performed my standard optimised biochemical analysis in terms of DMMB, hydroxyproline and DNA assays. In addition to my previously stated controls, I included a dexamethasone + TGFβ$_1$ treatment to compare the effect of CNP with the most commonly used method of stem cell differentiation in the literature, plus a CNP only treatment to distinguish if CNP itself had potential as a chondro-inductive agent like TGFβ. Furthermore, I optimised a method for alcian blue staining of AFSC/agarose constructs, optimised primer binding efficiency for 3 chondrogenic genes (SOX-9, aggrecan and COL2a1) and optimised a method for imaging of collagen deposition using SHG microscopy. In this way, I was able to visualise proteoglycan and collagen deposition by cells while also determining any differences in gene expression depending on treatment. To my knowledge, no other group has investigated the use of CNP as a chondro-inductive or chondro-supportive agent in the differentiation of AFSCs within an agarose construct model over 28 days.

4.2 Methods

4.2.1 RNA extraction optimisation methods

For all methods of RNA isolation investigated, extraction was performed within a Class II fume hood that had been thoroughly wiped down and sprayed liberally with RNase away to remove any RNA degrading RNases from the work area. Only essential instrumentation such as a mini centrifuge, heat block, pipettes and sterile filter tips were allowed within the setup area once wiped with RNase away. Gloves were worn at all times when handling RNase away as it can be a skin irritant and to prevent contact of RNases on the skin from contaminating the samples. Surgical masks were also worn as an extra precaution. All constructs used for the extractions were identical in terms of the dimensions (5 x 5 mm), cell seeding density (4 x 10^6 cells/ml) and amount of time in culture (21 days). A simplified overview of methods investigated is depicted in **Figure 4.2**.

Method 1: Buffer QG expired

Buffer QG (Qiagen Ltd, UK) was preheated within a heat block at 42°C for 10 minutes. AFSC/agarose samples were taken directly from a Heracell incubator (Thermofisher, Scientific, UK), removed from their well plates, rinsed briefly in D-PBS and then inserted into the heated Buffer QG (600 μl per construct) within an RNase free 1 ml Eppendorf tube. The tubes containing buffer QG and constructs were then placed within the heat block for a further 10 minutes to ensure adequate digestion of the agarose construct and lysis of the cell membranes present in the samples. Sample tubes were then transferred to a dry rack within the hood whereby 100 μl of isopropanol was added, mixed briefly by pipetting and then the total volume added to a RNeasy spin column. The spin columns were then centrifuged at maximum speed (12,225 x g) for 1 minute at room temperature. Following this the flow through was discarded and the spin column placed back in the same collection tube. 500 μl of the Buffer QG was again inserted into the spin column to ensure the complete removal of agarose from the spin column and centrifuged once again at 12,225 x g for 1 minute. Flow through was again discarded, then 750 μl of Buffer RPE (Qiagen Ltd, UK) was added to the spin column. The spin column was centrifuged again at 12,225 x g for 1 minute, flown through discarded and then the spin column was placed within a fresh microfuge tube. To elute the RNA, 400 μl of RNase free H_2O was added to the centre of the spin column

and then centrifuged at 12,225 x g for 1 minute. The spin column was then removed from the tube and the sample kept on ice immediately.

Method 2: Tilwani method

Many of the steps here were shared with that of Method 1 but a few simple changes were made. Firstly, each construct was incubated with 750 μl of buffer QG in order to digest the agarose and cell membrane rupture. 125 μl of isopropanol was then added instead of the 100 μl stated previously, with the resulting fluid yield requiring 2 centrifugation steps since the maximum volume contained within a RNeasy mini spin column is 700 μl. Centrifugation steps were also altered to reduce the speed and time of the table top centrifuge to 4293 x g for 15 seconds only. Following this, the addition of 700 μl of RW1 buffer (Qiagen Ltd, UK) was added to remove any proteins present within the sample. The samples were then treated with RPE buffer as in the other method with the addition of an extra centrifugation step with the empty RNeasy spin column to remove any excess solution that might still be present within the column. Elution was repeated in same way as Method 1.

Method 3: TRIzol extraction

Chloroform, TRIzol and 70% ethanol solutions were all pre-chilled on ice before the extraction was started. Isopropanol was kept at room temperature within a dry rack. Samples were removed from their well plates, placed within 1 ml cryovials and immediately snap frozen using liquid nitrogen within a dewar for 5 minutes. A sterile ball bearing was then placed within each cryovial which were then inserted into a Qiagen tissue lyser (Qiagen Ltd, UK). 50 oscillations per second for 1 minute was performed to grind the snap-frozen sample into powder format. 500 μl of TRIzol was then added to each cryovial and left to thaw for 5 minutes at room temperature. All homogenised sample were then transferred to an RNase free microfuge tube and placed on ice. 200 μl of chilled chloroform was added to each tube containing TRIzol and mixed thoroughly using a vortex. Samples were then centrifuged for 5 minutes at 12000 x g at 4°C. Hereby 3 layers were observed and the top layer (aqueous phase) was transferred to a fresh RNase free microfuge tube (approximately 300 - 400 μl total). Care was taken not to disturb the other layers present as these contained contaminants such as DNA, proteins and lipids. 500 μl of isopropanol was then added to the extracted layer and left at room temperature for 10 minutes to allow precipitation of the RNA from the sample. This was followed by centrifugation at 12,000 x g for a

further 10 minutes whereby an RNA pellet would form at the base of the tube. Once the supernatant was removed, the sample was washed in 1 ml of 70% ethanol, mixed by gentle inversion so as to not disturb the pellet and centrifuged again for 5 minutes at 7500 x g. The supernatant was then removed once again and inverted to air dry for a further 10 minutes. 100 μl of RNase free water was then used to resuspend the pellet prior to further purification steps.

Purification was achieved using the Qiagen RNeasy minikit (Qiagen Ltd, UK). Briefly, 350 μl of buffer RLT and 250 μl of 100% ethanol was added to the sample and transferred to a RNeasy mini spin column. Samples were then centrifuged for 1 minute at 8000 x g. The follow through was then discarded and 700 μl of RW1 buffer added before repetition of the centrifugation step again. DNase treatment was applied here by adding 80 μl of DNase 1 solution to the sample and incubating for 30 minutes. Following this 350 μl of buffer RW1 was added, centrifuged and removed before adding 500 μl buffer RPE. RPE buffer was incubated with the sample for 5 minutes then centrifuged as prior. Finally, 500 μl of 75% ethanol was added to the spin column and centrifuged for 2 minutes at 8000 x g before discarding and air drying the spin column. The column was then centrifuged with no additional liquid to help facilitate the removal of trace ethanol. The spin column was then transferred to a fresh microfuge tube and then 50 μl of RNase free water added to the tube before final elution (1 minute at 10,000 x g).

Method 4: Ogura method

Following the initial TRIzol method until the 70% ethanol wash step, the precipitant was dissolved in 200 μl of potassium thiocyanate buffer (NTC buffer, Macherey-Nagel, Germany) and incubated at 50°C for 10 minutes. Afterwards, the sample was then mixed with 70% ethanol and transferred to a silica spin column (Nucleospin Gel and PCR Clean up column, Macherey-Nagel, Germany) and centrifuged at 4293 x g for 1 minute. The follow through was then discarded and replaced with NT3 buffer (Macherey-Nagel, Germany) to wash the column, discarded again and then the RNA was eluted by the addition of low ionic strength NE buffer (Macherey Nagel, Germany).

Method 5: Buffer QG fresh

This method is identical to Method 1 except fresh Buffer QG, RPE and spin columns were purchased and used.

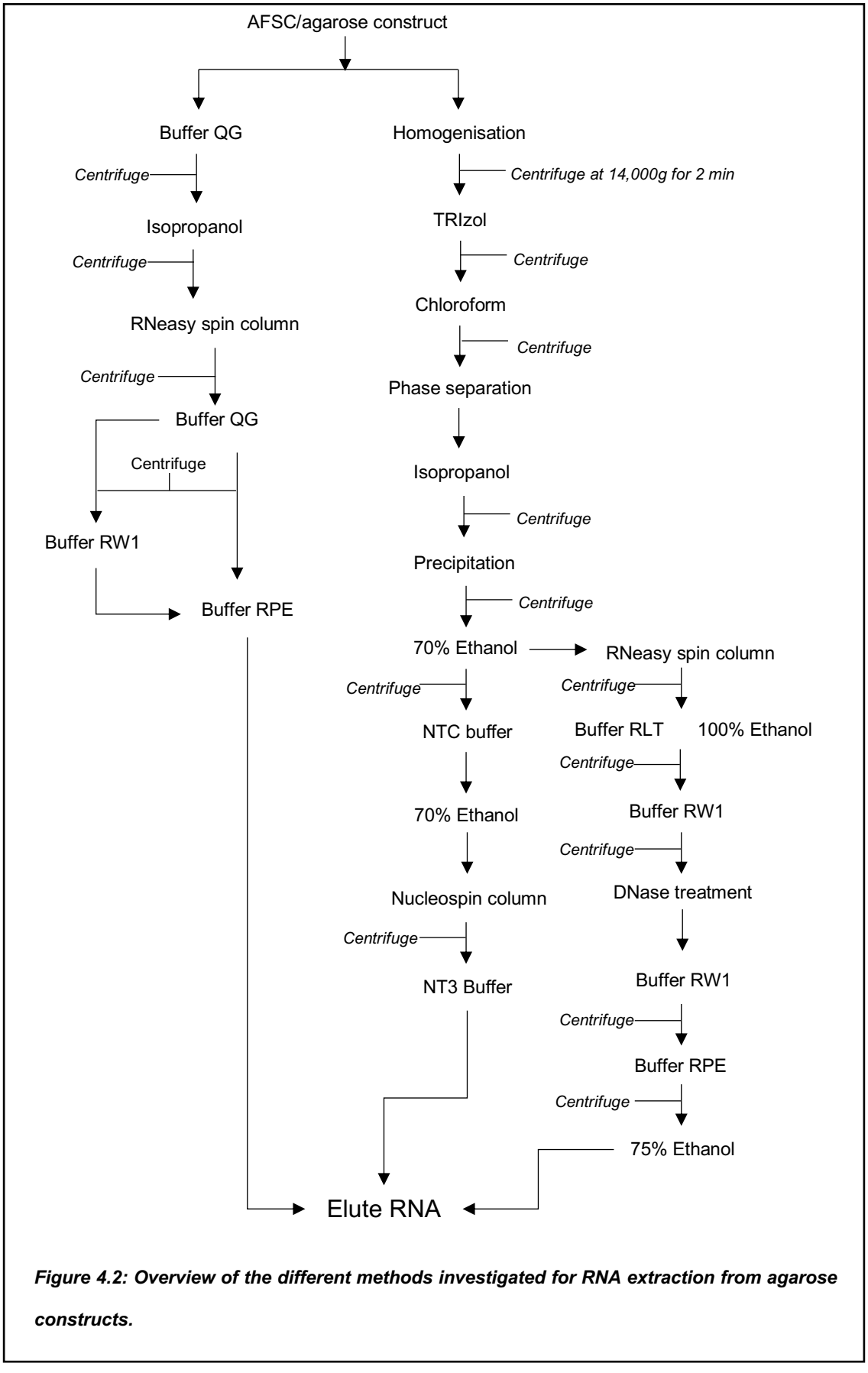

Figure 4.2: Overview of the different methods investigated for RNA extraction from agarose constructs.

DNase treatment

For all procedures, DNase treatment was carried out by adding 1 µl of DNase I enzyme and 10x DNase buffer to the RNA sample and incubating it for 20 minutes at 37°C. Another incubation period then followed for 2 minutes at room temperature, after adding 4 µl of DNase inactivating reagent to the tube. The resulting slurry was pelleted by carrying out centrifugation at 14,000 x g for 1 minute at 40°C. The RNA containing solution was then transferred into a new microfuge tube and kept on ice prior to RNA quantification or stored at -70°C. This procedure is summarised in **Figure 4.3**.

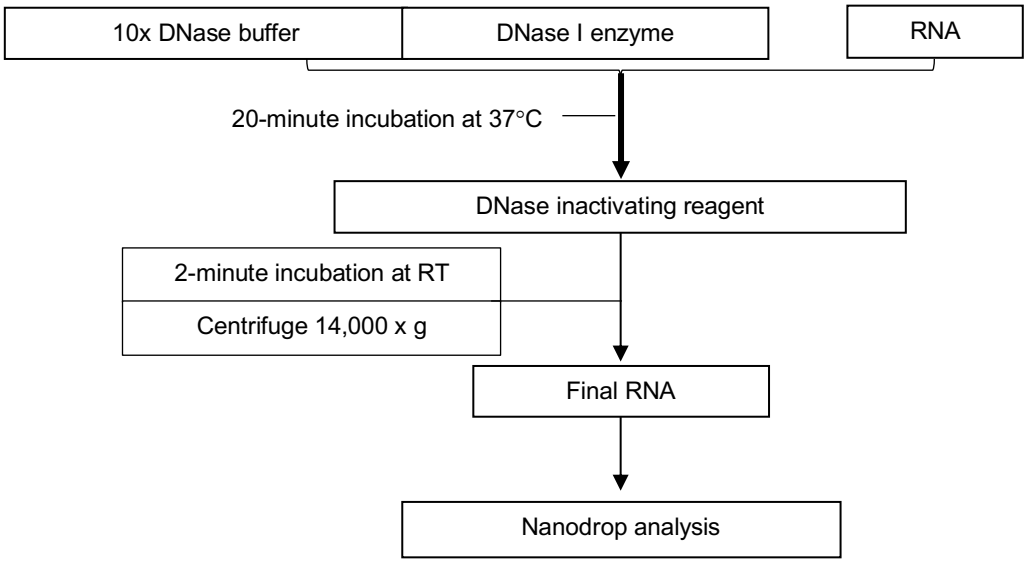

Figure 4.3: DNase treatment of samples.

Nanodrop quantification

To quantify the RNA present, a Nanodrop One spectrophotometer (Thermofisher Scientific, UK) was used. In brief, the pedestal was wiped over using Kimwipes (Sigma-Aldrich Ltd, UK) before loading 1 µl of RNase free water to the pedestal to blank the Nanodrop system to allow quantification of only the RNA within the sample. 1 µl of RNA containing solution was then added to the pedestal whereby yield and purity were quantified. For long term storage samples were kept in -80°C, otherwise samples were immediately converted to cDNA format. Nanodrop analyses of samples were recorded and displayed in **Figures 4.4, 4.5** and **4.6**.

Result of optimisation

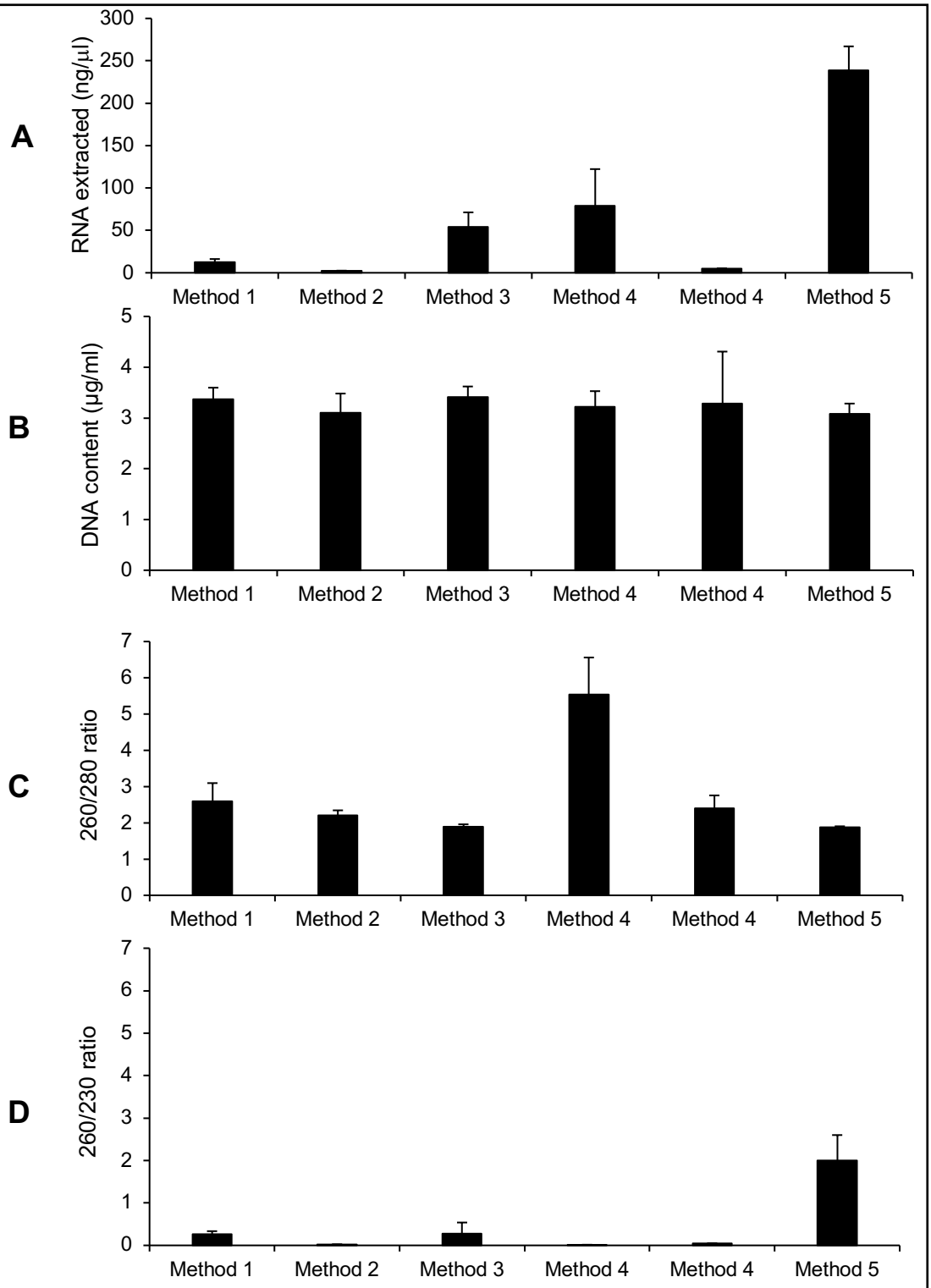

Figure 4.4: Comparison of RNA yield and purity between different extraction methods.

A: *Average RNA yield extracted from AFSC/agarose samples using various RNA extraction methods.* ***B****: Average DNA yield from AFSC/agarose constructs harvested from the same population of those tested for RNA extraction.* ***C****: Average 260/280 ratio from AFSC/agarose samples using the different extraction methods* ***D****: Average 260/230 ratio from AFSC/agarose samples using the different extraction methods. (N = 8 - 25 replicates). Error bars: ± SEM.*

Method	Nanodrop Analysis
Method 1	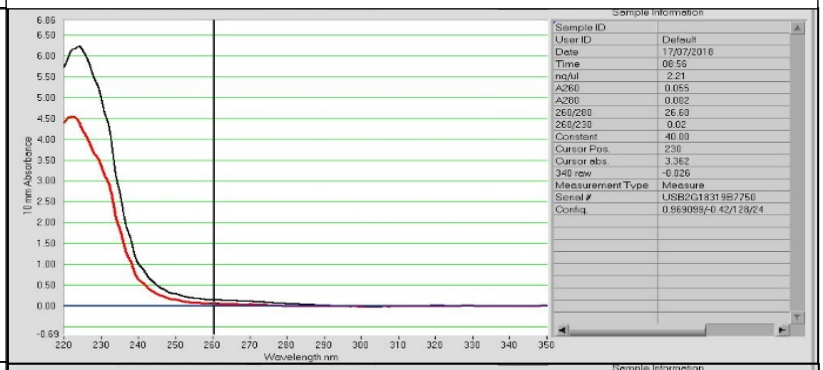
Method 2	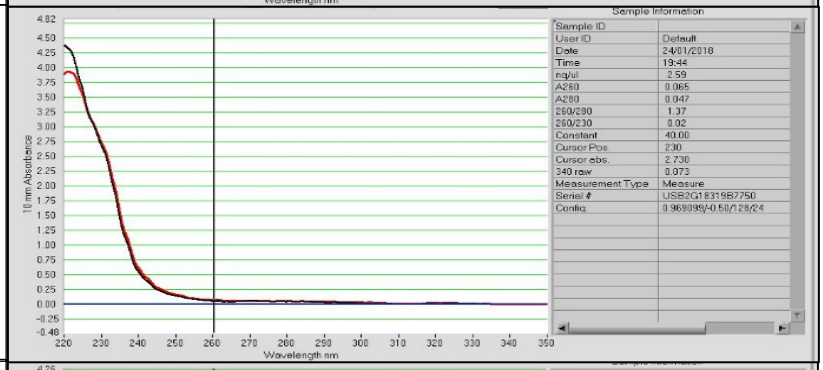
Method 3	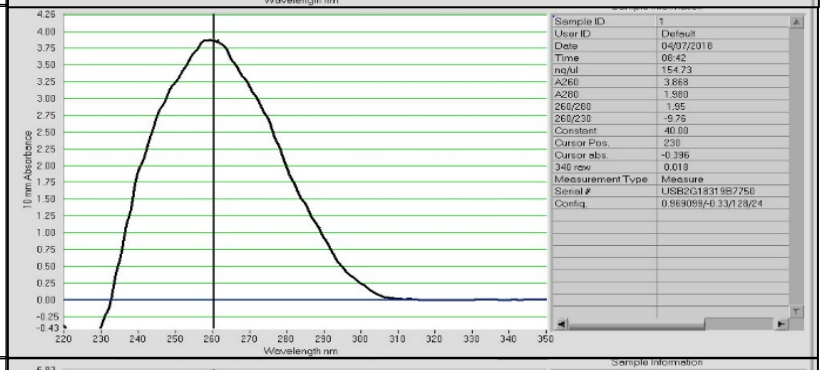
Method 4	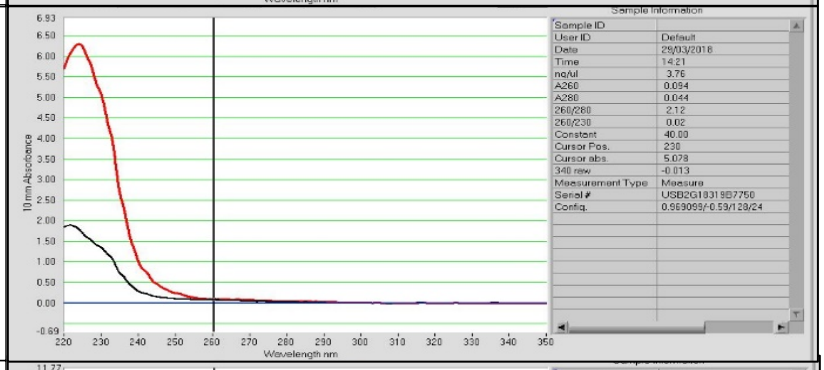
Method 5	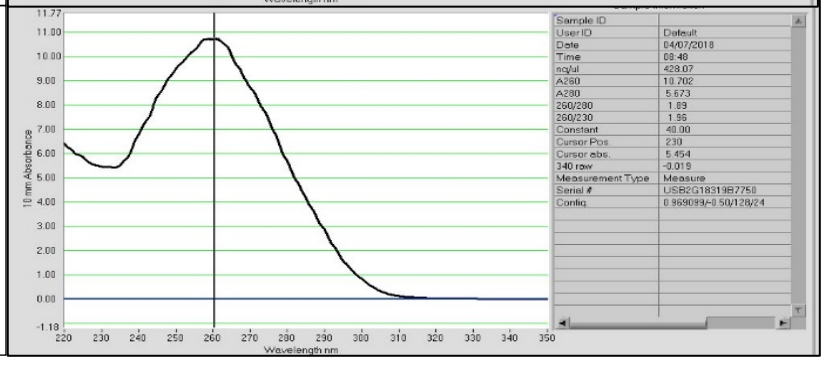

Figure 4.5: Representative Nanodrop plots from each RNA extraction method.

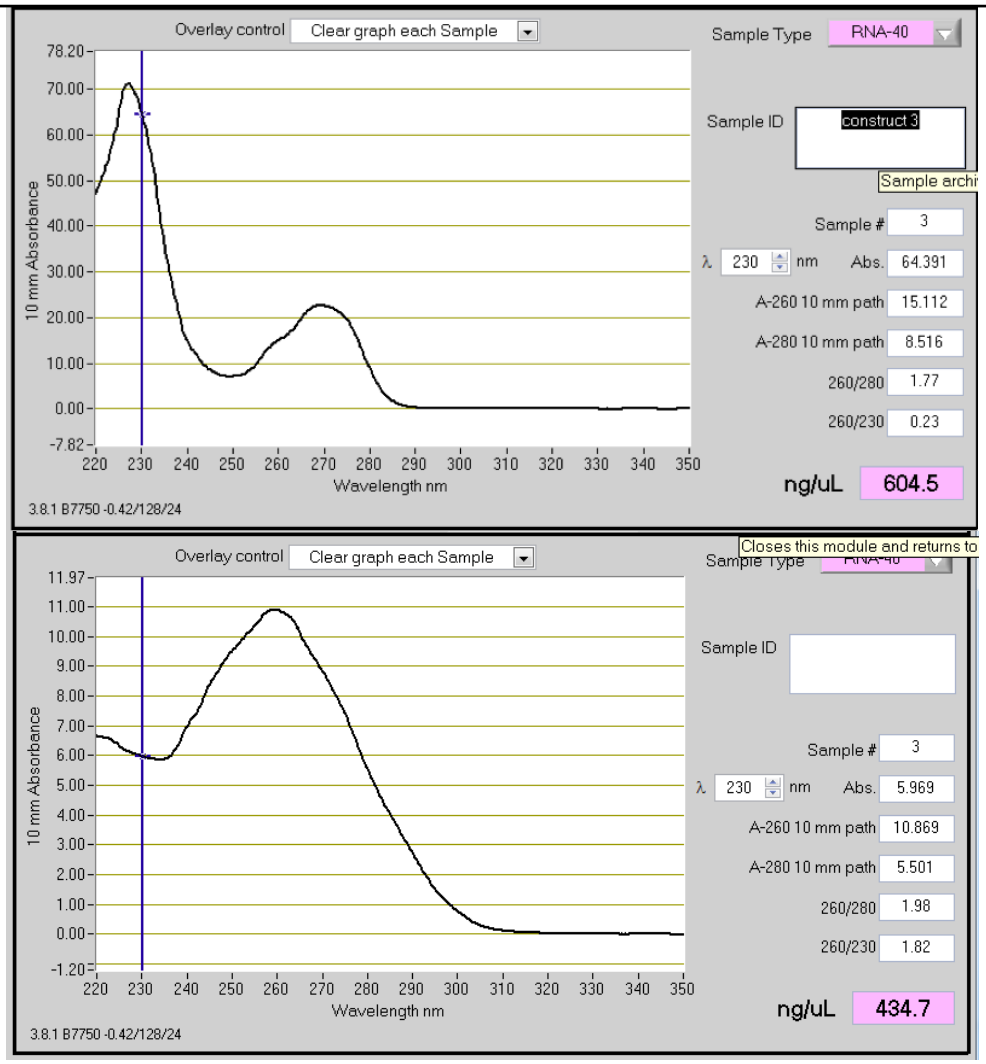

Figure 4.6: An example of a contaminated RNA sample. A*: Nucleic acid peak at 230 nm greatly outweighs the peak seen at 260 nm indicating that the substantial yield is an overestimation of the actual content. Purification of this sample is required.* ***B****: Sample A following purification. Note the improved 260/280 ratio and much improved 260/230 ratio. The peak at 230 nm has decreased significantly indicating a removal of contaminants that absorb at that absorbance. This sample is therefore suitable for cDNA synthesis.*

In summary, the use of fresh buffer QG, buffer RPE and spin columns provided the highest yields and purity of RNA for cDNA synthesis and PCR analysis compared to all other methods investigated (**Figure 4.4**, **4.5** and **4.6**). However, it must be noted that this method still was not effective 100% of the time suggesting that extraction of RNA from cell seeded agarose hydrogels is still difficult to achieve. This difficulty has also been noted by several other groups who indicate that the formation of ionic complexes between negatively charged RNA and positively charged regions of the matrix often results in a low yield of RNA.

4.2.2 First strand cDNA synthesis by reverse transcription

Conversion of total RNA into high-quality full-length cDNA was performed using the Enhanced Avian Reverse Transcription First Strand Synthesis Kit (Sigma-Aldrich Ltd, UK). Nuclease free water and 1 μl of Oligo $(dT)_{23}$ primer was first added to a 100 μl thin walled PCR microcentrifuge tube before 50 - 200 ng of total RNA was transferred into the tube. The constituents were then mixed and immediately placed on ice making a total volume of 10 μl. The tube was then placed into a Techgene thermal cycler (Techne, UK) for 5 minutes at 70°C to denature the total RNA. While this was performed, a mastermix was prepared using 10x buffer for eAMV-RT (1x final concentration), enhanced avian RT enzyme (1 unit/μl), RNase inhibitor (1 unit/μl), deoxynucleotide mix (500 μM each dNTP) and water. Once the RNA denaturation was complete, the tube was immediately placed on ice to prevent RNA from aggregating. 10 μl of the mastermix was then transferred to the tube containing denatured RNA to make a 20 μl total reaction volume and mixed with gentle pipetting. The reaction mixture was then centrifuged briefly in a minicentrifuge to make sure that the volume was at the bottom of the tube. Finally, the tube was transferred to the thermal cycler again and heated for 1 hour at 42°C. Following this step, the resultant cDNA was stored at -20°C until required.

4.2.3 RT-qPCR primer optimisation

Optimal hybridisation and priming are an essential part of PCR assay development as they concentration can enhance sensitivity, reproducibility and specificity. Each primer/target structure has a unique optimal thermodynamic stability, therefore identifying the optimum stable combination of primer to cDNA will produce the most repeatable experiments. A cDNA serial dilution series was therefore performed (1 in 5) which extended beyond both highest and lowest levels of target expected in order to calculate the primer binding efficiency. Dissociation/melt curves were included to analyse the PCR specificity and check for the formation of primer-dimers in the sample during final analysis.

Optimisation Method

To ensure uniform mixture of PCR reaction components, qPCR mastermixes were produced for each sample and primer pair containing Kapa SYBR green I fluorescent dye (2x) (Kapa Biosystems, USA), specific primer pairs (Sigma-Aldrich Ltd, UK), ROX high standard (Kapa Biosystems, USA), nuclease free water and cDNA sufficient to produce triplicate reactions (**Table**

4.2). ROX high was included as a reference dye to normalise the fluorescent reporter signal as an internal reference for non-PCR related fluctuations in fluorescence especially in terms of background noise and machine excitation and detection variations. All mastermixes were made in thin walled PCR microcentrifuge tubes before plating. Template free controls were produced by replacing cDNA with H_2O.

Table 4.2: qPCR mastermix recipe*

Reagent	Volume/μl
SYBR green	45
Forward primer	0.9
Reverse primer	0.9
Water	32.76
ROX high	1.44
cDNA	9

**Mastermixes are made 1.2x excess to ensure sufficient volume for plating. Total volume sufficient for 3 replicates.*

Forward and reverse human primers were purchased from Sigma-Aldrich at 100 μM stock concentration for the genes SOX-9, COL2a1, beta actin and aggrecan. For primer optimisation, these primers were diluted to 50, 25 and 12.5 μM concentrations in preparation for their addition to PCR mastermixes. When added to the mastermix they produced concentrations of 500, 250 and 125 nM concentrations of primers in each mastermix. Stock cDNA prepared from AFSC containing samples were prepared at concentrations of 200 nM and serially diluted 1 in 5 to produce concentrations of 200, 40, 8, 1.6 and 0.32 nM. When added to the mastermixes, these would produce concentrations of 20, 4, 0.16 and 0.032 nM concentrations of cDNA. cDNA template free controls were included for each reaction performed. Each mastermix was mixed thoroughly before pipetting 25 μl of mixture into each well of a clear 96 well PCR plate. The plate was then briefly centrifuged for 1 minute at 50 x g. Following the plate preparation, thermal cycling was performed using the StepOnePlus PCR system (Thermofisher Scientific, UK) with the following thermocycling conditions for quantitative PCR:

- 1 cycle 95°C for 10 minutes
- 40 cycles: 95°C for 15 seconds, 60°C for 1 minute
- 1 cycle: 95°C for 15 seconds, 60°C for 1 minute, 95°C for 15 seconds

Threshold cycle (Ct) values produced were analysed using StepOne v2.3 software. Amplification plots were generated for each reaction with fluorescence (δRn) against cycle number. The threshold remained unchanged for all experiments within the lower third of the linear phase of the amplification plot. Mean Ct values were normalised to day 0 beta actin endogenous control data whereby the Pfaffl method was used to calculate gene expression fold changes.

Primer efficiency calculation

A plot of Ct versus the log of nucleic acid input levels was performed and a linear regression applied. The reaction efficiency from the slope of the line was calculated using the following equation:

$$Efficiency = 10^{(-1/slope)} - 1$$

The correlation coefficient of the line (R^2 value) is used to show how well the data fits on a straight line with R^2 values of 0.99 desirable. For a 100% PCR reaction the amount of PCR product from each reaction will double following each cycle, resulting in a standard curve of gradient -3.33. Any slope between -3.9 and -3.0 is acceptable for determining efficiency.

Result of optimisation

Primer name	Forward Sequence	Reverse Sequence
Beta Actin	ACTCTCCCTCCTCCTCTT	AAGGCAACTTTCGGAACG

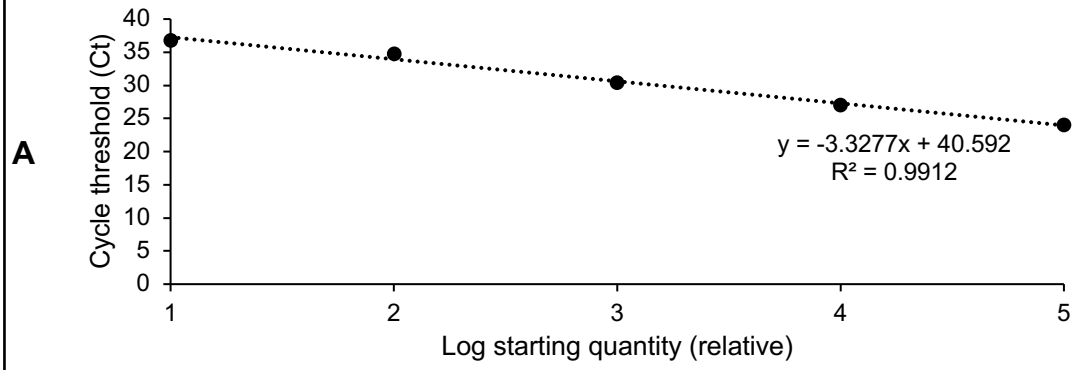

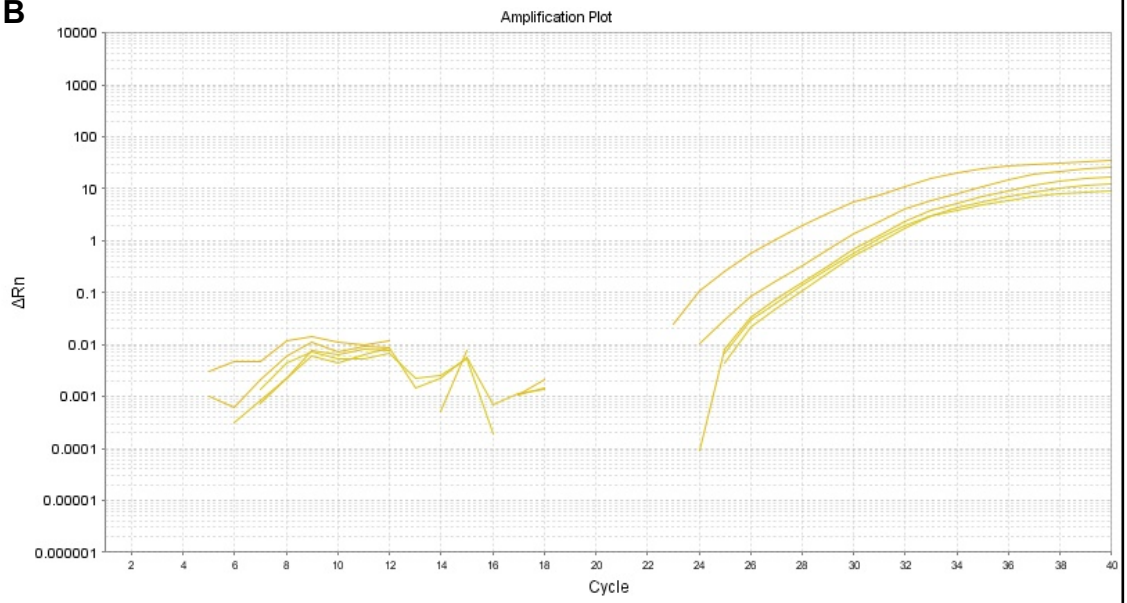

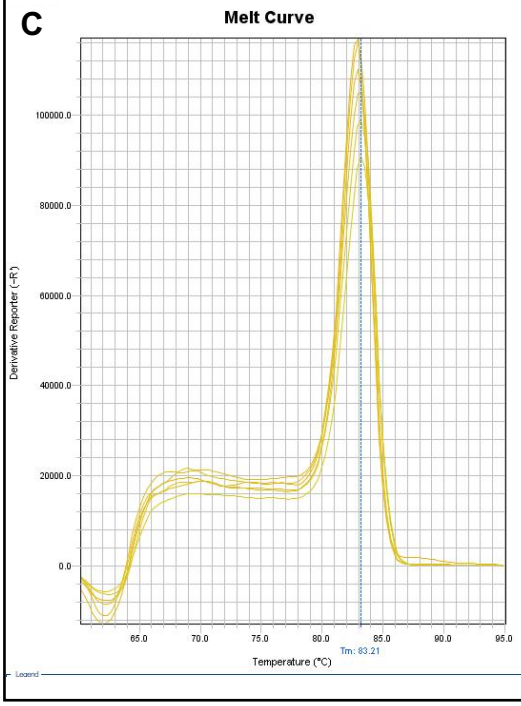

Figure 4.7: Primer optimisation for beta actin.

***A**: Standard curve indicating initial copy number of template versus threshold cycle (Ct). Real time PCR of 5-fold serial dilutions of human AFSC cDNA was performed using 500 nM of a beta actin forward and reverse primer. Reactions (3 replicates per dilution). Primer reaction efficiency = 0.99. **B**: Amplification plot of serial dilution. **C**: A rise in absorbance intensity in the melt curve indicates the dissociation of double stranded DNA during heating. The single amplification peak indicates a high standard of primer specificity without primer-dimer formation.*

Primer name	Forward Sequence	Reverse Sequence
Aggrecan	AACAGTGCCATCATTGCC	CTCATCCTTGTCTCCATAGC

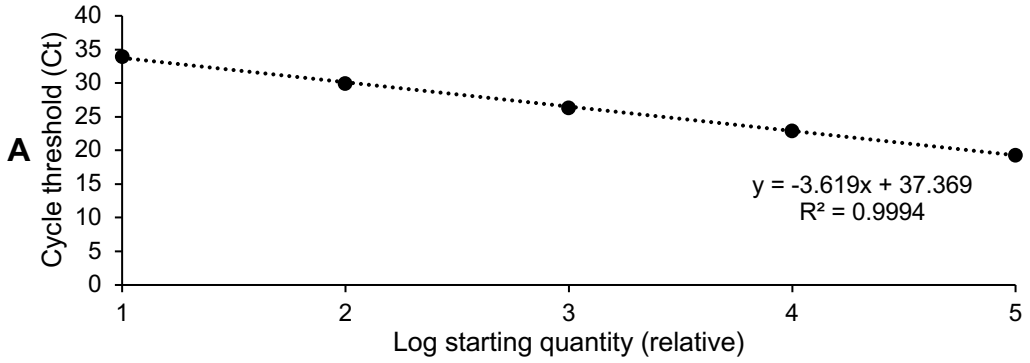

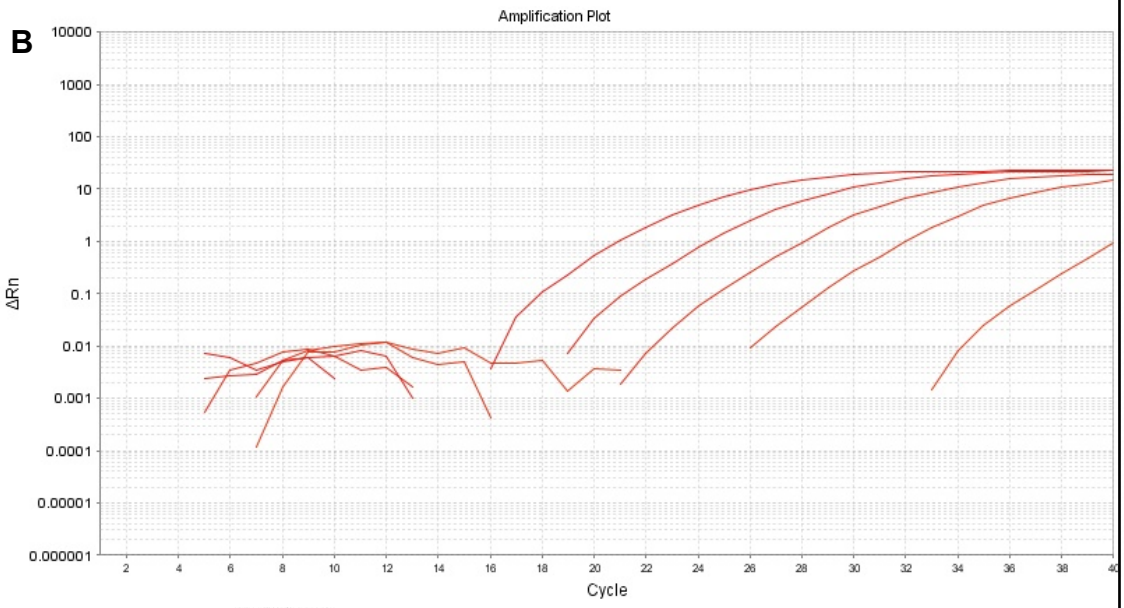

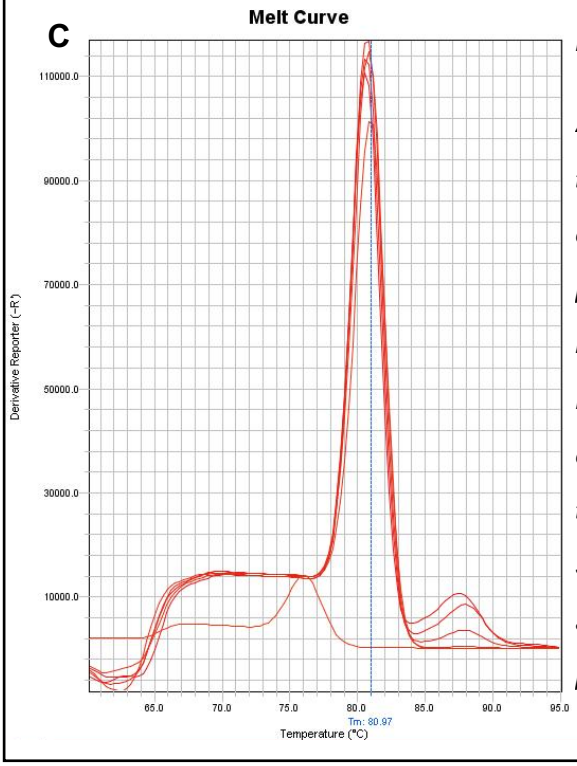

Figure 4.8: Primer optimisation for aggrecan.

***A**: Standard curve indicating initial copy number of template versus threshold cycle (Ct). Real time PCR of 5-fold serial dilutions of human AFSC cDNA was performed using 250 nM of aggrecan forward and reverse primer. Reactions (3 replicates per dilution). Primer reaction efficiency 0.91. **B**: Amplification plot of serial dilution. **C**: A rise in absorbance intensity in the melt curve indicates the dissociation of double stranded DNA during heating. The single amplification peak indicates a high standard of primer specificity without primer-dimer formation.*

Primer name	Forward Sequence	Reverse Sequence
COL2A1	GGAGTCAAGGGTGATCGT	CTTGTGCACCAGCTTCTC

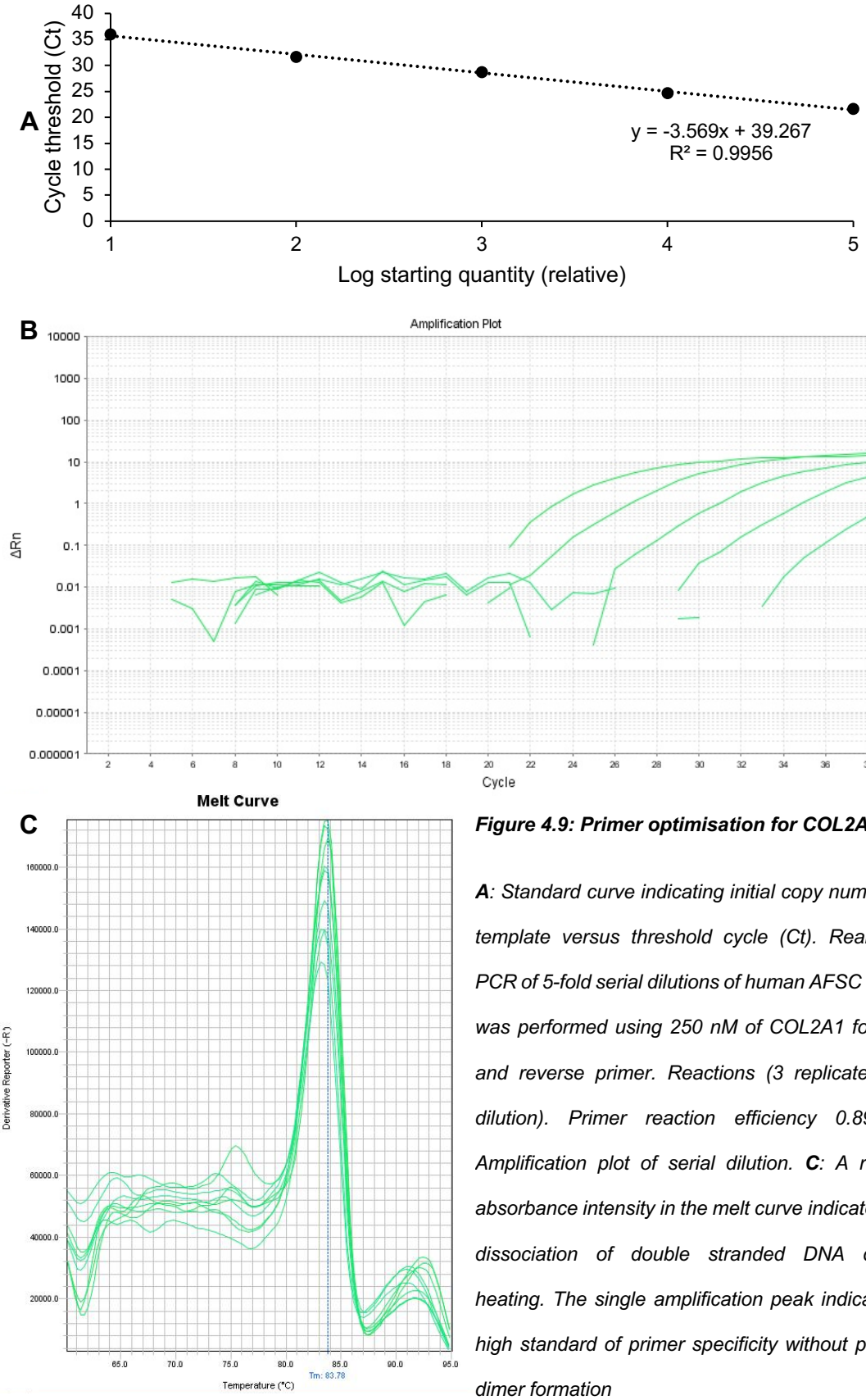

Figure 4.9: Primer optimisation for COL2A1.

A*: Standard curve indicating initial copy number of template versus threshold cycle (Ct). Real time PCR of 5-fold serial dilutions of human AFSC cDNA was performed using 250 nM of COL2A1 forward and reverse primer. Reactions (3 replicates per dilution). Primer reaction efficiency 0.89.* ***B****: Amplification plot of serial dilution.* ***C****: A rise in absorbance intensity in the melt curve indicates the dissociation of double stranded DNA during heating. The single amplification peak indicates a high standard of primer specificity without primer-dimer formation*

Primer name	Forward Sequence	Reverse Sequence
SOX-9	GTACCCGCACTTGCACAAC	GTAATCCGGGTGGTCCTTCT

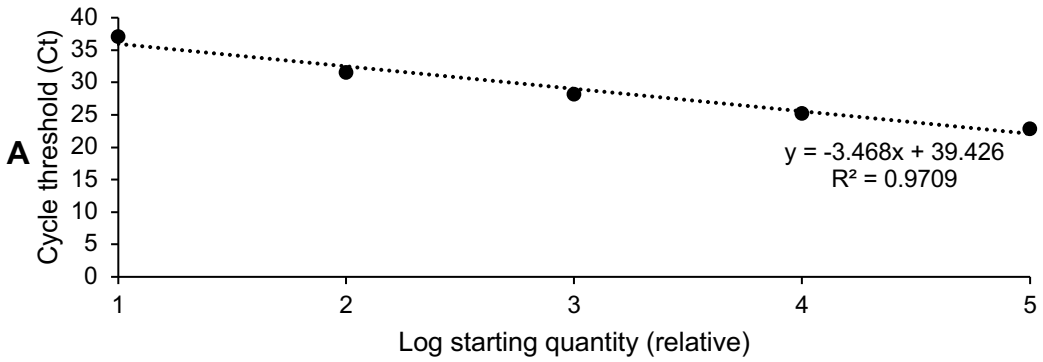

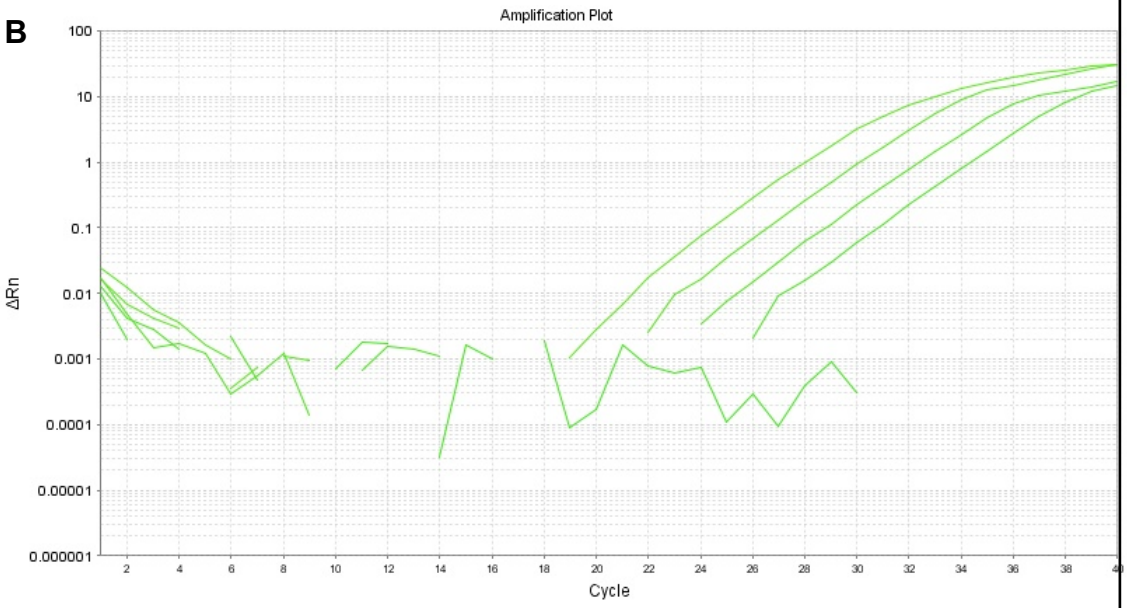

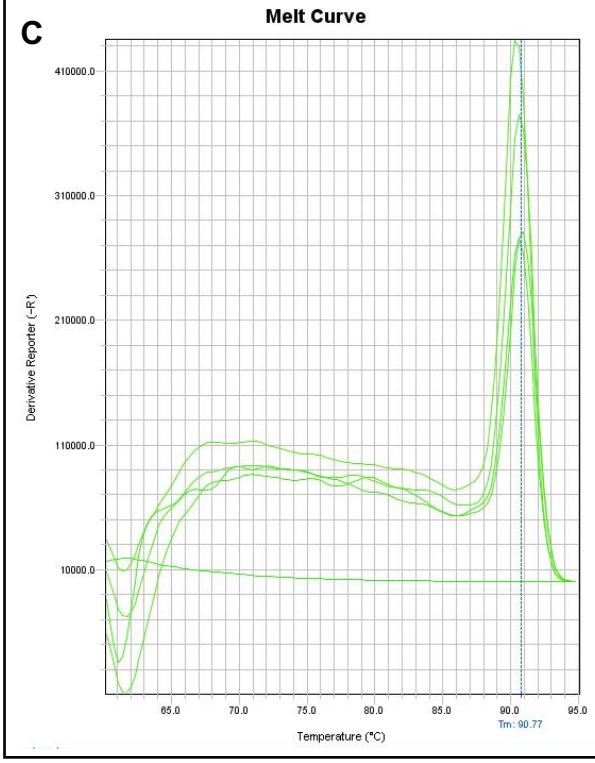

Figure 4.10: Primer optimisation for SOX-9.

***A**: Standard curve indicating initial copy number of template versus threshold cycle (Ct). Real time PCR of 5-fold serial dilutions of human AFSC cDNA was performed using 500 nM of SOX-9 forward and reverse primer. Reactions (3 replicates per dilution). Primer reaction efficiency 0.93. **B**: Amplification plot of serial dilution. **C**: A rise in absorbance intensity in the melt curve indicates the dissociation of double stranded DNA during heating. The single amplification peak indicates a high standard of primer specificity without primer-dimer formation*

Following primer optimisation performed in **Figures 4.7, 4.8, 4.9** and **4.10**, we distinguished the following optimal concentrations of primer for use with AFSCs:

Beta actin: 500nM

Aggrecan: 250nM

SOX-9: 500nM

COL2a1: 250nM

4.2.4 Pfaffl method analysis of PCR data

For gene expression analysis, relative quantification of the target gene against a reference gene (beta actin) was performed in order to obtain the relative expression ratio, which incorporates the PCR efficiency values calculated in **Figures 4.7**, **4.8**, **4.9** and **4.10**. Relative quantification of the target gene was estimated by normalising the target to the reference gene (Beta actin) and to the calibrator sample (patient matched day 0 control) by a comparative Ct approach. For each sample, the ratio of target Ct and reference Ct was calculated using the Pfaffl method which uses the equation below. Ratios were expressed on a logarithmic scale (arbitrary units).

$$\text{Gene expression ratio} = \frac{\text{Primer efficiency of GOI}^{\,\delta Ct\ GOI}}{\text{Primer efficiency of HKG}^{\,\delta Ct\ HKG}}$$

Whereby GOI = gene of interest and HKG = housekeeping gene.

4.2.5 Optimisation of hydrogel embedding and histological staining procedures

Principle

Histology from hydrogel samples is typically not shown in many papers due to the difficulty in producing high quality histological staining and preservation of the structure for analysis. Samples for histology can be prepared in 2 ways; paraffin embedding or cryo-embedding. Prior to embedding, samples require a period of fixation in order to preserve cell morphology and hydrogel architecture, inactivate proteolytic enzymes and prevent microbial contamination before undergoing any histological treatments and this is typically achieved using fixatives such as paraformaldehyde (PFA) or glutaraldehyde. Fixation works by forming covalent cross links such as methylene bridges between functional groups present in the sample and the formaldehyde itself. This crosslinking thereby acts to preserve the sample by producing an insoluble network without altering the cell structure too greatly. Following this, the constructs can be embedded in either paraffin or a cryoembedding compound such as optimal cutting temperature compound (OCT). When embedding for cryosectioning an issue can arise with the formation of ice crystals (similar to the problem of cryopreservation of cells). In order to reduce this incidence and preserve how the cells appear within the construct, cryoprotectants are employed. In this case, a hypertonic sucrose series is employed in order to gradually replace the water content found within the cells. By doing this, the formation of ice crystals is avoided and hence the cells are preserved so that they can be observed when stained. Paraffin embedding and cryo-embedding procedures were investigated.

Optimisation method

AFSC/agarose constructs were initially bisected using a no.10 scalpel to expose mid sagittal and axial sections prior to fixation (**Figure 4.11A and B**).

Fixation method: Based on previous method by (Bernstein et al., 2009). In brief, hydrogels were transferred to autoclaved glass vials and fixed with acetone for 5 minutes at -20°C (Sigma-Aldrich Ltd, UK). Acetone was replaced with methanol (5 minutes, -20°C) followed by an isopropanol extraction series (75% for 15 minutes, 96% repeated twice for 30 minutes, 100% repeated twice for 30 minutes and xylene for the final 20 minutes.

Paraffin embedding - Following fixation, samples were the beads were then embedded in paraffin by an automated series of formalin (1 hour at 37°C), 70% ethanol (2 x 45 minute washes at 37°C),

100% industrial methylated spirits (2 x 60 minute, 1 x 90 minute and 1 x 120 minute at 37°C) and xylene (1 x 90, 1 x 150 and 1 x 120 minutes) for hand embedding within paraffin wax. A small amount of molten wax was placed into the mould and allowed to cool slightly then a sample was placed in the centre. Paraffin was allowed to solidify to hold the sample in position. The tissue cassette was then placed on top of the mould and hot paraffin added from the dispenser and allowed to cool for 30 minutes.

OCT cryoembedding - Following fixation methods, each sample was rinsed briefly in ddH_2O and suspended within sucrose solutions of 5% (30 minutes to 1 hour), 15% (overnight) and 30% (overnight) concentrations. Samples were then transferred into a prepared flexible mould and coated in OCT compound until suitably covered so that the sample was completely immersed. The samples were then transferred to a prepared dewar containing liquid nitrogen, flash frozen and then stored at -80°C for long term storage or dry ice for transfer to a cryostat.

Sectioning of paraffin samples

All optimisation samples were sectioned at 10 µm thickness using a ThermoScientific Microm HM325 microtome and mounted on standard microscope slides. In brief, the paraffin embedded samples were stored on ice to cool the sample and aid sectioning. The sample was placed into the microtome and orientated to the inserted blade. Sections of 10 - 30 µm were first cut to ensure correct orientation of the blade to the sample and to expose the surface level of the embedded sample before being reduced to 6 µm. Sections were then cut sequentially and picked up by tweezers. Sections were then introduced to the surface of a preheated water bath at 40°C before being applied to microscope slide and dried overnight at 37°C.

Sectioning of OCT samples

Setup is displayed in **Figure 4.11C**. All optimisation samples were sectioned at 6 µm thickness using a Leica CM3050 S cryostat and mounted on Superfrost slides. Slides were then stored on ice prior to staining. Sections were stained with either Haematoxylin & Eosin (H&E), picosirius red or alcian blue for the presence of GAGs.

Microscopy

Sections were visualised using a Zeiss Axioskope microscope with Infinity3s camera and Infinity capture software. Images taken at x 1.25 and x 20 magnifications.

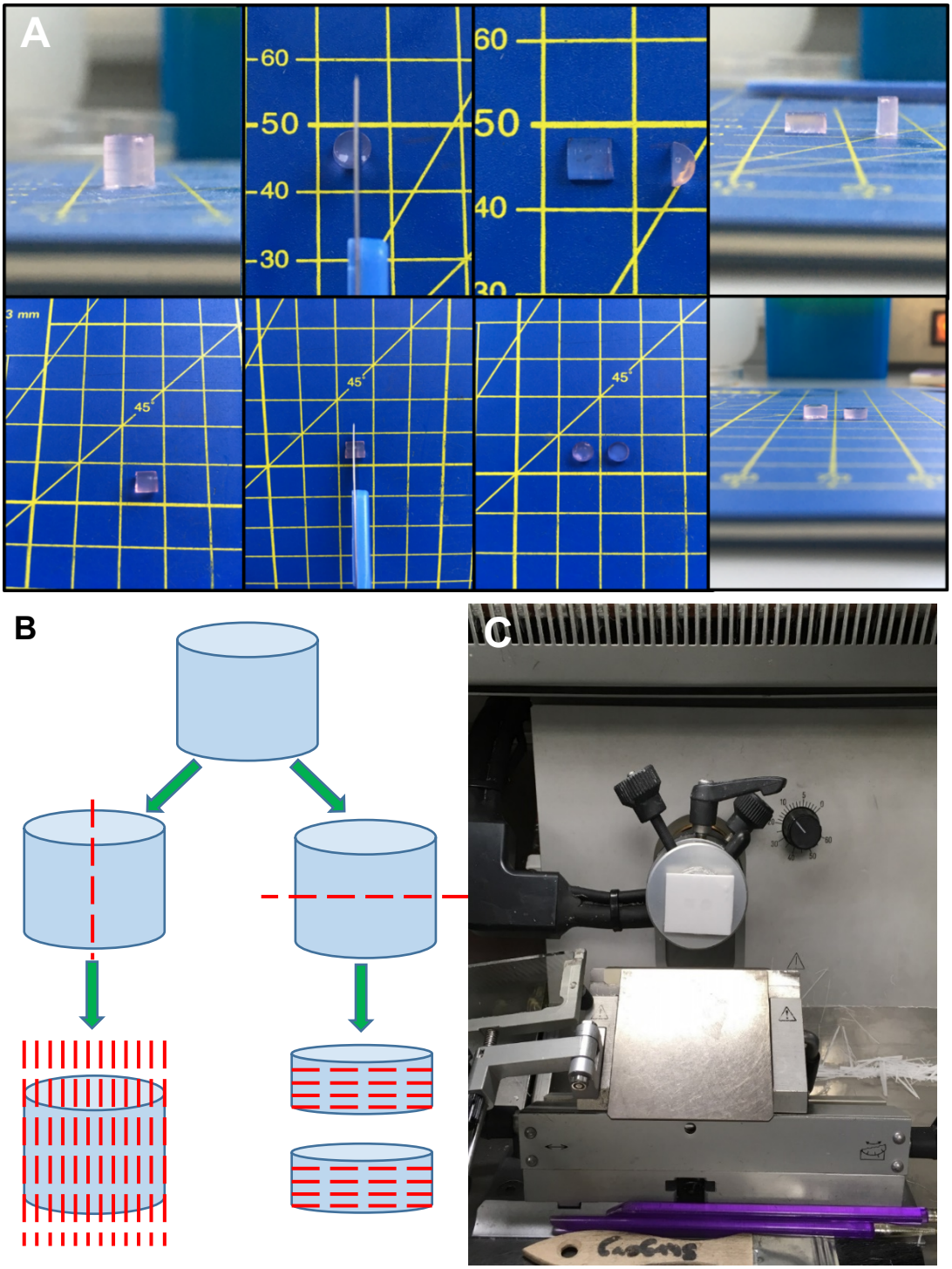

Figure 4.11: Preparation of agarose constructs within cryostat. *Following fixation and sucrose cryoprotection, samples were placed upright and bisected centrally to produce 2 exact halves of the construct (**A + B**). Subsequently one edge was then placed flat on its horizontal plane prior to OCT embedding. Secondly constructs were placed on their side and bisected centrally again. This produced 2 parts of the construct with the core and longitudinal sections of the construct exposed. Following snap freezing, samples were placed within cryostat pedestal for sectioning (**C**).*

Histological staining

For all paraffin embedded sections prior to staining the following steps were undertaken. Firstly, the samples were rehydrated by placing the microscope slides into histoclear baths for 5 minutes and repeated once more. Following this, the samples were added to an ethanol series of baths including 100%, 95% and 70% with each bath repeated twice for 3 minutes to ensure rehydration before rinsing in water. For cryoembedded samples, sections were allowed to air dry within a fume hood for 20 minutes prior to any staining procedure. All stains were kept at room temperature for 30 minutes prior to staining commencement.

H&E staining: This staining method is commonly used to identify cell types and cellular components in tissue. Haematoxylin is used to stain the cell nucleus blue while eosin stains the cytoplasm of the cell red producing a characteristic purple colour to the stained section. Since haematoxylin (Sigma-Aldrich Ltd, UK) and eosin solutions were premade, the following procedure was followed:

Sections were exposed to haematoxylin stain first for 8 minutes then placed under running water to remove any excess stain for a period of 5 minutes. Sections were then placed into the eosin solution for 2 minutes before being placed into an ethanol series of 96% ethanol for 30 seconds and 2 washes in 100% ethanol for 30 seconds. Finally, slides were placed in histoclear for 10 seconds. Moisture was allowed to evaporate from the surface of the slide in addition to gentle wiping of excess histoclear from the slide, before a drop of distyrene, plasticiser and xylene mounting solution (DPX, Sigma-Aldrich Ltd, UK) was applied without any air bubbles and a coverslip (24 mm x 60 mm) placed above the samples. The DPX was allowed to spread under the coverslip and over the samples.

Picosirius red: a strong, linear, anionic dye comprised of six sulfonate groups which are able to associate with cationic collagen fibres. This dye is typically used to stain muscle tissue sections.

The following procedure was followed for both paraffin and OCT embedded samples:

Solution A: 0.5 g of Direct Red 80 was added to 500 ml of picric acid solution.

Solution B: 5 ml glacial acetic acid was added to 1 litre of tap

Sections were exposed to solution A for 60 minutes, solution B for 30 seconds twice, deionised water for 30 seconds twice. Ethanol series was then used including 95% (twice for 20 seconds

each), 100% ethanol (twice for 20 seconds) and histoclear for 3 minutes. A drop of DPX was then added before coverslip attachment.

Alcian blue: a dark blue copper containing dye used to stain acidic polysaccharides such as glycosaminoglycans and other types of mucopolysaccharides.

Alcian blue solution (pH 1.0): 400 ml of 0.1 M hydrochloric acid was first made by adding 3.3 ml of 38% HCl to 395 ml of deionised water and topped up to 400 ml. 4 grams of alcian blue powder was then added to this solution and filtered using Whatman paper. The prepared solution was viable for up to 6 months and stored at room temperature.

Nuclear Fast Red solution: 20 grams of aluminium sulphate was dissolved in 400 ml of deionised water followed by 0.4 grams of nuclear fast red. The solution was then boiled on a heat plate and allowed to cool. Once cooled the solution was filtered using Whatman paper and a grain of thymol added as a preservative. The prepared solution was viable for up to 6 months and stored at room temperature.

Sections were loaded into a slide holder and introduced to the alcian blue solution for 5 minutes at room temperature. Afterwards, the slides were removed and washed 3 times with deionised water before adding to the nuclear fast red solution for a further 5 minutes at room temperature. Following this, the slides were removed and washed with tap water 4 times. Slides were then dried carefully, DPX applied to the surface of the microscope slide and coverslip mounted. Coverslip edges were again covered with nail varnish to secure coverslip to the slide and protect the sample.

Result of optimisation

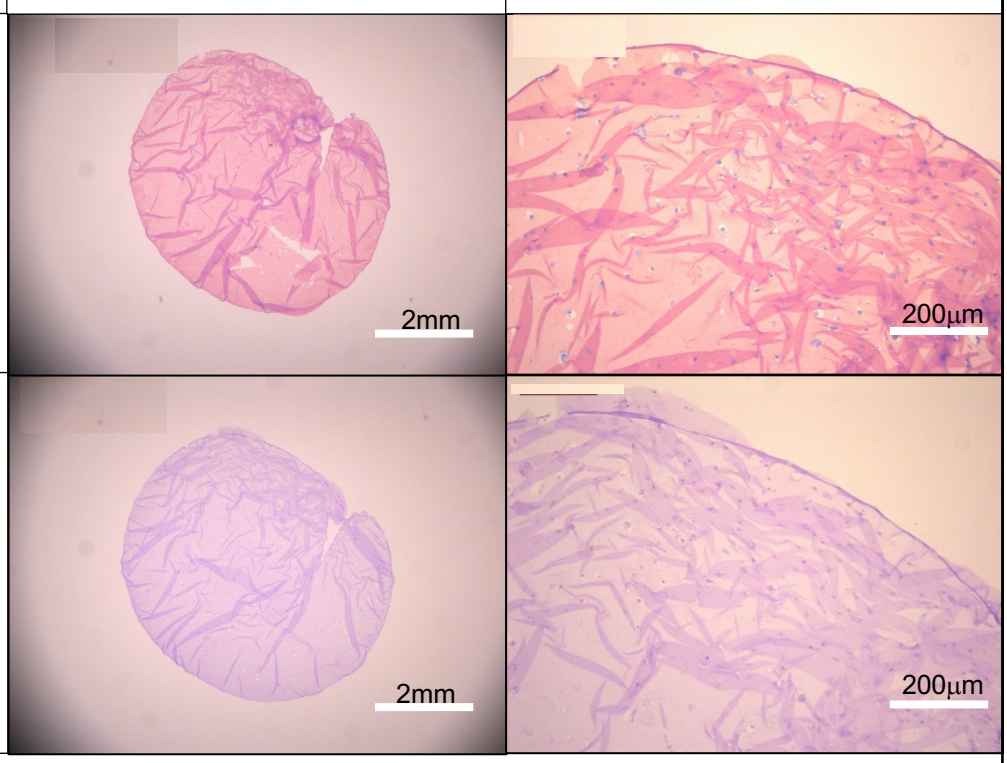

Figure 4.12: Paraffin embedding of hydrogel construct resulted in severe folding hydrogel samples. *Intense background staining of the hydrogel and extensive folding of the sample was apparent post paraffin embedding and sectioning, obscuring any specific staining attributed to the cells or ECM components and was unsuitable as a method of processing hydrogel samples.*

The sectioning procedure of paraffin embedded agarose samples caused a significant shrinkage of the hydrogel (**Figure 4.12**). During sample sectioning, the hydrogel expands creating the wrinkled appearance in each section. This directly affects the appearance of the section and the ability to discern useful information regarding the cells embedded within the sample. In contrast, cryoembedded samples demonstrated much clearer sections with no wrinkling as seen in the paraffin embedded samples (**Figure 4.13**). However, sectioning of the cryoembedded samples required a large amount of care and delicacy as the sections could easily split. Another problem associated with the histology process was the widespread non-specific background staining apparent in all the stains used (**Figure 4.12**). H&E and picrosirius staining in particular showed complete background staining of the gel itself making it difficult to distinguish any cellular architecture or collagen deposition.

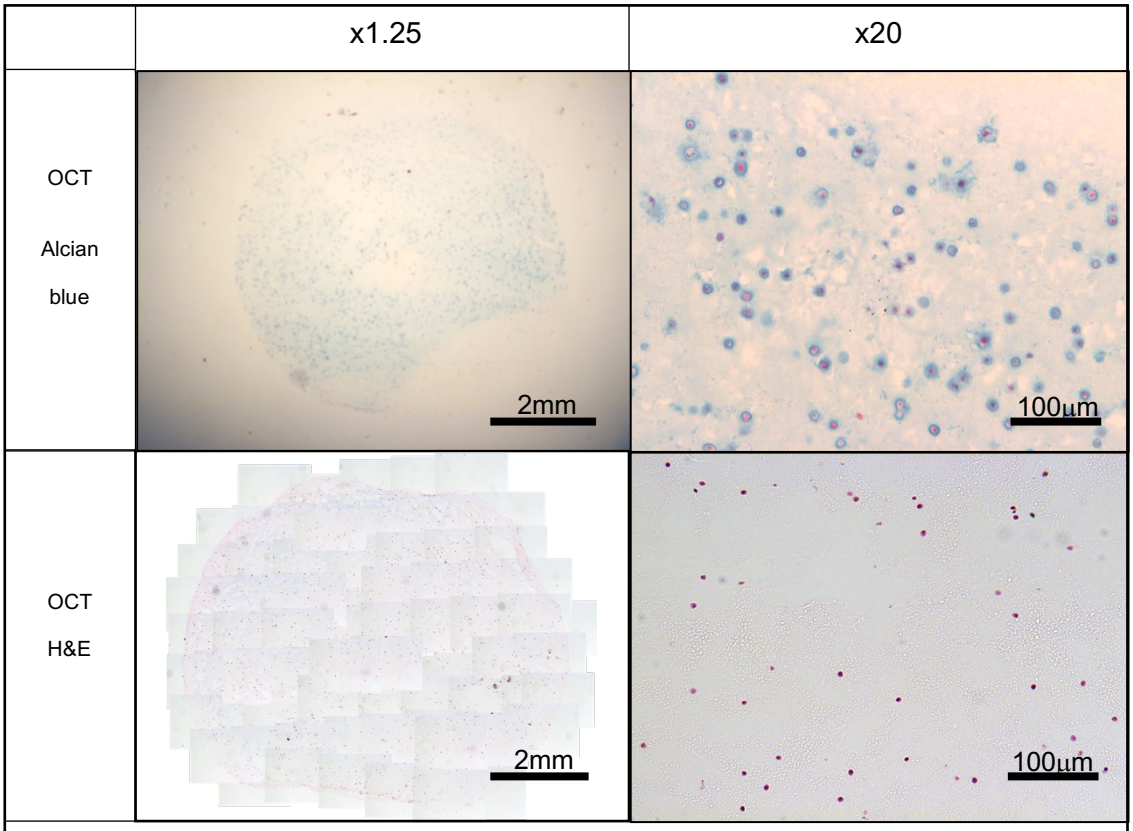

Figure 4.13: OCT embedding of hydrogel construct eliminates the severe folding seen in paraffin embedded samples. *While still showing some non-specific staining, the alcian blue staining protocol used showed specific staining of cells via nuclear fast red counterstain and specific positive staining of proteoglycans (alcian blue). H&E staining showed cell specific staining only.*

However, the alcian blue staining protocol with nuclear fast red counterstain offered the least amount of non-specific background staining and allowed the observation of pericellular proteoglycan deposition. Therefore, for histological staining AFSC/agarose samples were OCT embedded, cryo-sectioned and stained using alcian blue with a nuclear fast red counterstain (**Figure 4.13**).

4.2.6 Histology analysis

To perform image analysis and quantification, the image processing package Fiji was used (Schindelin, 2012). The following plugins were used to perform analysis of the prepared histological sections: Plot profiling: Dynamic ROI Profiler (Clojure) by Albert Cardona and Analyse Particles: Quick PALM by Ricardo Henriques. In brief, the histology collage was opened in the Fiji program and the area of the construct was selected using a circular area selection whereby it was converted into a 16 bit black and white image and threshold adjusted to isolate the cells within the image from the background (**Figure 4.14B**). This processed black and white image was then analysed using the 'Analyse Particles' plugin to count the individual number of cells within the processed image (**Figure 4.1C and D**). Smaller particles were excluded by applying 200-infinity and the fill hole parameter applied to avoid double counts. Further information including the number of counts and average size of each point read was also recorded.

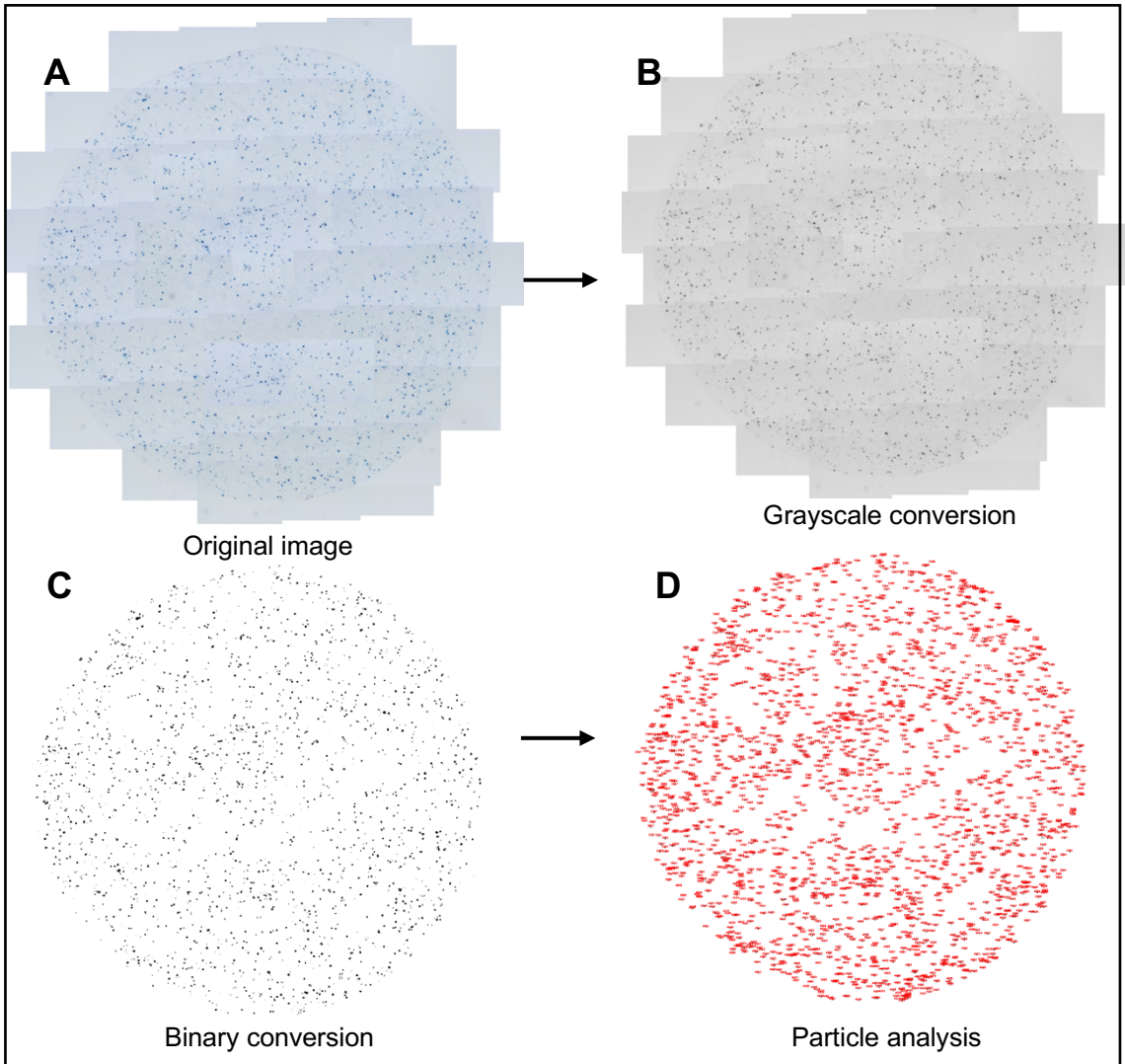

Figure 4.14: Key steps in image processing for cell count within AFSC/agarose constructs using Fiji software.

4.2.7 Second Harmonic Generation Microscopy (SHG)

SHG microscopy was performed using two photon confocal imaging on a Leica TCS SP8 AOBS multi photon confocal laser scanning microscope equipped with Coherent Chameleon Ultra, Ti Sapphire mode locked femtosecond IR laser. Collagen was excited at 900 nm and SHG signal detected using a non-descanned transmitted light detector with a 435 - 455 nm bandpass filter with a pump wavelength of 880 nm at 80 femtosecond pulse width and a 25 x 0.95 NA water immersion objective. The pinhole was set to maximum throughout imaging. Images were collected with a 25x objective. DAPI staining was also performed to label cell nuclei. Samples were acquired at 2 μm z-section intervals using the data acquisition system and Leica LAS X software; which can control the motorized stage containing the sample. The parameters for laser power, detector gain and offset remained constant for each sample so that direct comparisons could be made per treatment option. Data was collected at a resolution of 1024 x 1024 at a speed of 600 Hz with bidirectional mode enabled to allow scanning in both directions. A line average of 3 was used in order to reduced background noise.

4.2.8 Chondrogenic differentiation experiment

Chondrogenic differentiation medium was identical to that described in **Chapter 2.2**. Each construct was supplied with an identical volume of differentiation medium and growth factor concentrations as previously stated also. The end point of culture was maintained at 28 days. Culture medium was exchanged every 3 days as previously performed. In addition to the previous treatments and controls utilised, I included CNP only treatment (100 nM, GenScript, USA), CNP + TGFβ_1 (100 nM + 10 ng/ml respectively) treatment, CNP + TGFβ_3 (100 nM + 10 ng/ml respectively) treatment and finally Dex + TGFβ_1 (100 nM + 10 ng/ml respectively).

4.2.9 Biochemical assays

DMMB, Hoechst and hydroxyproline assay protocols were unchanged from **Chapters 2.2.12**, **2.2.13** and **3.2.3**. Each construct was also processed identically to the methods stated previously.

4.2.10 Statistics

All results in this study were shown as the mean from replicates and individual experiments with error bars representing the SEM. Shapiro Wilk normality test was used to determine statistical significance of non-normally distributed data between means (determined

using SPSS software, version 10, IBM, USA). The number of patients and replicates are indicated in figure legends. In all comparisons, $p<0.05$ was considered statistically significantly for tests comparing treatment conditions vs controls and inter-treatment comparisons.

4.3 Results

4.3.1 Temporal effect of CNP supplementation on GAG synthesis, hydroxyproline synthesis and DNA content of AFSC/agarose constructs suggests positive effect when applied in concert with TGFβ.

The statistical differences observed were based on comparing the averages of different treatment conditions. The ability of CNP to influence GAG synthesis in AFSC/agarose constructs was compared to that of Chang, Basal medium, TGFβ$_1$, TGFβ$_3$, CNP + TGFβ$_1$, CNP + TGFβ$_3$ and Dex + TGFβ$_1$ over a period of up to 28 days. Treatment of constructs with exogenous CNP did not result in any clear differences to control samples at all time points in terms of GAG synthesis, DNA content and collagen synthesis (**Figure 4.15, 4.16 and 4.17**; $p>0.05$). Treatment with either TGFβ$_1$ or TGFβ$_3$ resulted in significant increases in GAG synthesis and collagen synthesis relative to controls and CNP treated samples (**Figure 4.15B** and **C, Figure 4.16B and C**; $p<0.01$). Further to this, no obvious differences were detected between CNP + TGFβ$_1$ and CNP + TGFβ$_3$ treated AFSC/agarose constructs in terms of GAG synthesis, DNA content changes and hydroxyproline synthesis ($p>0.05$; **Figure 4.15C**). Direct comparisons between TGFβ$_1$ or TGFβ$_3$ treated samples with CNP + TGFβ$_1$ and CNP + TGFβ$_3$ counterparts for GAG synthesis, showed statistically significant differences between CNP + TGFβ$_1$ and CNP + TGFβ$_3$ treatments compared to TGFβ$_{1/3}$ treated samples (**Figure 4.15C**). After 28 days of culture, combination treatment samples were all significantly higher compared to single factor treatments. No statistical differences were observed after only 14 days of culture between these groups in terms of GAG and collagen synthesis.

For collagen synthesis, statistically significant differences were only detected after 21 and 28 days of culture in TGFβ isoform treated samples and combination treated samples (CNP + TGFβ$_1$, CNP + TGFβ$_3$, Dex + TGFβ$_1$) No differences were detected when comparing the combination treatments with single TGFβ isoform treatment (**Figure 4.16A, B and C**).

DNA content changes were detected as early as 14 days of culture whereby samples treated with either TGFβ isoform alone or combination treatments resulted in statistically significant increases relative to control samples. This trend continued at 21 and 28 days of culture. No differences in DNA content were observed between single factor TGF treatment and combination treatments either (**Figure 4.17A**, **B** and **C**; $p>0.05$).

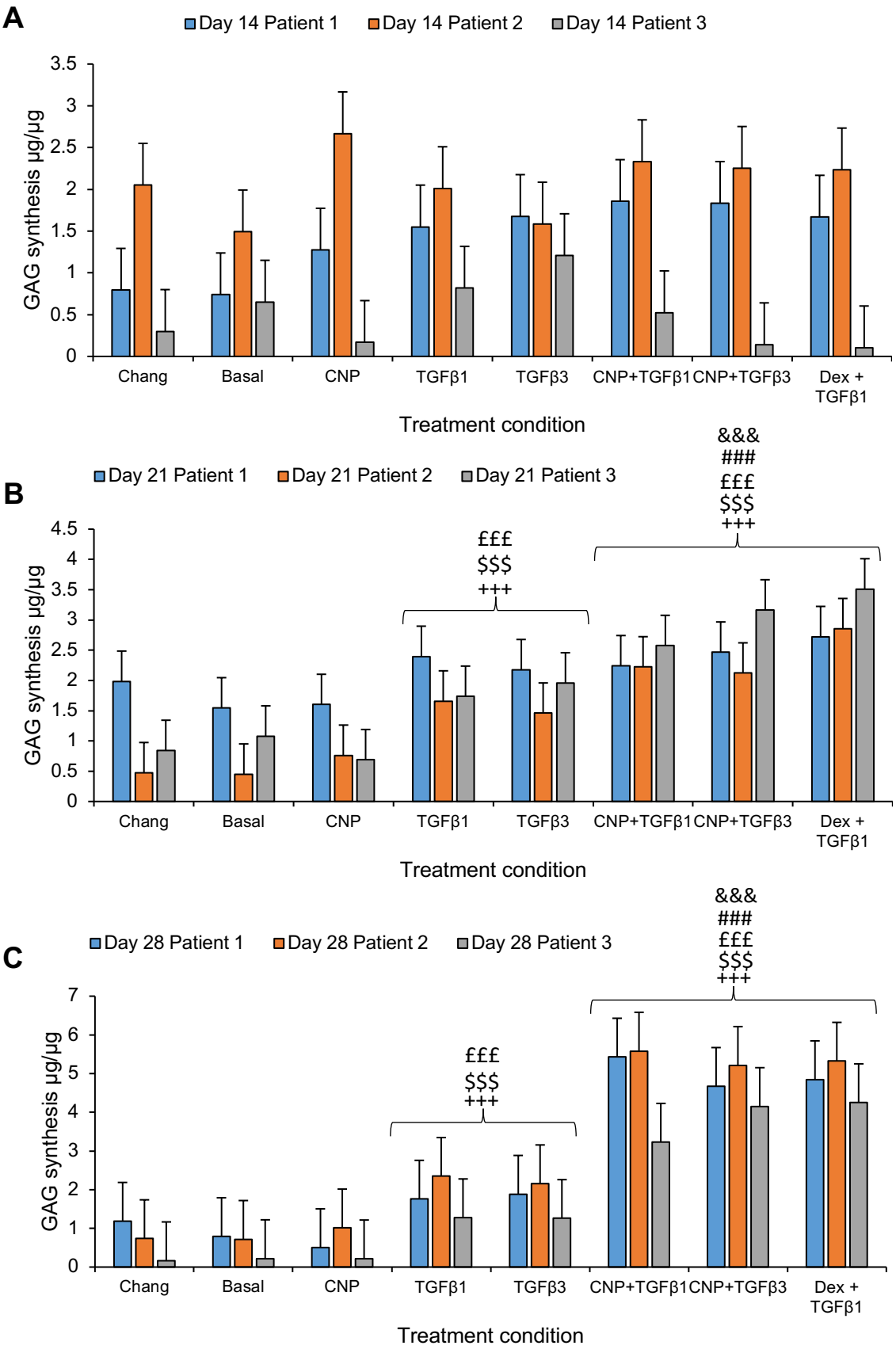

Figure 4.15 CNP alone does not stimulate GAG synthesis. *+++ indicates with Chang, $$$ with Basal, £££ with CNP, ### with TGFβ_1 and &&& with TGFβ_3. Brackets indicate the same statistical differences appear at the different time points. N = 3 per condition and time point with 12 replicates. Error bars indicate ± SEM. Data normalised to day 0.*

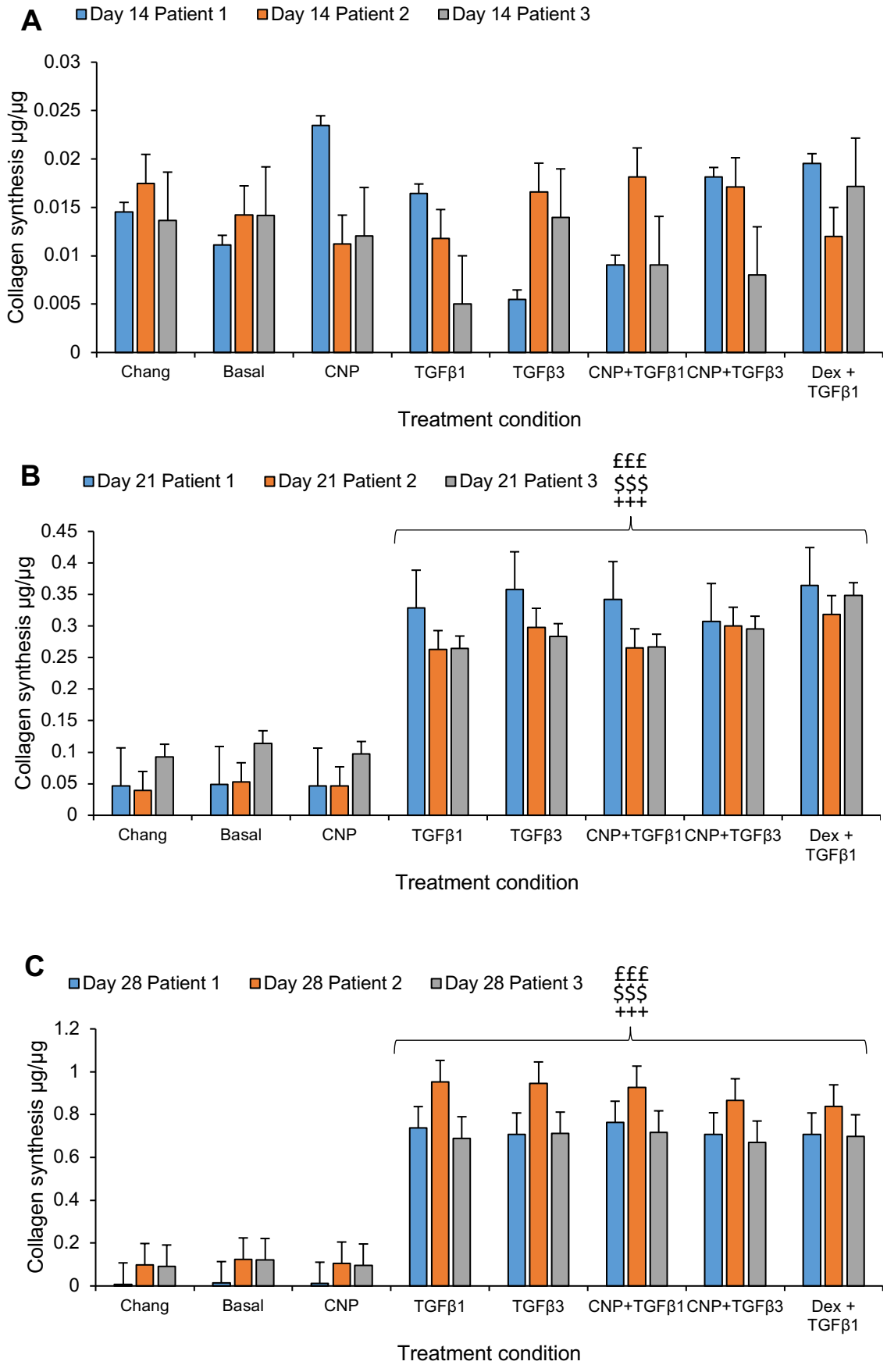

Figure 4.16: CNP alone does not stimulate collagen synthesis*. +++ indicates with Chang, $$$ with Basal, £££ with CNP. Brackets indicate the same statistical differences appear at the different time points. N = 3 per condition and time point with 12 replicates. Error bars indicate ± SEM. Data normalised to day 0.*

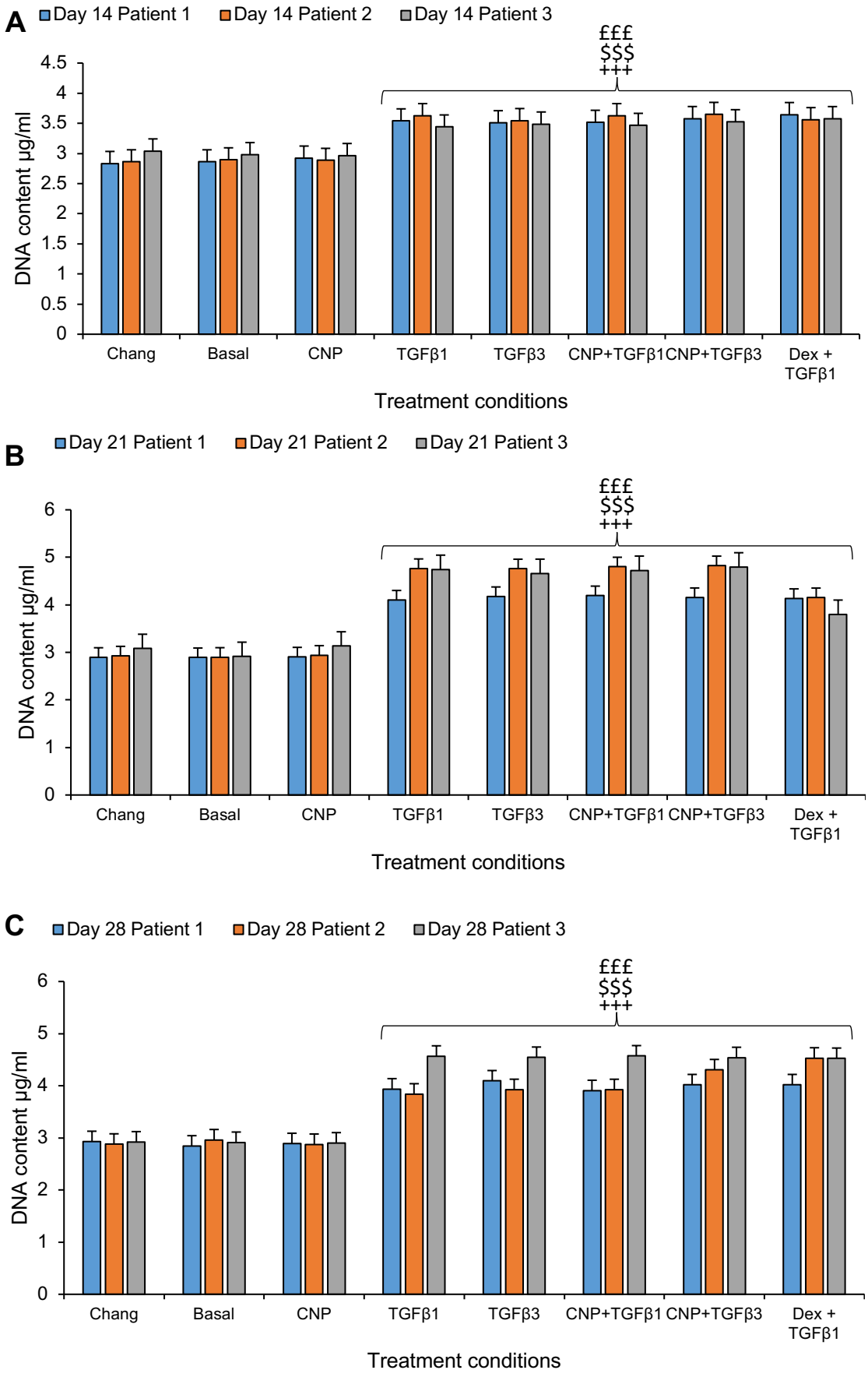

Figure 4.17: CNP addition does not significantly enhance DNA content. *+++ = significantly different to Chang treatment, $$$ = significantly different to basal medium, £££ = significantly different to CNP. N = 3 per condition and time point with 12 replicates. Error bars indicate ± SEM. Data normalised to day 0.*

4.3.2 Exogenous treatment of Dex + TGFβ, CNP + TGFβ1/TGFβ3 or CNP alone does not affect chondrogenic gene expression in AFSC/agarose constructs after 28 days of culture relative to day 0.

SOX-9 gene expression increased for all treated constructs compared to day 0 control (**Figure 4.17A**). However, the only statistically significant change in gene expression was detected when comparing CNP + TGFβ1 to day 0 control ($p<0.001$).

Similarly, COL2a1 gene expression increased in all treatment conditions compared to control ($p<0.01$, **Figure 4.17B**). The greatest increase was observed in Dex + TGFβ1 treated sample, showing 146 times increase in gene expression relative to day 0 control. In contrast, CNP treatment alone only resulted in a 25-fold increase in COL2a1 expression. However, no statistically significant differences were detected when comparing all treatment conditions to day 0 control and also when comparing treatments ($p>0.05$).

In the case of aggrecan expression, whilst treatment with CNP + TGFβ1, CNP + TGFβ3 and Dex + TGFβ1 all resulted in increased aggrecan gene expression relative to day 0 control, treatment with CNP did not (**Figure 4.17C**). No statistically significant differences were detected between day 0 and treated samples

Analysis included 4 patients' cells (N = 3 replicates) where error bars represent the standard error of the mean. Gene expression was normalised to patient matched day 0 control samples and presented as relative gene expression to day 0 untreated samples with gene amplification efficiency values taken into account during the calculation.

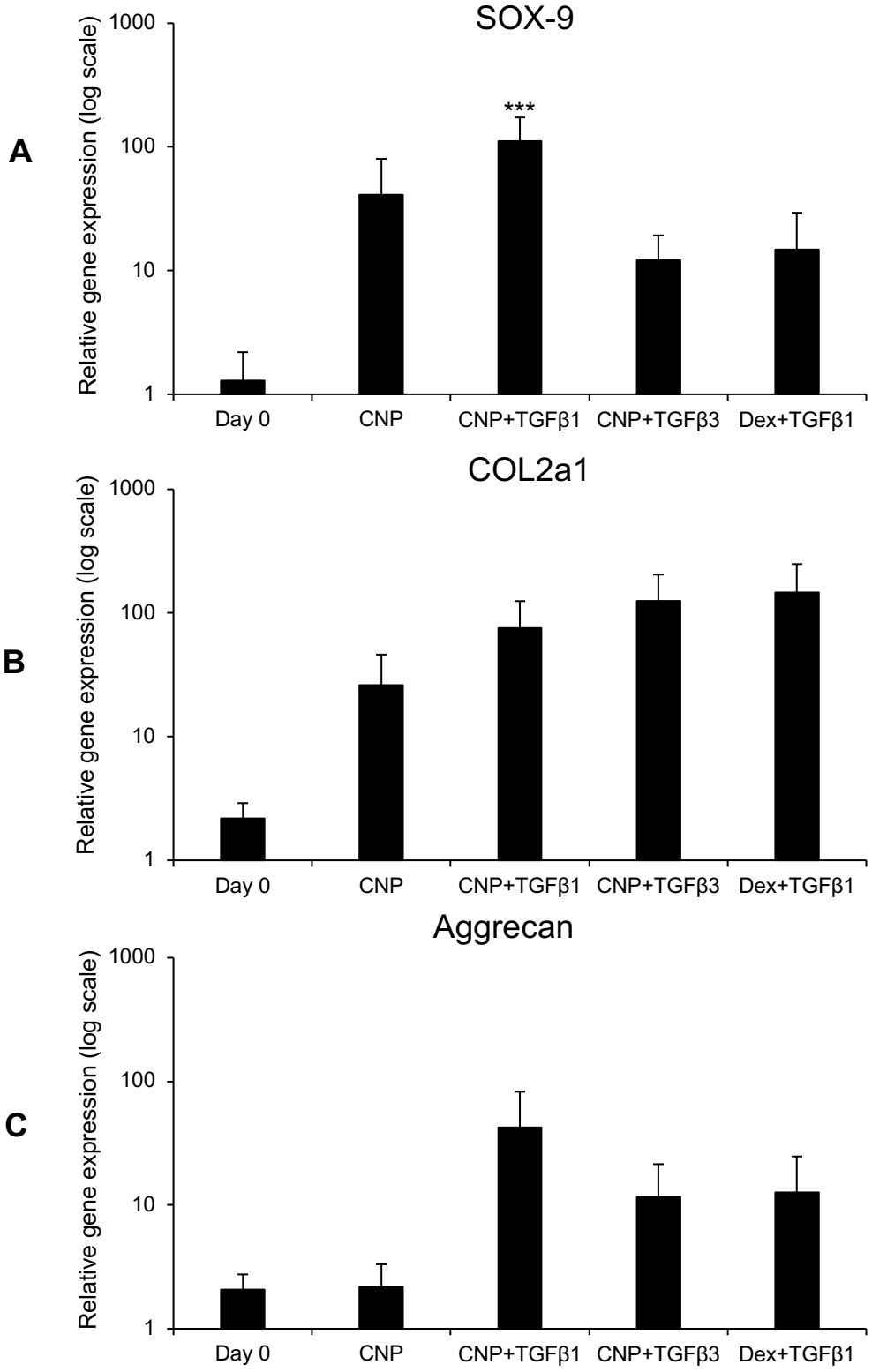

Figure 4.18: Relative gene expression for SOX-9, aggrecan and COL2a1 with y-axis presented as a logarithmic scale. *Analysis included 4 patients, with 3 replicates performed during analysis per patient. Error bars represent the standard error of the mean. The only statistically significant difference detected was observed when comparing CNP + TGFβ_1 treated sample to day 0 when measuring SOX-9 expression ($p<0.05$). *** indicates statistically significant difference with day 0 ($p<0.01$).*

4.3.3 Histological analysis of AFSC/agarose constructs treated with CNP +TGFβ_1, CNP + TGFβ_3, indicates weak positive pericellular proteoglycan deposition

Following cryo-preparation and cryo-sectioning of AFSC/agarose day 0 control and treated constructs, alcian blue staining with nuclear fast red counterstain was performed on axial and mid-sagittal sections of 6 μm thickness. Day 0 controls demonstrated no positive alcian blue staining with only cell nuclei stained due to the counterstain used (**Figure 4.18**). Homogenous cell distribution was identified using the Image J plugin and visual confirmation. AFSCs clearly displayed strong positive alcian blue staining around the cells when treated with dexamethasone and TGFβ_1 after 28 days of culture (**Figure 4.21**). This strong staining was evident in both axial and mid-sagittal sections (**Figure 4.421A** and **C**). Positive staining was also evident in CNP + TGFβ_1 and CNP + TGFβ_3 treated samples but to a much lesser extent than in the dexamethasone + TGFβ_1 treated sample (**Figure 4.19** and **Figure 4.20** respectively). All treated samples demonstrated more positive alcian blue staining compared to the day 0 control. The distribution of cells throughout the treated constructs was determined by counting the number of individual dots of a specific minimum and maximum size which would indicate a cell as the image was scanned from left to right. For all sections scanned, the distribution of cells appeared homogenously distributed (**Figure 4.18C and F, Figure 4.19C and F, Figure 4.20C and F, Figure 4.21C and F**).

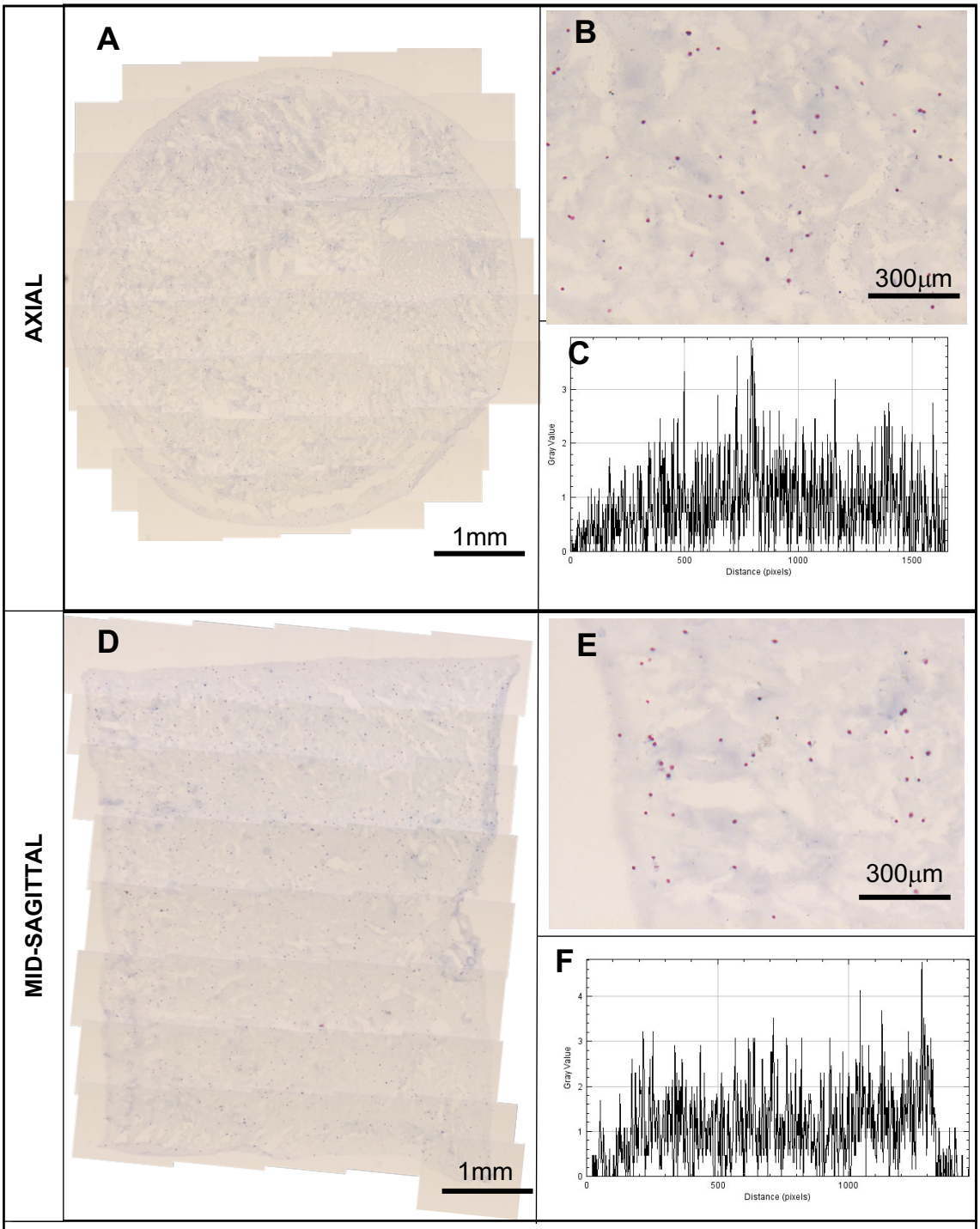

Figure 4.19: Alcian blue staining of AFSC/agarose day 0 control are negative for proteoglycan deposition. *Day 0 controls sections demonstrate largely homogenous distribution of cells within the constructs but show no positive alcian blue staining of proteoglycan deposition with only nuclei stained.* ***A + D****: Collage of x20 images taken of construct axial (****A****) and mid sagittal (****D****) sections of AFSC/agarose construct from day 0.* ***B + E****: x20 magnification image of sample negative for proteoglycan.* ***C + F****: Pixel count of collage image scanning from left to right to demonstrate cellular distribution through construct. Steep changes in distribution are attributed to the folding of the section on the slide. N = 1.*

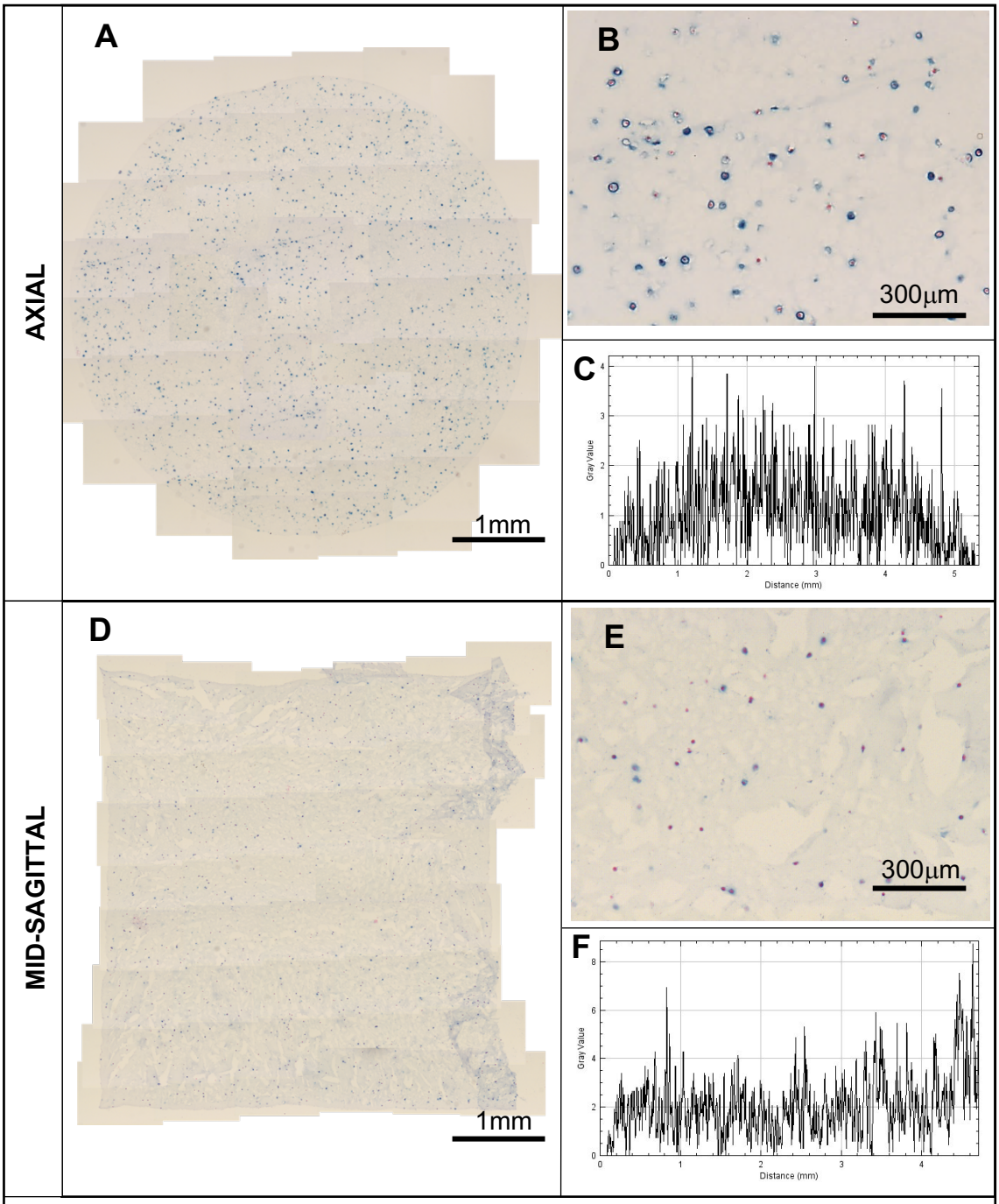

Figure 4.20: Alcian blue staining for proteoglycans within AFSC/agarose constructs treated with CNP + TGFβ_3 is positive. *CNP + TGFβ_3 histological sections demonstrate homogenous distribution of cells within the constructs and weak positive alcian blue staining of proteoglycan deposition.* ***A + D****: Collage of x20 images taken of construct axial (**A**) and mid-sagittal (**D**) sections of AFSC/agarose construct cultured with CNP + TGFβ_3. Axial section stains more positive for proteoglycan compared to the mid-sagittal sections.* ***B + E****: Example images x20 magnification of positive alcian blue staining of cells within the treated construct.* ***C + F****: Pixel count of collage image scanning from left to right to demonstrate cellular distribution through construct. N = 1.*

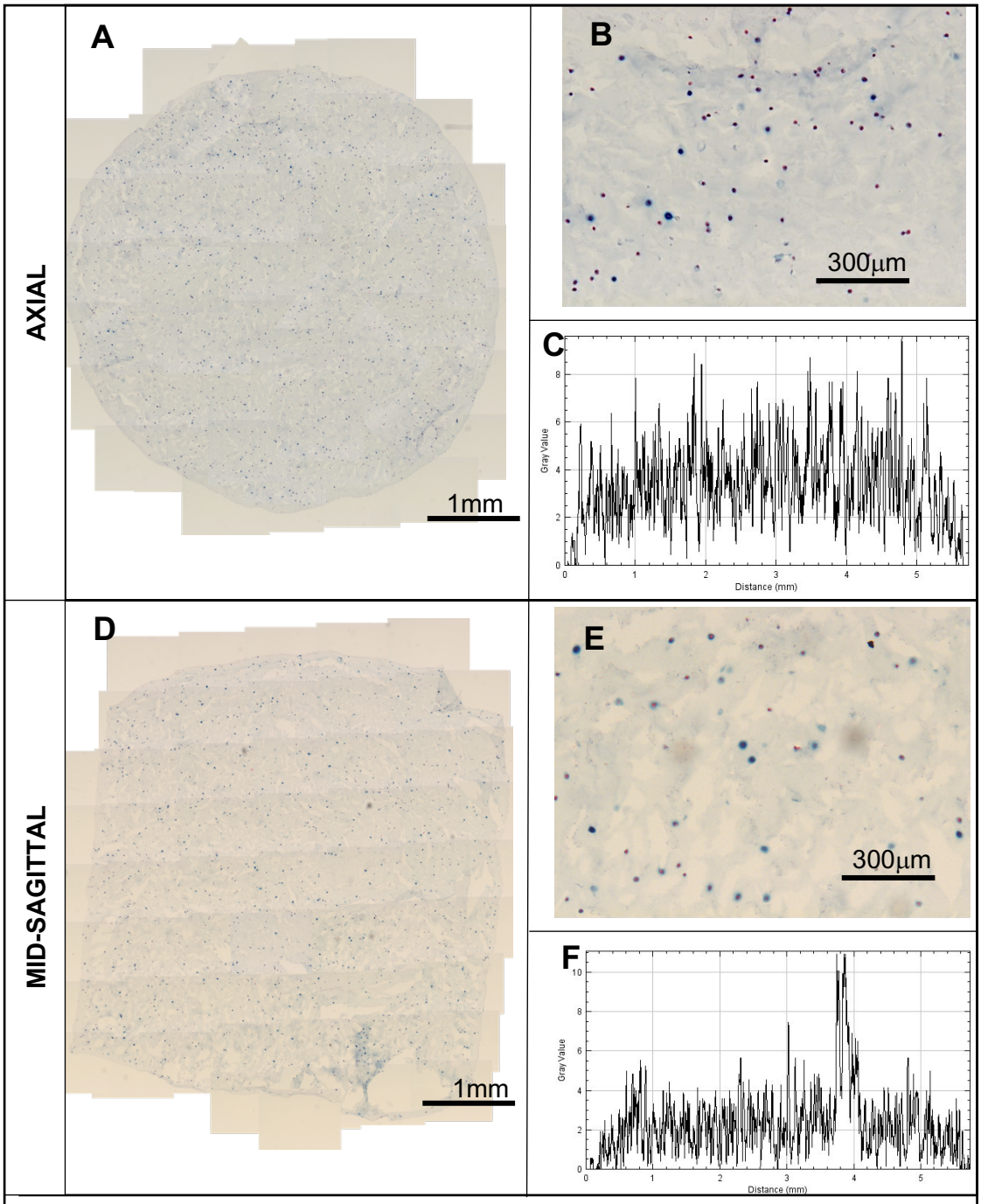

Figure 4.21: Alcian blue staining for proteoglycans within AFSC/agarose constructs treated with CNP + TGFβ_1 is positive. *CNP + TGFβ_1 histological section demonstrated a generally homogenous distribution of cells within the constructs and positive for alcian blue staining of proteoglycan deposition.* ***A + D****: Collage of x20 images taken of construct axial (**A**) and mid sagittal (**D**) sections of AFSC/agarose construct. Stronger alcian blue staining was observed in axial section compared to mid-sagittal.* ***B + E****: Example images x20 magnification of positive alcian blue staining of cells within the treated construct.* ***C + F****: Pixel count of collage image scanning from left to right to demonstrate cellular distribution through construct. N = 1.*

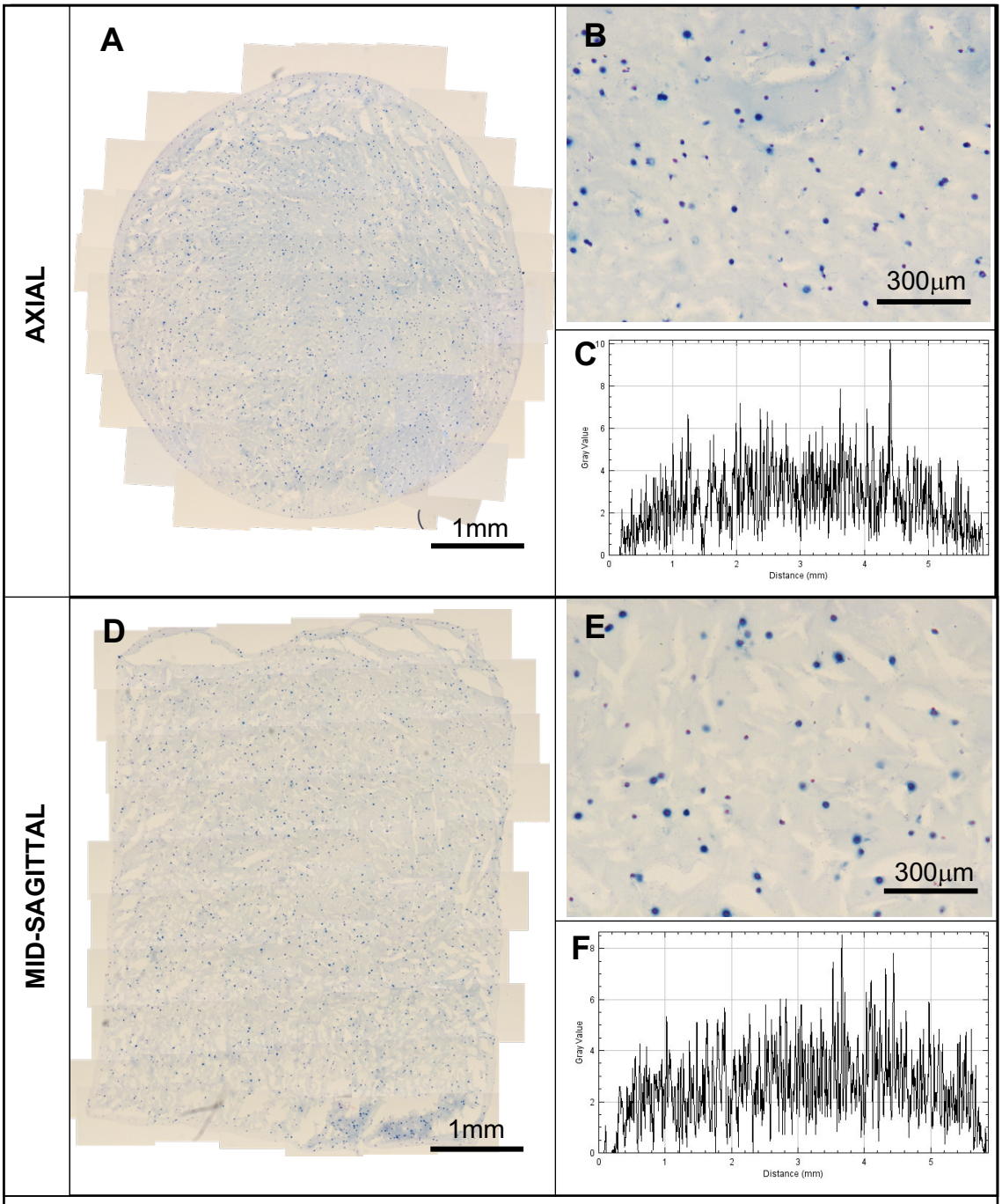

Figure 4.22: Alcian blue staining of AFSC/agarose constructs treated with dexamethasone and TGFβ_1 is strongly positive. *The dexamethasone + TGFβ_1 treated construct demonstrates largely homogenous distribution of cells within the constructs and shows clearly strong positive alcian blue staining for proteoglycans.* ***A + D****: Collages of x20 images taken of the construct at axial (****A****) and mid sagittal (****D****) orientations.* ***B + E****: x20 magnification of positive alcian blue staining of cells within the treated construct.* ***C + F****: Pixel count of collage image scanning from left to right to demonstrate cellular distribution throughout the construct. N = 1.*

4.3.4 SHG imaging indicates collagen deposition in AFSC/agarose constructs but levels are significantly less than positive control samples.

The ability of AFSCs to produce collagen in response to growth factor stimulation was assessed using SHG imaging of AFSC/agarose constructs across an area of 500 μm x 500 μm sample region (**Figure 4.22**). A positive control containing bovine chondrocytes cultured for 48 hours was used as a comparator. Imaging of the constructs in all treatment conditions did not produce clear widespread production of collagen fibres. Rather, areas where cells were in extremely close proximity often correlated with more evident collagen fibre deposition. The amount of collagen deposition appeared similar in all treatment conditions investigated for 28 days but was significantly lower compared to the positive control. Cell nuclei showed rounded morphology in all cases.

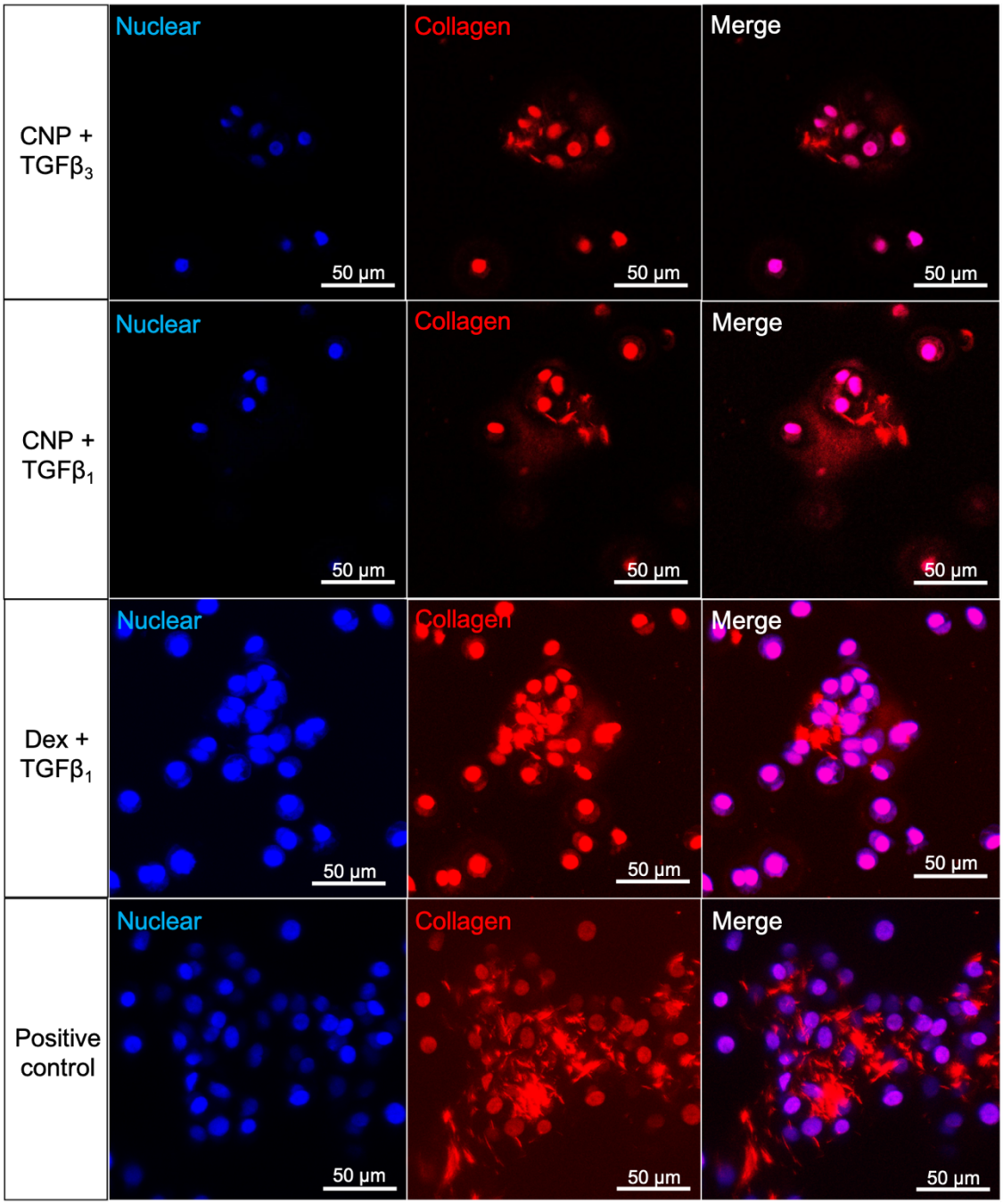

Figure 4.23: Second harmonic generation imaging of collagen deposition in day 28 treated samples compared to a bovine chondrocyte positive control cultured for 48 hours. *At 28 days, pericellular deposition of collagen is noted around clusters of cells in all treated samples. The collagen detected showed no specific orientation or organisation in AFSC/agarose constructs as well as in bovine chondrocyte/agarose constructs. Collagen detection was less distributed throughout the entire area of the construct scanned in AFSC/agarose constructs regardless of treatment compared to bovine chondrocyte/agarose constructs. Representative of N = 2 experiments.*

4.4 Summary of results

- CNP + TGFβ and Dex + TGFβ demonstrate collagen deposition according to SHG imaging of day 28 constructs but is lower than that of tissue derived bovine chondrocytes.
- CNP alone does not enhance chondrogenic differentiation of AFSC/agarose constructs in terms of GAG synthesis, hydroxyproline synthesis or DNA content.
- CNP with TGFβ$_1$ or TGFβ$_3$ enhances GAG synthesis, hydroxyproline synthesis and DNA content over 28 days compared to single factors.
- Weak positive alcian blue staining for proteoglycans is present in CNP + TGFβ$_1$ or TGFβ$_3$ treated samples but is more evident in Dex + TGFβ$_1$ treated sample compared to day 0 control.
- Statistically significant SOX-9 gene expression changes detected only when comparing CNP + TGFβ$_1$ treated sample to day 0.
- No statistically significant changes in terms of aggrecan and COL2a1 gene expression when comparing treated samples to day 0 or inter-treatment comparisons.

4.5 Discussion

The work described in this Chapter set out to investigate the effect of CNP on human AFSC chondrogenic differentiation over a period of 28 days. Specifically, I examined the effect of CNP alone or in combination with TGFβ_1 or TGFβ_3 on GAG synthesis, hydroxyproline synthesis and DNA content over 28 days of culture compared to day 0 control, non-growth factor treated controls (Basal, Chang) and the traditional differentiation method which utilises Dex and TGFβ_1. Furthermore, the study developed a simple *in vitro* hydrogel model by optimising protocols for sectioning of AFSC/agarose constructs, SHG imaging of collagen within AFSC/agarose constructs, RNA extraction from AFSC/agarose constructs and primer efficiency optimisation for the genes aggrecan, SOX-9, COL2a1 and beta actin when using AFSCs.

4.5.1 CNP enhances TGFβ mediated GAG synthesis of human AFSCs

CNP alone was insufficient to enhance chondrogenic differentiation of AFSCs within agarose constructs (**Figure 4.15A-C**). This was specifically shown by the lack of statistical differences when comparing GAG synthesis, collagen synthesis and DNA content relative to control samples (all $p>0.05$). To my knowledge this is the first study to directly test this using AFSCs. In contrast, when supplemented with the chondrogenic growth factor TGFβ, the GAG synthesis of AFSCs treated with CNP became greatly enhanced compared to control and single factor treated samples (**Figure 4.16A**, $p<0.01$). This effect was independent of the TGFβ isoform used, with no statistically significant differences observed between CNP + TGFβ_1 and CNP + TGFβ_3 ($p>0.05$). The finding that CNP enhanced TGFβ mediated chondrogenic differentiation is congruent with that of Tezcan and Kocamaz who also associated this effect when investigating MSC chondrogenic differentiation (Tezcan et al., 2010, Kocamaz et al., 2012).

Patient 3's cells in **Figure 4.16A**, showed that GAG synthesis was attenuated when treated with combination treatments especially dexamethasone + TGFβ_1 relative to single factor treatment at 14 days of treatment (**Figure 4.16A**). However, the effect of the treatment was recovered after 21 and 28 days of culture. An explanation for this could be due to patient variation but this wouldn't explain the recovery of the positive effect at the later time points investigated. Most likely an error occurred during analysis. However, to confirm this a repeat of the sample analysis or the overall experiment would be required ideally using more samples/biological repeats. In contrast, DNA content increases were statistically significantly higher in CNP + TGFβ_1

and CNP + TGFβ_3 treated samples compared to Dex + TGFβ_1 treatment. This suggests that Dex + TGFβ supplementation confers a greater enhancement to chondrogenic differentiation in terms of ECM synthesis, whilst CNP + TGFβ confers a benefit to cellular proliferation. This observation could be dependent on the concentration of CNP applied to this culture, since low concentrations of CNP have been associated previously with increase proliferation in chondrocytes (Woods et al., 2007).

Combination treatment of CNP + TGFβ_1 or CNP + TGFβ_3 or Dex + TGFβ_1 achieved GAG synthesis levels of 5.4, 5.3 and 5.5 μg/μg DNA respectively. Collagen synthesis levels were measured at 0.79, 0.75 and 0.75 μg/μg DNA for CNP + TGFβ_1 or CNP + TGFβ_3 or Dex + TGFβ_1 treated samples respectively. When put into context with other published work, these values are significantly lower. Partly this is due to the differences in cell seeding density used, but even when that is taken into account, the sheer scale of difference is quite vast and indicates that this model is unsuitable for a practical application but more useful as a method to study different treatments of stem cells within a 3D model.

Importantly when compared to the single factor treatments of TGFβ_1 or TGFβ_3 treatments, no statistically significant differences in collagen synthesis were observed when compared against the combination treatments, indicating that CNP has no effect on this part of ECM deposition (**Figure 4.15C** and **4.16C**). This correlates with findings by Kocamaz et al who demonstrated that inhibition of CNP or its receptor did not affect type II collagen mRNA expression (Kocamaz et al., 2012). If CNP does not directly affect the expression and therefore transcription of collagen, the lack of differences between single factor treatment and combination treatments could be explained in this way.

4.5.2 SHG imaging and histological staining are positive for ECM deposition in CNP + TGFβ isoform treated samples

Following the biochemical investigation, SHG imaging indicated that the collagen deposition was of a pericellular localisation and did not appear to be different when comparing the treatment options assessed, at least from a visual perspective (**Figure 4.22**). However, when compared to tissue derived chondrocytes embedded within agarose constructs for 48 hours, the amount of collagen deposition is much lower. This suggests that while ECM synthesis may be occurring, the cells are still unable to produce ECM molecules to the same extent as native cells

derived from tissue at least at this stage of the differentiation protocol. The lack of any fibrillar structures or any directionality in the SHG signal suggests that the collagen deposited here does not bear resemblance to the tissue structure of articular cartilage. The limited penetration depths of SHG from only 100 - 300 μm using the laser excitation used here, means that imaging of entire constructs is extremely difficult, expensive and logistically impractical given the size of the hydrogel construct used here (5 mm x 5 mm). Each scan performed in this experiment required over 1 hour of imaging time to complete. As such, the areas scanned here offers only a small glimpse regarding collagen deposition within the core of these constructs but not a full representation of the entire construct. Given the sheer cost of using this equipment due to the Ti:Sapphire laser source, and the inability to distinguish between fibrillar collagen types, techniques such as immunolabelling of specific collagens may be a more suitable method of determining collagen deposition in this particular model.

In terms of proteoglycan deposition, alcian blue staining of 6 μm histological sections of CNP + TGFβ$_1$ or CNP + TGFβ$_3$ constructs demonstrated weak positive staining for proteoglycans especially in mid-sagittal sections (**Figure 4.19** and **4.20**). This suggests a homogenous differentiation is occurring in the samples after 28 days. This level of proteoglycan staining in agarose constructs was also observed by Ahearne et al who showed after 21 days a similar level of pericellular accumulation of GAG was achieved compared to my study after 28 days. Given that the cell density used in Ahearn's study was much higher than the one used herein (1.5 x 10^7 cells/ml) this could explain why similar levels of alcian blue staining are observed in separate studies (Ahearne and Kelly, 2013). Alcian blue staining appears to be stronger in Dex + TGFβ$_1$ treated sample compared to CNP + TGFβ$_1$ or CNP + TGFβ$_3$ treated samples, especially when it comes to mid-sagittal sections (**Figure 4.21**). This is in agreement with the biochemical analysis of GAG synthesis performed earlier whereby statistically significant increases were observed in Dex + TGFβ$_1$ treated samples compared to CNP + TGFβ isoform treatments (**Figure 4.15A**).

4.5.3 CNP supplementation does not affect chondrogenic gene expression of human AFSCs after 28 days of culture

The finding that no statistically significant changes in gene expression for aggrecan and COL2a1 was surprising given the identification of proteoglycan and collagen deposition via biochemical, histological and SHG analysis (**Figure 4.17A-C**). However, the lack of statistical

power in terms of limited sample size, difficulties in terms of RNA extraction and the sheer amount of time required to perform the culture experiments mean this is not wholly unexpected. Aggrecan expression in particular has been associated with a transient expression over time, reliant on mechanical stimulation (Palmer et al., 2001). In addition, Greenbaum et al demonstrated that there are likely 3 significant mechanisms that explain differences between mRNA expression and detectable protein levels; 1) post transcriptional mechanisms that convert the mRNA to protein, 2) *in vivo* half-lives of the translated proteins and 3) experimental error and noise (Greenbaum et al., 2003). In terms of post transcriptional regulation occurring, many of these mechanisms are poorly defined but could explain the discrepancy observed here. Alternatively, experimental error is also potentially likely but would require further repeats of the experiment to confirm.

Gene expression as a measure of stem cell differentiation is a notoriously difficult and potentially unreliable method of assessment. Whilst gene expression changes might not be observed at the time point that I extracted my mRNA sample, it might have been upregulated at an earlier time point explaining the deposition of proteoglycans observed in the histological samples. In addition, aggrecan has previously been disputed as a good marker of chondrogenesis as some groups have found its expression to be constitutive event in MSCs (Cho et al., 2004). However, this event has not been noted when using AFSCs or agarose hydrogels previously. It should also be noted that patient variability is likely to result in some differences but cannot be avoided, therefore expansion of the number of samples and replicates would be required during analyses to minimise this concern.

4.6 Summary

In summary, for the first time I have identified that CNP is not a suitable enhancer of chondrogenic differentiation of human AFSCs on its own, but the evidence supports the use of CNP to support chondrogenic differentiation of stem cells mediated by TGFβ_1 or TGFβ_3 supplementation. However, further clarification of the effect that CNP has on TGFβ meditated differentiation is required in terms of the expression of further target chondrogenic genes and hypertrophic genes to fully characterise the effect of the peptide on this process compared to other established treatments.

Chapter 5: The effect of CNP microcapsules on ECM synthesis of bovine chondrocyte embedded within agarose constructs.

5.1 Introduction

In recent years, the use of tailorable vesicles for the release of bioactive molecules to stimulate a biological effect has been increasing. Several different carrier systems have been developed from nanoparticles (Boisselier and Astruc. D, 2009), dendrimers (Palmerston Mendes et al., 2017, Madaan et al., 2014) and even liposomes (Sercombe et al., 2015), each having unique characteristics suitable for practical applications such as drug delivery, chemical synthesis and even catalysis. Out of all of these technologies though, layer by layer assembled multilayer capsules have been intensively studied for use as a multifunctional system that is capable of stimuli responsiveness, stability and a broad range of novel functionalisation. Like many inventive technologies, layer by layer (LbL) assembly is based on a simple idea. Basic electrostatic interactions between two oppositely charged electrolytes, as proposed first by Decher et al and later built upon by Sukhorukov et al, around a spherical dissolvable core template results in the formation of reproducible, hollow shell formations referred to as microcapsules (MC) (Decher et al., 1992, Decher, 1997, Sukhorukov et al., 1998). The ability to tailor the size, composition and surface functionality has resulted in a truly amenable technology for a host of purposes. By altering the composition of these microcapsules using different polyelectrolytes, the resulting microcapsule can be biodegradable or non-biodegradable (Loca et al., 2014). This can directly affect the fate of microcapsules if engulfed by cells; biodegradable microcapsules will be broken down and release their contents whilst synthetic polymer microcapsules can remain intact and release their payload over time (Luo et al., 2016). The functional groups and structures present on different polyelectrolytes as well as environmental factors such as pH and salt concentration can directly affect the properties of the resultant polyelectrolytes produced.

Arguably the most important consideration in terms of microcapsules is the entrapment of cargo substances within the capsule's cavity which can be achieved in a multitude of ways. Proteins, polymers, DNA, enzymes and even small inorganic molecules can be incorporated into the core template of the microcapsules through co-precipitation (Volodkin et al., 2004) or following the removal of the template itself via diffusion through the microcapsules porous shells (Shchukin and Sukhorukov, 2003). The native conditions in which the microcapsules are formed allows the incorporation of these bioactive molecules (Luo et al., 2016) and the multilayer structure of the microcapsule essentially protects the cargo from degradation such that the microcapsule can be delivered to the site of action and released. Whilst in some microcapsules this release can be

mediated by the application of external stimuli such as physical (e.g. magnetic fields), chemical (e.g. pH) and biological (e.g. biodegradation) approaches, the porous network structure of microcapsules allows the permeability of molecules less than 5 kDa in size.

The ECM tightly regulates cell behaviour though its major components such as water, structural proteins and glycoproteins but also possess cell surface immobilised proteins and proteoglycans capable of binding and sequestering growth factors. In doing so, the ECM is capable of regulating the effect of these growth factors either by preventing overstimulation of the cells by sequestering them or through release of sequestered growth factors by enzymatic degradation of the ECM (Ferrara, 2010). The context and method of presentation of growth factors to the cells is itself an important factor. The ECM therefore plays a pivotal role in dictating growth factor activity and cellular response. One of the previous major criticisms for tissue engineered scaffold materials was viewing the scaffolds as simply a structure to place the cells when in reality the scaffold material acts as a surrogate for the inherent ECM of tissue and plays a much more significant role. Due to this, there has been growing interest in the incorporation of bioactive molecules within scaffold materials of tissue engineered products for the purpose of enhancing cell behaviour regulation or stem cell homing (Wu et al., 2018). The most obvious example of this is the use of RGD motifs which allow greater cell interaction with their surrounding material thereby affecting stem cell behaviour (Tahlawi et al., 2019). However, the incorporation of biomolecules into scaffold materials is costly due to the technical challenge of incorporating such molecules and sometimes the lack of appropriate materials in which these molecules can be attached. Even if growth factor incorporation into the scaffold material is possible, enzymatic degradation of these materials by the cells is sometimes difficult, resulting in a reduced release of the growth factor to stimulate the cells and therefore a reduced effect.

In terms of *in vitro* research, the application of exogenous growth factors to culture medium in order to affect the cellular response of cells within 3D materials is commonly performed and routinely effective. However, since the exogenous application of bioactive molecules is reliant on passive diffusion of the agent through culture medium and scaffold materials to the cells within, this has several implications. Firstly, most bioactive molecules used to elicit cellular responses possess short half-lives when free in solution. As such the bioactivity of these agents could be affected by this process. For example, CNP has a half-life of just under 2.6 minutes when in humans (Hunt et al., 1994). In addition, the fact that growth factors are not directly applied to cells

in cases of encapsulated systems requires much higher doses of growth factor to be applied to the culture medium in order to allow sufficient active growth factor to stimulate the cells. From a financial perspective, the use of high doses of growth factors to elicit cellular responses in these systems when much lower doses are required on a local level to facilitate the effect is a significant limitation. It is here that microcapsule technology offers a potential solution. Due to the low cost of the materials required, the ease with which synthesis can be performed and the vast range of functionalities possible; microcapsules offer a unique and versatile way to locally release a bioactive compound. Gradual release of a bioactive molecule such as a growth factor or peptide from microcapsules incorporated into a scaffold, could mimic the turnover events that occur *in vivo* which allows the release of sequestered growth factors from the ECM. In this way, a tissue engineered construct can more closely replicate what occurs *in vivo* and potentially enhance cellular response for example in terms of ECM synthesis.

The established model of differentiation in the previous chapters of this thesis utilises low gelling agarose as the means to provide a 3D environment for AFSC chondrogenic differentiation. Therefore, it would make sense to investigate the application of microcapsule technology to determine if local release through this method can instigate a positive effect on the cells in terms of differentiation. Ideally, microcapsule release of a growth factor such as TGFβ would be a good way of investigating this theory. However, given the relative molecular weight of TGFβ is 25 kDa, its size precludes passive release from simple microcapsule structures. In contrast, since CNP is a biological molecule of ~2.2 kDa size, it has potential as a candidate for passive release from LbL microcapsules. However, from the differentiation investigation in the previous chapter I noted that CNP alone does not constitute any effect on ECM synthesis in AFSC/agarose constructs. Therefore, to test the use of microcapsules within agarose hydrogels to enhance cell ECM synthesis, I sought to first test this technology on an alternate readily available cell type that has a previously demonstrated response to CNP; bovine chondrocytes. Bovine chondrocytes have previously been shown to be responsive to CNP microcapsule release when applied to the surface of a cartilage explant (Peake et al., 2015). By manufacturing and supplying CNP containing microcapsules to bovine chondrocyte/agarose constructs, I sought to determine whether the passive release of CNP from these structures enhances the ECM synthesis derived from these cells (**Figure 5.1**). If successful, this research would then pave the way for further investigation into the use of CNP microcapsules on AFSC differentiation, encapsulation of other

bioactive agents into the microcapsule structures or the development of more complex stimuli activated microcapsules to deliver larger more complex growth factors to stem cells within an agarose construct such as this.

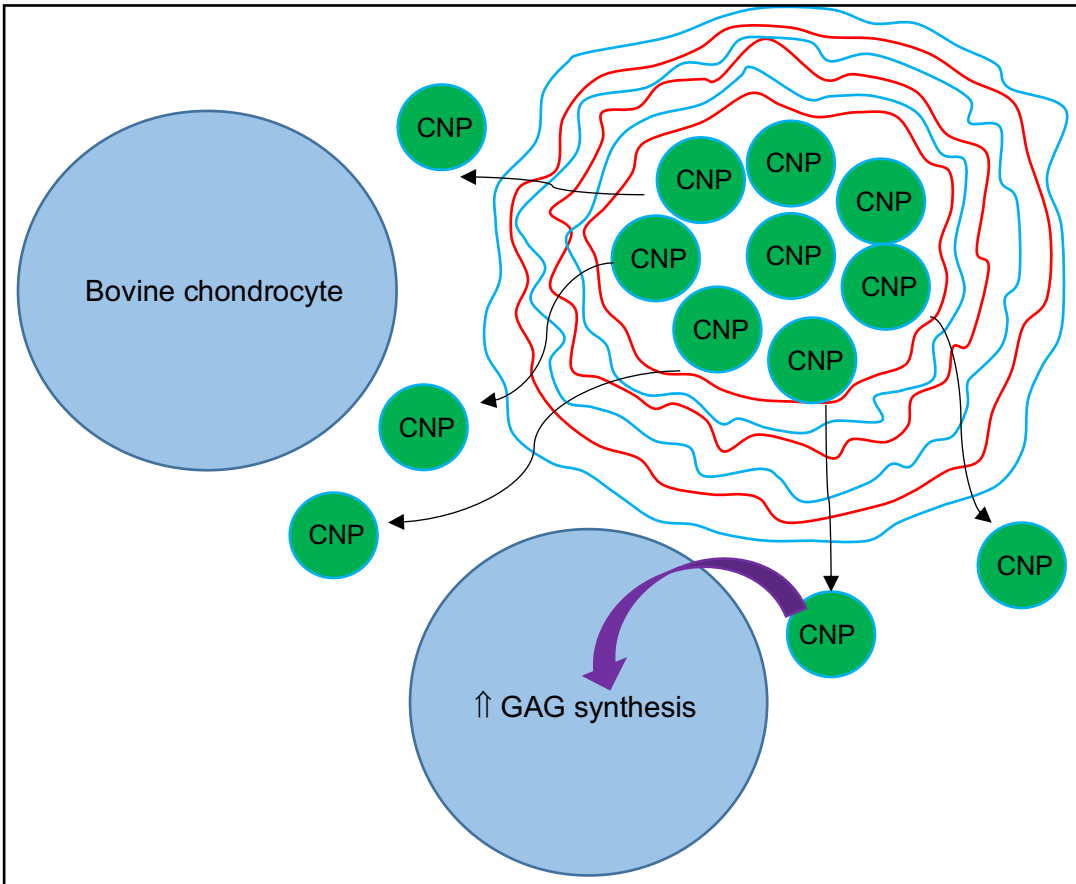

Figure 5.1: Localised passive release of CNP from polyelectrolyte microcapsules to stimulate proteoglycan synthesis of bovine chondrocytes.

5.2 Methods

Materials used: Poly-L-arginine hydrochloride (PLA, 15 - 70 kDa), dextran sulphate sodium salt (DS, 100 kDa), calcium chloride, sodium carbonate and all other salts were purchased from Sigma Aldrich Ltd, UK. Other reagents including tetramethylrhodamine (TRITC) were purchased from Thermofisher Scientific, UK).

5.2.1 CNP preparation and labelling

Fluorescent labelling of CNP was performed using the Pierce FITC Antibody Labelling Kit (Thermofisher Scientific, UK) according to the manufacturer's instructions. A 2 mg/ml solution of CNP (purity 95.1%) in 50 mM PBS was added to NHS-fluorescein isothiocyanate (FITC) and then incubated with FITC for 1 hour at room temperature. To purify the protein, the FITC labelled CNP was mixed with purification resin within a spin column and centrifuged for 30 - 45 seconds at 1000 x g to remove unbound dye. To measure the degree of labelling, fluorescence readings were taken at excitation 480 nm and emission 520 nm using a microplate reader (Fluostar, BMG Labtech, UK) and CNP concentration was determined using a Nanodrop ND-1000 Spectrophotometer at absorbance 280 nm and 495 nm (LabTech, UK). From this, the total amount of labelled CNP available was deduced. FITC labelled CNP was then stored at -20°C prior to use.

5.2.2 TRITC labelling of poly-L-arginine (PLA)

Poly-L-arginine was first dissolved in 0.1 M borate acid buffer at pH 8 - 9 (titrated with NaOH) at 2 mg/ml concentration. Separately TRITC was dissolved in ethanol at 1 mg/ml (5 ml). The TRITC solution was slowly added to the polymer solution while stirring with a magnetic stirrer, and then left to stir for 24 hours. After that, the solution obtained was transferred to into 25 kDa cut-off dialysis membrane and dialysed against deionized water for 1 week or until the water outside showed fluorescence traces. Water was changed at least twice a day during this process. TRITC labelled PLA was then stored at 4°C.

5.2.3 Microcapsule synthesis and characterization

All microcapsules used within these experiments were prepared using the layer by layer assembly technique using well established protocols of depositing alternately charged polyelectrolytes (poly-L-arginine hydrochloride and dextran sulfate onto $CaCO_3$ templates. To successfully load CNP into the microcapsule cores, 100 µg was co-precipitated into the sacrificial

$CaCO_3$ templates formed by vigorous agitation of 0.33 M $CaCl_2$ AND 0.33 M Na_2CO_3. Oppositely charged 2 mg/ml polyelectrolytes PLA (positively charged) and DS (negatively charged) in 0.15 M NaCl were alternately adsorbed for 15 minutes before agitation with the calcium cores, 3 washing steps using ddH_2O and centrifuged briefly before the next polyelectrolyte added (**Figure 5.2**). After a triple bilayer was formed the calcium carbonate cores were dissolved using 0.2 M EDTA (pH 6.5) twice for 15 minutes followed by washing in EDTA and H_2O and centrifugation steps. Microcapsules were stored at 4°C for a maximum of 1 week due to their inherent leakiness. CNP free microcapsules were kept for up to 1 month at 4°C. For fluorescent visualisation, the second positive layer was replaced with TRITC-PLA. Six layers were deposited for all the capsules before dissolving the templates with 0.2 M EDTA solution.

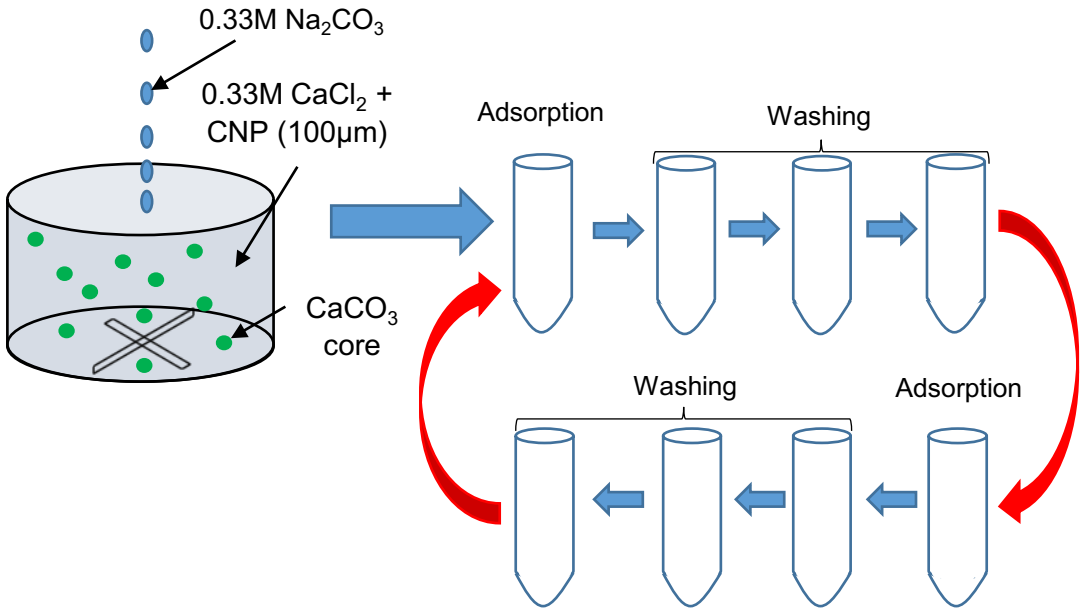

Figure 5.2: CNP microcapsule synthesis process. *Incorporation of CNP inside of a microcapsule structures requires early addition during the sacrificial core formation step where it is incorporated and protected during the layer by layer assembly process. Adsorption of a positive polyelectrolyte layer (PLA) was always initiated first and finished with a negatively charged polyelectrolyte layer (DS). EDTA was used to dissolve the calcium carbonate core and liberate the bound CNP within.*

5.2.4 Microcapsule counting

To count the number of microcapsules the stock volume was diluted 1/100 in H_2O. 10 µl of microcapsule suspension was placed on a disposable C-Chip haemocytometer (NanoEnTek Inc, USA) and counted using a Leica DMI4000B Epifluorescence microscope using its brightfield capacity at magnification of x 20 (**Figure 5.3**). FITC labelled CNP microcapsules were also

visualised under the microscope at emission 525 nm. TRITC labelled empty microcapsules were visualised at emission 630 nm.

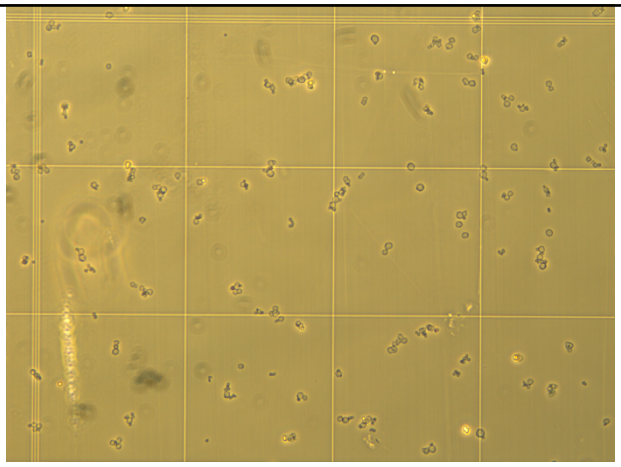

Figure 5.3: Counting microcapsules. *Representative image of microcapsule counting within disposable haemocytometer grid at x20 magnification.*

5.2.5 Estimating CNP content of microcapsules and release profile

Each wash fraction throughout the microcapsule synthesis phase was collected and stored at -20°C during synthesis steps. CNP concentration in each wash fraction was then measured by comparing the signal from each wash fraction against a standard curve generated using known concentrations of CNP - FITC (0 - 20 μg/ml, **Figure 5.4**). Fluorescence was measured using a fluorescence spectrometer (FLUOstar, BMG Labtech, UK) at excitation 485 nm and emission 520 nm. The amount of CNP in each wash fraction was calculated by multiplying the CNP concentration measured in the sample against the volume of the wash fraction solution. The values from each wash fraction were then collated and subtracted from the initial quantity of CNP used to make the microcapsules to calculate the encapsulation efficiency of CNP within the CNP microcapsules.

To determine release profile in solution, supernatant samples were taken periodically from CNP-FITC loaded microcapsule stock solutions (N = 3) every 12 hours for 4 days and analysed using a Nanodrop Spectrophotometer. The CNP-FITC standard curve was then used to calculate the release profile at each time point and expressed as a mean value.

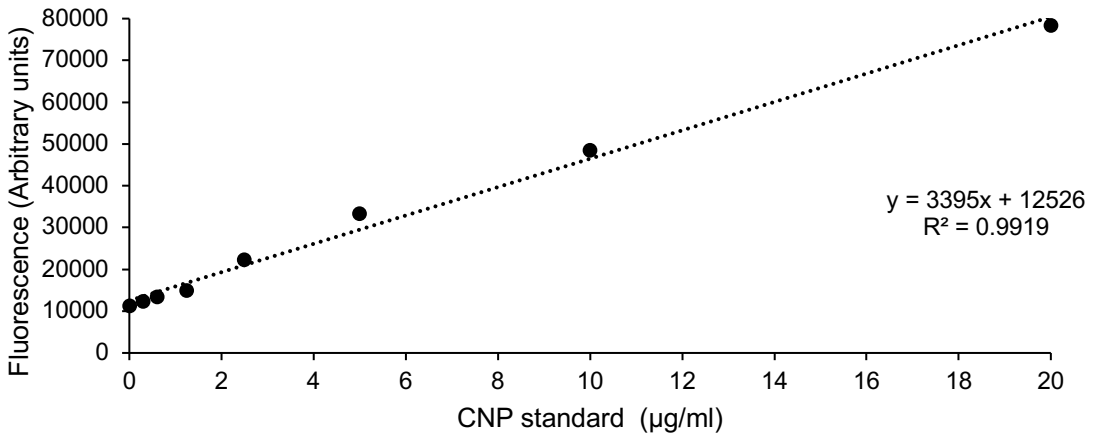

Figure 5.4: CNP standard curve. *Representation of standard curve to derive concentration of CNP in wash fractions.*

5.2.6 Culture medium

The culture medium used for experimental work involving bovine chondrocytes was prepared using the following reagents (**Table 5.5**). Dulbecco's Modified Eagle's Medium (DMEM), was supplemented with 20% FCS, penicillin/streptomycin, 4-(2-hydroxyethyl)-1-piperazineethanesulfonic acid (HEPES) buffer, L-glutamine and L-ascorbic acid (all components from Sigma-Aldrich Ltd, UK). The resulting solution was filtered using a 0.22 μm pore sized cellulose acetate filter for sterility. The prepared culture medium was then aliquoted into 50 ml sterile universal containers (Sterilin, UK) and stored at 4°C or at -20°C. Immediately prior to use, the culture medium was heated within a water bath for 25 minutes at 37°C. Constructs were cultured in a standard Heracell incubator at 37°C at 5% CO_2. The culture medium of constructs was changed every 48 hours.

Figure 5.5: Reagents used for bovine chondrocyte culture medium.

Reagent	Final concentration	Quantity
DMEM	N/A	500 ml
FCS	20% (w/v)	125 ml
HEPES	20 mM	10 ml
L-glutamine	2 μM	5 ml
Penicillin/streptomycin	5 μg/ml	5 ml
L-ascorbic acid	0.85 μM	0.075 g

5.2.7 Pronase and collagenase solutions

Isolation of bovine chondrocytes from bovine articular cartilage tissue required the use of the enzymes pronase and collagenase. Since pronase and collagenase are enzymes, their activity varied depending on the batch supplied by Sigma-Aldrich Ltd. Pronase powder (Sigma-Aldrich Ltd, UK) was added to a specific volume of prepared culture medium to produce a solution with an activity of 33 units/ml. For example, pronase with activity 5.9 units/mg would be added to 175 ml of culture medium. The solution was then sterile filtered using a 0.22 μm pore sized cellulose acetate filter, aliquoted and stored at -20°C for up to 1 year.

For the collagenase solution, collagenase powder derived from clostridium histolyticum (Sigma-Aldrich Ltd, UK) was added to an aliquot of culture medium to produce a solution with activity of 100 units/ml. The solution was filtered using a 0.22 μm pore sized cellulose acetate filter, aliquoted and stored at -20°C for up to 1 year.

5.2.8 Isolation of primary bovine chondrocytes from metacarpalphalangeal joints

Bovine chondrocytes (bACs) used in this study were derived from the metacarpalphalangeal joints of newly slaughtered 18 - 24-month-old steers (N = 3) acquired from a local abattoir (Humphreys and Sons, Essex, UK) with authorisation of the relevant meat inspectors. The joints were initially washed thoroughly in hot water to remove the majority of contaminating biological matter attached to the hair and hooves of the joint. Following this, the joints were immersed in a 70% industrial methylated spirit solution for 5 minutes to remove residual smell. Finally, the joints were immersed in a 2% chemgene (STARLAB, UK) disinfectant bath for 10 minutes in order to kill any remaining infectious organisms on the surface of the joint. The prepared joints were then placed into a sterilised metal dissecting tray and transferred to a sterile class II cabinet.

Firstly, a no.21 scalpel blade was used to make a longitudinal cut along the length of the clean joint until reaching the pastern. A perpendicular cut was then made across the pastern just above the hoof. The hide of the joint was then peeled back from the underlying tissue beneath using the no.21 blade to expose the joint capsule. Before continuing, the tissue was sprayed briefly with 70% IMS and any remaining hairs on the tissue were removed using the no.21 blade. Care was taken not to cut further into the tissue using this non-sterile blade. Using a fresh no.11 blade, one insertion was made on each side of the joint capsule and the underlying ligaments and

tendons cut back in order to dislocate the joint and expose the condyle surface. A fresh no.10 blade was then used to cut slices of cartilage from the proximal surface of the condyle. Cartilage slices were immersed in warm EBSS within a 50 mm petri dish while the dissection was completed. Once the dissection was complete, the petri dish containing the cartilage slices was transferred to an incubator at 37°C, 5% CO_2 and 21% O_2 while the dissected joint was removed from the hood, disposed of and the hood cleaned to produce sterile conditions.

The petri dish containing the cartilage slices was then returned to the sterile hood and finely diced using 2 fresh no.10 scalpels using a scissor motion. The slices were then transferred to a falcon tube containing 10 ml of the prepared pronase solution for 1 hour at 37°C on a rollermixer. The pronase solution was then removed using a Pasteur pipette and replaced with 30 ml of collagenase solution. The cartilage/collagenase falcon tube was then further incubated at 37°C on a rollermixer for a maximum of 16 hours. After this process, the cell supernatant was passed through a 70 μm pore cell sieve into a fresh falcon tube, centrifuged at 300 x g for 5 minutes using a mid-bench centrifuge (ALC International Multispeed Model PK131R). Once complete the supernatant was removed, cell pellet washed twice in fresh warm culture medium before resuspended in 20 ml of culture medium (DMEM + 20% FCS). A cell count and viability assessment of the solution was performed using the standard Trypan blue dye exclusion protocol stated in **Chapter 2**. On average, 2 – 4 x 10^7 cells are liberated from each joint per dissection with a viability of between 95 - 100%.

5.2.9 Microcapsule incorporation into bovine chondrocyte/agarose construct

Cells were resuspended in culture medium at a concentration of 8 x 10^6 cells/ml in preparation for the production of 3D chondrocyte/agarose constructs. Prepared CNP containing and blank microcapsules were added to the cell suspension in differing volumes to produce constructs with different numbers of microcapsules incorporated. A 6% (w/v) suspension of agarose type VII in EBSS (Sigma-Aldrich Ltd, UK) was autoclaved at 121°C for 45 minutes, transferred to a 60°C oven to cool for 1 hour and then to a 37°C oven to further cool on rollers. An equal volume of cell suspension was then added to the agarose solution to yield a cell concentration of 4 x 10^6 cells/ml in 3% (w/v) agarose with either 300,000, 500,000, 3,000,000 or 5,000,000 CNP containing microcapsules.

Constructs were then seeded transferred to a 24 well plate with 1 construct per well distributed. 3 ml of chondrogenic media was applied to maintain cell viability within the constructs. Control conditions included constructs without cells, constructs with only cells, constructs with empty microcapsules and constructs containing cells with CNP microcapsules. Exogenous CNP (100 nM) was applied to some constructs containing cells in order to provide a comparison. At the end of the culture period, constructs and media samples were transferred into Eppendorf tubes and store at -20°C for long term storage before biochemical analysis.

5.2.10 Microcapsule characterisation

SEM was used on microcapsules loaded with or without CNP to compare morphological characteristics. In brief, samples were prepared by applying a drop of the particle suspension onto a glass coverslip and allowed to air dry overnight. The samples were then sputter coated using gold and analysed using 10 kv electron beam with spot size 3.5. Mean diameter of the microcapsules was calculated by measuring a minimum of 50 particles for each formulation. Microcapsules within agarose constructs were imaged using Zeiss LSM710 Confocal and Elyra PS.1 Super-resolution microscope. DAPI staining was used to visualise the cell nucleus (blue) while microcapsules were visualised as red and green was used to identify CNP in the core of microcapsules.

5.2.11 DMMB assay & Hoechst assay

DMMB and Hoechst assays were performed identically to the method explained in **Chapter 2**.

5.2.12 Statistical analysis

All data are displayed as mean ± SEM values. Statistical analysis for biochemical data was conducted using Mann Whitney U test with Bonferroni correction to compare differences between treatment groups. In all cases, a significance level of 5% was considered significant ($p<0.05$).

5.3 Results

5.3.1 CNP lost in process of creating CNP microcapsules

By the end of the microencapsulation process a 2 ml stock solution was derived which contained on average 5 x 10^6 – 1 x 10^7 microcapsules/ml. From the fluorescence standard curve assay used I calculated that the encapsulation efficiency was calculated as 67% based on a loss of 33.12 μg of CNP in the collated wash fractions from the initial 100 μg supplied during the sacrificial core construction. Based on the amount of CNP detected in the wash fractions collected, I identified that most of the CNP lost during the microcapsule synthesis process occurred immediately after the formation of the sacrificial cores (13 μg, approximately 40% of the total CNP lost). Following this step, the average loss of CNP detected in the wash fractions reduced consistently over time with only a few deviations (**Figure 5.6A and B**). For example, after application of the first PLA layer, the amount of CNP detected was 2.3 μg/ml whereas following EDTA treatment near the end of the formation process the amount of CNP detected was 0.65 μg/ml. Microcapsule release profiles from the CNP containing microcapsules was measured at between 0.86% and 1.04% of total CNP contained within the microcapsule at each time point investigated (**Figure 5.6C**) based on 3 separate CNP-microcapsule solutions. This release profile is consistent with previous CNP microcapsules synthesised by the Chowdhury group (Peake et al., 2015). This release was relative stable over the time period investigated with no statistically significant differences in release calculated.

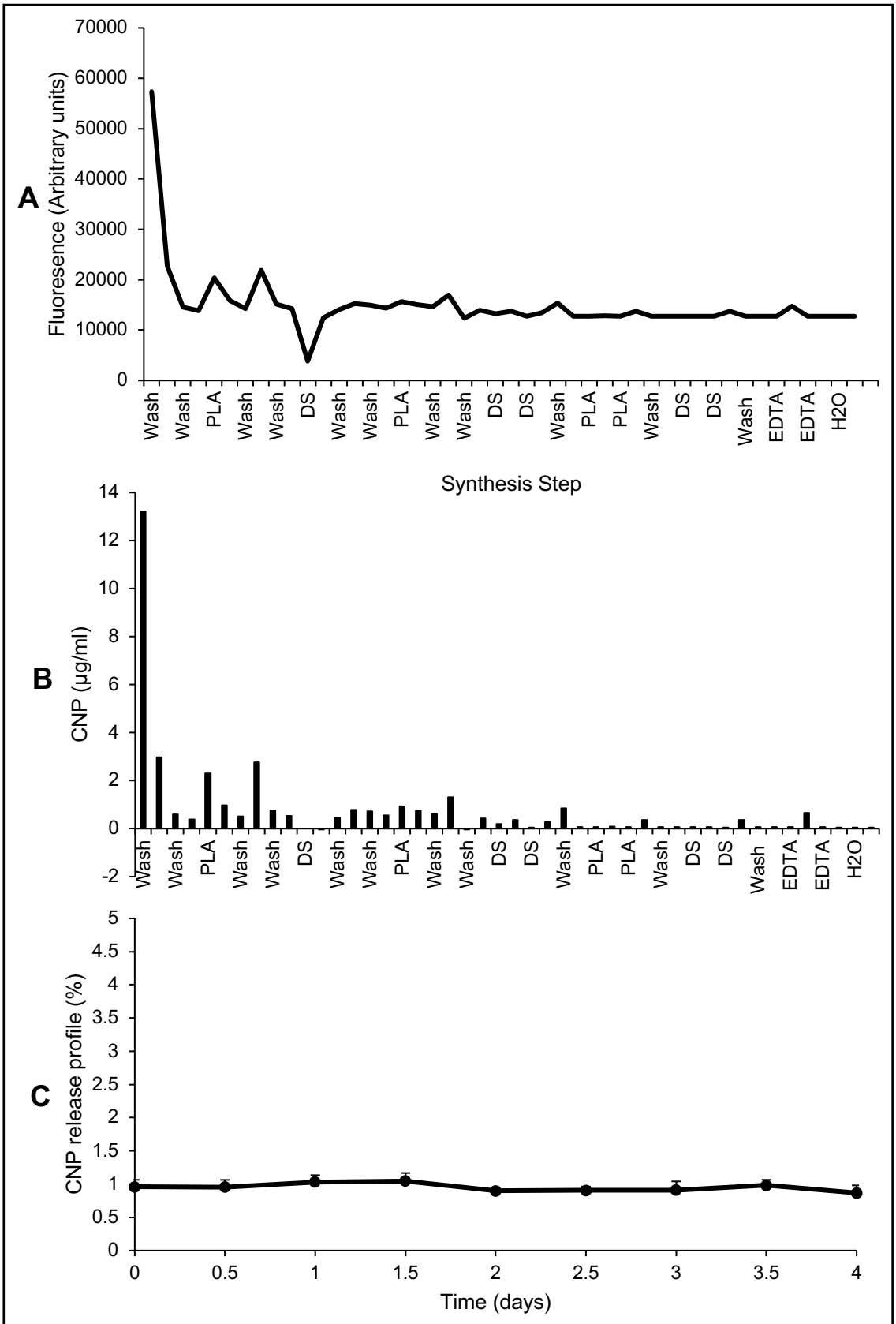

Figure 5.6: CNP is lost during the microencapsulation process but a consistent release profile is detected in solution. A*: Fluorescence detected in the wash fractions during CNP microcapsule synthesis were collated and compared to a standard curve to calculate CNP concentration in each wash fraction (**B**). **C**: CNP release profile over a period of 4 days. N = 3 for all graphs. Error bars indicate ± SEM.*

5.3.2 Localised release of CNP from polyelectrolyte microcapsules results in enhanced GAG synthesis compared to exogenous application

I examined the effect of different numbers of microcapsules loaded with CNP on bAC/agarose constructs in terms of GAG synthesis and DNA content compared to day 0 control and exogenous CNP (100 nM) application to culture medium. My results indicated that the application of the CNP microcapsules to bAC/agarose constructs resulted in a statistically significant increase in GAG synthesis for all quantities assessed compared to day 0 ($p<0.01$, **Figure 5.7A**). Application of exogenous CNP also stimulated increased GAG synthesis relative to the controls ($p<0.01$).

CNP microcapsules had a concentration dependent effect on GAG synthesis. For example, application of 300,000 and 500,000 microcapsules resulted in GAG synthesis of 8.4 and 8.5 μg/μg DNA respectively, while 3,000,000 and 5,000,000 microcapsules resulted in GAG synthesis of 7.6 and 7.2 μg/μg DNA respectively (**Figure 5.7A**). In contrast, blank microcapsules whilst still stimulating an increase in GAG synthesis relative to day 0 control, showed statistically lower levels of GAG synthesis relative to CNP containing MC constructs. By examining the effect of the local release of CNP from microcapsules compared to exogenous CNP at a concentration of 100 nM. In untreated controls I observed statistically significant increases in GAG synthesis in CNP microcapsule constructs compared to the exogenously applied CNP ($p<0.01$). Total DNA levels remained stable throughout the culture period between 2.5 and 3.5 μg/ml for all conditions investigated (**Figure 5.7B**)

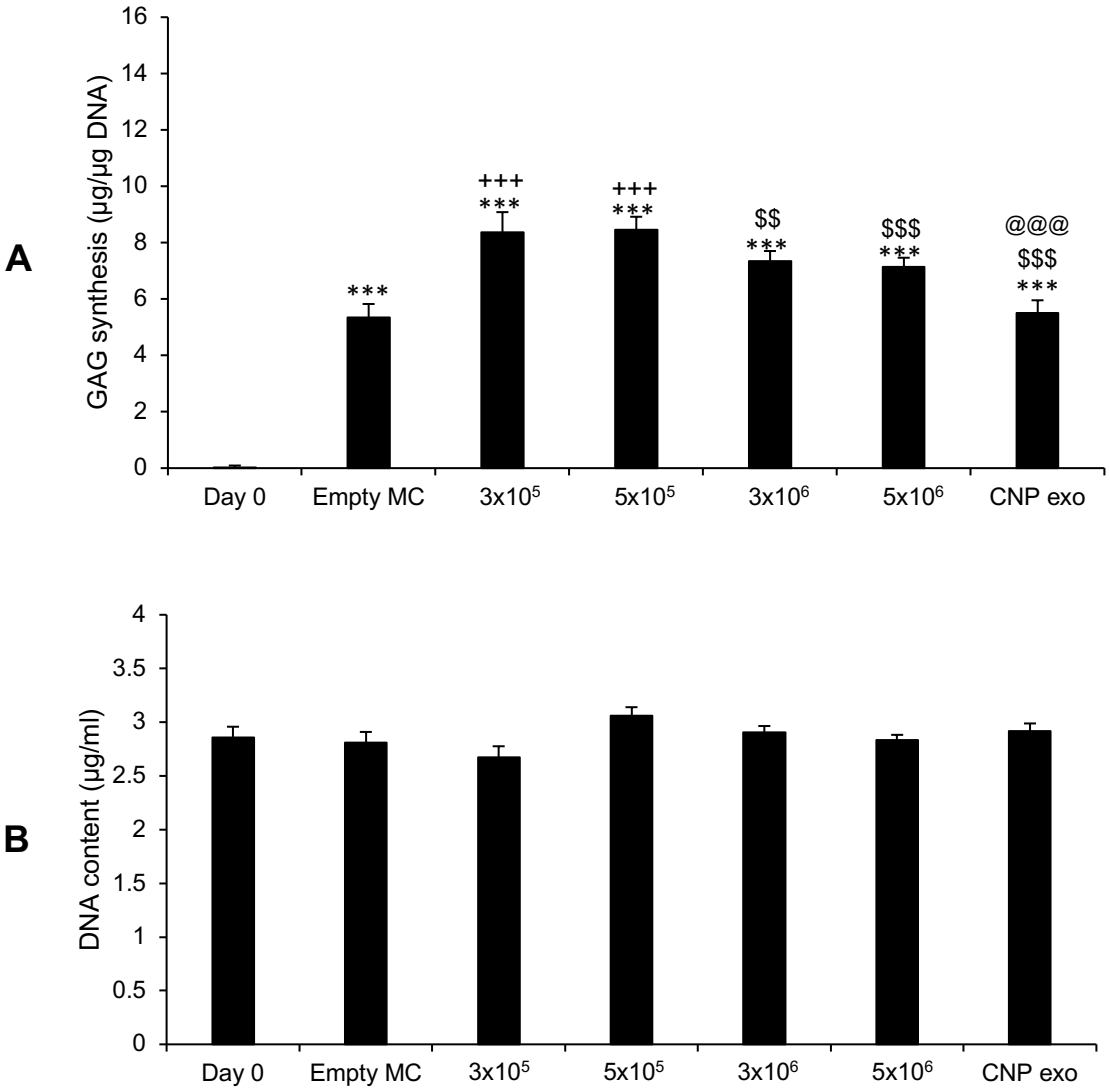

Figure 5.7: CNP microcapsule incorporation enhances GAG synthesis but is limited by concentration. *All constructs with MCs incorporated (empty and CNP containing) resulted in increased GAG synthesis compared to day 0 control. All CNP microcapsule containing constructs resulted in statistically significant increases in GAG synthesis compared to exogenous application. Statistically significant differences inverse relationship was detected when comparing 500,000 microcapsules to 3 x 10^6 and 5 x 10^6 with GAG synthesis. N = 3. Error bars indicate ± SEM. *** indicates difference compared to day 0, ++ indicates difference to empty MC, $$ indicates difference to 5 x 10^5, £££ indicates difference to 3 x 10^5, &&& indicates difference to 3 x 10^6, @@@ indicates difference to 5 x 10^6.*

5.3.3 CNP microcapsule characterisation

Incorporation of CNP did not significantly affect the morphological characteristics of the microcapsule (**Figure 5.8A**) with similar diameter (5 μm) and shape observed compared to empty microcapsules (**Figure 5.8B**). Confocal microscopy showed a distinct localisation of CNP within the core of the microcapsule structure highlighted by the presence of the TRITC labelled PLA layer surrounding it demonstrating a size comparable to the cell nucleus also pictured (**Figure 5.8C**). Some incomplete digestion of the CNP/$CaCO_3$ cores was detected (**Figure 5.8D**) but the majority of the microcapsules investigated demonstrated successful removal of the sacrificial core. Confocal imaging indicated clustering of microcapsules around cells with some observations of microcapsule internalisation.

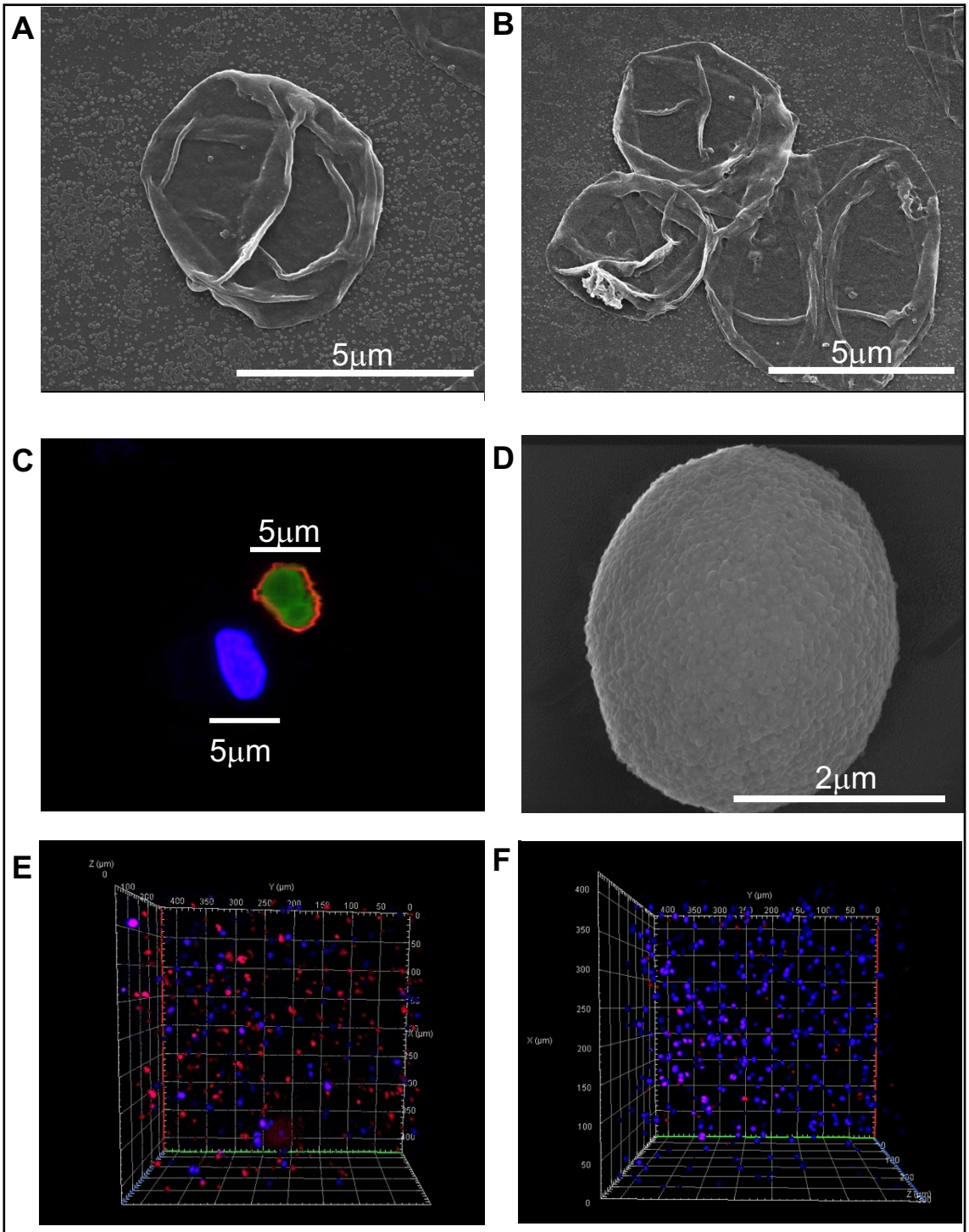

***Figure 5.8: Representative electron micrographs of CNP microcapsule structure. A + B**: SEM imaging showed uniform microcapsules with a characteristic folded pancake structure caused by drying from the sample preparation process for imaging. No morphological differences were detected in size or shape when comparing CNP microcapsules (**A**) to empty microcapsules (**B**). **C**: Microcapsule structure contains FITC labelled CNP and demonstrates size relative to a DAPI labelled cell nucleus. **D**: An example of an undigested core indicated that not all sacrificial cores were successfully digested using EDTA but the relative scarcity of them in the sample imaged suggested this was an uncommon event. **E + F**: Examples of microcapsule internalisation from day 0 (**E**) to day-2 (**F**).*

5.4 Summary of results

- Encapsulation of CNP in PLA/DS microcapsules resulted in 67% incorporation efficiency with an average 1% release rate from the structures.
- Incorporation of 3 x 10^5 and 5 x 10^5 CNP containing microcapsules resulted in the highest amount of GAG synthesis in bAC/agarose constructs compared to controls.
- Incorporation of 3 x 10^6 and 5 x 10^6 CNP containing microcapsules resulted in statistically significant decreases in GAG synthesis compared to 3 x 10^5 and 5 x 10^5 CNP containing microcapsules.
- Exogenous CNP application was statistically significantly lower compared to constructs containing CNP releasing microcapsules.
- Exogenous CNP application was not statistically significantly different compared empty microcapsules incorporated into the bAC/agarose construct.
- Confocal microscopy demonstrated the localisation of FITC-CNP within the core of the microcapsules produced.
- No morphological differences are detected when comparing CNP containing microcapsules with empty microcapsules as confirmed by SEM imaging.

5.5 Discussion

In this chapter, I successfully labelled CNP with the fluorescent marker FITC, synthesised polyelectrolyte microcapsules containing FITC labelled CNP by alternate deposition of PLA and DS on $CaCO_3$ sacrificial cores, characterised the loss and release rate of CNP from these microcapsules and measured the GAG synthesis resulting from the application of different numbers of CNP containing microcapsules into bAC/agarose constructs.

5.5.1 CNP containing microcapsules show no morphological differences compared to empty microcapsules

SEM studies revealed that CNP containing microcapsules were morphologically similar to empty microcapsules in terms of diameter and shape with only a small number of undigested cores detected in the samples imaged (**Figure 5.8A** and **B**). Visualisation of microcapsules within the hydrogel construct using SEM was unsuccessful, likely due to the collapse of the microcapsule structures during drying. Visualisation using fluorescence microscopy was more successful, with the addition of a TRITC-PLA layer allowing visualisation of microcapsules relative to cell nuclei (**Figure 5.8C**). Visualisation of FITC-CNP proved more problematic, requiring a high magnification to identify FITC-CNP within the core of the microcapsules but was achieved. Examples of microcapsule internalisation by cells was observed in some instances (**Figure 5.8E** and **F**) but were infrequently observed events. Due to the biodegradable nature of the microcapsule synthesis materials, this was unlikely to detrimentally affect the cells.

5.5.2 CNP is lost during the LbL microencapsulation process

Detection of CNP within the wash fractions taken during the microcapsule procedure indicates a significant loss of the original peptide of up to 33% especially following the first wash after CNP incorporation into the sacrificial core template (**Figure 5.6A** and **B**). This could possibly suggest some CNP was loosely bound to the exterior of the sacrificial core templates that was washed off during the initial steps. The CNP release profile measured over 4 days indicated a consistent steady release rate be sufficient for a prolonged period of time in excess of the investigation performed here based on the estimated amount incorporated into the microcapsule structure. This release rate is consistent with previous CNP microcapsules manufactured using the layer by layer assembly method as demonstrated by Peake et al. Given the daily release rate and the concentration of CNP calculated to be encapsulated within the microcapsules

synthesised, the expectant concentration of CNP released from the stock of microcapsules is 700 nM. Based on the average number of microcapsules synthesis in the stock solution ($2x10^7$), the amount of CNP released from $3x10^5$ microcapsules would be 10.5 nM, $5x10^5$ would be 17.5 nM, $3x10^6$ would be 100.5 nM and $5x10^6$ would be 175 nM. Relative to the 100 nM supplied via exogenous means this indicates that supply of $3x10^6$ and $5x10^6$ microcapsules releases similar concentration of CNP to the exogenous supply, whilst the supply of $3x10^5$ and $5x10^5$ microcapsules releases 10-fold less CNP. This therefore supports the idea that the higher concentration of CNP of 100 nM supplied either on a localised level or via exogenous entry is less effective than a lower concentration released on a localised level. Oversupply of CNP has been associated with a reduction in GAG synthesis when applied to BM-MSCs so this effect is at least to a certain degree supported by previous literature (Tezcan et al., 2010).

5.5.3 Microcapsule release of CNP demonstrates a dose dependent response on GAG synthesis in bAC/agarose constructs

My investigation encompassed a range of different microcapsule numbers within bAC/agarose constructs to ascertain if a concentration dependent effect was evident (**Figure 5.7A** and **B**). Empty microcapsules and exogenously applied CNP resulted in similar levels of GAG synthesis (5.3 and 5.5 μg/μg DNA respectively) with no statistically significant differences detected between the two groups. Since dextran sulfate is derived from glucose, it is possible that the internalised microcapsules I observed in some cases served as a glycolytic food source for the bACs and stimulated metabolic process including GAG synthesis. Work by Scholnick et al previously demonstrated that dextran sulfate can inhibit or consistently stimulate glycolysis in ascites tumour cells (Scholnick et al., 1973). However, no previous study to my knowledge has observed this in bovine chondrocytes so would warrant further investigation.

In contrast, the application of 500,000 CNP containing microcapsules demonstrated the greatest increase in GAG synthesis (8.5 μg/μg DNA) compared to 300,000 CNP MCs (8.4 μg/μg DNA). However, this response was also limited as the application of 3,000,000 and 5,000,000 CNP containing microcapsules resulted in statistically significant decreases in GAG synthesis (7.4 and 7.1 μg/μg DNA respectively) relative to the 300,000 and 500,000 MC containing samples. Significantly, statistical differences were detected when comparing samples with CNP microcapsules incorporated and exogenously applied CNP to culture medium (**Figure 5.7A**). Here, GAG synthesis from samples with CNP microcapsules were significantly higher than those

from cells treated with the exogenous peptide ($p<0.01$). This suggests that localised release of CNP is conducive to an enhanced ECM synthesis response.

The level of GAG synthesis occurring in bAC/agarose constructs relative to other literature is slightly lower than expected given the cell source and time frame investigated here. For example, Tilwani et al published data which showed that bAC/agarose constructs of identical agarose concentration, oxygen tension, cell type and culture duration (as used herein) produced GAG synthesis levels of 12 μg/μg DNA in untreated/unstimulated samples (Tilwani et al., 2017). When compared to my CNP treated condition, which is known to stimulate GAG synthesis in bovine chondrocytes, this poses a puzzling question. One potential explanation for this deviation could be in the donors used. Since this was designed as a pilot study, the number of replicates and donors used for these experiments (N = 3, 3 replicates) is different to the Tilwani study (N = 2, 8 replicates) and so variations in GAG synthesis levels could be attributed to this. In addition, damage to the joints from which I derived the articular chondrocytes can potentially stress the cells to produce inflammatory cytokines that can reduce GAG synthesis when incorporated into the agarose constructs. Furthermore, I used the optimised DMMB assay for agarose constructs that I developed in **Chapter 2** which used a reduced pH of 1.5 compared to the pH 3.0 used in Tilwani's experiments which could also explain this discrepancy.

5.6 Summary

This aspect of my thesis successfully synthesised, characterised and analysed the effect of CNP containing polyelectrolyte microcapsules on the GAGs synthesis of bovine articular chondrocytes embedded within an agarose construct. Furthermore, the application of CNP containing microcapsules resulted in an enhancement in GAG synthesis relative to day 0 control and exogenous application, but this effect was also shown to be concentration limited. For the first time, I demonstrate that polyelectrolyte release of a chondro-supportive peptide can enhance ECM synthesis and could provide an application for stem cell differentiation experiments in the future.

The overall fate of the microcapsules following CNP release is unknown but given the biodegradable nature of the materials used in this investigation the long-term implications to surrounding cells should be limited. To confirm this, *in vivo* experiments need to be performed to adequately assess this within an agarose hydrogel. In addition, encapsulation within the

microcapsule structure was theorised to protect the CNP given its short half-life. This short half-life is typically due to breakdown by proteolytic enzymes within the cell so encapsulation should not affect this process. To confirm this, analysis of the released supernatant of CNP microcapsules on cells responsive to CNP over the duration of a prolonged period (7 - 28 days) could be performed to determine whether the peptide is still biologically active.

Chapter 6: Final Discussion and Future Work

6.1 Introduction

My approach in this thesis was to effect a thorough, step wise evaluation of a simple hydrogel model to achieve chondrogenic differentiation of human AFSCs. In doing so, I sought to carefully identify how AFSCs change through early to late stages of a chondrogenic differentiation protocol within a 3D environment. I then progressed to use this model to ascertain the effect of the peptide CNP on this process. Finally, I applied polyelectrolyte microcapsules containing CNP to investigate their potential in the hydrogel model to mediate cellular response in terms of ECM synthesis using bovine articular chondrocytes. In this Chapter, I have aimed to summarise the findings (**Figure 6.1**) and provide the limitations of the experimental approaches taken herein. Finally, I conclude this thesis by providing potential avenues of future work that builds on the investigations performed here and the principal conclusions that I have attained.

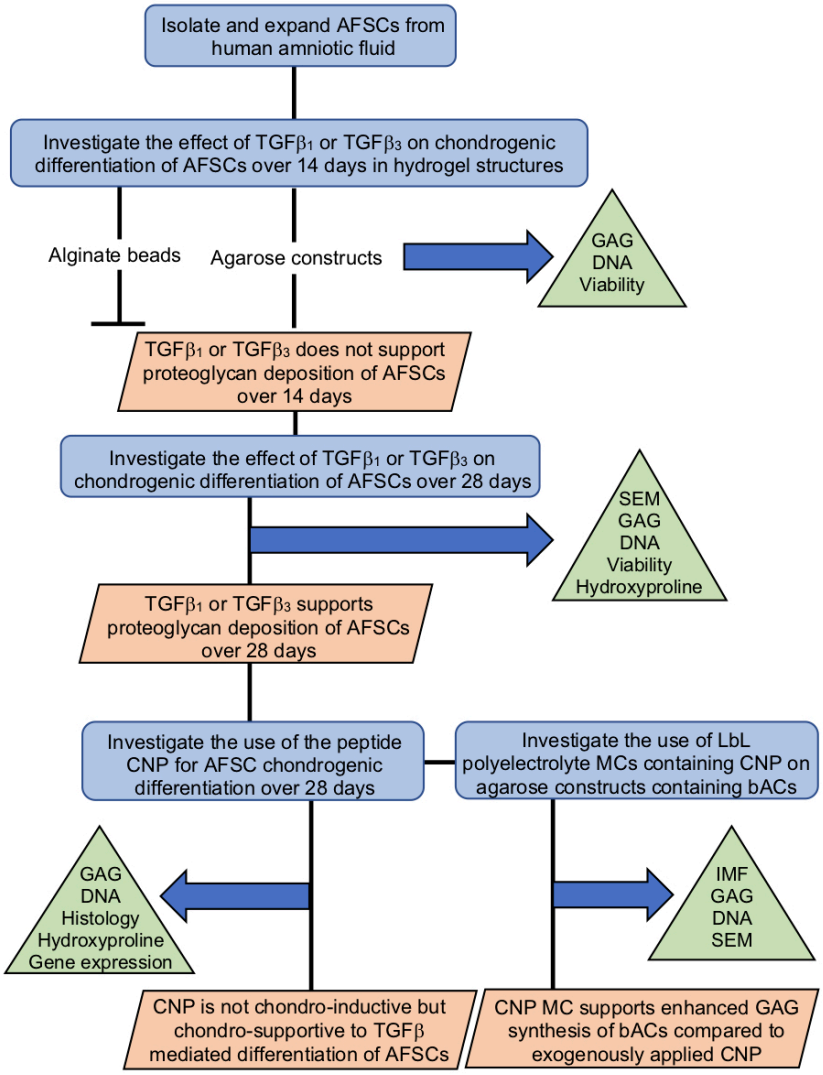

Figure 6.1: Overview of experiments performed, methods and findings. *Flowchart symbols indicate the investigations performed (blue boxes), the techniques utilised to achieve each aim (green triangle) and the principle conclusions (orange parallelograms).*

6.2 Scientific findings

6.2.1 Analysis of chondrogenic differentiation achieved in an agarose construct model over 14 days indicates an emphasis on cell proliferation rather than GAG synthesis.

My initial investigation characterised the biochemical and viability changes associated with embedding AFSCs within alginate beads and agarose constructs up to 14-days of culture (**Chapter 2**). I demonstrated that within the first 14 days of my differentiation protocol, only TGFβ_1-treated alginate beads showed a clear decrease in GAG synthesis at day 14. TGFβ_3 treatment did not constitute any differences in GAG synthesis at either day 7 or 14. For AFSC/agarose constructs, treatment with TGF$\beta_{1/3}$ did not confer any statistically significant change. In contrast, a marked increase in DNA content was observed when AFSC/alginate beads and AFSC/agarose constructs were treated with TGFβ_1 or TGFβ_3 compared to all controls. This observation therefore suggested that at early stages, the cells are proliferating more than they are synthesising proteoglycans, potentially in an effort to recapitulate early stages of stem cell aggregation which occurs in early limb formation.

Viability of the AFSC/agarose constructs was shown to be consistent for all treatment conditions with no statistical differences observed. This indicated that treatment of the cells with TGFβ did not enhance nor reduce cellular viability compared to the control treatments after 14 days of culture. These values were consistent between the edge and core samples of the constructs investigated. In contrast, while AFSC/alginate bead samples did not demonstrate any statistically significant differences at 7 days of culture, overt decreases in viability were observed at 14 days of culture. This observation also further indicated that treatment with TGFβ_1 or TGFβ_3 resulted in an increased decrease in viability of AFSCs compared to controls. No clear differences were detected between TGFβ_1 and TGFβ_3 treatment in this regard. Despite these decreases in viability, viability of AFSCs within the alginate beads was still high at over 85% for all treatment conditions.

I also found that alginate beads were an unsuitable method for further investigation as the bead structure began to degrade within the first 14 days of culture. This observation has not previously been noted by other groups, with others able to successfully culture stem cell/alginate bead structures for as long as 28 days (Shalini and Debnath, 2015, Deng et al., 2012, Ma et al., 2003). However, differences in cell density used and viscosity of alginate utilised could contribute

to this, thereby suggesting that the alginate used for these experiments is not suitable for stem cell differentiation over a prolonged period of culture. *In summary, the characterisation of early stage AFSC chondrogenic differentiation within simple hydrogel models and the effect of different TGFβ isoforms on this process is an important evaluation that can elucidate our understanding of how AFSCs undergo this procedure.*

6.2.2 Analysis of chondrogenic differentiation achieved in agarose model over 28 days indicates greater emphasis on GAG synthesis in TGFβ treated samples.

I further characterised the effect of TGFβ_1 or TGFβ_3 treatment on AFSC/agarose constructs over a full 28-day culture period by investigating biochemical and morphological changes, this time incorporating analysis of hydroxyproline content normalised to DNA content and SEM imaging to achieve this (**Chapter 3**). From my investigation, GAG synthesis and hydroxyproline content was enhanced by TGFβ_1 alone and TGFβ_3 alone compared to controls. From SEM imaging, the most obvious morphological changes observed was the initial presence of filopodia like structures within the first 7 days of agarose culture and the apparent loss of these structures by the end of my investigation at 28 days. Taken together, these findings suggested that the cells initially were attempting to interact with the surrounding environment and between 14 and 28 days began to stimulate the production and release of proteoglycans and collagens.

Overall, the basic hydrogel model of AFSCs embedded within agarose constructs shown here supports a level of chondrogenic differentiation. However, in contrast to other published work the level of GAG synthesis and collagen synthesis achieved here after 28 days was substantially lower than that of other studies. This could therefore indicate the importance of cell seeding density in relation to chondrogenic differentiation of stem cells or potential limitations in the differentiation potential of AFSCs to the chondrogenic lineage. No differences were observed between TGFβ_1 or TGFβ_3 treatment, thereby suggesting that the mode of chondrogenic differentiation triggered by these growth factors are likely similar. Given the similarities between the structural and signalling pathways that these isoforms utilise this observation is not unexpected and does have some agreement with other studies who also determine a lack of difference between the isoforms effects within an *in vitro* hydrogel model. *In summary, further culture of AFSC/agarose constructs is possible and results in an increase in GAG synthesis and*

hydroxyproline content. However, when put into context with other established published work the levels observed within my model constitute a reduced level of ECM synthesis in comparison.

6.2.3 Analysis of CNPs effect on AFSC/agarose chondrogenic differentiation indicates positive effect on GAG synthesis when used with TGFβ treated sample.

After demonstrating that the use of a single factor such as TGFβ to achieve chondrogenic differentiation to be possible, I sought to determine the effect of the peptide CNP on this process via solitary application or in conjunction with established chondro-inductive growth factors TGFβ_1 or TGFβ_3 (**Chapter 4**). Whilst I observed that the application of CNP alone did not constitute any effect to ECM synthesis relative to control samples, its use in conjunction with TGFβ_1 or TGFβ_3 was able to support an enhanced differentiation effect on par with the traditionally used Dex + TGFβ_1 treatment. This was also confirmed by SHG imaging which indicates a pericellular localisation of collagen around cells in these combination treatment conditions but no formation of large fibre networks was shown to be present. Importantly when compared to TGFβ_1 or TGFβ_3 treatments, no differences in collagen synthesis were observed in terms of collagen synthesis, indicating that CNP has no effect on this part of ECM deposition.

Histological analysis of OCT embedded AFSC/agarose constructs revealed weak positive alcian blue staining localised to pericellular matrix surrounding the cells in CNP + TGFβ_1 or CNP + TGFβ_3 samples compared to Dex + TGFβ_1 sample but all treated conditions resulted in significantly more alcian blue staining than the day 0 control sample. This observation confirmed my biochemical analysis which indicated obvious increases in GAG synthesis for these treatment conditions compared to day 0 controls. The analysis of gene expression changes also revealed only one marked difference when comparing CNP + TGFβ_1 treatment with control for SOX-9 gene expression. All other genes investigated, whilst demonstrating fold changes compared to control did not demonstrate any statistical significance. This therefore suggested that prolonged culture of my AFSC/agarose constructs and treatment with combination therapies did not trigger any significant differences in terms of chondrogenic gene expression compared to control. Considering that gene expression analysis is usually subject to temporal changes, when put into context of the weak positive alcian blue staining suggests that the chondrogenic differentiation achieved in the AFSCs was poor. This is in congruence with my findings in **Chapter 3**.

In summary, CNP alone is insufficient to affect AFSC chondrogenic differentiation but when used in conjunction with the established chondrogenic growth factor TGFβ was shown to act as a chondro-supportive agent for TGFβ mediated chondrogenic differentiation in terms of proteoglycan deposition as confirmed by biochemical and histological analysis. This effect was also shown to be comparable to that of the traditionally utilised Dex + TGFβ_1 treatment. However, CNP application did not enhance collagen synthesis of TGFβ treated samples relative to samples treated with TGFβ isoforms alone suggesting a restricted role.

6.2.4 Microcapsule encapsulation of CNP promotes greater GAG synthesis in compared to exogenous application in bAC/agarose constructs.

A wide variety of growth factors and other molecules are used to study and enhance chondrogenesis of stem cells for a tissue engineering application. However, given the high doses required for exogenous application and the relative costing of growth factors etc, the ability to supply a chondro-inductive or chondro-supportive agent to cells over a long period of time at a reduced dosage/day would make this model much more feasible for further investigation. Thus, I designed and performed a pilot investigation into the use of polyelectrolyte microcapsules containing CNP on the GAG synthesis of bovine articular chondrocytes (**Chapter 5**).

From this investigation, I successfully synthesised CNP containing polyelectrolyte microcapsules from PLA and DS and characterised them morphologically using SEM and confocal imaging techniques. No morphological differences were observed between empty microcapsules and CNP containing microcapsules according to SEM imaging. In addition, the application of CNP containing polyelectrolyte microcapsules stimulated an obvious increase in GAG synthesis relative to exogenous application of CNP and the application of empty microcapsules. However, this effect did show signs of limitation whereby the application of 3 x 10^6 and 5 x 10^6 microcapsules resulted in a diminishment of this effect relative to the application of 3 x 10^5 and 5 x 10^5 microcapsules. This therefore indicated that the application of too much CNP on a local level can actually inhibit GAG synthesis, which is in accordance with similar studies albeit using exogenously applied CNP (Tezcan et al., 2010). The successful encapsulation/release of CNP and effect on encapsulated cells is certainly a promising result and could open the way to investigate their application to *in vivo* models of osteoarthritis such as the Dunkin Hartley guinea pig (Kuyinu et al., 2016). For example, microencapsulation of CNP can

theoretically protect the peptide from potential breakdown by upregulated MMPs present within the diseased joint where it can exert its beneficial effects.

In summary, my findings demonstrated that microcapsule technology has potential advantages for use in a 3D hydrogel system relative to exogenous application but much more characterisation and investigation into the encapsulation of other pro-chondrogenic growth factors must be performed in order to fully ascertain the possibility of this technology for this purpose.

6.3 Limitations in approach and potential solutions

The use of alginate constructs of identical size and shape to those of the agarose constructs investigated would have been more appropriate to allow direct comparison of the 2 hydrogel materials for the purpose of chondrogenic differentiation of AFSCs. To create an alginate construct, a stainless-steel mould similar in design and identical in dimensions to the one used to make agarose constructs is required. By applying and securing a dialysis membrane to the surface of a mould using screws, the AFSC/alginate suspension could be held in place within the mould's wells whilst allowing diffusion of the gelling ions into the alginate solution for crosslinking to occur. After 2 hours in an incubator the dialysis membrane would be removed, and the constructs popped out of the mould wells using a Pasteur pipette. A similar methodology has been used by Ragan et al with apparent success (Ragan et al., 1999). Alternatively, dialysis membrane tubing of diameter 5 mm could be used whereby the cell/alginate solution is transferred inside the tubing, the ends tied off and transferred to a gelling solution for 2 hours. However, this method is much more awkward to perform and difficult to ensure uniform sizes of constructs.

Another potential limitation is the quantification of viability. Manually counting based on a grid is subject to human error much like quantification of cells using a haemocytometer. As such the use of an automated method using software such as ImageJ for automated cell counting from images or the use of an automated cell counter such as a ViCell would be a more accurate reliable method that could be used for these measurements. I noted that encapsulation of AFSCs in agarose results in an initial decrease in viability compared to a method such as alginate incorporation. This is likely a result of the gelling solution being too warm, causing thermal stress to the cells and apoptosis. The use of a sensitive temperature probe could be used in order to indicate accurately when the temperature is most suitable for cellular encapsulation and improve the initial cell viability.

Morphological characterisation of cells within complex physiological or manufactured materials is often achieved using scanning electron microscopy. However, conventional SEM techniques requires the sample to be in a vacuum (10^{-7} to 10^{-9} Torr) and removal of the hydrogel's natural hydrated state. Since hydrogel structures are maintained by water absorbed by the polymer network, this inherently affects how reliable the images observed in the prepared sample relate to the actual state during culture. Specialised microscopy techniques do exist that are able to characterise the morphology of hydrogels in their hydrated state such as environmental SEM (ESEM). Although it must be noted that techniques such as these do have increased user cost compared to conventional vacuum SEM. Environmental SEM differentially pumping the microscope column to produce a graduated vacuum from the specimen to the electron gun. By maintaining a high humidity, specific temperature and pressure within the microscope chamber, ionising collisions between the electrons and water vapour molecules generate positive ions which attract to the sample and neutralise the specimens charge. The hydrated environment also allows the sample to stay hydrated. Whilst the resolution offered by the ESEM is lower than that of conventional SEM, the lack of sample preparation steps except for fixation, a lower chance of image artefact formation and the maintenance of the hydrated hydrogel state offers several advantages that should produce a more accurate representation of how the cells are sustained within the agarose construct.

While I have demonstrated that chondrogenic differentiation, at least from a biochemical standpoint, is facilitated by agarose encapsulation and treatment with TGFβ_1 or TGFβ_3, the use of agarose itself as a scaffold material is potentially problematic. *In vivo*, humans lack the enzymes required to break down agarose (Emans et al., 2010). As a true tissue engineered material is meant to degrade over time as the body naturally replaces the inserted material with native tissue, this is a significant issue. As the mechanical properties of agarose are much less than that of native cartilage, this could present a focal point of weakness within the tissue and increase the chances of degradation of the structure if applied to an osteochondral defect. In addition, research conducted in 2011 indicated that chondrogenically primed stem cells when applied *in vivo* within an agarose gel demonstrate an increase in calcification markers (Vinardell et al., 2011). Therefore, this suggests that an agarose model is better suited as a means to investigate the differentiation of AFSCs and not as a defect implant.

The lack of statistically significant differences observed in analysis of common gene expression markers, despite the presence of fold changes compared to control, could suggest that my study lacked statistical power. To avoid that situation, a study whereby the majority of samples are devoted to gene expression analysis would be appropriate. The genes analysed in this study were all positive chondrogenic markers, but further analysis is essential to determine if hypertrophic markers or osteogenic markers (MMP-13, ALP, collagen X) were also enhanced as a result of differentiation. This is especially important as some groups have suggested that TGFβ_1 treatment predisposes cells to a hypertrophic phenotype and it would be interesting to observe if CNP has any effect on this incidence (Lolli et al., 2018). Similarly, histological staining used here is restricted to confirmation of proteoglycan deposition by cells only. It would be useful to discern and support any gene expression data to show if osteogenic or myogenic markers were also present. For example, alizarin red solution is commonly used to look at mineralisation to confirm osteogenic differentiation. The investigation of CNP only, TGFβ_1 only and TGFβ_3 only controls for histological analysis would have been beneficial to provide a more complete overview of the treatment conditions investigated for biochemistry and would be beneficial to correlate whether the increases in proteoglycan synthesis observed in controls was also identified at a histological level. SHG, while useful to look at collagen deposition, could not be used to distinguish accurately what type of collagen was being produced by the cells. This is a significant limitation in regard to identifying whether the collagen being produced by the cells is supportive of hypertrophic tissue or mature cartilage. Immunohistochemistry could therefore be a useful technique to apply in this circumstance as it can be used to identify type I and type II collagen deposition in histological samples although there is some debate regarding whether this staining is specific enough to yield definitive conclusions.

In terms of the CNP microcapsule work, the obvious limitation relative to the rest of this thesis was the xenogeneic cell source used. However, there are appropriate reasons for this. Firstly, since this investigation serves as a pilot study to investigate whether the application of microcapsules to a 3D hydrogel is possible and worthwhile, the use of xenogeneic cells avoids wasting the limited supply of AFSCs available. Secondly, I showed in **Chapter 4** that CNP has no effect on GAG synthesis of AFSCs when applied exogenously to culture medium on its own. Thirdly, whilst human chondrocytes might be more relevant for a potential clinical application, human chondrocytes are less readily available since they are usually only sourced from patients who have an underlying disease or tissue damage and are inherently variable based on the anisotropy of the tissue itself. Since bovine articular cartilage is relatively easy to procure, financially reasonable to purchase, well characterised,

possess similar biochemical properties and identical phenotypes to human articular chondrocytes (Buschmann et al., 1992); the use of bovine articular chondrocytes for this pilot study was warranted.

As a small study, the N numbers used in this investigation is small in terms of donor cells despite standard numbers of replicates per treatment group. It would therefore be worthwhile to increase the number of donors used in this investigation to increase statistical power. In addition, expanding the scope of microcapsule numbers investigated would have been useful to determine an optimum concentration required to produce an optimum level of GAG synthesis enhancement. Since I demonstrated that extremely high numbers of microcapsules were detrimental to GAG synthesis in bACs, it would be useful to distinguish the effect microcapsules within the range of 50,000 to < 3,000,000 MCs to see how the cells react to the localised release. In this way a concentration profile could be determined. The incorporation of an untreated cell only control with no exogenous treatment applied would be beneficial to do a comparison with exogenous CNP treatment and the different microcapsule combinations. Also, given the microcapsule to cell ratio was <12.5 and the microcapsules synthesised were made using biodegradable materials, the chances of significant toxicity in this experiment were reasonably low. However, this should still be checked further by performing viability profiling of unlabelled CNP and microcapsules structures so as to avoid confusion between live cells (green) with FITC-CNP and dead cells (red) with TRITC-PLA.

The amount of CNP lost during the initial CNP microcapsule manufacture stage is a significant issue. Peake et al noted only a loss of less than 20% of the initial CNP supplied during their microcapsule synthesis which whilst not as high detected in my experiments is still a significant loss and limitation of this method (Peake et al., 2015). For a peptide such as CNP which presents a significant investment, 0.5 mg of CNP can cost as high as £352 from some suppliers at the time of writing, a loss of this amount is from a financial perspective troubling and could have significant effects on the feasibility of applying this technology to the clinic.

Another potential limitation of the passive release microcapsule model is an issue of overstimulation. Whilst, prolonged release of a bioactive molecule is often desirable and avoids the issue of reapplication, there is potential for an overstimulation of the cells to occur by the released molecule. Since passive release is not governed by an external stimulus, if excessive activation of a signalling pathway that is resulting in undesirable effects begins to occur, there is no way of stopping the process without disruption of the entire agarose construct used here. This

might potentially explain why I saw a decrease in GAG synthesis in bAC/agarose constructs that contained 3,000,000 and 5,000,000 microcapsules. Tezcan et al demonstrated the effect of CNP on GAG synthesis in MSCs becomes diminished at concentrations of 1μM (Tezcan et al., 2010). In that way, stimulus responsive microcapsule technology is a much more desirable method to achieving long term coaxing of a specific cellular response.

One final general limitation for this research is the availability of AFSCs for testing. Although extraction of AFSCs is easily performed from the fluid extracted during procedures such as amniocentesis, the incidence of these procedures is reducing following the advent of non-invasive prenatal screening tests such as NACE®. These tests require a simple blood sample to be taken from the mother in order to analyse DNA in the maternal plasma related to the foetus via next generation sequencing. Whilst AFSCs can still be derived from other essential procedures such as amniodrainage and during laser interventions, the number of AFSCs that can be isolated from these procedures is much lower than that of amniocentesis. With an increasing interest in the use of these cells for medical and tissue engineering applications, such a small supply of AFSC samples will make performing in vitro studies more difficult, especially in regard to obtaining sufficient independent samples in which to perform a complex study.

6.4 Future research

The experimental studies performed within this thesis have provided a basis for investigating a variety of different aspects regarding chondrogenic differentiation of human AFSCs, the effect of CNP on this process and the utilisation of microcapsule technology within a 3D model to affect cellular response. As discussed in the limitations section of this chapter, the investigations performed require further follow up and in-depth evaluation to fully characterise and conclude the effect of TGFβ isoforms, CNP and CNP containing MCs on AFSC chondrogenic differentiation. Below is a flowchart proposing further investigations that follow on directly from the work performed here, followed by in-depth explanations of the rationale for each point.

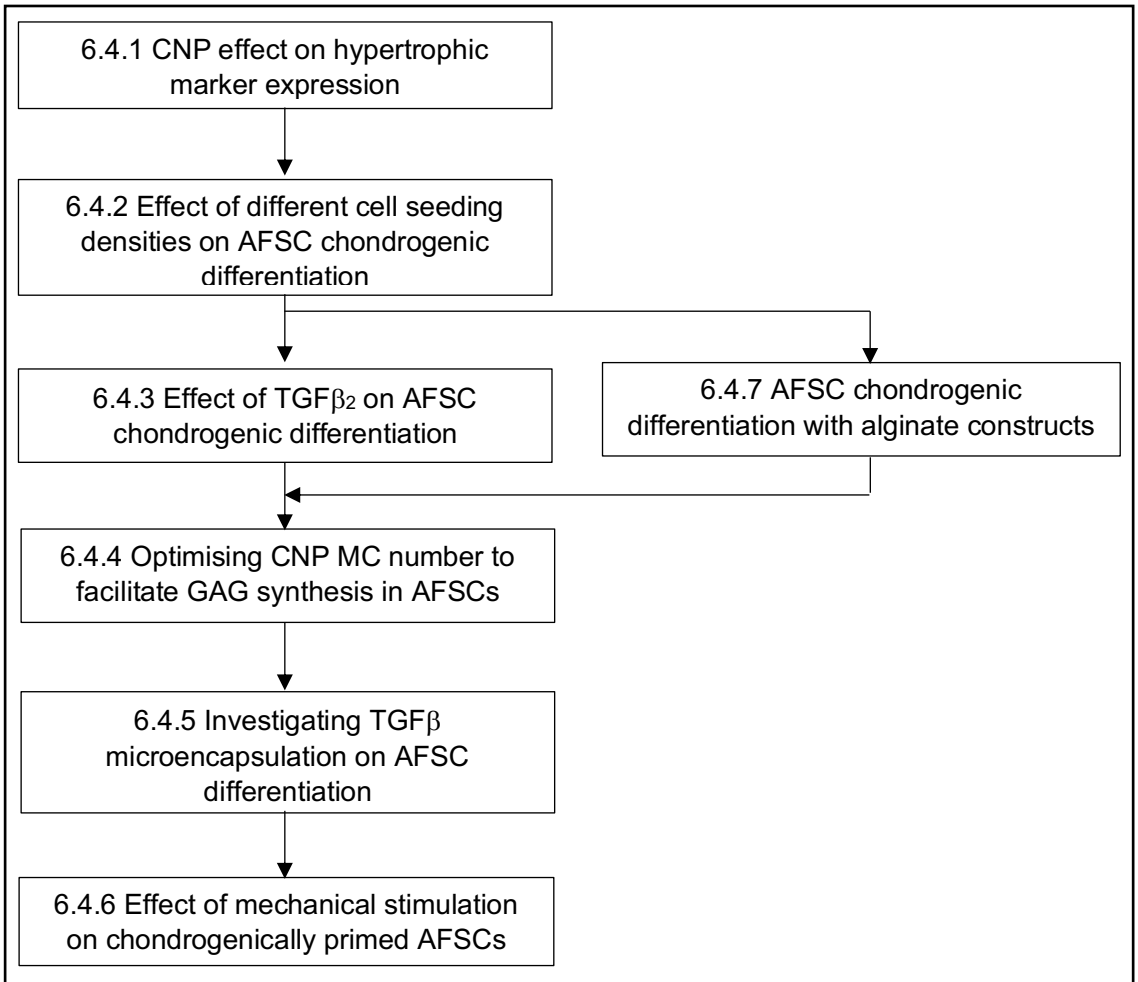

Figure 6.2: Flowchart indicating a potential workflow that can be followed to further build upon and characterise the events investigated in this thesis.

6.4.1 The effect of CNP on hypertrophic marker expression

One of the major problems in terms of applying this knowledge to future research is primarily a financial one. From the data I have acquired, no statistically significant difference was detected between CNP + TGFβ isoform treatment with Dex + TGFβ$_1$ treatment after 28 days of culture. The one caveat before a definitive judgement can be made is the effect that CNP has on the expression of hypertrophic/osteogenic markers. Dexamethasone has previously been implicated in enhancing chondrogenic gene expression (SOX-9, COL2b1, aggrecan) in addition to enhancing hypertrophic markers such as Runx2, ALP and osteocalcin. Therefore, it is essential to fully evaluate the effect of CNP on AFSC chondrogenic differentiation by identifying its effect on the expression of these hypertrophic markers as well as COL1 and COLX in a much more expanded study to ensure appropriate statistical power. In addition to this, histological examination of hypertrophic/osteogenic markers should be performed through staining to support the findings of the gene expression data retrieved. A more complete understanding of CNP's effect on this process can therefore be achieved and a determination as to whether CNP is a more appropriate supplement to this process than dexamethasone can be assessed.

6.4.2 Effect of different cell seeding densities on AFSC chondrogenic differentiation.

Healthy articular cartilage contains 9.6 x 10^6 chondrocytes/cm^3 (Hunziker et al., 2002). However for chondrogenic differentiation of stem cells, different seeding densities have been used in a variety of matrix environments and chondrocyte sources (Heywood et al., 2004, Watt, 1988). Bernstein et al. demonstrated that a high cell density (7 x 10^7) of chondrocytes within alginate hydrogels did not constitute a significant enhancement in collagen synthesis or gene expression compared to a 'low' cell density of 4 x 10^6 per ml, with reduced fibrocartilage markers seen in the low cell density group indicating low cell density would be more important for overall chondrogenic development (Bernstein et al., 2009). Other groups have utilised cell densities as high as 2 - 5 x 10^7 of MSCs to achieve sufficient chondrogenic differentiation (Thorpe et al., 2013). A recent study looking at cell seeding densities for chondrogenic differentiation of BM-MSCs performed by Bornes et al showed that cell seeding density of 5 x 10^7 bovine BM-MNCs resulted in the highest levels of aggrecan, collagen II mRNA, GAG synthesis and Bern score compared to all other densities investigated (Bornes et al., 2016). Since my study has limitations in terms of the level of GAG and hydroxyproline synthesis occurring, it would be beneficial to investigate whether an optimum cell density exists to achieve chondrogenic differentiation of AFSCs within

this model. This could be achieved by culturing AFSC/agarose constructs of increasing density for the same period of time whereby the methods optimised within this thesis can be used to compare the biochemical, histological and gene expression changes occurring. The optimum cell density can therefore be determined by also assessing these factors against the viability of the cells after 28 days.

6.4.3 Effect of TGFβ_2 on AFSC chondrogenic differentiation.

Mesenchymal condensation and chondrogenesis of mesenchymal progenitor cells is promoted by TGFβ_1, TGFβ_2 and TGFβ_3 signalling but its role as an essential factor is debated (Tuli et al., 2003, Song et al., 2007, Shull et al., 1992, Pelton et al., 1991). Studies regarding the role of TGFβ in early development are difficult to perform due to the perinatal lethality induced when specific TGFβ isoforms are knocked out. Despite this, defects in chondrogenesis have been detected upon the loss of TGFβ_2 which display general chondrodysplasias and blocking of Shh signalling to prevent hypertrophic differentiation *ex vivo* (Sanford et al., 1997, Alvarez et al.). However, when deletion of TGFβ_2 occurs at later stages of limb development, the defects are not evident suggesting a specific role during pre-chondrogenic stages. Few studies have looked at the impact of TGFβ_2 on chondrogenic differentiation despite research indicating it plays a more integral role in the early chondrogenic differentiation stages. Of the studies that have been performed, no difference was reported in effect compared to TGFβ_1 and TGFβ_3 treatment (Jakobsen et al., 2014, Mueller et al., 2010). This would be in agreement with my findings in which no differences between TGFβ_1 and TGFβ_3 were detected. Nevertheless, this would therefore be an area of important investigation to determine if chondrogenic differentiation of AFSCs within this model is independent of TGFβ isoform used. This could easily be achieved by utilising the framework initially investigated in this thesis and improved upon by the suggestions made in 6.4.1 and 6.4.2, with the addition of TGFβ_2 and CNP + TGFβ_2 treatment conditions.

6.4.4 Optimising CNP MC number to facilitate GAG synthesis in AFSCs.

Whilst I demonstrated the local release of CNP from polyelectrolyte microcapsules within the agarose construct enhanced bAC GAG synthesis, the more relevant investigation to be performed is the effect of CNP microcapsule incorporation on human AFSC differentiation. In terms of analysis, the application of this technology could have much wider connotations in addition to enhancing GAG synthesis of cells. Gene expression within cells is a dynamic process that experiences careful regulation in order to maintain chondrocytes in their mature state. While

many groups are able to demonstrate that pro-chondrogenic gene expression occurs during chondrogenic differentiation of stem cells, it is often associated with upregulation of hypertrophic and osteogenic genes also. It is possible that the prolonged activation of pro-chondrogenic genes through the exogenous application of growth factors contributes to this upregulation of undesirable genes which contribute to hypertrophic and endochondral ossification processes. By carefully regulating the application of growth factors in a more physiological environment, it is possible that the desirable aspects of this differentiation ca be achieved whilst minimising the undesirable events. Therefore, if future investigations apply this technology for stem cell differentiation purposes, the effect of localised release of peptide on chondrogenic/hypertrophic gene expression would be an important observation to make in addition to biochemical and histological analysis. This investigation could be achieved by repeating the methodology laid out in **Chapter 5** of this thesis but changing the number of MCs utilised and of course switching the cell type encapsulated to AFSCs. In addition to these studies, whilst it is possible to characterise the release rates of CNP from MCs in solution, the release rate when placed in the hydrogel construct is likely to be different or demonstrate alterations in kinetics. This could be another area of novel investigation to characterise the release of peptide load from LbL MCs within an agarose construct. A time lapse study using confocal microscopy imaging could potentially be utilised to investigate the release of fluorescently labelled peptide from the LbL MCs over a defined time period to characterise this.

6.4.5 Analysis of the effect of TGFβ microencapsulation on chondrogenic differentiation.

TGFβ similarly shares a short half-life to CNP and would benefit from long term, stable effective local delivery in a similar way (Shen et al., 2018). Covalent tethering of $TGF\beta_1$ within PEG hydrogels has already demonstrated the promotion of chondrogenic differentiation in MSCs, so an investigation into the localised release of TGFβ from microcapsule carriers within an agarose hydrogel would be warranted (McCall et al., 2012). However, more recently nanofiber scaffold based release of $TGF\beta_3$ was also shown to driving synovium derived stem cells towards a fibrocartilage cell fate (Qu et al., 2019). Despite this, localised release of microencapsulated $TGF\beta_1$ for AFSC differentiation within a 3D model would be an interesting research question to answer. As a much larger molecule (25 kD relative to CNPs 2.197 kDa) the use of a passive release mechanism as used in my investigation would be inappropriate as the growth factor would remain entrapped within the polyelectrolyte layers. However, if applied to a stimuli responsive

microcapsule release system, such as ferromagnetic microcapsules which releases its payload when exposed to a magnetic field, this could facilitate carefully managed release of TGFβ to the cells (**Figure 6.3**). Ferromagnetic microcapsules would possess several advantages to other stimuli activated microcapsules such as (ultraviolet) UV and infra-red (IR) responsive microcapsules because the magnetic fields applied are unlikely to negatively impact the viability or responses of cells. Several groups have already indicated successful stimuli dependent release of microcapsules payloads using this technology.

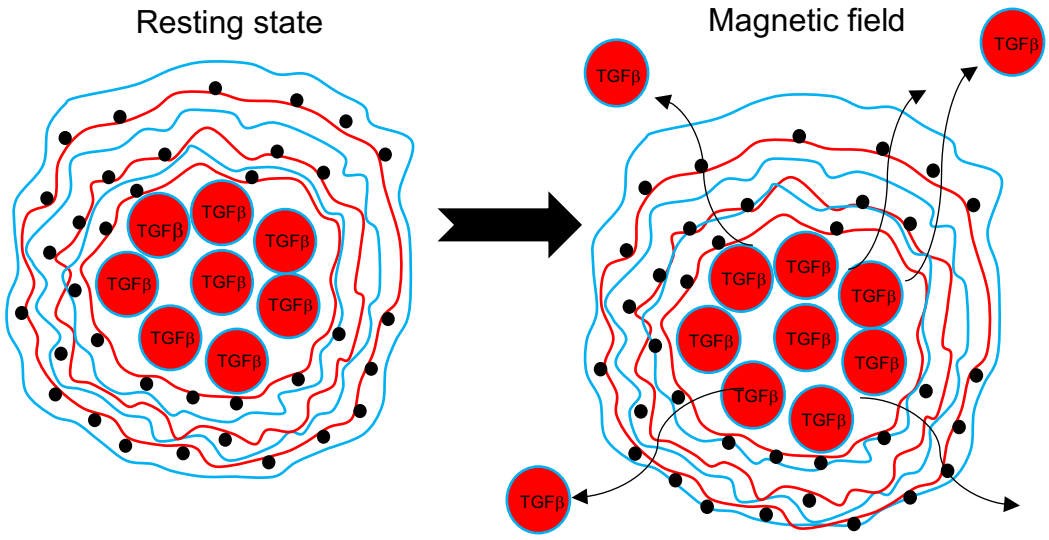

Figure 6.3: Potential application of ferromagnetic responsive TGFβ containing microcapsules. *Ferromagnetic particles within polyelectrolyte layer can effectively make microcapsules leakier to facilitate release of payload, in this case TGFβ, in response to a magnetic field.*

Therefore, incorporation of ferromagnetic particles into a biodegradable LbL polyelectrolyte microcapsules would need to be performed and optimised. Following this, a method for the encapsulation of TGFβ within these structures would need to be developed before an investigation into how responsive the produced microcapsules are to a magnetic field. Once the stimulus responsiveness of the MCs and the identification of release is identified, then the application of these MCs to an AFSC laden hydrogel construct could be performed and investigated.

6.4.6 Effect of mechanical stimulation on chondrogenically primed AFSCs.

The indication of a pericellular matrix deposition of the cells suggests that the cells could be attempting to stimulate mechanotransduction pathways after 28 days of culture. However, given the relatively low level of collagen and GAG detected in my samples, application of

mechanical stimulation is potentially detrimental to the survival of the cells within an agarose construct. Once identification of the optimum cell density to perform chondrogenic differentiation of AFSCs is performed and well characterised, the application of mechanobiology studies could be utilised here to investigate the effect of mechanical stimuli on chondrogenically primed AFSC GAG synthesis (**Figure 6.4**). The most effective way of performing this would be through the use of a cell straining apparatus whereby physiological load can be applied of between 0 - 15% strain amplitude with sinusoidal waveform and a frequency of 1Hz (Lee and Bader, 1997). In addition, if this apparatus was implemented into an oxygen-tension controlled incubator such as a Biospherix, the effect of hypoxic oxygen tensions could also be investigated on this process.

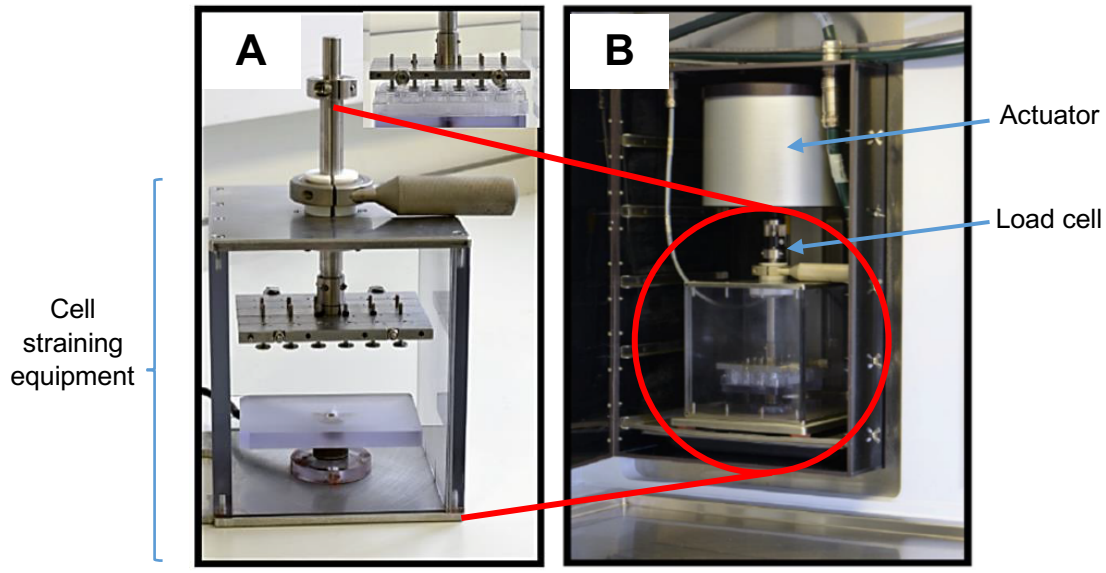

***Figure 6.4: Cell straining apparatus for mechanobiology studies. A**: Example of Bose bioreactor cell straining apparatus consisting of compressive mounting plate and loading pins. **B**: The electromagnetically controlled vertical actuator and load cell attached to the cell straining apparatus (BOSE ElectroForce System Group, Minnesota, USA). Figure modified from (Tilwani, 2016).*

To complement these studies, RAMAN spectroscopy could be used to identify the presence of any calcifications that develop within the construct as a result of de-differentiation of the cells over time or mineralisation as a consequence of osteogenic differentiation (Henrionnet et al., 2017). RAMAN spectroscopy uses the principle of vibrational inelastic light scattering of an incident laser shining on a sample to provide biomolecular and structural information regarding the sample. This technology has previously been used to look at the zonal organisation of articular cartilage and tissue engineered cartilage (Bergholt et al., 2016). If used in concert with mechanical characterisation of the tissue engineered construct, both the mechanical properties (local elastic

modulus) and the tissue engineered construct's organisation in terms of collagen, GAG and water could be well established and compared to native tissue. In this way, a different perspective is provided to support biochemical, gene expression and imaging techniques that I have used in this thesis.

6.4.7 AFSC chondrogenic differentiation within 3D alginate constructs.

The use of alginate constructs of identical size and shape to the agarose constructs used in this thesis would have been ideal for a direct comparison of the hydrogel materials employed for the encapsulation of AFSCs. With the construction of a simple mould with attachable glass plating that can be secured via screws and a piece of standard dialysis membrane, this should be a methodology that is achievable to perform (**Figure 6.5**). Following the proposed optimisation of cell seeding density for constructs as outlined in **Chapter 6.4.2**, AFSC differentiation could be investigated again and prolonged culture used to determine if this hydrogel material is sufficient for this purpose.

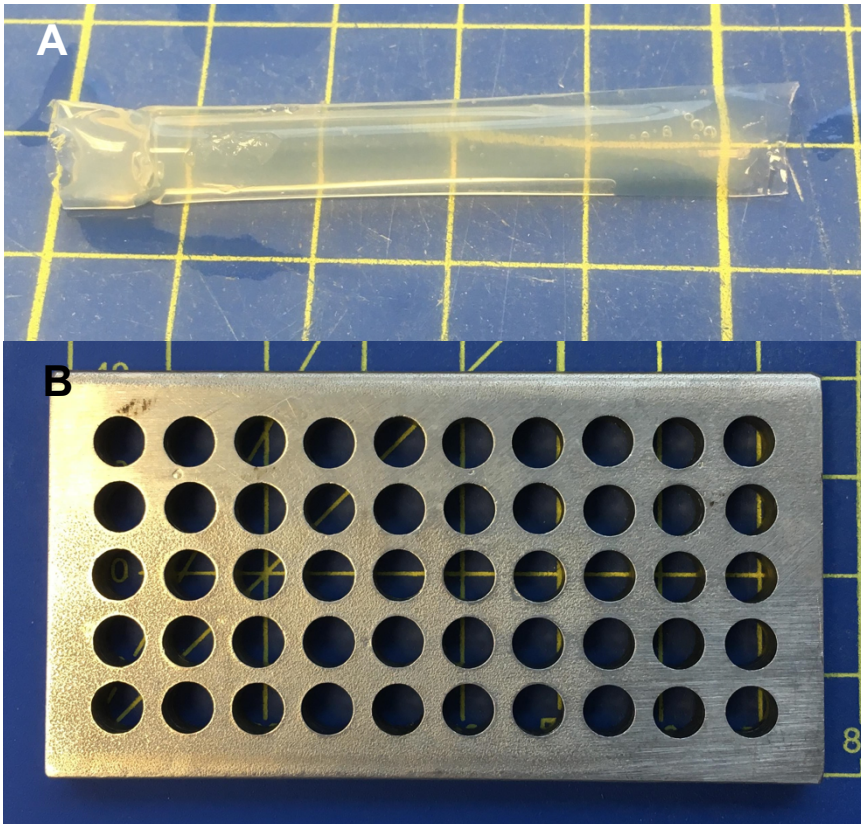

***Figure 6.5: Alginate construct example. A**: Example of alginate construct that can be made using dialysis tubing. **B**: Example of the mould used to create 5 x 5 mm agarose constructs. The insertion of screw points into the stainless-steel mould could allow attachment of dialysis membrane to the mould for alginate construct construction.*

6.4.8 Clinical implications

With the findings presented here, the application of an AFSC embedded hydrogel has a limited application for cartilage repair in the clinic without longer term culture in order to stimulate further ECM synthesis (>4 weeks). Given the weak mechanical properties of hydrogels, the application of an AFSC embedded hydrogel is limited without structural modifications or a therapy designed to utilise this effect. However, the basic methodologies developed here and optimised can be used to help differentiate any stem cells into lineages whereby a 3D environment is beneficial. The immunologic properties, or lack thereof of immunogenic properties, for AFSCs presents a desirable situation in terms of a cell only implantation, provided that the cells remain *in situ* and differentiate correctly to the mature chondrocyte phenotype. Incorporation of magnetic nanoparticles may be an avenue of research to maintain the cells within a specific location however incorporation of cells like this requires further experimental testing regarding how the cells process these nanoparticles over the long term.

Future application of AFSCs is potentially limited for a cartilage repair purpose. The lack of substantial ECM synthesis in terms of GAG and collagen within the experiments performed here suggests that either further optimisation to stimulate these processes is needed or that the cell type itself is limited in terms of chondrogenic differentiation. In comparison to MSC chondrogenic differentiation, the work presented here also indicates a reduced capacity to meet the needs of a clinically applied tissue engineered tissue. More recent work has focused on the use of AFSCs to differentiate along a cardiomyogenic lineage and the results have been promising, showing a greater potential relative to bone marrow mesenchymal stem cells (Jain, 2019).

Whilst the immunologic properties of AFSCs are desirable, the lack of availability of AFSCs provides a limitation especially given the preference for expectant mothers to select non-invasive procedures for karyotype testing. More expansive *in vitro* and *in vivo* studies would therefore be limited and effectively provides a bottleneck in terms of further advancement to assess the utility of these cells for other applications. The future of these cells is therefore potentially ambiguous. However, the advancement of biobanking and research cell bank productions could potentially make the scientific investigations of these cells easier.

6.5 Thesis conclusions

Overall, this research has furthered current understanding by:

- Successfully characterising of the biochemical changes that occur in human AFSCs over 14 days when encapsulated in alginate beads and agarose constructs and subjected to a defined TGFβ mediated chondrogenic differentiation protocol.
- Demonstrating the limitation of alginate beads for human AFSC chondrogenic differentiation for longer than 14 days of culture.
- Revealing that ECM synthesis of human AFSCs is enhanced within a simple agarose construct following a defined TGFβ mediated chondrogenic differentiation protocol over 21 and 28 days.
- Indicating the ECM synthesis of human AFSCs undergoing this chondrogenic differentiation protocol is not influenced by the TGFβ isoform utilised.
- Identifying CNP is not a chondro-inductive agent for human AFSC chondrogenic differentiation.
- Identifying CNP acts as a chondro-supportive agent for the TGFβ mediated differentiation of human AFSCs.
- Revealing an application of CNP containing polyelectrolyte microcapsules can be conducive to enhancing ECM synthesis of cells within a 3D hydrogel model compared to exogenous application.

My thesis has therefore laid the groundwork for several promising areas of investigations by future researchers in this field that can contribute to the development of a robust 3D hydrogel model for *in vitro* study of AFSC and other stem cell chondrogenic differentiation experiments. My work has also opened up a new avenue of enquiry into the use of microcapsule technology to enhance this process within 3D culture models.

National conference/symposium contributions

Oral presentations

- Taylor, J. R. M.; David, A. L.; De Coppi, P.; Chowdhury, T. T. *The effect of CNP on the chondrogenic differentiation of foetal derived stem cells (AFSCs).* Stem Cell Regenerative Medicine meeting, Institute of Child Health, UCL, London.

  Date: Tuesday 11th July 2017.

- Taylor, J. R. M.; David, A. L.; De Coppi, P.; Chowdhury, T. T. *The effect of CNP on the chondrogenic differentiation of foetal derived stem cells (AFSCs).* Russel Binions Memorial Symposium 2018, QMUL, London

  Date: Thursday 26th April 2018.

Poster presentations

- Industrial Liaison Forum 2016: *The effect of CNP and TGFβ on foetal stem cell differentiation for chondrogenesis.*

  School of Engineering and Materials Science, QMUL, London, UK.

  Date: Friday 11th November 2016.

- Rosetrees Symposium 2016: *The effect of CNP on foetal derived stem cell differentiation and GAG production in an alginate bead model.*

  Blizard Institute, QMUL, London, UK.

  Date: Wednesday 21st September 2016.

- Industrial Liaison Forum 2017: *Microcapsules encapsulated with CNP enhance GAG synthesis in chondrocyte/agarose constructs.*

  School of Engineering and Materials Science, QMUL, London, UK.

  Date: 22nd November 2017.

- BiomedEng18 conference: *CNP with TGFβ enhanced chondrogenic differentiation of human amniotic fluid stem cells cultured in agarose constructs. Poster 63.*

  Imperial College, London, UK.

  Date: Thursday 6th and Friday 7th September 2018.

List of Awards

3rd place for oral presentation in the Queen Mary 3-minute thesis competition finals 2016.

Date received: Thursday 16th June 2016.

QMUL Skill points record

Mr JRM Taylor (130474511)

Progress

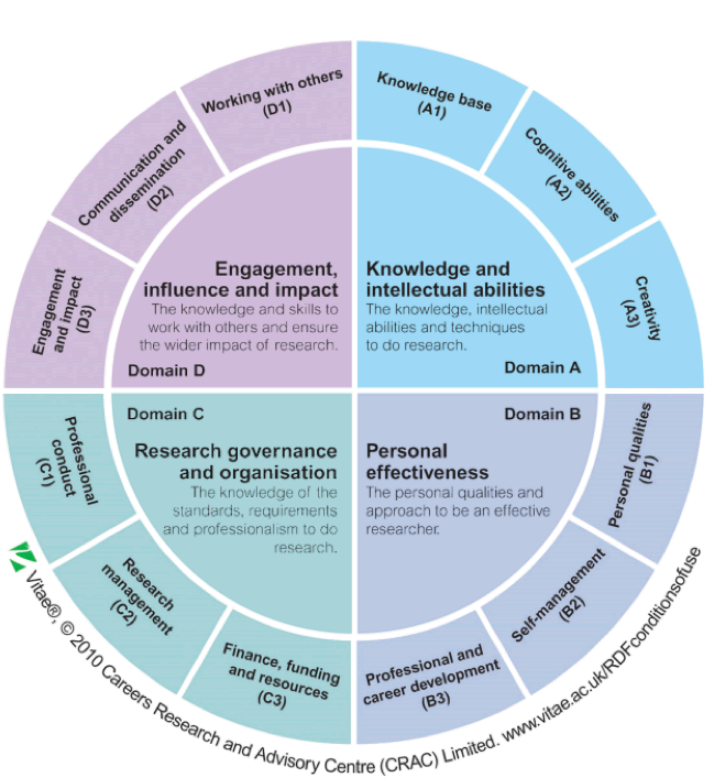

Personal Details

Full Name: James Robert Miles Taylor
Username: [redacted]
Telephone: [redacted]
Enrolment Status: R-E-E
Course Name: PhD FT Medical Engineering
Start Date: 28-Sep-2015
Route: RSMEN
Faculty: Science and Engineering
Department: School of Engineering and Materials Science - Engineering

Gender: Male
Email: [redacted]
Mobile: [redacted]
Programme: RRPF-QMENNG1 PhD FT Engineering
Award Code: RP
Expected End Date: 28-Sep-2019
School: School of Engineering and Materials Science

Supervisors

Title	Given Names	Last Name	Telephone	Email	Active
Dr	Tina Tanveer	Chowdhury		t.t.chowdhury@qmul.ac.uk	true
Prof	Adrian Jonathan	Hobbs		a.j.hobbs@qmul.ac.uk	true

Points Summary

Year	Type	Pts:	A	B	C	D	Total	Cap:	A	B	C	D	Total
1st	*Conference Attendance (One day)*		9.0	6.0	0.0	0.0	15.0						
	Conference Attendance (Two days)		6.0	4.0	0.0	0.0	10.0						
	Conference attendance sub-total		**16.5**	**11.0**	**0.0**	**0.0**	**27.5**						
	Doctoral College event/course		0.0	4.0	3.0	4.0	11.0						
	GRADFEST		4.0	4.0	0.0	4.0	12.0						
	Health and Safety		0.0	0.0	5.0	0.0	5.0						
	Other course/event attendance		2.0	3.0	0.0	2.0	7.0						
	Researcher Development Course		12.0	31.5	13.0	9.0	65.5						
	Course/event attendance sub-total		**18.0**	**42.5**	**21.0**	**19.0**	**100.5**						
	Outreach/public engagement		0.0	0.0	0.0	23.0	23.0						
	Outreach/public engagement sub-total		**0.0**	**0.0**	**0.0**	**23.0**	**23.0**						
	Seminar attendance (single)		10.5	1.0	0.0	0.0	11.5						
	Seminar attendance sub-total		**10.5**	**1.0**	**0.0**	**0.0**	**11.5**						
	Mentoring/supervising of Project Student		6.0	3.0	0.0	6.0	15.0						
	Teaching/demonstrating/marking/preparation		0.0	3.0	0.0	3.0	6.0						
	Teaching sub-total		**6.0**	**6.0**	**0.0**	**9.0**	**21.0**						
	Year 1 Total (with caps applied)		51.0	60.5	21.0	51.0	183.5						

Year	Type	Pts:	A	B	C	D	Total	Cap:	A	B	C	D	Total
2nd	*Doctoral College event/course*		0.5	1.0	0.5	1.0	3.0						
	Other course/event attendance		11.0	6.0	0.0	4.0	21.0						
	Researcher Development Course		0.5	3.0	0.5	2.0	6.0						
	Course/event attendance sub-total		**12.0**	**10.0**	**1.0**	**7.0**	**30.0**						
	Outreach/public engagement		0.0	0.0	0.0	13.0	13.0						
	Outreach/public engagement sub-total		**0.0**	**0.0**	**0.0**	**13.0**	**13.0**						
	Seminar attendance (single)		1.5	0.0	0.0	0.0	1.5						
	Seminar attendance sub-total		**1.5**	**0.0**	**0.0**	**0.0**	**1.5**						
	Teaching/demonstrating/marking/preparation		0.0	5.8	0.0	5.8	11.5						
	Teaching sub-total		**0.0**	**5.8**	**0.0**	**5.8**	**11.5**						
	Year 2 Total (with caps applied)		13.5	15.8	1.0	25.8	56.0						
4th	*Educational Development Course*		0.0	4.0	0.0	5.0	9.0						
	Course/event attendance sub-total		**0.0**	**4.0**	**0.0**	**5.0**	**9.0**						
	Year 4 Total (with caps applied)		0.0	4.0	0.0	5.0	9.0						
Total	*Conference Attendance (Half day)*		1.5	1.0	0.0	0.0	2.5						
	Conference Attendance (One day)		9.0	6.0	0.0	0.0	15.0						
	Conference Attendance (Two days)		6.0	4.0	0.0	0.0	10.0						
	Conference attendance sub-total		**16.5**	**11.0**	**0.0**	**0.0**	**27.5**		**18.0**	**12.0**			**30.0**
	Doctoral College event/course		0.5	5.0	3.5	5.0	14.0						
	Educational Development Course		0.0	4.0	0.0	5.0	9.0						
	GRADFEST		4.0	4.0	0.0	4.0	12.0						
	Health and Safety		0.0	0.0	5.0	0.0	5.0				10.0		10.0
	Other course/event attendance		13.0	9.0	0.0	6.0	28.0						
	Researcher Development Course		12.5	34.5	13.5	11.0	71.5						
	Course/event attendance sub-total		**30.0**	**56.5**	**22.0**	**31.0**	**139.5**						
	Outreach/public engagement		0.0	0.0	0.0	36.0	36.0					60.0	60.0
	Outreach/public engagement sub-total		**0.0**	**0.0**	**0.0**	**36.0**	**36.0**						
	Seminar attendance (single)		12.0	1.0	0.0	0.0	13.0						
	Seminar attendance sub-total		**12.0**	**1.0**	**0.0**	**0.0**	**13.0**		**30.0**				**30.0**
	Mentoring/supervising of Project Student		6.0	3.0	0.0	6.0	15.0		8.0	4.0		8.0	20.0
	Teaching/demonstrating/marking/preparation		0.0	8.8	0.0	8.8	17.5			15.0		15.0	30.0
	Teaching sub-total		**6.0**	**11.8**	**0.0**	**14.8**	**32.5**						
	Total (with caps applied)		64.5	80.2	22.0	81.8	248.5						
	Grand Total (with caps applied)		**64.5**	**80.2**	**22.0**	**81.8**	**248.5**						
	Target		60.0	20.0	15.0	30.0	210.0						

Pending Activities

Nothing found to display

Activity Record

Type	Code	Title	Provider	From	To	Hours	A	B	C	D	Total
Health and Safety		Lab Awareness	Chris Mole	30-Sep-2015 00:00	30-Sep-2015 00:00	2.0	0.0	0.0	2.0	0.0	2.0
Researcher Development Course	DC100	PhD Induction	Doctoral College	07-Oct-2015 09:30	07-Oct-2015 17:00	0.0	0.0	2.0	3.0	2.0	7.0
Doctoral College event/course	DC100	PhD Induction	Doctoral College	07-Oct-2015 09:30	07-Oct-2015 17:00	0.0	0.0	2.0	3.0	2.0	7.0
Conference Attendance (One day)		IOB Launch Event	IOB	08-Oct-2015 00:00	08-Oct-2015 00:00	0.0	3.0	2.0	0.0	0.0	5.0
Researcher Development Course	RD101	Getting Started with your PhD	Centre for Academic and Professional Development	26-Oct-2015 13:30	26-Oct-2015 16:30	0.0	0.0	1.0	1.0	1.0	3.0
Teaching/demonstrating/marking/preparation	MAT311	Demonstrating GAG assay	SEMS	02-Nov-2015 00:00	06-Nov-2015 00:00	6.0	0.0	3.0	0.0	3.0	6.0
Seminar attendance (single)		SEMS PhD talk by Professor Steve Dunn	SEMS	13-Nov-2015 00:00	13-Nov-2015 00:00	0.0	0.5	0.0	0.0	0.0	0.5
Researcher Development Course	RS002	The seven secrets of highly successful research students	Centre for Academic and Professional Development	12-Jan-2016 14:00	12-Jan-2016 16:30	0.0	0.0	1.5	0.0	1.0	2.5
Researcher Development Course	RC202	Academic Career Planning for PhD Students	QM Careers	20-Jan-2016 14:00	20-Jan-2016 17:00	0.0	0.0	3.0	0.0	0.0	3.0
Researcher Development Course	RD102	Managing Your Research Project	Centre for Academic and Professional Development	28-Jan-2016 10:00	28-Jan-2016 16:30	0.0	0.0	3.0	3.0	0.0	6.0
Researcher Development Course	RD109	Speed-reading for Researchers	Centre for Academic and Professional Development	01-Feb-2016 13:30	01-Feb-2016 16:30	0.0	0.0	3.0	0.0	0.0	3.0

Type	Code	Title	Provider	From	To	Hours	A	B	C	D	Total
Researcher Development Course	RC216	CVs and Applications for Jobs Outside Academia	Centre for Academic and Professional Development	03-Feb-2016 10:00	03-Feb-2016 13:00	0.0	0.0	3.0	0.0	0.0	3.0
Seminar attendance (single)		Chemistry of individual molecules through a lens of transmission electron microscope	MRI	10-Feb-2016 00:00	10-Feb-2016 00:00	0.0	0.5	0.0	0.0	0.0	0.5
Seminar attendance (single)	RES-SEM-SING	Research seminar (singular)	Any provider	17-Feb-2016 00:00	17-Feb-2016 00:00	0.0	0.5	0.0	0.0	0.0	0.5
Seminar attendance (single)		Evening Talk and discussion with Amrita Ahluwalia	WISE @ QMUL	24-Feb-2016 00:00	24-Feb-2016 00:00	0.0	1.0	1.0	0.0	0.0	2.0
Researcher Development Course	RS405	Career management for Non-Academic Career Paths	Centre for Academic and Professional Development	24-Feb-2016 14:00	24-Feb-2016 17:00	0.0	0.0	3.0	0.0	0.0	3.0
Researcher Development Course	RC326	Interview Skills for PhD Students	Centre for Academic and Professional Development	03-Mar-2016 10:00	03-Mar-2016 13:00	0.0	0.0	3.0	0.0	0.0	3.0
Seminar attendance (single)		Mechanobiology and the Primary Cilium	Inaugral Lecture by Professor Martin Knight	09-Mar-2016 00:00	09-Mar-2016 00:00	0.0	0.5	0.0	0.0	0.0	0.5
Researcher Development Course	RC212	Doctoral Transitions: Career networking event for those with a STEM background	QM Careers	10-Mar-2016 18:00	10-Mar-2016 20:00	0.0	0.0	1.5	0.0	0.0	1.5
Researcher Development Course	RD203	Reading Strategically and Analytically	Centre for Academic and Professional Development	14-Mar-2016 10:00	14-Mar-2016 13:00	0.0	3.0	0.0	0.0	0.0	3.0
Health and Safety	HS013	Working Safely with Biological Hazards	Dr M Ariyanayagam/SEMS	15-Mar-2016 00:00	15-Mar-2016 00:00	3.0	0.0	0.0	3.0	0.0	3.0
Seminar attendance (single)		Approaches to corneal tissue engineering: Top-down or bottom-up?	IOB	16-Mar-2016 00:00	16-Mar-2016 00:00	0.0	0.5	0.0	0.0	0.0	0.5
Seminar attendance (single)		Biomimetic Approaches to Growing Biological Rubber Bands	IOB	16-Mar-2016 00:00	16-Mar-2016 00:00	0.0	0.5	0.0	0.0	0.0	0.5
Researcher Development Course	RD112	Research it! : Information research skills for Science and Engineering	Centre for Academic and Professional Development	17-Mar-2016 10:00	17-Mar-2016 12:00	0.0	2.0	0.0	0.0	0.0	2.0
Researcher Development Course	RD208	Making a Poster Presentation	Centre for Academic and Professional Development	23-Mar-2016 10:00	23-Mar-2016 13:00	0.0	0.0	0.0	0.0	3.0	3.0
Seminar attendance (single)		Introduction to App Development Session 1	WISE@QMUL	29-Mar-2016 00:00	29-Mar-2016 00:00	0.0	2.0	0.0	0.0	0.0	2.0
Researcher Development Course	RC217	Linkedin Secrets for Researchers: how to find jobs beyond academia.	Centre for Academic and Professional Development	30-Mar-2016 11:30	30-Mar-2016 13:00	0.0	0.0	1.5	0.0	0.0	1.5
Seminar attendance (single)		Introduction to App Development Session 2	WISE@QMUL	05-Apr-2016 00:00	05-Apr-2016 00:00	0.0	2.0	0.0	0.0	0.0	2.0
Researcher Development Course	RD104	Critical Thinking	Centre for Academic and Professional Development	07-Apr-2016 10:00	07-Apr-2016 13:00	0.0	3.0	0.0	0.0	0.0	3.0
Researcher Development Course	RSAP	Academic Progressions	Centre for Academic and Professional Development	07-Apr-2016 14:00	07-Apr-2016 16:00	0.0	0.0	1.0	1.0	0.0	2.0
Seminar attendance (single)		Introduction to App Development Session 3	WISE@QMUL	12-Apr-2016 00:00	12-Apr-2016 00:00	0.0	2.0	0.0	0.0	0.0	2.0
Researcher Development Course	RD002	Cafe Scientifique	Centre for Academic and Professional Development	12-Apr-2016 18:00	12-Apr-2016 20:30	0.0	0.0	1.0	0.0	0.0	1.0
Conference Attendance (One day)		London Polymer Group 2nd Symposium	London Polymer Group	13-Apr-2016 00:00	13-Apr-2016 00:00	0.0	3.0	2.0	0.0	0.0	5.0
Researcher Development Course	RD005	How to use Endnote for Science and Engineering	Centre for Academic and Professional Development	14-Apr-2016 14:00	14-Apr-2016 16:00	0.0	2.0	0.0	0.0	0.0	2.0
Outreach/public engagement		The Bioengineering Experience	IOB/Dr Tina Chowdhury	21-Apr-2016 00:00	21-Apr-2016 00:00	10.0	0.0	0.0	0.0	10.0	10.0
Researcher Development Course	RD007	Introduction to the 3-Minute Thesis Competition	Centre for Academic and Professional Development	28-Apr-2016 10:00	28-Apr-2016 12:00	0.0	0.0	0.0	2.0	0.0	2.0
Researcher Development Course	RD001	LATeX Tutorial for Beginners	Centre for Academic and Professional Development	28-Apr-2016 15:00	28-Apr-2016 17:00	0.0	2.0	0.0	0.0	0.0	2.0
Other course/event attendance		Workshop on 3D Image Visualisation, Analysis and Model Generation with Simpleware	Simpleware	03-May-2016 00:00	03-May-2016 00:00	0.0	1.0	0.0	0.0	0.0	1.0
Researcher Development Course	FD	Fellowship Day	Centre for Academic and Professional Development	24-May-2016 13:00	24-May-2016 16:00	0.0	0.0	2.0	3.0	0.0	5.0
Seminar attendance (single)		Molecular Biomechanics and Mechanobiology	IOB	03-Jun-2016 00:00	03-Jun-2016 00:00	0.0	0.5	0.0	0.0	0.0	0.5

Type	Code	Title	Provider	From	To	Hours	A	B	C	D	Total
Researcher Development Course	DC101	1st year PhD day: Maximising the Impact of Conferences and Networking	Centre for Academic and Professional Development	03-Jun-2016 09:30	03-Jun-2016 14:00	0.0	0.0	2.0	0.0	2.0	4.0
Doctoral College event/course	DC101	1st year PhD day: Maximising the Impact of Conferences and Networking	QMUL	03-Jun-2016 09:30	03-Jun-2016 14:00	0.0	0.0	2.0	0.0	2.0	4.0
Outreach/public engagement		Staying Strong - Joints in Space	IOB/QMUL Community Festival/Dr Tina Chowdhury	04-Jun-2016 00:00	04-Jun-2016 00:00	7.0	0.0	0.0	0.0	7.0	7.0
Other course/event attendance	DEN6407	IOB Symposium	IOB	06-Jun-2016 00:00	06-Jun-2016 00:00	0.0	1.0	1.0	0.0	0.0	2.0
Other course/event attendance		3 minute thesis vocal training	CAPD	09-Jun-2016 00:00	09-Jun-2016 00:00	0.0	0.0	2.0	0.0	2.0	4.0
Conference Attendance (One day)		Institute for Womens Health Annual Conference	Institute for Womens Health	14-Jun-2016 00:00	14-Jun-2016 00:00	0.0	3.0	2.0	0.0	0.0	5.0
GRADFEST	GF2016	Easy tricks in ImageJ	Doctoral College	15-Jun-2016 16:00	15-Jun-2016 18:00	0.0	2.0	0.0	0.0	0.0	2.0
GRADFEST	GF2016	3 Minute Thesis Final (presenting)	Doctoral College	16-Jun-2016 13:00	16-Jun-2016 14:30	0.0	2.0	4.0	0.0	4.0	10.0
Mentoring/supervising of Project Student		Masters student mentoring for presentation	Supervisor - T. Chowdhury	28-Jun-2016 00:00	28-Jun-2016 00:00	0.0	2.0	1.0	0.0	2.0	5.0
Outreach/public engagement		QMUL Science Festival	QMUL	06-Jul-2016 00:00	06-Jul-2016 00:00	6.0	0.0	0.0	0.0	6.0	6.0
Mentoring/supervising of Project Student		Mentoring Masters student through project	n/a	13-Jul-2016 00:00	13-Jul-2016 00:00	0.0	2.0	1.0	0.0	2.0	5.0
Mentoring/supervising of Project Student		Mentoring Masters student through project	IOB/Dr Tina Chowdhury	27-Jul-2016 00:00	27-Jul-2016 00:00	0.0	2.0	1.0	0.0	2.0	5.0
Conference Attendance (Two days)		Inaugural UK Regenerative Medicine Conference	Catapult & UK Regenerative Medicine Platform	20-Sep-2016 00:00	21-Sep-2016 00:00	0.0	6.0	4.0	0.0	0.0	10.0
Conference Attendance (Half day)		Rosetrees Symposium	Rosetrees Trust	21-Sep-2016 00:00	21-Sep-2016 00:00	0.0	1.5	1.0	0.0	0.0	2.5
Outreach/public engagement		Big Bang Event at Pennthorpe school	Pennthorpe school	14-Oct-2016 00:00	14-Oct-2016 00:00	7.0	0.0	0.0	0.0	7.0	7.0
Seminar attendance (single)		Cartilage, bone and joint regeneration using biomaterials, stem cells and 3D bioprinting	IOB	19-Oct-2016 00:00	19-Oct-2016 00:00	0.0	0.5	0.0	0.0	0.0	0.5
Teaching/demonstrating/marking/preparation		Teaching demonstrating for module MAT311	SEMS	31-Oct-2016 00:00	31-Oct-2016 00:00	3.5	0.0	1.8	0.0	1.8	3.5
Teaching/demonstrating/marking/preparation		Teaching demonstrating for module MAT311	SEMS	04-Nov-2016 00:00	04-Nov-2016 00:00	4.0	0.0	2.0	0.0	2.0	4.0
Other course/event attendance		IRC Celebration Event	IOB	11-Nov-2016 00:00	11-Nov-2016 00:00	0.0	8.0	3.0	0.0	4.0	15.0
Teaching/demonstrating/marking/preparation		Teaching demonstrating for module MAT311	SEMS	14-Nov-2016 00:00	14-Nov-2016 00:00	4.0	0.0	2.0	0.0	2.0	4.0
Other course/event attendance		Industrial Liason Forum (ILF)	SEMS	29-Nov-2016 00:00	29-Nov-2016 00:00	0.0	3.0	3.0	0.0	0.0	6.0
Seminar attendance (single)		Osteoinductive coatings to control bone tissue formation - seminar	IOB	18-Jan-2017 00:00	18-Jan-2017 00:00	0.0	0.5	0.0	0.0	0.0	0.5
Researcher Development Course	DC200	2nd Year PhD Cohort day: Understanding the impact of your research	Doctoral College	15-Feb-2017 13:00	15-Feb-2017 18:00	0.0	0.5	1.0	0.5	1.0	3.0
Doctoral College event/course	DC200	2nd Year PhD Cohort day: Understanding the impact of your research	Doctoral College	15-Feb-2017 13:00	15-Feb-2017 18:00	0.0	0.5	1.0	0.5	1.0	3.0
Seminar attendance (single)		Unravelling how bi-directional cell-biomaterial interactions direct stem cell fate in 3D	IOB	08-Mar-2017 00:00	08-Mar-2017 00:00	0.0	0.5	0.0	0.0	0.0	0.5
Researcher Development Course	RD100	Working With Your Supervisor	Centre for Academic and Professional Development	13-Mar-2017 14:00	13-Mar-2017 17:00	0.0	0.0	2.0	0.0	1.0	3.0
Outreach/public engagement		The Bioengineering Experence	Dr Tina Chowdhury	28-Apr-2017 00:00	28-Apr-2017 00:00	6.0	0.0	0.0	0.0	6.0	6.0
Educational Development Course	GT101	Teach your first session - Science and Engineering	QMUL	03-Jan-2019 09:30	03-Jan-2019 16:30	0.0	0.0	3.0	0.0	3.0	6.0

Supplementary materials

Example consent forms used to procure amniotic fluid from patients

University College London Hospitals NHS
NHS Foundation Trust

Fetal Medicine Unit
Elizabeth Garrett Anderson Wing
University College Hospital
235 Euston Road
London
NW1 2BU

Direct line: 020 3447 9872
Fax: 020 7387 9984
Switchboard: 020 3456 7890

Version no. 2.0
Date: 12th May 2016
Ethics: 14/LO/0863
Participant ID:_____

CONSENT FORM – Labour Ward

Study title: **Amniotic Fluid, placental and fetal stem cells at birth**

Researchers: **Dr Anna David, Consultant in Fetal Medicine**
Dr Paul Winyard, Consultant in Paediatric Nephrology
Mr Paolo de Coppi, Consultant Paediatric Surgeon

		Please initial box
1.	I confirm that I have read and understood the information sheet dated 28 April 2016 version 2.0 for the above study and have had the opportunity to ask questions	
2.	I confirm that I have had sufficient time to consider whether or not I want to be included in the study	
3.	I understand that my participation is voluntary and that I am free to withdraw at any time, without giving any reason, without my medical care or legal rights being affected	
4.	I understand that sections of any of my and my child's medical notes may be looked at by the researchers/ sponsor organisation where it is relevant to my taking part in research. I give permission for these individuals to have access to my records	
5.	I agree to take part in the above study	
6.	I agree to gift to the researchers samples of my amniotic fluid, amniotic membrane, umbilical cord blood, umbilical cord, placenta and any intellectual property	
7.	I consent to have my samples stored in a cell Biobank and consent to have a blood test to screen for infection	
8.	I consent to storage and use of these cells for any ethically (and future ethically) approved medical research or clinical trial	
9.	I agree to samples being sent to laboratories working on the research	

Name of participant	Date	Signature
Name of person taking consent	Date	Signature
Dr Anna David	07852 220375	a.david@ucl.ac.uk
Researcher to be contacted (if there are any problems)	Phone Number.	Email address

1 form for patient; 1 to be kept as part of the study documentation; 1 to be kept with hospital notes

uclh University College Hospital | National Hospital for Neurology and Neurosurgery | Eastman Dental Hospital | Royal National Throat, Nose and Ear Hospital | Heart Hospital | Royal London Hospital for Integrated Medicine

Version No. 2.0
Date: 28th April 2016
Ethics: 14/LO/0863

University College London Hospitals NHS
NHS Foundation Trust

PARTICIPANT INFORMATION SHEET – Labour Ward
Study title: Amniotic Fluid, placental and fetal stem cells at birth

Researchers: **Dr Anna David, Consultant in Fetal Medicine**
Dr Paul Winyard, Consultant in Paediatric Nephrology
Mr Paolo de Coppi, Consultant Paediatric Surgeon

You are being invited to take part in a research study. Before you decide it is important for you to understand why the research is being done and what it will involve. Please take time to read the following information carefully and ask us if there is anything that is not clear.

What is the purpose of the study? We would like to find out whether we can grow stem cells from amniotic fluid, placental tissue and fetal fluid, and whether proteins found in the fluid can be used to indicate long term outcome for problems such as kidney disease.

Stem cells have the remarkable potential to develop into many different cell types in the body. Serving as a repair system for the body, they can theoretically divide without limit to replenish other cells as long as the person or animal is still alive. When a stem cell divides, each new cell has the potential to either remain a stem cell or become another type of cell with a more specialised function, such as a muscle cell, a red blood cell, or a brain cell for example. Adults have stem cells that are commonly collected from the bone marrow. Recent studies have found stem cells in the amniotic fluid and the placenta. Stem cells are more abundant in the fetus than the adult. They may be better **able to divide, grow and develop into different cell types.**

We would like to study **amniotic fluid, placental and fetal stem cells** to find out about their characteristics, how they grow and what tissues they can turn into. We will grow them in the laboratory to see if they can repair damaged tissues such as muscle and bone, and analyse the proteins in the amniotic fluid to look for crucial growth factors and chemicals which tell us about the baby's condition. We are keen to check whether genes that are missing in genetic diseases can be introduced into stem cells. We also want to monitor how cells behave in the body and some cells may be introduced into animals to do this. These animal studies have received ethical approval and are in accordance with relevant legislation. In the future it might be possible to use corrected stem cells to treat people with genetic diseases. For example, a stem cell from a patient with thalassaemia, a genetic disease that causes severe anaemia, could have a gene inserted to correct the anaemia. Introduction of the corrected stem cell into the affected patient might then cure the disease.

We are hoping that our research will show that these stem cells are a potential **treatment of diseases in newborn babies**. Our early data has shown that amniotic fluid stem cells might be useful to treat necrotizing enterocolitis, a serious gut disease that affects up to 1 in 10 premature neonates. These stem cells may also be useful for repairing congenital structural problems in babies such as hernias. For these reasons we would also like to store some cells and tissues for future ethically approved clinical trials in a special cell biobank. To ensure that any cells that are biobanked for potential use as a treatment are free from infection, we would like to collect a sample of your blood (20mls or equivalent to 4 teaspoons) to test for infections such as HIV, hepatitis and toxoplasma. If you would prefer not to biobank the samples, we would still like to study them in our research but we would not use them for future therapy, and you would not be asked to give a blood sample.

We are also performing research to improve our understanding of the placenta, and how it works in health and disease. The placenta is a complex organ, which provides the growing baby with all the oxygen and nutrients it needs in the womb. Despite it being essential to a healthy pregnancy, it is the organ we know least about. We are developing novel imaging methods at UCLH to analyse the placenta after it is delivered. This will help us to better understand the placenta, how it functions, and how it changes in different diseases. The methods we develop may be used clinically in the future to help healthcare professionals make decisions to manage pregnancies better.

Why have I been invited to participate? We are asking pregnant woman who attend UCLH to deliver their baby whether they would take part in this study.

Do I have to take part? There is no obligation to take part and your decision will not have any affect on your future medical care. It is up to you to decide whether you would like to be involved. We will give you this information sheet to look at and keep, then ask if you are happy to sign a consent form. You are still free to withdraw at any time without giving a reason even if you decide to take part.

What will happen to me if I take part? The placenta, umbilical cord and amniotic membranes that deliver after your baby is born are checked by your midwife and then usually discarded. We would like to collect samples of the amniotic membrane, placental cells or whole placenta, the umbilical cord blood and umbilical cord from your placenta after it has been checked. If your baby is born by Caesarean section, the amniotic fluid is usually collected during surgery and discarded at the end of the operation. We will collect a sample of amniotic fluid if

you deliver your baby by Caesarean section for research and biobanking. We will only take samples from your placenta, umbilical cord or the amniotic fluid for research and for biobanking purposes if otherwise discarded. We are asking for your permission to store and use these tissues or cells for ethically approved research studies and clinical trials. If you agree to biobank your samples we will collect a sample of your blood (20mls or equivalent to 4 teaspoons) from your arm to test for infections. By gifting the samples to the Principal Investigator, you will give up all rights over the samples. If you agree to the cells being stored in the biobank for future therapeutic use, **you retain the right to withdraw them from the biobank after which they will be destroyed**. After seven years, the cells may become unsuitable for future therapeutic use but they can still continue to be used for research purposes.
We will assign to the samples and the information we collect about you a unique identifying number so that the information becomes anonymous to the researchers. **You do not have to do anything different during your tests or during the rest of your pregnancy if you take part in this study.**

What tests will be done on the amniotic fluid, placental and fetal cells? We will study the chemicals and proteins in the amniotic fluid, how the cells grow and develop, what cell types they become and whether corrective genes can be introduced into them. For some studies the sample may leave the UK for analysis in other countries, but your personal details will not be revealed. If you agree to biobank the cells we will store them for future ethically approved research and clinical studies, and you will retain the right at any time over the next 30 years, to request these cells or tissues are removed from the biobank and then destroyed.

For the imaging studies the whole placenta will be taken to the lab where we will visualise the placenta using different imaging modalities.
Will you require access to my medical records? We may need to access your or your baby's medical records, and may collect limited clinical information about you and your baby, such as pregnancy complications and outcome. These will all be kept confidential.

What are known risks of the study? There are no additional risks to your health or the health of your baby from taking part in the research because there are no extra procedures. All of the samples are being collected as part of your normal clinical tests, and we will just use the extra material which would normally be thrown away. Collection of a small blood sample has momentary discomfort and occasionally results in bruising to your arm.

What are the possible benefits of taking part? There will be no immediate benefits to your pregnancy, but this research may help us to treat patients with congenital diseases or structural abnormalities better in the future.

What if something goes wrong? As there is no extra intervention being performed other than taking some of your blood, we do not expect any risks. If you are harmed by taking part in this research project, there are no special compensation arrangements. If you are harmed due to someone's negligence, then you may have grounds for a legal action but you may have to pay for it. Regardless of this, if you wish to complain, or have any concerns of this study, the normal National Health Service complaints mechanisms should be available to you.

Will my taking part in this study be kept confidential? All information collected about you during the research will be kept strictly confidential and samples will be anonymised to the individual researchers. Any information about you, which leaves the hospital will have your name, hospital or NHS number and addressed removed so that you cannot be recognised from it. All data will be kept safe and secure in accordance with the Data Protection Act 1998 and will be collected, stored and handled by the researchers listed at UCL.

Who is organising and funding the research? The research is organised by the Tissue Engineering Laboratory and the Nephro-Urology Unit, both at UCL Institute of Child Health and Great Ormond Street Hospital and the UCL Institute for Women's Health. It is funded by the Royal Society, UCLH Charities, Kids Kidney Research, Sparks, Wellcome Trust and the European Union. Imaging research is funded by the Wellcome Trust and Engineering and Physical Sciences Research Council.

What will happen to the results of the research study? The results will be analysed, presented in scientific meetings and published in peer reviewed journals. Your identity will not be revealed in any report or publication. You may obtain a copy a copy of the results from Dr Anna David at the Institute for Women's Health at UCL (a.david@ucl.ac.uk)

The Bloomsbury Research Ethics Committee has reviewed this study and given its approval.

Contact for further information:
Dr Eleni Antoniadou 07708 666945
Dr Anna David 07852 220 375
Dr Rosalind Pratt 07958 044337

Thank you for taking part in this study!

Equipment used for RNA optimisation, cDNA synthesis and RT-qPCR.

A: Qiagen Tissue lyser

B: Nanodrop One

C: Techgene thermal cycler

D: StepOnePlus System

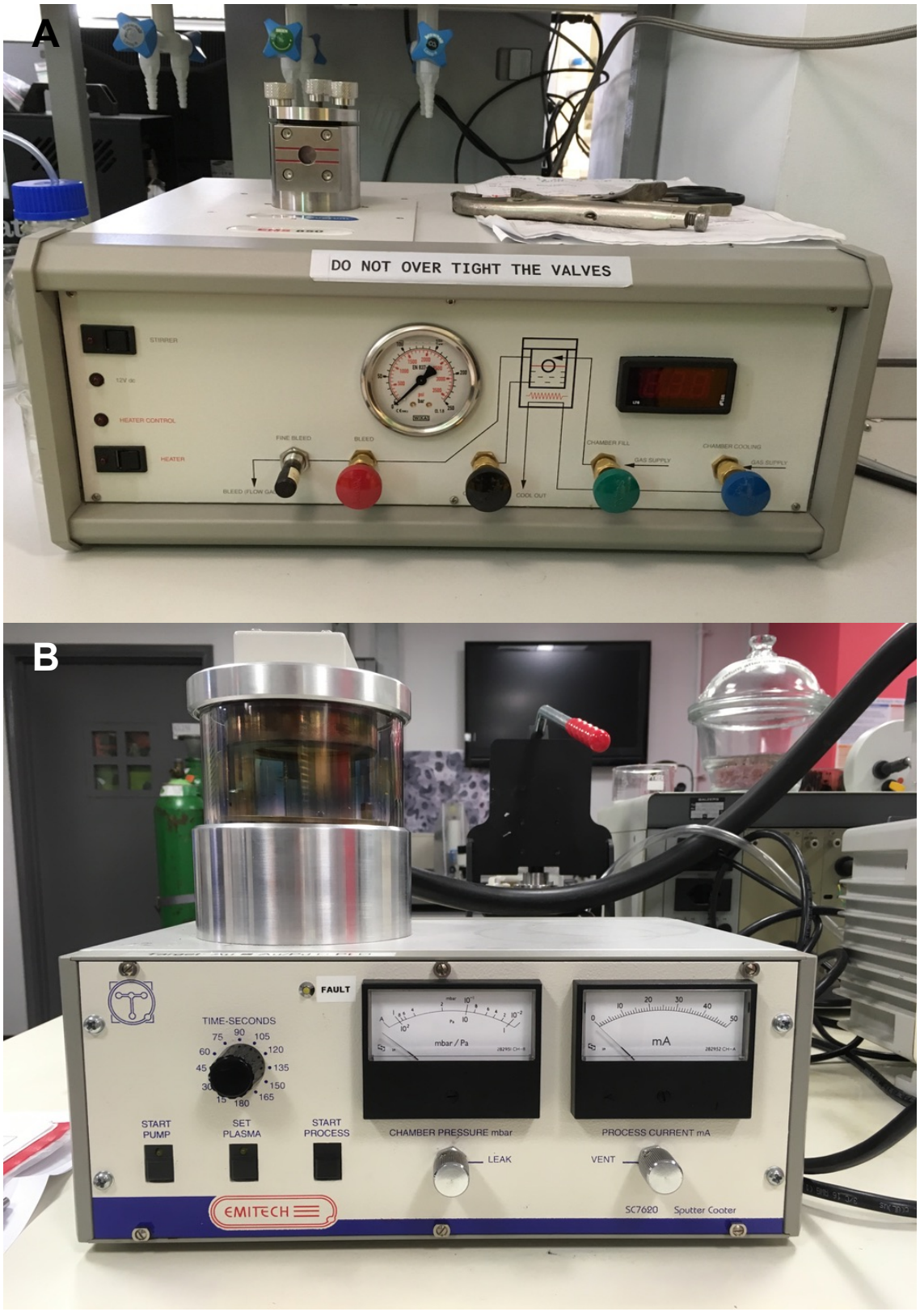

Equipment used for preparation of hydrogel and microcapsule samples for SEM.

A: Critical Point Dryer

B: EMITECH sputter coater

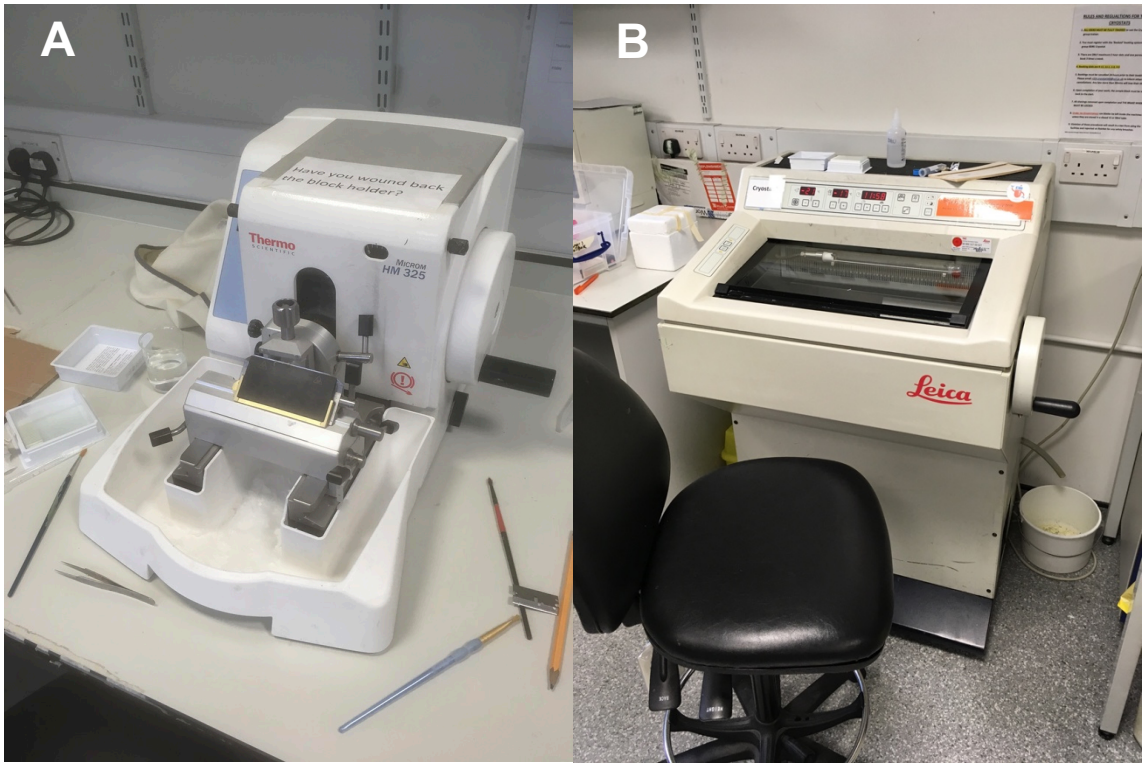

Equipment used for sectioning of hydrogel samples prior to histology.

A: ThermoScientific HM325 microtome

B: Leica cryostat

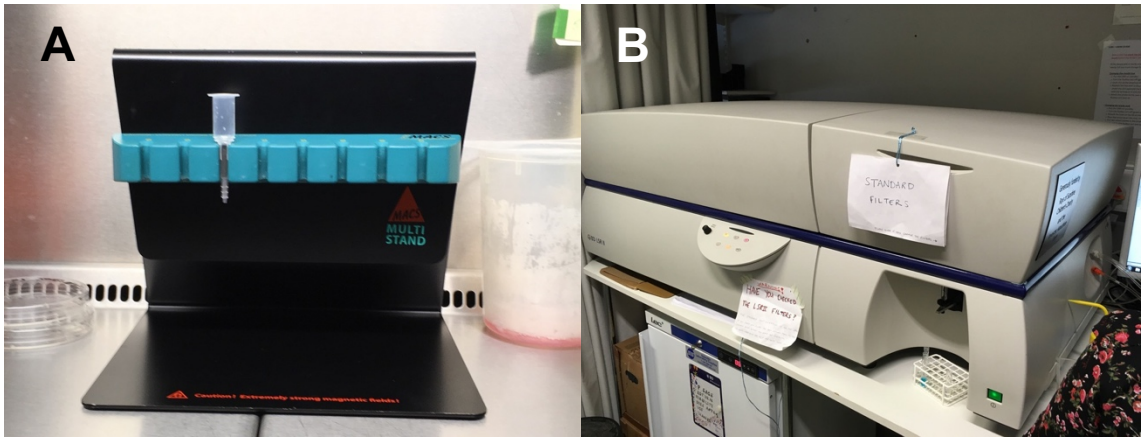

Equipment used for MACS and FACS analysis of AFSCs.

A: OCTOMACS separator

B: BD LSRII cytometer

References

AGOSTON, H., BAYBAYAN, L. & BEIER, F. 2006. Dexamethasone stimulates expression of C-type Natriuretic Peptide in chondrocytes. *BMC Musculoskelet Disord,* 7**,** 87.

AGOSTON, H., KHAN, S., JAMES, C. G., GILLESPIE, J. R., SERRA, R., STANTON, L. A. & BEIER, F. 2007. C-type natriuretic peptide regulates endochondral bone growth through p38 MAP kinase-dependent and -independent pathways. *BMC Dev Biol,* 7**,** 18.

AHEARNE, M. & KELLY, D. J. 2013. A comparison of fibrin, agarose and gellan gum hydrogels as carriers of stem cells and growth factor delivery microspheres for cartilage regeneration. *Biomed Mater,* 8**,** 035004.

ALOE, L., TUVERI, M. A., CARCASSI, U. & LEVI-MONTALCINI, R. 1992. Nerve growth factor in the synovial fluid of patients with chronic arthritis. *Arthritis Rheum,* 35**,** 351-355.

ALVAREZ, J., SOHN, P. & ZENG, X. TGFb2 mediates the effects of Hedgehog on hypertrophic differentiation and PTHrP expression. *Development,* 129**,** 1913–1924.

ARTHRITIS RESEARCH UK 2013. Osteoarthritis in general practice. *In:* UK, A. R. (ed.).

ARTHRITIS RESEARCH UK 2018. State of Musculoskeletal Health 2018. *In:* UK, A. R. (ed.).

AUGUSTYNIAK, E., TRZECIAK, T., RICHTER, M., KACZMARCZYK, J. & SUCHORSKA, W. 2015. The role of growth factors in stem cell-directed chondrogenesis: a real hope for damaged cartilage regeneration. *Int Orthop,* 39**,** 995-1003.

AWAD, H. A., WICKHAM, M. Q., LEDDY, H. A., GIMBLE, J. M. & GUILAK, F. 2004. Chondrogenic differentiation of adipose-derived adult stem cells in agarose, alginate, and gelatin scaffolds. *Biomaterials,* 25**,** 3211-22.

BAKSH, D., YAO, R. & TUAN, R. S. 2007. Comparison of Proliferative and Multilineage Differentiation Potential of Human Mesenchymal Stem Cells Derived from Umbilical Cord and Bone Marrow. *Stem Cells,* 25**,** 1384–1392.

BARRY, F., BOYNTON, R. E., LIU, B. & MURPHY, J. M. 2001. Chondrogenic differentiation of mesenchymal stem cells from bone marrow: differentiation-dependent gene expression of matrix components. *Exp Cell Res,* 268**,** 189-200.

BARTELS, C. F., BÜKÜLMEZ, H., PADAYATTI, P., RHEE, D. K., VAN RAVENSWAAIJ-ARTS, C. & PAULI, R. M. 2004. Mutations in the transmembrane natriuretic peptide receptor NPR-B impair skeletal growth and cause acromesomelic dysplasia, type Maroteaux. *Am J Hum Genet,* 75**,** 27-34.

BARTLETT, W., SKINNER, J. A., GOODING, C. R., CARRINGTON, R. W. J., FLANAGAN, A. M. & BRIGGS, T. W. R. 2005. Autologous chondrocyte implantation versus matrix-induced autologous chondrocyte implantation for osteochondral defects of the knee. *Journal of Bone and Joint Surgery,* 87B**,** 640–645.

BASAD, E., ISHAQUE, B., BACHMANN, G., STURZ, H. & STEINMEYER, J. 2010. Matrix-induced autologous chondrocyte implantation versus microfracture in the treatment of cartilage defects of the knee: a 2-year randomised study. *Knee surgery, sports traumatology, arthroscopy: official journal of the ESSKA,* 18**,** 519–527.

BEHREND, M., KLUGE, E., VON WASIELEWSKI, R. & KLEMPNAUER, J. 2002. The mechanical influence of tissue engineering techniques on tracheal strength: an experimental study on sheep trachea. *J Invest Surg,* 15**,** 227-36.

BERGHOLT, M. S., ST-PIERRE, J. P., OFFEDDU, G. S., PARMAR, P. A., ALBRO, M. B., PUETZER, J. L., OYEN, M. L. & STEVENS, M. M. 2016. Raman Spectroscopy Reveals New Insights into the Zonal Organization of Native and Tissue-Engineered Articular Cartilage. *ACS Cent Sci,* 2**,** 885-895.

BERNSTEIN, P., DONG, M., GRAUPNER, S., CORBEIL, D., GELINSKY, M., GUNTHER, K. P. & FICKERT, S. 2009. Sox9 expression of alginate-encapsulated chondrocytes is stimulated by low cell density. *J Biomed Mater Res A,* 91**,** 910-8.

BERTOLINI, D. R., NEDWIN, G. E., BRINGMAN, T. S., SMITH, D. D. & MUNDY, G. R. 1986. Stimulation of bone resorption and inhibition of bone formation in vitro by human tumour necrosis factors. *Nature,* 319**,** 516-518.

BERTOLO, A., ARCOLINO, F., CAPOSSELA, S., TADDEI, A. R., BAUR, M., POTZEL, T. & STOYANOV, J. 2015. Growth Factors Cross-Linked to Collagen Microcarriers Promote Expansion and Chondrogenic Differentiation of Human Mesenchymal Stem Cells. *Tissue Eng Part A,* 21**,** 2618-28.

BIAN, L., ZHAI, D. Y., TOUS, E., RAI, R., MAUCK, R. L. & BURDICK, J. A. 2011. Enhanced MSC chondrogenesis following delivery of TGF-beta3 from alginate microspheres within hyaluronic acid hydrogels in vitro and in vivo. *Biomaterials,* 32**,** 6425-34.

BLUNK, T., SIEMINSKI, A. L., GOOCH, K. J., COURTER, D. L., HOLLANDER, A. P., MENAHEM NAHIR, A., LANGER, R., VUNJAK-NOVAKOVIC, G. & FREED, L. E. 2002. Differential Effects of Growth Factors on Tissue-Engineered Cartilage. *Tissue Engineering,* 8.

BO, H., WU, J. P., KIRK, T. B., CARRINO, J. A., XIANG, C. & XU, J. 2014. High-resolution measurements of the multilayer ultra-structure of articular cartilage and their translational potential. *Arthritis Research & Therapy,* 16**,** 1-16.

BOCK, T., SCHILL, V., KRAHNKE, M., STEINERT, A. F., TESSMAR, J., BLUNK, T. & GROLL, J. 2018. TGF-beta1-Modified Hyaluronic Acid/Poly(glycidol) Hydrogels for Chondrogenic Differentiation of Human Mesenchymal Stromal Cells. *Macromol Biosci,* 18**,** e1700390.

BOISSELIER, E. & ASTRUC. D 2009. Gold nanoparticles in nanomedicine: preparations, imaging, diagnostics, therapies and toxicity. *Chemical Society Reviews,* 38**,** 1759-1782.

BORNES, T. D., JOMHA, N. M., MULET-SIERRA, A. & ADESIDA, A. B. 2016. Optimal Seeding Densities for In Vitro Chondrogenesis of Two- and Three-Dimensional-Isolated and -Expanded Bone Marrow-Derived Mesenchymal Stromal Stem Cells Within a Porous Collagen Scaffold. *Tissue Eng Part C Methods,* 22**,** 208-20.

BRAY, D. 2000. Critical Point Drying of Biological Specimens for Scanning Electron Microscopy. *Supercritical Fluid Methods and Protocols* 235-243.

BRITTBERG, M., LINDAHL, A., NILSSON, A., OHLSSON, C., ISAKSSON, O. & PETERSON, L. 1994. Treatment of deep cartilage defects in the knee with autologous chondrocyte transplantation. *New England Journal of Medicine,* 331**,** 889-895.

BRITTBERG, M., PETERSON, L., SJÖGREN-JANSSON, E., TALLHEDEN, T. & LINDAHL, A. 2003. Articular cartilage engineering with autologous chondrocyte transplantation: A review of recent developments. *J Bone Joint Surg Am,* 85-A**,** 109-115.

BUSCHMANN, M. D., GLUZBAND, Y. A., GRODZINSKY, A. J., KIMURA, J. H. & HUNZIKER, E. B. 1992. Chondrocytes in agarose culture synthesize a mechanically functional extracellular matrix. *J Orthop Res,* 10**,** 745–758.

BUXTON, A. N., BAHNEY, C. S., YOO, J. U. & JOHNSTONE, B. 2011. Temporal exposure to chondrogenic factors modulates human mesenchymal stem cell chondrogenesis in hydrogels. *Tissue Eng Part A,* 17**,** 371-80.

CANANZI, M., ATALA, A. & DE COPPI, P. 2009. Stem cells derived from amniotic fluid: new potentials in regenerative medicine. *Reprod Biomed Online,* 18**,** 17-27.

CANCEDDA, R., DOZIN, B., GIANNONI, P. & QUARTO, R. 2003. Tissue engineering and cell therapy of cartilage and bone. *Matrix Biology,* 22**,** 81-91.

CARRARO, G., PERIN, L., SEDRAKYAN, S., GIULIANI, S., TIOZZO, C., LEE, J., TURCATEL, G., DE LANGHE, S. P., DRISCOLL, B., BELLUSCI, S., MINOO, P., ATALA, A., DE

FILIPPO, R. E. & WARBURTON, D. 2008. Human amniotic fluid stem cells can integrate and differentiate into epithelial lung lineages. *Stem Cells,* 26**,** 2902-11.

CAVANAUGH, J. T. 2007. *Rehabilitation strategies following articular cartilage sugery in the knee*, Humana Press.

CHANGOOR, A., NELEA, M., METHOT, S., TRAN-KHANH, N., CHEVRIER, A., RESTREPO, A., SHIVE, M. S., HOEMANN, C. D. & BUSCHMANN, M. D. 2011. Structural characteristics of the collagen network in human normal, degraded and repair articular cartilages observed in polarized light and scanning electron microscopies. *Osteoarthritis Cartilage,* 19**,** 1458-68.

CHEN, P., ZHU, S. & WANG, Y. 2014. The amelioration of cartilage degeneration by ADAMTS-5 inhibitor delivered in a hyaluronic acid hydrogel. *Biomaterials,* 35**,** 2827-2836.

CHERIAN, J. J., PARVIZI, J., BRAMLET, D., LEE, K. H., ROMNESS, D. W. & MONT, M. A. 2015. Preliminary results of a phase II randomized study to determine the efficacy and safety of genetically engineered allogeneic human chondrocytes expressing TGF-beta1 in patients with grade 3 chronic degenerative joint disease of the knee. *Osteoarthritis Cartilage,* 23**,** 2109-2118.

CHEVALIER, X., GOUPILLE, P. & BEAULIEU, A. D. 2009. Intraarticular injection of anakinra in osteoarthritis of the knee: a multicenter, randomized, double blind, placebo-controlled study. *Arthritis Rheum,* 61**,** 344-352.

CHO, J. H., KIM, S. H., PARK, K. D., JUNG, M. C., YANG, W. I., HAN, S. W., NOH, J. Y. & LEE, J. W. 2004. Chondrogenic differentiation of human mesenchymal stem cells using a thermosensitive poly(N-isopropylacrylamide) and water-soluble chitosan copolymer. *Biomaterials,* 25**,** 5743-51.

CHUSHO, H., TAMURA, N., OGAWA, Y., YASODA, A., SUDA, M., MIYAZAWA, T., NAKAMURA, K., NAKAO, K., KURIHARA, T., KOMATSU, Y., ITOH, H., TANAKA, K., SAITO, Y., KATSUKI, M. & NAKAO, K. 2001. Dwarfism and early death in mice lacking C-type natriuretic peptide. *Proc Natl Acad Sci U S A,* 98**,** 4016-21.

CLARKE, E. P., CATES, G. A., BALL, E. H. & SANWAL, B. D. 1991. A collagen binding protein in the endoplasmic reticulum of myoblasts exhibits relationship with serine protease inhibitors. *J. Biol. Chem,* 266**,** 17230 – 17235.

COHEN, S. B., PROUDMAN, S. & KIVITZ, A. J. 2011. A randomized, double blind study of AMG 108 (a fully human monoclonal antibody to IL-1R1) in patients with osteoarthritis of the knee. *Arthritis Research & Therapy,* 13**,** R125.

CRAWFORD, D. C., DEBERARDINO, T. M. & WILLIAMS, R. J. R. 2012. NeoCart, an autologous cartilage tissue implant, compared with microfracture for treatment of distal femoral cartilage lesions: an FDA phase-II prospective, randomized clinical trial after two years. *The Journal of bone and joint surgery American volume,* 94**,** 979-989.

CRAWFORD, D. C., HEVERAN, C. M., CANNON, W. D. J., FOO, L. F. & POTTER, H. G. 2009. An autologous cartilage tissue implant NeoCart for treatment of grade III chondral injury to the distal femur: prospective clinical safety trial at 2 years. . *The American journal of sports medicine,* 37**,** 1334–1343.

DANIELS, K. & SOLURSH, M. 1991. Modulation of chondrogenesis by the cytoskeleton and extracellular matrix. *J Cell Sci,* 100**,** 249-254.

DASHTDAR, H., MURALI, M. R., SELVARATNAM, L., BALAJI RAGHAVENDRAN, H., SUHAEB, A. M., AHMAD, T. S. & KAMARUL, T. 2016. Ultra-structural changes and expression of chondrogenic and hypertrophic genes during chondrogenic differentiation of mesenchymal stromal cells in alginate beads. *PeerJ,* 4**,** e1650.

DAVATCHI, F., SADEGHI ABDOLLAHI, B., MOHYEDDIN, M. & NIKBIN, B. 2016. Mesenchymal stem cell therapy for knee osteoarthritis: 5 year follow up of three patients. *Int J Rheum Dis,* 19**,** 219-225.

DAYER, J. M., BEUTLER, B. & CERAMI, A. 1985. Cachectin/tumor necrosis factor stimulates collagenase and prostaglandin E2 production by human synovial cells and dermal fibroblasts. *J Exp Med,* 162**,** 21638.

DE COPPI, P., BARTSCH, G., JR., SIDDIQUI, M. M., XU, T., SANTOS, C. C., PERIN, L., MOSTOSLAVSKY, G., SERRE, A. C., SNYDER, E. Y., YOO, J. J., FURTH, M. E., SOKER, S. & ATALA, A. 2007. Isolation of amniotic stem cell lines with potential for therapy. *Nat Biotechnol,* 25**,** 100-6.

DE VRIES-VAN MELLE, M. L., TIHAYA, M. S., KOPS, N., KOEVOET, W., MURPHY, J. M., VERHAAR, J. A. N., ALINI, M., EGLIN, D. & VAN OSCH, G. 2014. Chondrogenic differentiation of human bone marrow-derived mesenchymal stem cells in a simulated osteochondral environment is hydrogel dependent. *European Cells and Materials,* 27**,** 112-123.

DECHER, G. 1997. Fuzzy nanoassemblies: toward layered polymeric multicomposites. *Science,* 277**,** 1232-1237.

DECHER, G., HONG, J. D. & SCHMITT, J. 1992. Buildup of ultrathin multilayer films by a self-assembly process: III. Consecutively alternating adsorption of anionic and cationic polyelectrolytes on charged surfaces. *Thin Solid Films,* 210–211**,** 831-835.

DENG, Y., LI, T.-Q., YAN, Y.-E., MAGDALOU, J., WANG, H. & CHEN, L.-B. 2012. Effect of nicotine on chondrogenic differentiation of rat bone marrow mesenchymal stem cells in alginate bead culture. *Bio-Medical Materials and Engineering,* 22**,** 81-87.

DEXHEIMER, V., FRANK, S. & RICHTER, W. 2012. Proliferation as a requirement for in vitro chondrogenesis of human mesenchymal stem cells. *Stem Cells Dev,* 21**,** 2160-9.

EBERT, J. R., ROBERTSON, W. B., WOODHOUSE, J., FALLON, M., ZHENG, M. H. & ACKLAND, T. 2011. Clinical and magnetic resonance imaging-based outcomes to 5 years after matrix-induced autologous chondrocyte implantation to address articular cartilage defects in the knee. *The American journal of sports medicine,* 39**,** 753–763.

EHRENHOFER, A., ELSTNER, M. & WALLMERSPERGER, T. 2018. Normalization of hydrogel swelling behavior for sensoric and actuatoric applications. *Sensors and Actuators B: Chemical,* 255**,** 1343-1353.

EMANS, P. J., VAN RHIJN, L. W., WELTING, T. J., CREMERS, A., WIJNANDS, N., SPAAPEN, F., VONCKEN, J. W. & SHASTRI, V. P. 2010. Autologous engineering of cartilage. *Proc Natl Acad Sci U S A,* 107**,** 3418-23.

ENOBAKHARE, B. O., BADER, D. L. & LEE, D. A. 1996. Quantification of sulfated glycosaminoglycans in chondrocyte/alginate cultures, by use of 1,9-dimethylmethylene blue. *Anal Biochem,* 243**,** 189-191.

ESHED, I., TRATTNIG, S., SHARON, M., ARBEL, R., NIERENBERG, G. & KONEN, E. 2012. Assessment of cartilage repair after chondrocyte transplantation with a fibrin-hyaluronan matrix-correlation of morphological MRI, biochemical T2 mapping and clinical outcome. *European Journal of Radiology,* 81**,** 1216-1223.

EVANS, C. H., GHIVIZZANI, S. C. & ROBBINS, P. D. 2018. Arthritis gene therapy is becoming a reality. *Nat Rev Rheumatol,* 14**,** 381-382.

EYRE, D. R. 2004. Collagens and cartilage matrix homeostasis. *Clin Orthop Relat Res. ,* 427**,** S118–S122.

FARNDALE, R. W., SAYERS, C. A. AND BARRETT, A. J. 1982. A direct spectrophotometric microassay for sulfated glycosaminoglycans in cartilage cultures. . *Connect Tissue Res,* 9**,** 247-248.

FERRARA, N. 2010. Binding to the extracellular matrix and proteolytic processing: two key mechanisms regulating vascular endothelial growth factor action. *Mol Biol Cell,* 21**,** 687-90.

FLORINE, E. M., MILLER, R. E., PORTER, R. M., EVANS, C. H., KURZ, B. & GRODZINSKY, A. J. 2013. Effects of dexamethasone on mesenchymal stromal cell chondrogenesis and aggrecanase activity: comparison of agarose and self assembling peptide scaffolds. *Cartilage,* 4**,** 63-74.

FOOD, U. & ADMINISTRATION , D. 2015. Tanezumb Arthritis Advisory committee Briefing document. *In:* FDA (ed.). Silver Spring.

FOX, A. J. S., BEDI, A. & RODEO, S. A. 2009. The Basic Science of Articular Cartilage: Structure, Composition, and Function. *Sports Health,* 1**,** 461-468.

FRANTZ, C., STEWART, K. M. & WEAVER, V. M. 2010. The extracellular matrix at a glance. *J Cell Sci,* 123**,** 4195-4200.

FRISBIE, D. D., CROSS, M. W. & MCILWRAITH, C. W. 2006. A comparative study of articular cartilage thickness in the stifle of animal species used in human pre-clinical studies compared to articular cartilage thickness in the human knee. *Vet Comp Orthop Traumatol,* 19**,** 142-146.

GELSE, K. 2003. Collagens—structure, function, and biosynthesis. *Advanced Drug Delivery Reviews,* 55**,** 1531-1546.

GILBERT, R. W. D., VICKARYOUS, M. K. & VILORIA-PETIT, A. M. 2016. Signalling by Transforming Growth Factor Beta Isoforms in Wound Healing and Tissue Regeneration. *J Dev Biol,* 4.

GLEGHORN, J. P., LEE, C. S., CABODI, M., STROOCK, A. D. & BONASSAR, L. J. 2008. Adhesive properties of laminated alginate gels for tissue engineering of layered structures. *J Biomed Mater Res A,* 85**,** 611-8.

GOLDRING, M. B. 2010. Articular cartilage and subchondral bone in the pathogenesis of osteoarthritis. *Ann NY Acad Sci.,* 1192**,** 230–237.

GOLDRING, M. B., DAYER, J.-M. & GOLDRING, S. R. 2016. Osteoarthritis and the Immune System. 257-269.

GOLDRING, S. R. & GOLDRING, M. B. 2016. Changes in the osteochondral unit during osteoarthritis: structure, function and cartilage-bone crosstalk. *Nat Rev Rheumatol,* 12**,** 632-644.

GREENBAUM, D., COLANGELO, C., WILLIAMS, K. & GERSTEIN, M. 2003. Comparing protein abundance and mRNA expression levels on a genomic scale. *Genome Biology,* 4**,** 1-8.

GUILAK, F. 2005. The slippery slope of arthritis. *Arthritis Rheum,* 52**,** 1632-3.

GUILAK, F., NIMS, R. J., DICKS, A., WU, C. L. & MEULENBELT, I. 2018. Osteoarthritis as a disease of the cartilage pericellular matrix. *Matrix Biol,* 71-72**,** 40-50.

GUO J, J. G., MACCALLUM D. 1989. Culture and growth characteristics of chondrocytes encapsulated in alginate beads. . *Conn Tiss Res,* 19**,** 277-297.

HAGIWARA, H., SAKAGUCHI, H., ITAKURA, M., YOSHIMOTO, T., FURUYA, M., TANAKA, S. & HIROSE, S. 1994. Autocrine Regulation of Rat Chondrocyte Proliferation by Natriuretic Peptide C and Its Receptor, Natriuretic Peptide Receptor-B. *The Journal of Biological Chemistry,* 269**,** 10729-10733.

HARDIN, J. A., COBELLI, N. & SANTAMBROGIO, L. 2015. Consequences of metabolic and oxidative modifications of cartilage tissue. *Nat Rev Rheumatol,* 11**,** 521-9.

HEGERT, C., KRAMER, J., HARGUS, G., MÜLLER, J., GUAN, K., WOBUS, A. M., MÜLLER, P. K. & ROHWEDEL, J. 2002. Differentiation plasticity of chondrocytes derived from mouse embryonic stem cells. *Journal of Cell Science,* 115**,** 4617-4628.

HENRIONNET, C., LIANG, G., ROEDER, E., DOSSOT, M., WANG, H., MAGDALOU, J., GILLET, P. & PINZANO, A. 2017. Hypoxia for MSC expansion and differentiation: the best way for enhancing TGFß-induced chondrogenesis and preventing calcifications in alginate beads. *Tissue Engineering*.

HERLOFSEN, S. R., KUCHLER, A. M., MELVIK, J. E. & BRINCHMANN, J. E. 2011. Chondrogenic differentiation of human bone marrow-derived mesenchymal stem cells in self-gelling alginate discs reveals novel chondrogenic signature gene clusters. *Tissue Eng Part A,* 17**,** 1003-13.

HERNANDEZ, M. L., MILLS, K., ALMOND, M., TODORIC, K., ALEMAN, M. M., ZHANG, H., ZHOU, H. & PEDEN, D. B. 2015. IL-1 receptor antagonist reduces endotoxin-induced airway inflammation in healthy volunteers. *J Allergy Clin Immunol,* 135**,** 379-85.

HERNANDEZ, R. M., ORIVE, G., MURUA, A. & PEDRAZ, J. L. 2010. Microcapsules and microcarriers for in situ cell delivery. *Adv Drug Deliv Rev,* 62**,** 711-30.

HEYWOOD, H. K., SEMBI, P. K., LEE, D. A. & BADER, D. L. 2004. Cellular Utilization Determines Viability and Matrix Distribution Profiles in Chondrocyte-Seeded Alginate Constructs. *Tissue Engineering,* 10**,** 1467-1479.

HOLLIDAY, L. S., DEAN, A. D., GREENWALD, J. E. & GLUCKS, S. L. 1995. C-type natriuretic peptide increases bone resorption in 1,25-dihydroxyvitamin D3-stimulated mouse bone marrow cultures. *J Biol Chem,* 270**,** 18983-18989.

HUANG, A. H., FARRELL, M. J., KIM, M. & MAUCK, R. L. 2010. Long-term dynamic loading improves the mechanical properties of chondrogenic mesenchymal stem cell-laden hydrogel. *Eur Cell Mater,* 19**,** 72–85.

HUANG, B. J., HU, J. C. & ATHANASIOU, K. A. 2016. Cell-based tissue engineering strategies used in the clinical repair of articular cartilage. *Biomaterials,* 98**,** 1-22.

HUANG, T., SCHOR, S. L. & HINCK, A. P. 2014. Biological activity differences between TGF-beta1 and TGF-beta3 correlate with differences in the rigidity and arrangement of their component monomers. *Biochemistry,* 53**,** 5737-49.

HUAQING, Z. & CHANGHONG, C. 2015. Body mass index and risk of knee osteoarthritis: systematic review and meta-analysis of prospective studies. *British Medical Journal,* 5.

HUBBARD, C., MCNAMARA, J. T., AZUMAYA, C., PATEL, M. S. & ZIMMER, J. 2012. The hyaluronan synthase catalyzes the synthesis and membrane translocation of hyaluronan. *J Mol Biol,* 418**,** 21-31.

HULEJOVA, H., BARESOVA, V. & KLEZL, Z. 2007. Increased level of cytokines and matrix metalloproteinases in osteoarthritic subchondral bone. *Cytokine,* 38**,** 1516.

HUNT, P. J., RICHARDS, A. M., ESPINER, E. A., NICHOLLS, M. G. & YANDLE, T. G. 1994. Bioactivity and metabolism of C-type natriuretic peptide in normal man. *J Clin Endocrinol Metab,* 78**,** 1428–1435.

HUNTER, W. 1743. Of the structure and diseases of articulating cartilage. *Phil. Trans. R. Soc. London,* 42**,** 514-521.

HUNZIKER, E. B., QUINN, T. M. & HÄUSELMANN, H. J. 2002. Quantitative structural organization of normal adult human articular cartilage. *Osteoarthritis Cartilage,* 10**,** 564-572.

IGNAT'EVA, N. Y., DANILOV, N. A., AVERKIEV, S. V., OBREZKOVA, M. V., LUNIN, V. V. & SOBOL', E. N. 2007. Determination of hydroxyproline in tissues and the evaluation of the collagen content of the tissues. *Journal of Analytical Chemistry,* 62**,** 51-57.

JAKOBSEN, R. B., OSTRUP, E., ZHANG, X., MIKKELSEN, T. S. & BRINCHMANN, J. E. 2014. Analysis of the effects of five factors relevant to in vitro chondrogenesis of human mesenchymal stem cells using factorial design and high throughput mRNA-profiling. *PLoS One,* 9**,** e96615.

JOHNSTONE, B., HERING, T. M., CAPLAN, A. I., GOLDBERG, V. M. & YOO, J. U. 1998. In Vitro Chondrogenesis of Bone Marrow-Derived Mesenchymal Progenitor Cells. *Experimental Cell Research,* 238**,** 265-272.

JUNGEBLUTH, P., MOLL, G., BAIGUERA, S. & MACCHIARINI, P. 2012. Tissue-engineered airway: a regenerative solution. *Clin Pharmacol Ther,* 91**,** 81-93.

KAFIENAH, W., JAKOB, M., DEMARTEAU, O., FRAZER, A., BARKER, M. D. & MARTIN, I. 2002. Three-dimensional tissue engineering of hyaline cartilage: comparison of adult nasal and articular chondrocytes. *Tissue Eng,* 8.

KAFIENAH, W., MISTRY, S., DICKINSON, S. C., SIMS, T. J., LEARMONTH, I. & HOLLANDER, A. P. 2007. Three-dimensional cartilage tissue engineering using adult stem cells from osteoarthritis patients. *Arthritis Rheum,* 56**,** 177-87.

KANZAKI, T., OLOFSSON, A., MORÉN, A., WERNSTEDT, C., HELLMAN, U., MIYAZONO, K., CLAESSON-WELSH, L. & HELDIN, C.-H. 1990. TGF-β1 binding protein A component of the large latent complex of TGF-β1 with multiple repeat sequences. *Cell,* 61**,** 1051-1061.

KAWAMATA, H., FUJIMORI, T. & IMAI, Y. 2004. TSC-22 (TGF-beta stimulated clone-22): a novel molecular target for differentiation-inducing therapy in salivary gland cancer. *Curr Cancer Drug Targets,* 4**,** 521-529.

KEARNS, K., DEE, A., FITZGERALD, A., DOHERTY, E. & PERRY, I. 2014. Chronic disease burden associated with overweight and obesity in Ireland: the effects of a small BMI reduction at population level. *BMC Public Health,* 14.

KENNY, A. J., BOURNE, A. & INGRAM, J. 1993. Hydrolysis of human and pig brain natriuretic peptides, urodilatin, C-type natriuretic peptide and some C-receptor ligands by endopeptidase. *Biochem J. Chem,* 291**,** 83-88.

KIM, E., GUILAK, F. & HAIDER, M. A. 2008. The dynamic mechanical environment of the chondrocyte: a biphasic finite element model of cell-matrix interactions under cyclic compressive loading. *J Biomech Eng,* 130**,** 061009.

KIM, Y. I., RYU, J. S., YEO, J. E., CHOI, Y. J., KIM, Y. S., KO, K. & KOH, Y. G. 2014. Overexpression of TGF-beta1 enhances chondrogenic differentiation and proliferation of human synovium-derived stem cells. *Biochem Biophys Res Commun,* 450**,** 1593-9.

KISIDAY, J. D., FRISBIE, D. D., MCILWRAITH, C. W. & GRODZINSKY, A. J. 2009. Dynamic compression stimulates proteoglycan synthesis by mesenchymal stem cells in the absence of chondrogenic cytokines. . *Tissue Eng Part A,* 15**,** 2817–2824.

KNUDSON, C. B. & KNUDSON, W. 2001. Cartilage proteoglycans. *Semin Cell Dev Biol,* 12**,** 69-78.

KNUDSON, W., CASEY, B., NISHIDA, Y., EGER, W., KUETTNER, K. E. & KNUDSON, C. B. 2000. Hyaluronan Oligosaccharides Perturb Cartilage Matrix Homeostasis and Induce Chondrocytic Chondrolysis. *Arthritis & Rheumatism,* 43**,** 1165-1174.

KO, J. Y., KIM, K. I., PARK, S. & IM, G. I. 2014. In vitro chondrogenesis and in vivo repair of osteochondral defect with human induced pluripotent stem cells. *Biomaterials,* 35**,** 3571-81.

KOCAMAZ, E., GOK, D., CETINKAYA, A. & TUFAN, A. C. 2012. Implication of C-type natriuretic peptide-3 signaling in glycosaminoglycan synthesis and chondrocyte hypertrophy during TGF-beta1 induced chondrogenic differentiation of chicken bone marrow-derived mesenchymal stem cells. *J Mol Histol,* 43**,** 497-508.

KOH, Y. G. & CHOI, Y. J. 2012. Infrapatellar fat pad derived mesenchymal stem cell therapy for knee osteoarthritis. *Knee,* 19**,** 902-907.

KOH, Y. G., JO, S. B. & KWON, O. R. 2013. Mesenchymal stem cell injections improve symptoms of knee osteoarthritis. *Arthroscopy,* 29**,** 748-755.

KOLAMBKAR, Y. M., PEISTER, A., SOKER, S., ATALA, A. & GULDBERG, R. E. 2007. Chondrogenic differentiation of amniotic fluid-derived stem cells. *J Mol Histol,* 38**,** 405-13.

KREJCI, P., MASRI, B., FONTAINE, V., MEKIKIAN, P. B., WEIS, M., PRATS, H. & WILCOX, W. R. 2005. Interaction of fibroblast growth factor and C-natriuretic peptide signaling in regulation of chondrocyte proliferation and extracellular matrix homeostasis. *Journal of Cell Science,* 118**,** 5089-5100.

KRZESKI, P., BUCKLAND-WRIGHT, C. & BALINT, G. 2007. Development of musculoskeletal toxicity without clear benefit after administration of PG-116800, a matrix

metalloproteinase inhibitor, to patients with knee osteoarthritis: a randomized, 12 month, double blind, placeboi controlled study. *Arthritis Research & Therapy,* 9**,** R109.

KURTZ, S., ONG, K., LAU, E., MOWAT, F. & HALPERN, M. 2007. Projections of primary and revision hip and knee arthroplasty in the United States from 2005 to 2030. *J Bone Joint Surg Am,* 89**,** 780-5.

KUYINU, E. L., NARAYANAN, G., NAIR, L. S. & LAURENCIN, C. T. 2016. Animal models of osteoarthritis: classification, update, and measurement of outcomes. *J Orthop Surg Res,* 11**,** 19.

LANE, N. E., SCHNITZER, T. J. & BIRBARA, C. A. 2010. Tanezumab for the treatment of pain from osteoarthritis of the knee. *New England Journal of Medicine,* 363**,** 1521-1531.

LANG, K., SCHMID, F. X. & FISCHER, G. 1987. Catalysis of protein folding by prolyl isomerase. *Nature,* 329**,** 268-270.

LANGER, R. & VACANTI, J. P. 1993. Tissue engineering. *Science,* 260**,** 920-926.

LEE, D. A. & BADER, D. L. 1997. Compressive strains at physiological frequencies influence the metabolism of chondrocytes seeded in agarose. *J Orthop Res,* 15**,** 181-188.

LEROUX, M. A., GUILAK, F. & SETTON, L. A. 1999. Compressive and shear properties of alginate gel: Effects of sodium ions and alginate concentration. *Journal of Biomedical Materials Research Part A,* 47**,** 46–53.

LIETMAN, S. A. 2016. Induced pluripotent stem cells in cartilage repair. *World J Orthop,* 7**,** 149-155.

LIU, Y., CHEN, F., LIU, W., CUI, L., SHANG, Q. & XIA, W. 2002. Repairing large porcine full-thickness defects of articular cartilage using autologous chondrocyte- engineered cartilage. *Tissue Eng,* 8**,** 709–721.

LOCA, D., SEVOSTJANOVS, E., MAKRECKA, M., ZHARKOVA-MALKOVA, O., BERZINA-CIMDINA, L., TUPUREINA, V. & SOKOLOVA, M. 2014. Microencapsulation of mildronate in biodegradable and non-biodegradable polymers. *J Microencapsul,* 31**,** 246-53.

LOESER, R. F. 2014. Integrins and chondrocyte-matrix interactions in articular cartilage. *Matrix Biol,* 39**,** 11-6.

LOESER, R. F., GOLDRING, S. R., SCANZELLO, C. R. & GOLDRING, M. B. 2012. Osteoarthritis: a disease of the joint as an organ. *Arthritis Rheum,* 64**,** 1697-1707.

LOHAN, A., MARZAHN, U., EL SAYED, K., HAISCH, A., MÜLLER, R. D. & KOHL, B. 2014. Osteo- chondral articular defect repair using auricle-derived autologous chondrocytes in a rabbit model. *Ann Anat,* 196**,** 317–326.

LOLLI, A., COLELLA, F., DE BARI, C. & VAN OSCH, G. 2018. Targeting anti-chondrogenic factors for the stimulation of chondrogenesis: A new paradigm in cartilage repair. *J Orthop Res*.

LORENZO, P., BAYLISS, M. T. & HEINEGARD, D. 2004. Altered patterns and synthesis of extracellular matrix macromolecules in early osteoarthitis. *Matrix Biol,* 23**,** 381-391.

LOTY, S., FOREST, N., BOULEKBACHE, H. & SAUTIER, J. M. 1995. Cytochalasin D induces changes incell shape and promotes in vitro chondrogenesis: A morphological study. *BiolCell,* 83**,** 149-161.

LUE, S., KOPPIKAR, S., SHAIKH, K., MAHENDIRA, D. & TOWHEED, T. E. 2017. Systematic review of non surgical therapies for osteoarthritis of the hand: an update. *Osteoarthritis and Cartilage,* 25**,** 1379-1389.

LUNDBERG, P. & KUCHEL, P. W. 1997. Diffusion of Solutes in Agarose and Alginate Gels: 'H and 23Na PFGSE and 23Na TQF NMR Studies. *Magnetic Resonance in Medicine,* 37**,** 44-52.

LUO, D., GOULD, D. J. & SUKHORUKOV, G. B. 2016. Local and Sustained Activity of Doxycycline Delivered with Layer-by-Layer Microcapsules. *Biomacromolecules,* 17**,** 1466-76.

LUO, Y., SINKEVICIUTE, D., HE, Y., KARSDAL, M., HENROTIN, Y., MOBASHERI, A., ONNERFJORD, P. & BAY-JENSEN, A. 2017. The minor collagens in articular cartilage. *Protein Cell,* 8**,** 560-572.

MA, H.-L., HUNG, S.-C., LIN, S.-Y., CHEN, Y.-L. & LO, W.-H. 2003. Chondrogenesis of human mesenchymal stem cells encapsulated in alginate beads. *Journal of Biomedical Materials Research Part A,* 64A**,** 273-281.

MADAAN, K., KUMAR, S., POONIA, N., LATHER, V. & PANDITA, D. 2014. Dendrimers in drug delivery and targeting: Drug-dendrimer interactions and toxicity issues. *J Pharm Bioallied Sci.,* 6**,** 139–150.

MADRY, H., VAN DIJK, C. N. & MUELLER-GERBL, M. 2010. The basic science of the subchondral bone. *Knee Surg Sports Traumatol Arthrosc,* 18**,** 419-33.

MAHBOUDI, H., SOLEIMANI, M., ENDERAMI, S. E., KEHTARI, M., HANAEE-AHVAZ, H., GHANBARIAN, H., BANDEHPOUR, M., NOJEHDEHI, S., MIRZAEI, S. & KAZEMI, B. 2018. The effect of nanofibre-based polyethersulfone (PES) scaffold on the chondrogenesis of human induced pluripotent stem cells. *Artif Cells Nanomed Biotechnol,* 46**,** 1948-1956.

MAKSYMOWYCH, W. P., RUSSELL, A. S., CHIU, P., YAN, A., JONES, N., CLARE, T. & LAMBERT, R. G. W. 2012. Targeting tumour necrosis factor alleviates signs and symptoms of inflammatory osteoarthritis of the knee. *Arthritis Research & Therapy,* 14**,** 1-7.

MAN, G. S. & MOLOGHIANU, G. 2014. Osteoarthritis pathogenesis – a complex process that involves the entire joint *Journal of Medicine and Life,* 7**,** 37-41.

MARIJNISSEN, W. J., VAN OSCH, G. J., AIGNER, J., VAN DER VEEN, S. W., HOLLANDER, A. P. & VERWOERD-VERHOEF, H. L. 2002. Alginate as a chondrocyte-delivery substance in combination with a non-woven scaffold for cartilage tissue engineering. *Biomaterials,* 23.

MATSUKAWA, N., GRZESIK, W. J., TAKAHASHI, N., PANDEY, K. N., PANG, S., YAMAUCHI, M. & SMITHIES, O. 1999. The natriuretic peptide clearance receptor locally modulates the physiological effects of the natriuretic peptide system. *Proc. Natl. Acad. Sci. U. S. A.,* 96**,** 7403-7408.

MAUCK, R. L., BYERS, B. A., YUAN, X. & TUAN, R. S. 2007. Regulation of cartilaginous ECM gene transcription by chondrocytes and MSCs in 3D culture in response to dynamic loading. . *Biomech Model Mechanobiol,* 6**,** 113-125.

MAUCK, R. L., YUAN, X. & TUAN, R. S. 2006. Chondrogenic differentiation and functional maturation of bovine mesenchymal stem cells in long-term agarose culture. *Osteoarthritis Cartilage,* 14**,** 179-89.

MAVROGENIS, A. F., NOMIKOS, G. N., SAKELLARIOU, V. I., KARALIOTAS, G. I., KONTOVAZENITIS, P. & PAPAGELOPOULOS, P. J. 2009. Wear debris pseudotumor following total knee arthroplasty: a case report. *J Med Case Rep,* 3**,** 9304.

MCARDLE, C. A., OLCESE, J., SCHMIDT, C., POCH, A., KRATZMEIER, M. & MIDDENDORFF, R. 1994. C-type natriuretic peptide, (CNP) in the pituitary: is CNP an autocrine regulator of gonadotropes? *Endocrinology,* 135**,** 2794-2801.

MCCALL, J. D., LUOMA, J. E. & ANSETH, K. S. 2012. Covalently tethered transforming growth factor beta in PEG hydrogels promotes chondrogenic differentiation of encapsulated human mesenchymal stem cells. *Drug Deliv Transl Res,* 2**,** 305-12.

MEDICINE, U. N. L. O. 2015a. *Comparison of Autologous Chondrocyte Implantation Versus Mosaicoplasty: a Randomized Trial (Cartipatch).* [Online]. Available: https://clinicaltrials.gov/ct2/show/NCT00560664 [Accessed].

MEDICINE, U. N. L. O. 2015b. *Comparison of Microfracture Treatment and CARTIPATCH® Chondrocyte Graft Treatment in Femoral Condyle Lesions.* [Online]. Available: https://clinicaltrials.gov/ct2/show/NCT00945399 [Accessed].

MEDICINE, U. N. L. O. 2015c. Confirmatory Study of NeoCart in Knee Cartilage Repair.

MOOREFIELD, E. C., MCKEE, E. E., SOLCHAGA, L., ORLANDO, G., YOO, J. J., WALKER, S., FURTH, M. E. & BISHOP, C. E. 2011. Cloned, CD117 selected human amniotic fluid stem cells are capable of modulating the immune response. *PLoS One,* 6**,** e26535.

MOUW, J. K., CONNELLY, J. T., WILSON, C. G., MICHAEL, K. E. & LEVENSTON, M. E. 2007. Dynamic compression regulates the expression and synthesis of chondrocyte-specific matrix molecules in bone marrow stromal cells. *Stem Cells,* 25**,** 655–663.

MOW, V. C. & GUO, X. E. 2002. Mechano-electrochemical properties of articular cartilage: their inhomogeneities and anisotropies. *Annu Rev Biomed Eng,* 4**,** 175-209.

MOW, V. C., RATCLIFFE, A. & ROBIN POOLE, A. 1992. Cartilage and diarthrodial joints as paradigms for hierarchical materials and structures *Biomaterials,* 13**,** 67-97.

MOW, V. C., WANG, C. & HUNG, C. T. 1999. The extracellular matrix, interstitial fluid and ions as a mechanical signal transducer in articular cartilage. *Osteoarthritis and Cartilage,* 7**,** 41-58.

MU, Y., GUDEY, S. K. & LANDSTROM, M. 2012. Non-Smad signaling pathways. *Cell Tissue Res,* 347**,** 11-20.

MUELLER, M. B., FISCHER, M., ZELLNER, J., BERNER, A., DIENSTKNECHT, T., PRANTL, L., KUJAT, R., NERLICH, M., TUAN, R. S. & ANGELE, P. 2010. Hypertrophy in mesenchymal stem cell chondrogenesis: effect of TGF-beta isoforms and chondrogenic conditioning. *Cells Tissues Organs,* 192**,** 158-66.

MUELLER, M. B. & TUAN, R. S. 2008. Functional characterization of hypertrophy in chondrogenesis of human mesenchymal stem cells. *Arthritis Rheum,* 58**,** 1377-88.

MUIR, H. 1995. The chondrocyte, architect of cartilage. Biomechanics, structure, function and molecular biology of cartilage matrix macromolecules. *Bioessays,* 17**,** 1039-1048.

NATIONAL JOINT REGISTRY 2017. 14th Annual Report. Part two including data on clinical activity.

NEHRER, S., CHIARI, C., DOMAYER, S., BARKAY, H. & YAYON, A. 2008. Results of chondrocyte implantation with a fibrin-hyaluronan matrix: a preliminary study. *Clinical orthopaedics and related research,* 466**,** 1849–1855.

NIETHAMMER, T. R., PIETSCHMANN, M. F., HORNG, A., ROSSBACH, B. P., FICKLSCHERER, A. & JANSSON, V. 2014. Graft hypertrophy of matrix-based autologous chondrocyte implantation: a two-year follow-up study of NOVOCART 3D implantation in the knee. *ESSKA,* 22**,** 1329–1336.

OHTA, S., SHIMEKAKE, Y. & NAGATA, K. 1996. Molecular cloning and characterization of a transcription factor for the C-type natriuretic peptide gene promoter. *European Journal of Biochemistry,* 242**,** 460-466.

OLDEROY, M. O., LILLEDAHL, M. B., BECKWITH, M. S., MELVIK, J. E., REINHOLT, F., SIKORSKI, P. & BRINCHMANN, J. E. 2014. Biochemical and structural characterization of neocartilage formed by mesenchymal stem cells in alginate hydrogels. *PLoS One,* 9**,** e91662.

OLNEY, R. C. 2006. C-type natriuretic peptide in growth: a new paradigm. *Growth Horm IGF Res,* 16 Suppl A**,** S6-14.

OROZCO, L., MUNAR, A. & SOLER, R. 2013. Treatment of knee osteoarthritis with autologous mesenchymal stem cells: a pilot study. *Transplantation,* 95**,** 1535-1541.

PALMER, G. D., CHAO, P. H., RAIA, F., MAUCK, R. L., VALHMU, W. B. & HUNG, C. T. 2001. Time-dependent aggrecan gene expression of articular chondrocytes in response to hyperosmotic loading. *Osteoarthritis Cartilage,* 9**,** 761-70.

PALMERSTON MENDES, L., PAN, J. & TORCHILIN, V. P. 2017. Dendrimers as Nanocarriers for Nucleic Acid and Drug Delivery in Cancer Therapy. *Molecules,* 22.

PANADERO, J. A., LANCEROS-MENDEZ, S. & RIBELLES, J. L. 2016. Differentiation of mesenchymal stem cells for cartilage tissue engineering: Individual and synergetic effects of three-dimensional environment and mechanical loading. *Acta Biomater,* 33**,** 1-12.

PAS, H. I. M. F. L., WINTERS, M., HAISMA, H. J., KOENIS, M. J. J., TOL, J. L. & MOEN, M. H. 2017. Stem cell injections in knee osteoarthritis: a systematic review of the literature. *British Journal of Sports Medicine,* 51**,** 1125-1133.

PEAKE, N., SU, N., RAMACHANDRAN, M., ACHAN, P., SALTER, D. M. & BADER, D. L. 2013. Natriuretic peptide receptors regulate cytoprotective effects in a human ex vivo 3D/bioreactor model. *Arthritis Res Ther,* 15**,** R76.

PEAKE, N. J., PAVLOV, A. M., D'SOUZA, A., PINGGUAN-MURPHY, B., SUKHORUKOV, G. B., HOBBS, A. J. & CHOWDHURY, T. T. 2015. Controlled release of C-type natriuretic peptide by microencapsulation dampens proinflammatory effects induced by IL-1beta in cartilage explants. *Biomacromolecules,* 16**,** 524-31.

PEARLE, A. D., WARREN, R. F. & RODEO, S. A. 2005. Basic science of articular cartilage and osteoarthritis. . *Clin Sports Med,* 24**,** 1-12.

PELTON, R. W., SAXENA, B. & JONES, M. 1991. Immunohistochemical localization of TGF beta 1, TGF beta 2, and TGF beta 3 in the mouse embryo: expression patterns suggest multiple roles during embryonic development. *J Cell Biol,* 115**,** 1091–1105.

PELTTARI, K., STECK, E. & RICHTER, W. 2008. The use of mesenchymal stem cells for chondrogenesis. *Injury,* 39 Suppl 1**,** S58-65.

PELTTARI, K., WINTER, A., STECK, E., GOETZKE, K., HENNIG, T., OCHS, B. G., AIGNER, T. & RICHTER, W. 2006. Premature induction of hypertrophy during in vitro chondrogenesis of human mesenchymal stem cells correlates with calcification and vascular invasion after ectopic transplantation in SCID mice. *Arthritis Rheum,* 54**,** 3254-66.

PETERS, A. E., AKHTAR, R., COMERFORD, E. J. & BATES, K. T. 2018. The effect of ageing and osteoarthritis on the mechanical properties of cartilage and bone in the human knee joint. *Sci Rep,* 8**,** 5931.

PIETSCHMANN, M. F., NIETHAMMER, T. R., HORNG, A., GULECYUZ, M. F., FEIST-PAGENSTERT, I. & JANSSON, V. 2012. The incidence and clinical relevance of graft hypertrophy after matrix-based autologous chondrocyte implantation. *The American journal of sports medicine,* 40**,** 68-74.

PILZ, R. B. & CASTEEL, D. E. 2003. Regulation of gene expression by cyclic GMP. *Circ Res,* 93**,** 1034-46.

POOLE, C. A. 1997. Articular cartilage chondrons: form, function and failure. *J Anat,* 191**,** 1-13.

POTTER, L. R. 1998. Phosphorylation Dependent Regulation of the Guanylyl Cyclase Linked Natriuretic Peptide Receptor B: Dephosphorylation Is a Mechanism of Desensitization. *Biochemistry,* 37**,** 2422-2429.

PREITSCHOPF, A., SCHORGHOFER, D., KINSLECHNER, K., SCHUTZ, B., ZWICKL, H., ROSNER, M., JOO, J. G., NEHRER, S., HENGSTSCHLAGER, M. & MIKULA, M. 2016. Rapamycin-Induced Hypoxia Inducible Factor 2A Is Essential for Chondrogenic Differentiation of Amniotic Fluid Stem Cells. *Stem Cells Transl Med,* 5**,** 580-90.

PRITZKER, K. P., GAY, S., JIMENEZ, S. A., OSTERGAARD, K., PELLETIER, J. P., REVELL, P. A., SALTER, D. & VAN DEN BERG, W. B. 2006. Osteoarthritis cartilage histopathology: grading and staging. *Osteoarthritis Cartilage,* 14**,** 13-29.

PRUSA, A. R., MARTON, E., ROSNER, M., BERNASCHEK, G. & HENGSTSCHLAGER, M. 2003. Oct-4-Expressing Cells in Human Amniotic Fluid : a new source for stem cell research? *Human Reproduction,* 18**,** 1489-1493.

QU, D., ZHU, J. P., CHILDS, H. R. & LU, H. H. 2019. Nanofiber-based transforming growth factor-beta3 release induces fibrochondrogenic differentiation of stem cells. *Acta Biomater*.

RAGAN, P. M., BADGER, A. M., COOK, M., CHIN, V. I., GOWEN, M., GRODZINSKY, A. J. & LARK, M. W. 1999. Down-regulation of chondrocyte aggrecan and type-II collagen gene expression correlates with increases in static compression magnitude and duration. *J Orthop Res,* 17**,** 836-842.

RAMACHANDRAN, M., ACHAN, P., SALTER, D. M., BADER, D. L. & CHOWDHURY, T. T. 2011. Biomechanical signals and the C-type natriuretic peptide counteract catabolic activities induced by IL-1b in chondrocyte/agarose constructs. *Arthritis Research & Therapy,* 13**,** 1-12.

RATCLIFFE, A. & MOW, V. C. 1996. Extracellular Matrix. *In:* COMPER, W. D. (ed.) *Extracellular Matrix: Tissue Function.* Harwood Academic publishers.

RAU, R. 2002. Adalimumab (a fully human anti-tumour necrosis factor alpha monoclonal antibody) in the treatment of active rheumatoid arthritis: the initial results of five trials. *Ann Rheum Dis,* 61.

RESCA, E., ZAVATTI, M., MARALDI, T., BERTONI, L., BERETTI, F., GUIDA, M., LA SALA, G. B., GUILLOT, P. V., DAVID, A. L., SEBIRE, N. J., DE POL, A. & DE COPPI, P. 2015. Enrichment in c-Kit improved differentiation potential of amniotic membrane progenitor/stem cells. *Placenta,* 36**,** 18-26.

REXWINKLE, J. T., HUNT, H. K. & PFEIFFER, F. M. 2017. Characterization of the surface and interfacial properties of the lamina splendens. *Frontiers of Mechanical Engineering,* 12**,** 234-252.

RIDKER, P. M., EVERETT, B. M., THUREN, T., MACFADYEN, J. G., CHANG, W. H., BALLANTYNE, C., FONSECA, F., NICOLAU, J., KOENIG, W., ANKER, S. D., KASTELEIN, J. J. P., CORNEL, J. H., PAIS, P., PELLA, D., GENEST, J., CIFKOVA, R., LORENZATTI, A., FORSTER, T., KOBALAVA, Z., VIDA-SIMITI, L., FLATHER, M., SHIMOKAWA, H., OGAWA, H., DELLBORG, M., ROSSI, P. R. F., TROQUAY, R. P. T., LIBBY, P., GLYNN, R. J. & GROUP, C. T. 2017. Antiinflammatory Therapy with Canakinumab for Atherosclerotic Disease. *N Engl J Med,* 377**,** 1119-1131.

RODRIGUES, M. T., LEE, S. J., GOMES, M. E., REIS, R. L., ATALA, A. & YOO, J. J. 2012. Bilayered constructs aimed at osteochondral strategies: the influence of medium supplements in the osteogenic and chondrogenic differentiation of amniotic fluid-derived stem cells. *Acta Biomater,* 8**,** 2795-806.

ROUGHLEY, P. J. & MORT, J. S. 2014. The role of aggrecan in normal and osteoarthritic cartilage. *Journal of Experimental Orthopaedics,* 1**,** 1-11.

RUEDEL, A., HOFMEISTER, S. & BOSSERHOFF, A. 2013. Development of a model system to analyze chondrogenic differentiation of mesenchymal stem cells. *Int J Clin Exp Pathol,* 6**,** 3042-3048.

RYAN MC, S. L. 1990. Differential expression of a cysteine-rich domain in the amino-terminal propeptide of type II (cartilage) procollagen by alternative splicing of mRNA. *J Biol Chem,* 265**,** 10334–10339.

SAHA, N., MOLDOVAN, F., TARDIF, G., PELLETIER, J., CLOUTIER, J. & MARTEL-PELLETIER, J. 1999. Interleukin-1b–converting enzyme/caspase-1 in human osteoarthritic tissues. *Arthritis & Rheumatism,* 42**,** 1577-1587.

SAKLATVALA, J. 1986. Tumour necrosis factor alpha stimulates resorption and inhibits synthesis of proteoglycan in cartilage. *Nature,* 322**,** 5479.

SANFORD, L. P., ORMSBY, I. & GITTENBERGER-DE GROOT, A. C. 1997. TGFb2 knockout mice have multiple developmental defects that are nonoverlapping with other TGFb. *Development,* 124**,** 2659–2670.

SARIS, D., PRICE, A., WIDUCHOWSKI, W., BERTRAND-MARCHAND, M., CARON, J. & DROGSET, J. O. 2014. Matrix-Applied Characterized Autologous Cultured Chondrocytes

Versus Microfracture: Two-Year Follow-up of a Prospective Randomized Trial. *The American journal of sports medicine,* 42**,** 1384–1394.

SCHENK, R. K., EGGLI, P. S. & HUNZIKER, E. B. 1986. Articular cartilage morphology. *In:* KUETTNER, K. E., SCHLEYERBACH, R. & HASCALL, V. C. (eds.) *Articular Cartilage Biochemistry.* New York: Raven Press.

SCHINDELIN, J. A.-C., I. & FRISE, E. ET AL. 2012. Fiji: an open-source platform for biological-image analysis. *Nature methods,* 9**,** 676-682.

SCHOLNICK, P., LANG, D. & RACKER, E. 1973. Regulatory mechanisms in carbohydrate metabolism. *J. Biol. Chem,* 248**,** 5175-5182.

SCHWARCZ, H. P., ABUEIDDA, D. & JASIUK, I. 2017. The Ultrastructure of Bone and Its Relevance to Mechanical Properties. *Frontiers in Physics,* 5.

SEGUIN, C. A. & BERNIER, S. M. 2003. TNFalpha suppresses link protein and type II collagen expression in chondrocytes: role of MEK1/2 and NF-kappaB signaling pathways. *J Cell Physiol,* 197**,** 35669.

SEKIYA, I., LARSON, B. L., VUORISTO, J. T., REGER, R. L. & PROCKOP, D. J. 2005. Comparison of effect of BMP-2, -4, and -6 on in vitro cartilage formation of human adult stem cells from bone marrow stroma. *Cell Tissue Res,* 320**,** 269-76.

SEKIYA, I., VUORISTO, J. T., LARSON, B. L. & PROCKOP, D. J. 2002. In vitro cartilage formation by human adult stem cells from bone marrow stroma defines the sequence of cellular and molecular events during chondrogenesis. *Proc Natl Acad Sci U S A,* 99**,** 4397-402.

SELMI, T. A., VERDONK, P., CHAMBAT, P., DUBRANA, F., POTEL, J. F. & BARNOUIN, L. 2008. Autologous chondrocyte implantation in a novel alginate-agarose hydrogel: outcome at two years. *The Journal of bone and joint surgery,* 90**,** 597–604.

SERCOMBE, L., VEERATI, T., MOHEIMANI, F., WU, S. Y., SOOD, A. K. & HUA, S. 2015. Advances and Challenges of Liposome Assisted Drug Delivery. *Front Pharmacol,* 6**,** 286.

SHACHAR, M., TSUR-GANG, O., DVIR, T., LEOR, J. & COHEN, S. 2011. The effect of immobilized RGD peptide in alginate scaffolds on cardiac tissue engineering. *Acta Biomater,* 7**,** 152-62.

SHALINI, U. & DEBNATH, T. 2015. Development of 3D Alginate encapsulation for better chondrogenic differentiation potential than the 2D pellet system. *Journal of Stem Cell Research & Therapy,* 05.

SHANG, X., WANG, Z. & TAO, H. 2017. Mechanism and therapeutic effectiveness of nerve growth factor in osteoarthritis pain. *Therapeutic Clinical Risk Management,* 13**,** 951-956.

SHCHUKIN, D. G. & SUKHORUKOV, G. B. 2003. Selective YF3 nanoparticle formation in polyelectrolyte capsules as microcontainers for yttrium recovery from aqueous solutions. *Langmuir* 19**,** 4427-4431.

SHEN, H., LIN, H., SUN, A. X., SONG, S., ZHANG, Z., DAI, J. & TUAN, R. S. 2018. Chondroinductive factor-free chondrogenic differentiation of human mesenchymal stem cells in graphene oxide-incorporated hydrogels. *Journal of Materials Chemistry B,* 6**,** 908-917.

SHI, Q., QIAN, Z., LIU, D., SUN, J., XU, J. & GUO, X. 2017. Maintaining the Phenotype Stability of Chondrocytes Derived from MSCs by C-Type Natriuretic Peptide. *Front Physiol,* 8**,** 143.

SHINTANI, N. & HUNZIKER, E. B. 2011. Differential Effects of Dexamethasone on the Chondrogenesis of Mesenchymal Stromal Cells: Influence of Microenvironemnt, Tissue Origin and Growth Factor. *European Cells and Materials,* 22**,** 302-320.

SHIRASAWA, S., SEKIYA, I., SAKAGUCHI, Y., YAGISHITA, K., ICHINOSE, S. & MUNETA, T. 2006. In vitro chondrogenesis of human synovium-derived mesenchymal stem cells: optimal condition and comparison with bone marrow-derived cells. *J Cell Biochem,* 97**,** 84-97.

SHOICHET, M. S., LI, R. H., WHITE, M. L. & WINN, S. R. 1995. Stability of Hydrogels Used in Cell Encapsulation: An In Vitro Comparison of Alginate and Agarose. *Biotechnol Bioeng.,* 50**,** 374-81.

SHULL, M. M., ORMSBY, I. & KIER, A. B. 1992. Targeted disruption of the mouse transforming growth factor-beta 1 gene results in multifocal inflammatory disease. *Nature,* 359**,** 693–699.

SINGH, P., MARCU, K. B., GOLDRING, M. B. & OTERO, M. 2019. Phenotypic instability of chondrocytes in osteoarthritis: on a path to hypertrophy. *Ann N Y Acad Sci,* 1442**,** 17-34.

SMITH, M. D., TRIANTAFILLOU, S., PARKER, A., YOUSSEF, P. P. & COLEMAN, M. 1997. Synovial membrane inflammation and cytokine production in patients with early osteoarthritis. . *J Rheumatol,* 24**,** 36571.

SONG, J. J., ASWAD, R., KANAAN, R. A., RICO, M. C., OWEN, T. A., BARBE, M. F., SAFADI, F. F. & POPOFF, S. N. 2007. Connective tissue growth factor (CTGF) acts as a

downstream mediator of TGF-beta1 to induce mesenchymal cell condensation. *J Cell Physiol,* 210**,** 398-410.

SUDA, M., TANAKA, K., FUKUSHIMA, M., NATSUI, K., YASODA, A., KOMATSU, Y., OGAWA, Y., ITOH, H. & NAKAO, K. 1996. C-Type Natriuretic Peptide as an Autocrine/Paracrine Regulator

of Osteoblast. *Biochemical and Biophysical Research Communications,* 223**,** 1-6.

SUKHORUKOV, G. B., DONATH, E., DAVIS, S., LICHTENFELD, H., CARUSO, F., POPOV, V. I. & MÖHWALD, H. 1998. Stepwise polyelectrolyte assembly on particle surfaces: a novel approach to colloid design. . *Polymers for Advanced Technologies,* 9**,** 759-767.

TAHLAWI, A., KLONTZAS, M. E., ALLENBY, M. C., MORAIS, J. C. F., PANOSKALTSIS, N. & MANTALARIS, A. 2019. RGD-functionalized polyurethane scaffolds promote umbilical cord blood mesenchymal stem cell expansion and osteogenic differentiation. *J Tissue Eng Regen Med,* 13**,** 232-243.

TANGTRONGSUP, S. & KISIDAY, J. D. 2016. Effects of dexamethasone concentration and timing of exposure on chondrogenesis of equine bone marrow derived mesenchymal stem cells. *Cartilage,* 7**,** 92-103.

TARE, R. S., HOWARD, D., POUND, J. C., ROACH, H. I. & OREFFO, R. O. 2005. Tissue engineering strategies for cartilage generation--micromass and three dimensional cultures using human chondrocytes and a continuous cell line. *Biochem Biophys Res Commun,* 333**,** 609-21.

TAYLOR, K. B. & JEFFREE, G. M. 1969. A new basic metachromatic dye 1,9-dimethylmethylene blue. *Histological chemistry journal,* 1**,** 199-204.

TEIXEIRA, C. C., AGOSTON, H. & BEIER, F. 2008. Nitric oxide, C-type natriuretic peptide and cGMP as regulators of endochondral ossification. *Dev Biol,* 319**,** 171-8.

TEZCAN, B., SERTER, S., KITER, E. & TUFAN, A. C. 2010. Dose dependent effect of C-type natriuretic peptide signaling in glycosaminoglycan synthesis during TGF-beta1 induced chondrogenic differentiation of mesenchymal stem cells. *J Mol Histol,* 41**,** 247-58.

THOMPSON, C. 2013. *Interactions between primary cilia length and hedgehog signalling in response to mechanical and thermal stress* PhD, Queen Mary University of London.

THORPE, S. D., BUCKLEY, C. T., STEWARD, A. J. & KELLY, D. J. 2012. European Society of Biomechanics S.M. Perren Award 2012: the external mechanical environment can

override the influence of local substrate in determining stem cell fate. *J Biomech,* 45**,** 2483-92.

THORPE, S. D., NAGEL, T., CARROLL, S. F. & KELLY, D. J. 2013. Modulating gradients in regulatory signals within mesenchymal stem cell seeded hydrogels: a novel strategy to engineer zonal articular cartilage. *PLoS One,* 8**,** e60764.

TILLMANN, E. N. 2005. Untere Extremität. *Atlas der Anatomie des Menschen.* Berlin, Heidelberg: Springer Berlin Heidelberg.

TILWANI, R. K. 2016. *Low oxygen tension modulates the effects of TNFα and fibronectin fragments in compressed chondrocytes.* PhD, Queen Mary University of London.

TILWANI, R. K., VESSILLIER, S., PINGGUAN-MURPHY, B., LEE, D. A., BADER, D. L. & CHOWDHURY, T. T. 2017. Oxygen tension modulates the effects of TNFalpha in compressed chondrocytes. *Inflamm Res,* 66**,** 49-58.

TONNESEN, H. H. & KARLSEN, J. 2002. Alginate in drug delivery systems. *Drug Dev Ind Pharm,* 28**,** 621-30.

TULI, R., TULI, S., NANDI, S. & AL., E. 2003. Transforming growth factor-beta-mediated chondrogenesis of human mesenchymal progenitor cells involves N-cadherin and mitogen-activated protein kinase and Wnt signaling cross-talk. . *J Biol Chem,* 278**,** 41227–41236.

VINARDELL, T., BUCKLEY, C. T., THORPE, S. D. & KELLY, D. J. 2011. Composition-function relations of cartilaginous tissues engineered from chondrocytes and mesenchymal stem cells isolated from bone marrow and infrapatellar fat pad. *J Tissue Eng Regen Med,* 5**,** 673-83.

VINATIER, C., GAUTHIER, O., FATIMI, A., MERCERON, C., MASSON, M., MOREAU, A., MOREAU, F., FELLAH, B., WEISS, P. & GUICHEUX, J. 2009. An injectable cellulose-based hydrogel for the transfer of autologous nasal chondrocytes in articular cartilage defects. *Biotechnol Bioeng,* 102**,** 1259-67.

VOLODKIN, D. V., LARIONOVA, N. I. & SUKHORUKOV, G. B. 2004. Protein encapsulation via porous CaCO3 microparticles templating. *Biomacromolecules,* 5**,** 1962-1972.

WAGNER, W., HORN, P., CASTOLDI, M., DIEHLMANN, A., BORK, S., SAFFRICH, R., BENES, V., BLAKE, J., PFISTER, S., ECKSTEIN, V. & HO, A. D. 2008. Replicative senescence of mesenchymal stem cells: a continuous and organized process. *PLoS One,* 3**,** e2213.

WALDMAN, S. D., USMANI, Y., TSE, M. Y. & PANG, S. C. 2007. Differential Effects of Natriuretic Peptide Stimulation on Tissue-Engineered Cartilage. *Tissue Engineering*, 110306233438005.

WANG, G., EVANS, C. H., BENSON, J. M., HUTT, J. A., SEAGRAVE, J., WILDER, J. A., GRIEGER, J. C., SAMULSKI, R. J. & TERSE, P. S. 2016. Safety and biodistribution assessment of sc-rAAV2.5IL-1Ra administered via intra-articular injection in a mono-iodoacetate-induced osteoarthritis rat model. *Mol Ther Methods Clin Dev,* 3, 15052.

WANG, M., SAMPSON, E. R. & JIN, H. 2013. MMP13 is a critical target gene during the progression of osteoarthritis. *Arthritis Research & Therapy,* 15, R5.

WANG, Q. G., EL HAJ, A. J. & KUIPER, N. J. 2008. Glycosaminoglycans in the pericellular matrix of chondrons and chondrocytes. *J Anat,* 213, 266-73.

WANG, W., RIGUEUR, D. & LYONS, K. M. 2014. TGFbeta signaling in cartilage development and maintenance. *Birth Defects Res C Embryo Today,* 102, 37-51.

WATT, F. M. 1988. Effect of seeding density on stability of the differentiated phenotype of pig articular chondrocytes in culture. *Journal of Cell Science,* 89, 373-378.

WIGHT, T. N., TOOLE, B. P. & HASCALL, V. C. 2010. *Hyaluronan and the aggregating proteoglycans,* Mecham R. (eds), Springer, Berlin, Heidelberg.

WONG, M., WUETHRICH, P., EGGLI, P. & HUNZIKER, E. B. 1996. Zone-Specific Cell Biosynthetic Activity in Mature Bovine Articular Cartilage: A New Method Using Confocal Microscopic Stereology and Quantitative Autoradiography *Journal of Orthopaedic Research,* 14, 424-432.

WOODS, A., KHAN, S. & BEIER, F. 2007. C-type natriuretic peptide regulates cellular condensation and glycosaminoglycan synthesis during chondrogenesis. *Endocrinology,* 148, 5030-41.

WU, C., WU, F., PAN, J., MORSER, J. & WU, Q. 2003. Furin-mediated processing of Pro-C-type natriuretic peptide. *J Biol Chem,* 278, 25847-52.

WU, J., EYRE, D. R. & SLAYTER, H. S. 1987. Type VI collagen of the intervertebral disc. *Biochem. J.,* 248, 373-381.

WU, R.-X., XU, X.-Y., WANG, J., HE, X.-T., SUN, H.-H. & CHEN, F.-M. 2018. Biomaterials for endogenous regenerative medicine: Coaxing stem cell homing and beyond. *Applied Materials Today,* 11, 144-165.

XU, J., WANG, W., LUDEMAN, M., CHENG, K., HAYAMI, T., LOTZ, J. C. & KAPILA, S. 2008. Chondrogenic differentiation of human mesenchymal stem cells in three-dimensional alginate gels. *Tissue Eng Part A,* 14**,** 667-80.

YANAGISHITA M. 1993. Function of proteoglycans in the extracellular matrix. *Acta Pathol Jpn,* 43**,** 283-293.

YASODA, A., KOMATSU, Y., CHUSHO, H., MIYAZAWA, T., OZASA, A., MIURA, M., KURIHARA, T., ROGI, T., TANAKA, S., SUDA, M., TAMURA, N., OGAWA, Y. & NAKAO, K. 2004. Overexpression of CNP in chondrocytes rescues achondroplasia through a MAPK-dependent pathway. *Nat Med,* 10**,** 80-6.

YEH, L. C., ZAVALA, M. C. & LEE, J. C. 2006. C-type natriuretic peptide enhances osteogenic protein-1-induced osteoblastic cell differentiation via Smad5 phosphorylation. *J Cell Biochem,* 997**,** 494-500.

YOO, J. U., T.S. BARTHEL, K. NISHIMURA, L. SOLCHAGA, A.I. CAPLAN, V.M. GOLDBERG, B. JOHNSTONE 1998. The chondrogenic potential of human bone-marrow-derived mesenchymal progenitor cells. *J Bone Joint Surg Am,* 80**,** 1745–1757.

YORK HEALTH ECONOMICS 2017. The Cost of Arthritis: sCalculation conducted on behalf of Arthritis Research UK. *Unpublished*.

ZAK, L., ALBRECHT, C., WONDRASCH, B., WIDHALM, H., VEKSZLER, G. & TRATTNIG, S. 2014. Results 2 Years After Matrix-Associated Autologous Chondrocyte Transplantation Using the Novocart 3D Scaffold: An Analysis of Clinical and Radiological Data. *The American journal of sports medicine,* 42**,** 1618–1627.

ZHANG, L., SU, P., XU, C., YANG, J., YU, W. & HUANG, D. 2010. Chondrogenic differentiation of human mesenchymal stem cells: a comparison between micromass and pellet culture systems. *Biotechnol Lett,* 32**,** 1339-46.

ZHAO, G., YIN, S., LIU, G., CEN, L., SUN, J. & ZHOU, H. 2009. In vitro engineering of fibrocartilage using CDMP1 induced dermal fibroblasts and polyglycolide. *Biomaterials,* 30**,** 3241–3250.

ZHENG, J., LUO, W. & TANZER, M. L. 1998. Aggrecan Synthesis and Secretion. *The Journal of Biological Chemistry,* 273**,** 12999–13006.

ZHU, W., CUI, H., BOUALAM, B., MASOOD, F., FLYNN, E., RAO, R. D., ZHANG, Z. Y. & ZHANG, L. G. 2018. 3D bioprinting mesenchymal stem cell-laden construct with core-shell nanospheres for cartilage tissue engineering. *Nanotechnology,* 29**,** 185101.

ZULIANI, C. C., BOMBINI, M. F., ANDRADE, K. C., MAMONI, R., PEREIRA, A. H. & COIMBRA, I. B. 2018. Micromass cultures are effective for differentiation of human amniotic fluid stem cells into chondrocytes. *Clinics (Sao Paulo),* 73**,** e268.

ZUSCIK, M. J., HILTON, M. J., ZHANG, X., CHEN, D. & O'KEEFE, R. J. 2008. Regulation of chondrogenesis and chondrocyte differentiation by stress. *J Clin Invest,* 118**,** 429-38.